TECHNISCHE UNIVERSITÄT MÜNCHEN
FAKULTÄT FÜR CHEMIE

Development of Novel λ^3-*F*-Iodane Based Umpolung Strategies for the Chemoselective Synthesis of α-Functionalized Ketones

Gabriel Maria Kiefl

Vollständiger Abdruck der von der Fakultät für Chemie der Technischen Universität München zur Erlangung des akademischen Grades eines Doktors der Naturwissenschaften genehmigten Dissertation.

Vorsitzender:	Prof. Dr. Matthias Feige
Prüfer der Dissertation:	1. Prof. Dr. Tanja Gulder
	2. Prof. Dr. Lukas Hintermann

Die Dissertation wurde am 29.09.2021 bei der Technischen Universität München eingereicht und durch die Fakultät für Chemie am 10.11.2021 angenommen.

Part of the results presented in this thesis were already included in the following publications:

C. Brunner, A. Andries-Ulmer, **G. M. Kiefl**, T. Gulder; Hypervalent Fluoroiodane-Triggered Synthesis of Fluoro-Azabenzoxazepines and Azaindoles; *Eur. J. Org. Chem.* **2018**, 2615-2621.

G. M. Kiefl, T. Gulder; α-Functionalization of Ketones via a Nitrogen Directed Oxidative Umpolung; *J. Am. Chem. Soc.* **2020**, *142*, 20577-20582.

Hypervalent Iodane Triggered Umpolung of Ketones (Poster), 7th EuCheMS Chemistry Congress **2018**, Liverpool/England.

This work utilizes the convention to depict the relative configuration of racemates with straight bars (bold or hashed) and the absolute and relative configuration of enantiomerically pure or enriched compounds with wedged bonds (bold or hashed).

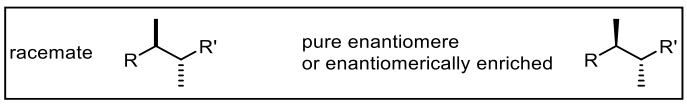

Danksagung

Ich bedanke mich ganz herzlich bei Frau Prof. Tanja Gulder für die Möglichkeit, meine Doktorarbeit in Ihrer Arbeitsgruppe anfertigen zu dürfen. Das entgegengebrachte Vertrauen und die uneingeschränkte fachliche als auch finanzielle Unterstützung weiß ich sehr zu schätzen.

Des Weiteren möchte ich mich natürlich auch bei der Arbeitsgruppe Tanja Gulder bedanken. Qingqi, Christoph, Steffi, Jarek, und Andi haben mich sofort in ihrer Mitte aufgenommen und die vielen gemeinsamen Abende werde ich nie vergessen. Auch Pierre, Simon, Julia, Wanying, Catharina, Anna, Bin-bin, Peng-yuan, Yang und Zuoyufan haben diese Zeit einzigartig gemacht.

Bei meinen Forschungspraktikanten Christian, Jonas, Nick, Alex und Vroni möchte ich mich für ihre Hilfe im Labor und ihrem Beitrag zu dieser Doktorarbeit herzlich bedanken.

Meiner Familie schulde ich Dank, die mich während des Studiums und der Promotion stets unterstützt und das Leben abseits der Chemie verschönert haben.

Abschließende möchte ich mich bei meiner Frau Simone bedanken, die mich unaufhörlich, immer wieder aufgebaut hat und auch an stressigen Tagen stets ein offenes Ohr hatte. Zuletzt danke ich auch noch meinem Sohn Hector, der sich meine Zeit in seinen ersten Lebensmonaten mit dieser Arbeit teilen musste, das aber immer mit einem Lachen getan hat.

Table of Contents

Abstract

The α-functionalization of carbonyls is a widely used synthetic method that grants access to valuable molecules and multiple fields of chemistry have found elegant approaches for the execution of suitable reaction pathways. The class of hypervalent iodane reagents have proven themselves to be excellent mediators for the oxidative Umpolung of ketones and play a valuable role in the introduction of nucleophiles into the nucleophilic α-position of ketones. The λ^3-iodanes enable a broad scope of introducible nucleophiles and demonstrate good tolerance towards functional groups. Nonetheless, several limitations, like the need for preformation of the respective silyl enol ether when using external nucleophiles or the problem of regioselectivity when both α-positions of the respective ketone are accessible, are still present.

We envisioned a non-covalent coordination of the Lewis acidic hypervalent iodane with a Lewis basic group in the substrate scaffold that would direct the reaction towards one selective α-position of the ketone and facilitate the introduction of external nucleophiles. Pyridine was chosen as the suitable Lewis basic moiety because of its already established affinity to form coordinative bonds with the iodane center of λ^3-iodanes. The ideal hypervalent iodane for this approach was found in a relatively novel, cyclic *F*-iodane that is bench-stable and moisture insensitive.

With the presented substrate directing method, a broad variety of protic *S*-, *N*- and *O*- nucleophiles were introduced selectively into the α-position of 2-pyridylacetone derivatives under exceptionally mild conditions, without the need for the careful preparation of a moisture and oxygen free atmosphere. Furthermore, quaternary carbon centers bearing a fluorine and fluoro-alcohols were obtained under slightly adapted reaction conditions.

The scope of the established method was extended to furnish complex α-functionalized ketones and imidazo[1,5-*a*]pyridines starting from pyridylstyrene derivatives in a one-pot cascade reaction. *S*-, *N*-, *O*- and even *C*-nucleophiles were introduced to obtain various α-functionalized ketones and alkylnitriles to gain access to unprecedented imidazo[1,5-*a*]pyridines. A substrate dependent product formation was discovered that can be used to selectively distinguish between three product classes by small adjustments of the reaction conditions and selection of the suitable substitution pattern in the substrates.

I. Theoretical Background

1. Introduction

During the course of a chemist's life at university an interesting phenomenon seems to take place, starting in the first semester and being at its maximum at the end of the doctorate phase. The accurate description of what you are actually doing all day becomes increasingly difficult to communicate to friends and family. While some are fortunate enough to have taken a path that led them to topics like light emitting diodes (LED) in inorganic chemistry or vaccines in biochemistry with easy to grasp real life applications, most organic chemists are stuck with the simple answer, that their research might lead one day to a new drug that helps cure a disease. And although the majority of people associate chemistry with organic chemistry, that does not help a great deal in trying to explain the highly specialized topic of one's thesis. Nonetheless, the exploration of new concepts, reaction pathways and reactivities in the synthesis of novel and known organic compounds is the foundation on which innovation can thrive and the possible future impact of the work presented in this thesis is yet to be determined.

One structural motif has played an essential role in the whole duration of this doctorate phase and that class of molecules are the pyridines. Despite the seemingly minor variation from benzene with the introduction of a nitrogen into the aromatic ring, pyridine (**1**, figure 1) possesses a vastly different reactivity[1] and although it is not widely common in nature, besides as traces e.g. in roasted coffee,[2] its derivatives are found abundantly in natural products.[3] The most prominent example is Nicotine (**2**) found in the *Nicotina tabacum* plant, known as tobacco.[4] With over 1.3 billion tobacco users worldwide in 2020[5] this pyridine containing molecule (**2**) has probably the most impact on the human population out of all natural products. Although Nicotine (**2**) is not the most harmful ingredient of cigarettes, it is still highly addictive and has negative effects on the development of a human fetus.[6] Nicotinic acid (**3**), also known as Niacin in an effort to detach itself from its namesake Nicotine (**2**) from which it can be synthesized by oxidation with nitric acid,[7] on the other hand is one of the three forms of vitamin B_3,[8] an essential nutrient that is further metabolized to a co-factor used in almost all redox reactions in the human body.[9] Another cofactor is Pyridoxal Phosphate (**4**), the active form of vitamin B_6, with the corresponding enzymes being used throughout all organisms.[10] Natural pyridine derivates like Malloapeltine (**5**), extracted from the root *Mallotus apelta* as a potent anti-HIV drug[11] and Streptonigrin (**6**), isolated from *Streptomyces foculus* as an anti-tumor and anti-microbial drug[12] have also found significant medicinal applications.

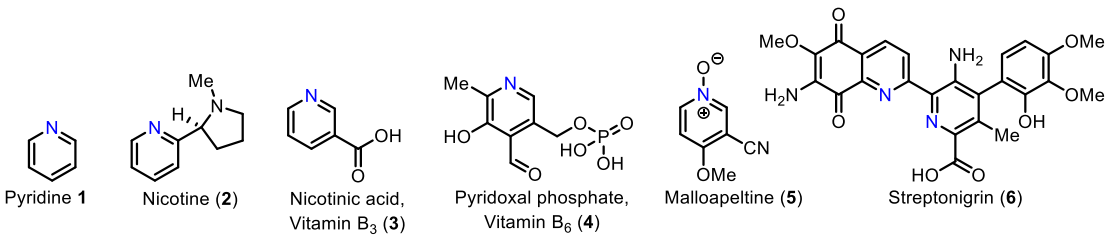

Figure 1: Pyridine and pyridine containing natural products.

Advances in organic chemistry expanded the possible selection for bio active compounds from natural products to novel, synthetic compounds and natural product derivatives that are tunable to maximize the efficacy. Pyridine containing molecules are once more showing their importance in medicinal chemistry as one of the most used heterocyclic structure in U.S. FDA approved pharmaceuticals[13] with broad applications[14] reaching from anti-microbial effects[15] to inhibiting enzyme activity.[16]

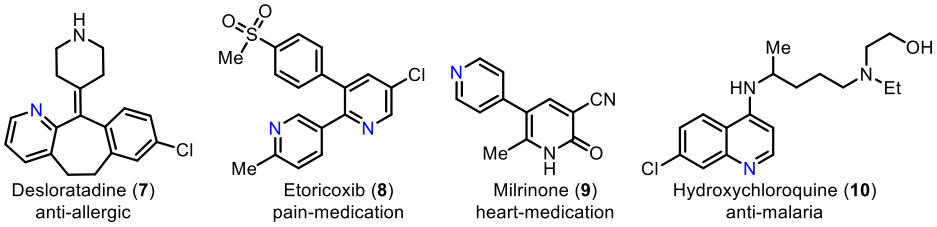

Figure 2: Pyridine-motif containing drugs.

Desloratadine (**7**, figure 2) is build up of a pyridine moiety condensed with a seven-membered ring and shows anti-allergic effects.[17] The bipyridine derivative Etoricoxib (**8**) is a pain medication[18] and Milrinone (**9**), containing a pyridine and a pyridone scaffold, has indication as a medication against acute heart failure, pulmonary hypertension, or chronic heart failure.[19] During the course of the COVID-19 pandemic in 2020, Hydroxychloroquine (**10**), originally developed as a precautionary anti-malaria drug,[20] was tested for its anti-viral activity against the SARS-CoV-2 but unfortunately did not show a beneficial effect during treatment and no decrease in mortality,[21] despite having the most prominent test patient of them all at that time, the president of the United States of America.

Furthermore, pyridine-based compounds play a fundamental role as agrochemicals. The fungicide Fluazinam[22] (**11**, figure 3), the herbicide Paraquat (**12**)[23] and the insecticide Imidacloprid (**13**)[24] are all widely used pesticides with the latter two being among the top 10 crop protecting products in 2013[25], despite Paraquat (**12**) being linked to causing Parkinson's disease[26] and being banned in the European Union since 2007.[27]

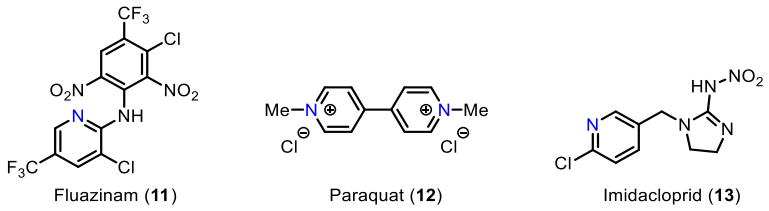

*Figure 3: Pyridine-based agrochemicals: fungicide **11**, herbicide **12**, and insecticide **13**.*

A reason for the substantial number of pyridine-based compounds found in nature, pharmaceuticals and agrochemicals is the significant decrease in hydrophobic constant compared to their benzenoid counterparts. The introduction of the electro negative nitrogen into the six membered ring causes an electron deficiency in the aromatic portion and an increase in polarity, rendering pyridines basic, electron poor aromatic substances with increased water miscibility and making its usage in predominantly aqueous environments more feasible. The lone pair of the nitrogen is not part of the π-system and thus of the aromatic system and is therefore free to interact with Lewis acids *via* direct σ-bonding or π-back bonding (figure 4).[28]

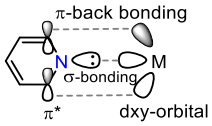

Figure 4: Orbital bonding possibilities of pyridine with a Lewis acid.

While there is an abundance of natural pyridine derivatives, their biosynthesis is still poorly understood. An exception is the Niacin (**3**) production in plants and mammals. Because of its significance and great value for humans, a multitude of studies have been conducted and the synthetic pathway is well understood.[29]

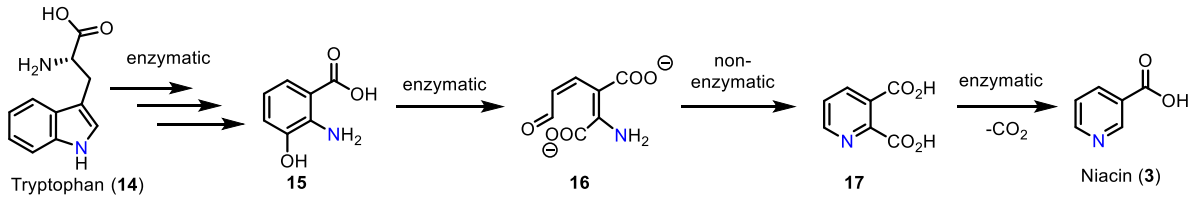

*Scheme 1: Schematic biosynthetic pathway to Niacin (**3**) from Tryptophan (**14**).*

Starting from Tryptophan (**14**, scheme 1), it is steadily converted through an enzyme catalyzed, oxidative pathway to 3-hydroxyanthranilate (**15**) and converted to the oxidized, open-form **16**. Interestingly, the step in which the pyridine ring is formed seems to proceed via a pericyclic, non-enzymatic pathway to build up quinolic acid (**17**).[30] Finally, Niacin (**3**) is formed after decarboxylation. Furthermore, this seems not to be an exclusive characteristic of the Niacin (**3**) biosynthesis but also for other natural pyridine derivatives,[31] showing vividly, that the aromatic pyridine ring is a stable and favored scaffold, which greatly facilitates its synthesis.

The procedure to synthesize pyridine, that is to date used on an industrial scale, is the since the early 20th century known Chichibabin condensation reaction (scheme 2).[32] The ammoniac forms an imine **19** with the aldehyde **18** and reacts in a Michael addition with the acrylaldehyde **20**. After proton migration, ring closure and autooxidation steps, pyridine **1** is formed.

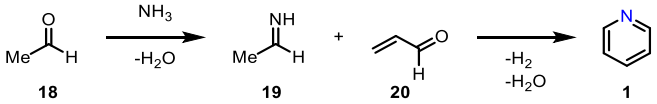

Scheme 2: Chichibabin condensation reaction.

As previously mentioned, pyridines can form significantly stronger interactions with electrophilic moieties than their benzenoid counterparts and have therefore found broad applications as ligands to metallic centers in catalysts. Examples of pyridine-based transition metal catalysts can be found in various fields of chemistry (figure 5). The photocatalyst $[Ru(bpy)_3]Cl_2$ **21** for instance can be used in ultraviolet and visible light to trigger transformations of organic molecules,[33] while the hafnium complex **22** catalyzes ethylene-α-olefin copolymerization reactions.[34] The famous Crabtree's catalyst (**23**) on the other hand is a highly potent pyridyl-complex that shows trans-selectivity[35] in the hydrogenation of olefines.[36] While not the most commonly used ligand in cross coupling reactions,

pyridyl-ligands in the form of Pd(II)-complex **24** are efficient catalysts for the Suzuki coupling of aryl halides under microwave irradiation in water.[37]

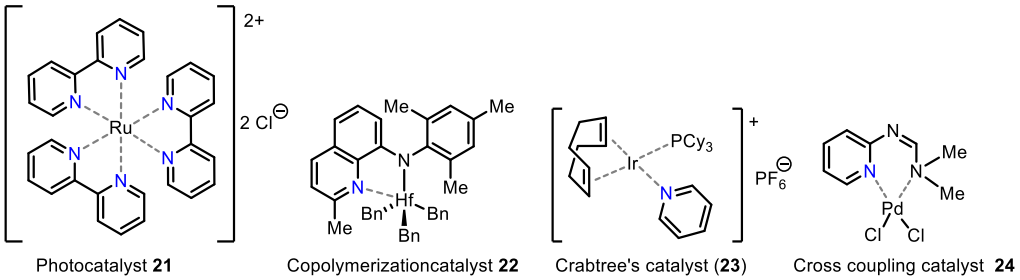

Figure 5: Transition-metal catalysts bearing pyridine ligands.

The dependence on precious metals in transition metal catalysis can be a significant disadvantage as it is susceptible to price and purity fluctuations and has serious environmental impacts caused by the mining.[38] The substitution to less problematic reagents if possible is therefore highly desirable. One class of reagents that has emerged as potential successors over the last decades are hypervalent iodane reagents. They display similar reactivity patterns as transition metal catalysts and are solely dependent on their synthetic availability. Their striking resemblance in reactivity can be recognized by comparing the catalytic cycles for the Negishi cross-coupling[39] (figure 6a) and the iodobenzene-catalyzed α-acetoxylation of ketones[40] (figure 6b). After the oxidative addition (A) of the substrate to the palladium, respectively the iodine, a ligand exchange (B) with the second substrate occurs. In the last step, the reductive elimination (C) to the product as well as to the catalyst in its initial state is carried out to complete the cycle.

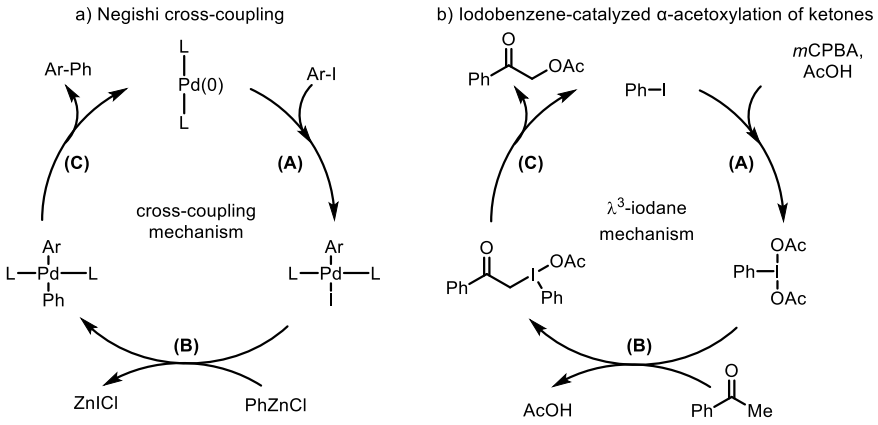

Figure 6: Catalytic cycles of a) the Negishi cross-coupling and b) the hypervalent iodane catalyzed α-acetoxylation of ketones.

Hypervalent iodanes do not only showcase similar reactivities to already established catalysts but possess unique characteristics that manifest themselves in unprecedented chemo- and regioselectivities that are unrivaled by conventional oxidative mediators. The Gulder group has already started to unravel new synthetic applications of a recently disclosed fluoro λ^3-iodane (**35**) in the conversion with styrene-derivates[41] and the further exploration of still untapped potential is the reason of this work focusing on strategies to utilize the fascinating reactivities of compound **35** in the development of novel Umpolung approaches as well as in one-pot cascade reactions.

2. State of the Art

2.1 Hypervalent λ³-*F*-Iodane 35

Hypervalence is the condition of ions or molecules of group 15-18 elements of the periodic table in which the octet rule is disregarded and the valence shell is occupied by more than eight electrons.[42] The hypervalent bonding is best described by a three-center four-electron (3c-4e) bond (figure 7).[43] The most prominent organic compounds that exploit the unique reactivities accompanied by hypervalent bonding are the hypervalent iodane reagents **25** with the 3c-4e bond between two horizontal ligands and the iodine.

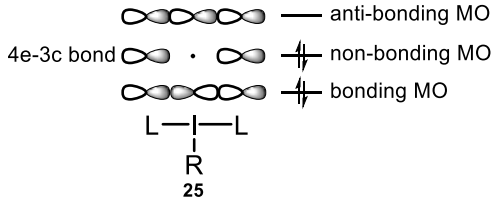

*Figure 7: General MO-scheme of the hypervalent bond in trivalent λ³-iodanes **25**.*

The first synthesis of a trivalent λ³-iodane was achieved by Willgerodt already in 1885[44] by letting iodobenzene **26** react with chlorine gas to obtain iodobenzene dichloride (**27)** as a yellow solid (figure 8a). This discovery sparked an enormous interest and although iodobenzene dichloride (**27**) itself is not widely used, derivatives thereof have proven themselves immensely useful (figure 8b). (Diacetoxyiodo)benzene (**28**, PIDA), Kosers's reagent (**29**) and the fluorination reagent **30** are among the most applied hypervalent iodane reagents in oxidation and atom transfer reactions.[43, 45] Besides these linear reagents, cyclic hypervalent iodanes **31**[46] and **32**[47] possessing a bidentate ligand, derived from 2-iodobenzoic acid, that lead to improved stability were discovered just a few years after compound **27** (figure 8c). Despite the early access to these compounds, cyclic species have only quite recently started to become versatile tools for novel reactions in organic synthesis.[48] Probably the most renowned cyclic hypervalent iodanes are Togni reagent I (**33**) and II (**34**), named after Professor Togni, who developed their synthesis in 2006[49] and is an eminent authority in the field of hypervalent iodine chemistry. Compounds **33** and **34** are highly effective and versatile tools for the electrophilic trifluoromethylation for a manifold of substrates.[50]

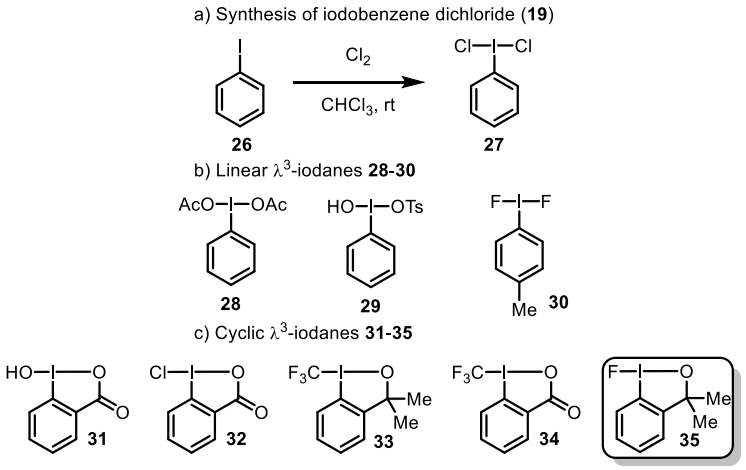

*Figure 8: a) Synthesis of compound **27** and selected examples of b) linear and c) cyclic trivalent λ³-iodanes **28**-**35**.*

Arguably the most important recent development in the field of novel, cyclic hypervalent iodane reagents was made by Legault and Prévost in 2012[51] with their disclosure of the synthesis and crystal structure of fluorobenziodoxole **35**. Since their focus was primarily on the crystal structure and not the yield, they did not employ additional effort to find the optimal conditions and did not specify the yield of compound **35** in their procedure for the conversion of 2-(2-Iodophenyl)-propan-2-ol **36** with Selectfluor® (**37**) to the desired product **35** (scheme 3a). A few months later, Togni *et al.*[52] used spray dried KF to convert the chloro iodane **38** to the *F*-iodane **35** in an excellent yield (scheme 3b), although their focus laid more on its use as an intermediate to obtain Togni reagent I (**33**). Another few months later, highlighting the great interest in this novel hypervalent iodane, Stuart *et al.*[53] developed an improved synthesis using cheap and mild conditions, making it widely available to the synthetic community (scheme 3c). Selectfluor® (**37**) or spray dried KF and an argon atmosphere were no longer needed and starting from 2-(2-Iodophenyl)-propan-2-ol **36**, *F*-iodane **35** was furnished in three simple steps. The bromoiodane **39**, obtained from the oxidation of compound **36** with *N*-bromosuccinimide (NBS) was converted to the hydroxyiodane **40** with potassium hydroxide. Fluoroiodane **35** was furnished in the key step by treating compound **40** with triethylamine trihydrofluoride and was obtained after a simple recrystallization in excellent yield and purity.

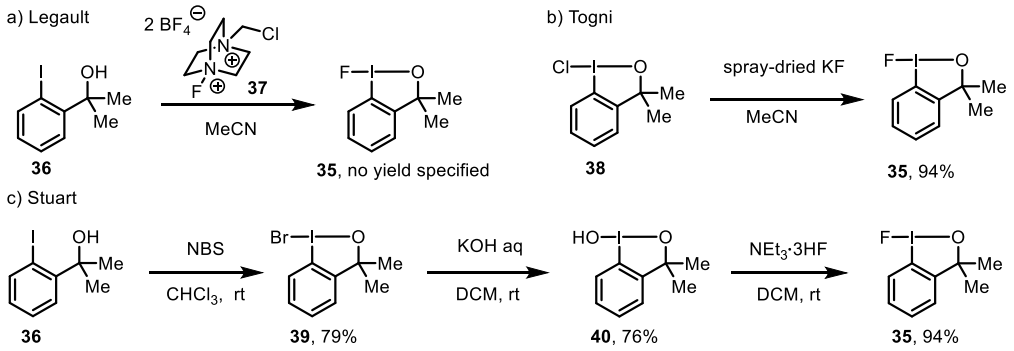

*Scheme 3: Synthetic pathways towards F-iodane **35** by a) Legault[51], b) Togni[52] and c) Stuart et al.[53]*

With easy access to this novel, moisture, air and bench stable reagent, applications were expected to be disclosed soon. Although *F*-iodane **35** is less reactive than the linear hypervalent iodane **30**, which was the standard fluorinating hypervalent iodane reagent,[45b] the lower synthetic effort needed to carry out fluorination reactions made the exploration of its applicability more than worthwhile, especially when considering that fluorine-containing molecules have found broad recognition in agrochemistry,[54] pharmaceutical products,[55] material science [56] and in diagnostics[57] due to beneficial characteristics of the respective molecules.

The first utilization of *F*-iodane **35** was disclosed by Stuart *et al.*[53] in the same publication as the improved synthesis. They were able to mono-fluorinate β-keto ester **40** to compound **41** under unusually mild conditions (scheme 4a). The difluorinated sideproduct was suppressed through addition of the NEt_3·3HF complex. The ability to directly fluorinate compounds sparked great interest and more applications followed rather quickly. The geminal oxofluorination of diazocarbonyl compound **42**

demonstrated the reactivity of *F*-iodane **35** in a completely different field of use.[58] The rhodium acetate catalyst **44** inserts itself into the diazo-carbon bond under cleavage of nitrogen and the formed rhodium-carbene complex is readily attacked by the alcohol **43**. The *F*-iodane **35** oxidizes the intermediate and introduces the fluorine into the structure to furnish the geminal oxofluorinated product **45**.[59] Furthermore, an unprecedented hypervalent iodane catalyzed Balz-Schiemann fluorination to transform arenediazonium salt **46** to the fluorinated aromatic compound **47** in a highly efficient manner and excellent yield was shown quite recently by Hu *et al.*[60] The affinity of *F*-iodane **35** towards allylic structures **48** was demonstrated by Szabo *et al.*[61] in their approach to introduce the fluorine and the iodine of the hypervalent reagent **35** into the product **49** by cleaving the aromatic iodine bond through palladium catalysis.

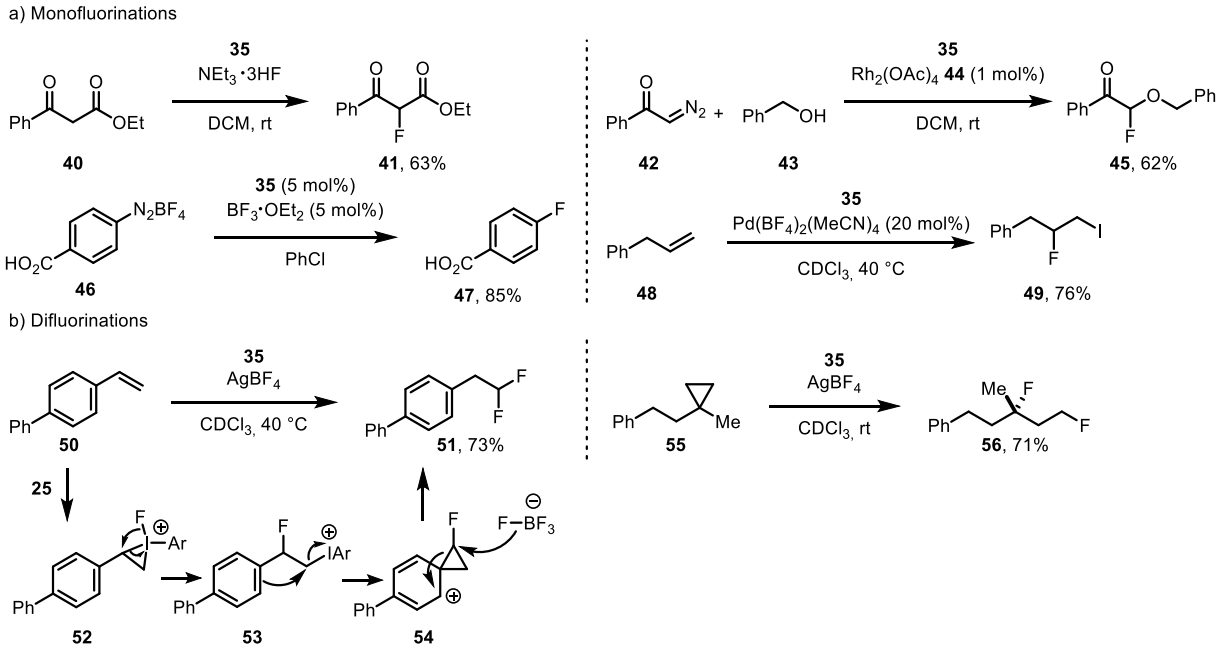

*Scheme 4: a) Mono- and b) difluorinations using the cyclic fluoro-benziodoxole **35**.*

Szabo *et al*. focused their studies on the conversion of double bonds with *F*-iodane **35** and achieved the synthesis of the geminal difluorinated compound **51** from the styrene derivative **50** using air- and moisture insensitive conditions (scheme 4b).[62] This reaction proceeds via an 1,2-aryl shift to obtain the geminal and not the vicinal difluorinated product. They described a plausible mechanism for this reaction in which the oxidation of the double bond forms the iodonium ion **52** and a subsequent fluorine migration occurs to furnish the 1,2-substituted alkyl **53**. In the key step, the aromatic ring attacks nucleophilic and cleaves the highly nucleofuge iodoaryl moiety to construct the spirocyclic **54**. Finally, an external fluoride is introduced and the geminal fluorinated product **51** obtained. The $AgBF_4$ was needed as an activator through coordination of the Lewis acid to the fluorine of the *F*-iodane **35**[63] and as an additional, external fluoride source. They successfully extended the substrate scope to α,α'-disubstituted styrenes in later years.[64] Furthermore, they showed that this approach was not exclusive to the conversion of styrene derivatives and disclosed a fluorinative ring-opening of cyclopropanes **55** to the 1,3-difluorinated linear alkyl-compounds **56**,[65] utilizing the $AgBF_4$ again as an activator and external fluoride source.

The apparent affinity of *F*-iodane **35** towards double bonds was further exploited in several approaches towards cyclic structures. Exchanging the external nucleophile with an intramolecular functional group led to highly interesting fluorinated cyclic scaffolds (scheme 5).

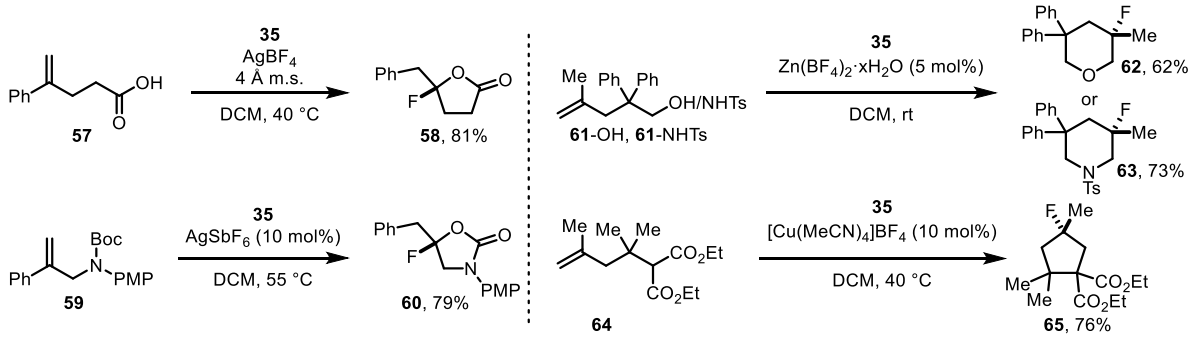

*Scheme 5: Synthesis of fluorinated, mono-cyclic structures using F-iodane **35** and an intramolecular, nucleophilic moiety.*

The treatment of the unsaturated carboxylic acid **57** with *F*-iodane **35** and $AgBF_4$ led to the five membered lactone **58**.[66] Once more, the reaction proceeds via an 1,2-aryl shift, but the cyclic structure is furnished by an intramolecular, nucleophilic attack of the carboxylic acid moiety instead of an external nucleophile. Substituting the carboxylic acid moiety to a nucleophilic carbamate group **59** gave the fluorinated *N*-aryl-oxazolidin-2-one **60** under slightly harsher conditions.[67] Szabo *et al.*[68] followed a similar approach but with *O*-, *N*- and *C*-nucleophilic moieties incorporated in alkenyl compounds **61**-OH, **62**-NHTs and **64**. Fluorinated heterocycles **62** and **63** were furnished with the help of zinc tetrafluoroborate and fluorinated cyclopentane derivative **65** was obtained with $[Cu(MeCN)_4]BF_4$ as the catalyst.

In 2016, our group joined the race to explore the synthetic value of the novel *F*-iodane **35**. Installing an amide moiety at the aromatic portion in the styrene derivative **66** opened the door for the straightforward synthesis of unprecedented fluoro-benzoxazepines (**67**, scheme 6).[41a]

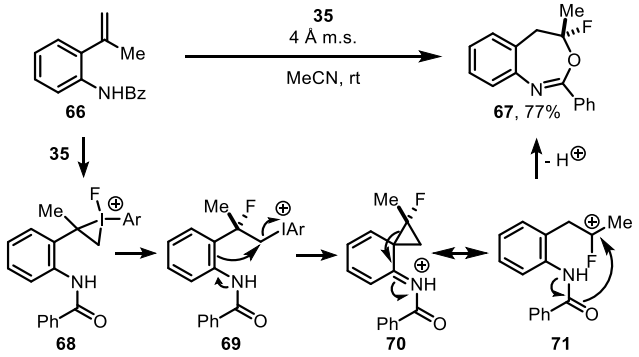

*Scheme 6: Synthesis of unprecedented fluoro-benzoxazepine **67** and the plausible mechanistic pathway.*

Computational studies on the mechanistic pathway towards these pharmacologically interesting, bicyclic molecules were done by the Cheng group[69] and refined by our own group.[41b] The density functional theory (DFT) calculations established the most plausible mechanism for this reaction with a rather surprising, fluoro carbocationic structure **71** at the defining step. The addition of the *F*-iodane **35** to the double bond towards structure **68**, fluorine migration to structure **69** and furnishing of the

spirocyclic structure **70**, with the positive charge stabilized at the amide-nitrogen, are all in accordance with the previously hypothesized mechanism for the conversion of styrenes **40** (scheme 4b) by Szabo *et al.*[62]. The opening of the spirocyclic structure **70** to the *F*-carbocation **71** was unexpected but can be rationalized when taking the 2p nonbonded electron-pair back bonding of the fluorine and the electron-donating effect of the Lewis basic amide-oxygen into account for the stabilization of the positive charge.[41b]

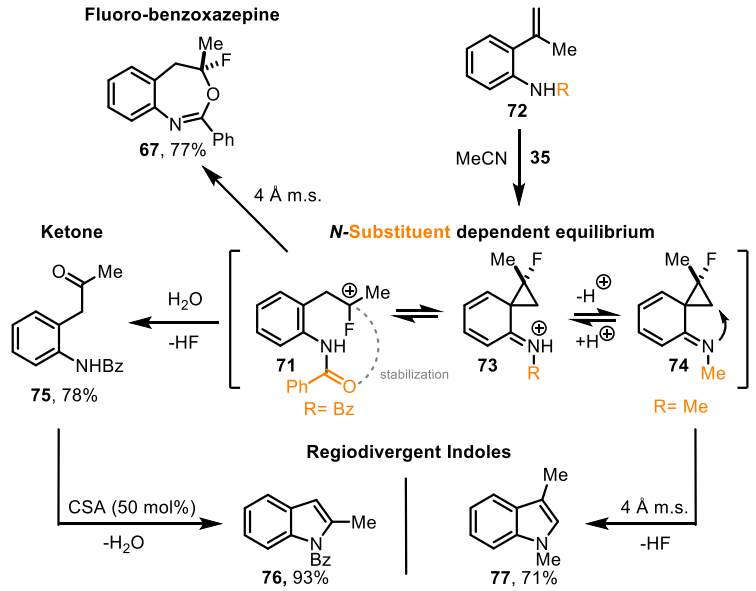

*Scheme 7: Reaction condition and N-substituent dependent synthetic pathways starting from styrene **72** with F-iodane **35**.*

Intrigued by this finding, follow up investigations into the conversions of the styrenes **72** were done[41b] (scheme 7). It was discovered that omitting the molecular sieve from the reaction conditions and thus permitting water to trap the *F*-carbocation intermediate **71** gave way to the ketone **75**. Varying the reaction conditions by adding the protic camphorsulfonic acid (CSA) as a catalyst led to indoles **76** via a further ring closing reaction without the need to isolate the intermediary ketone **75**. With this approach, starting from the same styrene **72** three different products (fluoro-benzoxazepine **67**, ketone **75** and indole **76**) can be obtained by simple adjustments of the reaction conditions in a straightforward manner. Even more fascinating was the realization that varying the *N*-substituent R from benzoyl to methyl led to the indole **77**. Since the indoles **76** and **77** are regiodivergent to each other, different mechanistic pathways have to be present for these conversions. Computational studies supported by experimental control reactions gave the answer and demonstrated that the spirocyclic *F*-cyclopropane **73** is the common intermediate for all styrene derivatives **72**. Depending on the stabilizing capabilities of the substituent R, either the open carbocationic structure **71** (R= Benzoyl) or the deprotonated intermediate **74** (R= Me) is favored and regiodivergent products are formed. The fluorine acts as a traceless directing group because of its essential role in the formation of the respective intermediates and subsequent elimination from the molecule.

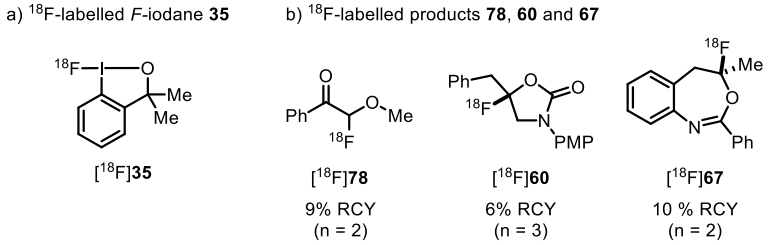

*Figure 9: ^{18}F-labelled a) F-iodane [^{18}F]**35** and b) fluorination products [^{18}F]**78**, [^{18}F]**60** and [^{18}F]**67**.*

The facile and straightforward introduction of fluorine into valuable scaffolds via the *F*-iodane **35** caught the attention of the radio labelling community. Using [^{18}F]-tetrabutylammonnium fluoride (TBAF) in the adapted synthesis of *F*-iodane [^{18}F]**35** (figure 9a) made way for the introduction of a positron emitting isotope ^{18}F in the already established oxyfluorination of diazoketones to compounds [^{18}F]**78**[70] and fluoro cyclization reactions to structures [^{18}F]**60**[67] and [^{18}F]**67**[71] (figure 9b) in good radiochemical yields (RCY). With a half-life of 109.7 minutes for fluorine-18, reactions must be quick and include as few steps as possible, which played perfectly into the strengths of the hypervalent iodane reagent **35**.

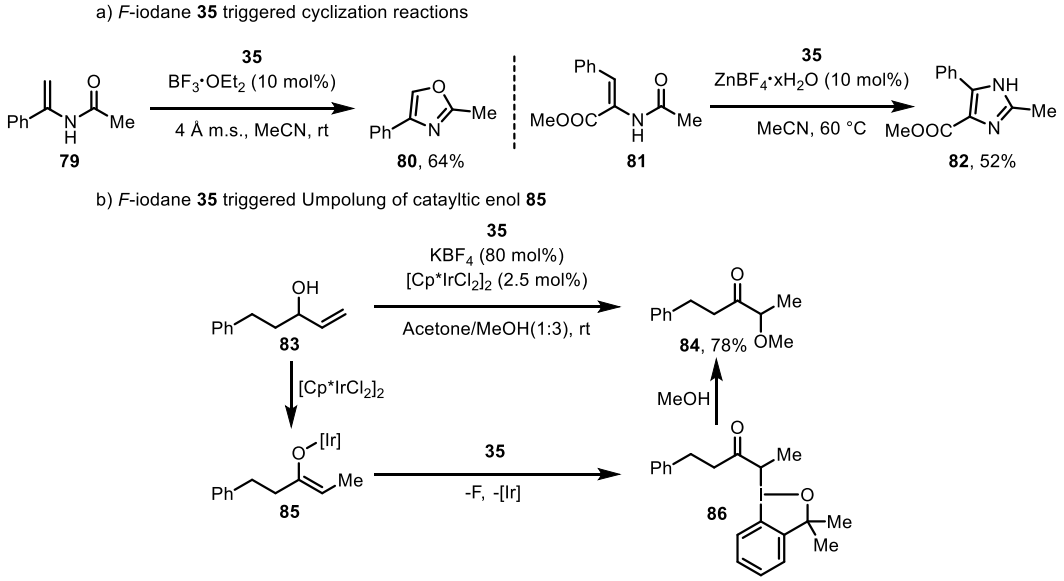

*Scheme 8: Reactions utilizing F-iodane **35** without the introduction of fluorine into the molecules.*

The introduction of the fluorine into intermediates or the final products was the main focus of most *F*-iodane **35** mediated reactions, but it was also utilized as solely an oxidative mediator in two more applications. The Ding group[72] achieved the conversion of *N*-acetyl enamines **79** and **81** to the oxazole **80** and imidazole **82** respectively by having the nucleophilic amide moiety directly at the reactive double bond (scheme 8a). Finally, the reaction of allyl alcohol **83** with *F*-iodane **35** to the α-functionalized ketone **84** was disclosed by the Martín-Matute group in 2019 (scheme 8b).[73] The iridium complex converts the allylic alcohol **83** into the enol **85**, which is readily oxidized by the *F*-iodane **35**. The hypervalent iodane attaches itself under cleavage of the fluorine in the α-position of the formed carbonyl **86**. Methanol substitutes in a subsequent nucleophilic attack the iodoaryl moiety, furnishing the ketone **84**. This is an elegant approach to selectively obtain ketones with only one of the two possible α-positions functionalized. Although the necessity for the preformation of the allyl alcohol **83** and iridium enol ether **85** implies additional effort and limitations in the usable substrates.

2.2 α-Functionalization of Ketones with λ^3-Iodanes

The introduction of a functional group into the α-position of ketones is among the most executed chemical transformation in organic chemistry. The intrinsic polarity of carbonyls **87** furnishes a nucleophilic character at the α-carbon center and therefore limits the employable reaction partners to electrophiles (scheme 9).[74]

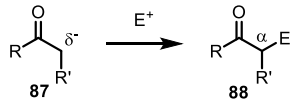

*Scheme 9: Intrinsic polarization and reactivity of ketones **87**.*

Needless to say, the chemistry community was not satisfied with this limitation and a concept to introduce nucleophiles had to be established. In 1977, Corey and Seebach[75] proposed the term Umpolung for transformations where the polarity of the reaction center is formally reversed during the reaction and applied this concept to introduce electrophiles to electrophilic acyl-carbon centers[76] (scheme 10a). The aldehyde **89** is converted into the dithioacetal intermediate **90** in the first step. After the following deprotonation by a strong organolithium base to the lithiated species **91**, the desired reaction with an electrophile can take place to obtain product **92** in a formal electrophile-electrophile reaction.

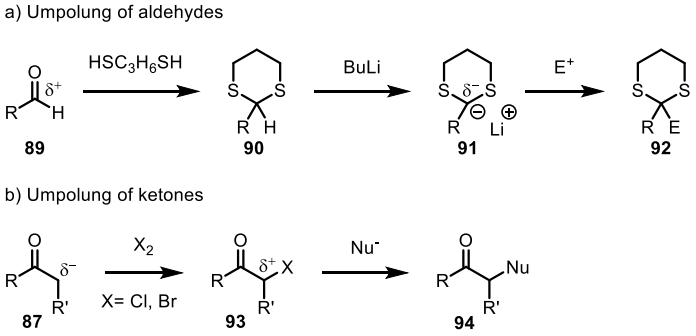

Scheme 10: General approaches utilizing the Umpolung concept.

For the reaction of a nucleophile with the nucleophilic α-carbon center of ketone **87**, this concept had to be adjusted (scheme 10b). By adding an electrophile to the ketone scaffold **87** and substituting it in a subsequent nucleophilic attack by the nucleophile leads to the desired α-functionalized product **94** and renders it a formal nucleophile-nucleophile reaction The two-step procedure opened the door for otherwise inaccessible ketones.[77] Probably the most prominent electrophilic mediators used in this approach are the halogens chlorine and bromine.[78] They react readily with ketones **87** to form α-haloketones **93**, effectively reversing the polarity at the α-carbon and are good leaving groups for the subsequent nucleophilic attack by the preferred nucleophile to furnish the α-functionalized ketone **94**.

The increased synthetic effort caused by the need for at least one intermediate and relatively harsh conditions drove the interest towards novel techniques and reagents that could achieve the desired conversions in a milder, less laborious manner. Once again, hypervalent iodane compounds emerged as convenient and broadly applicable mediators.

The first to combine the Umpolung of ketones with hypervalent iodane chemistry was the group of Mizukami in 1978,[79] around the same time as Seebach and Corey disclosed their seminal studies on the Umpolung of reactivity. By using the cheap and easy to synthesize PIDA (**28**) as an oxidative mediator, they were able to directly introduce a nucleophilic acetoxy functional group in α-position of the ketone **95** to obtain the carbonyl **96** (scheme 11).

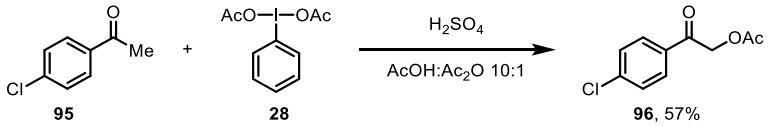

*Scheme 11: First application of a hypervalent iodane **28** in the Umpolung of ketone **95**.*

Other groups were quick to disclose further examples with similar approaches after this discovery and it ushered in the broad application of hypervalent iodane reagents as mediators in the α-functionalization of ketones (scheme 12).[80]

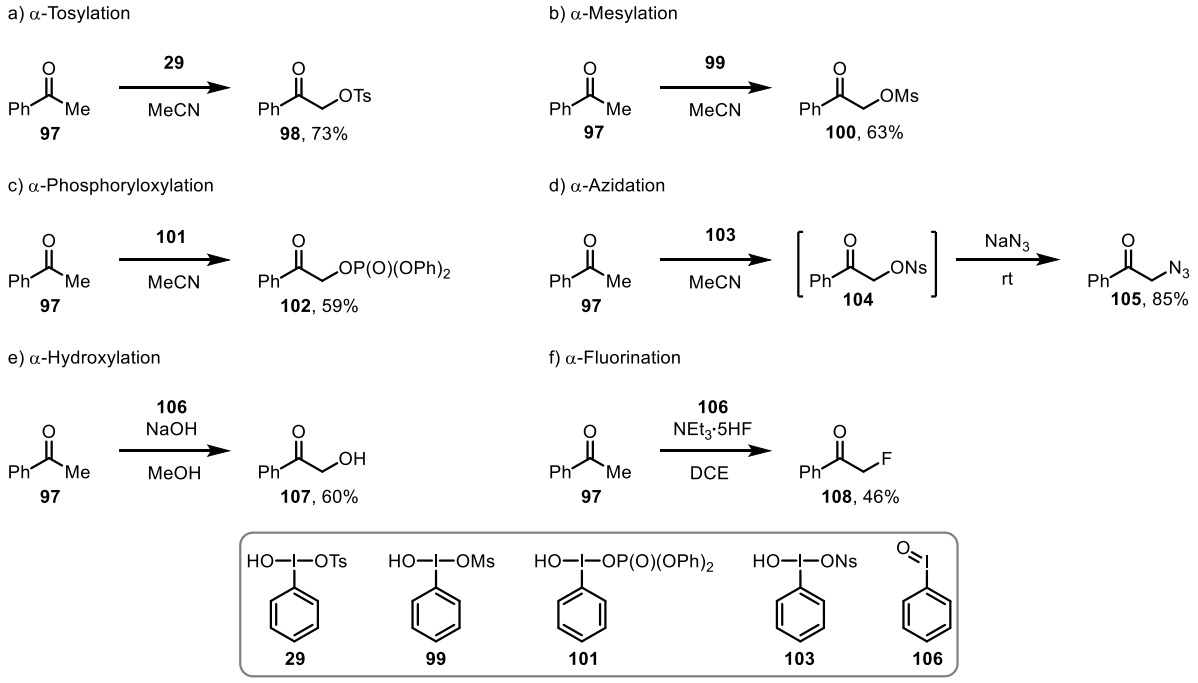

Scheme 12: Overview of α-functionalizations of simple ketones by hypervalent iodanes.

Koser *et al.*[81] made use of the tosyl-derivative **29** to introduce a tosyl group into the ketone scaffold **97** to obtain the functionalized product **98**. This reagent, now known as Koser's reagent was actually first synthesized by Neiland and Karele in 1970 from toluene sulfonic acid and PIDA (**28**),[82] but was greatly popularized by Koser and his group through extensive studies on its reactivity and applications.[83] Their attempts for α-mesylation (**100**)[84] and α-phosphoryloxylation (**102**)[85] of carbonyls using the respective λ^3-iodanes **99** and **101** were successful as well. The α-azidation of ketone **97** could not be achieved directly but the nosyl-derivative **103** was used by Shin *et al.*[86] to obtain the intermediate **104**, which was directly converted with sodium azide to the desired product **105**. The α-hydroxylation (**107**)[87] of ketone **97** was accomplished with another approach. Iodosobenzene **106** in methanol under basic conditions with NaOH converted the respective ketone **97** into the product **107**. The iodine-oxygen bond in reagent **106** is commonly depicted as a double bond for simplification reasons, but the polymeric

structure would actually be better described by a single dative bond between the iodine and the oxygen.[88] Muta *et al.*[89] were also able to utilize iodosobenzene **106** in their method to introduce a fluorine with the triethylamine 5HF complex as the fluorine source to obtain the fluorinated ketone **108**.

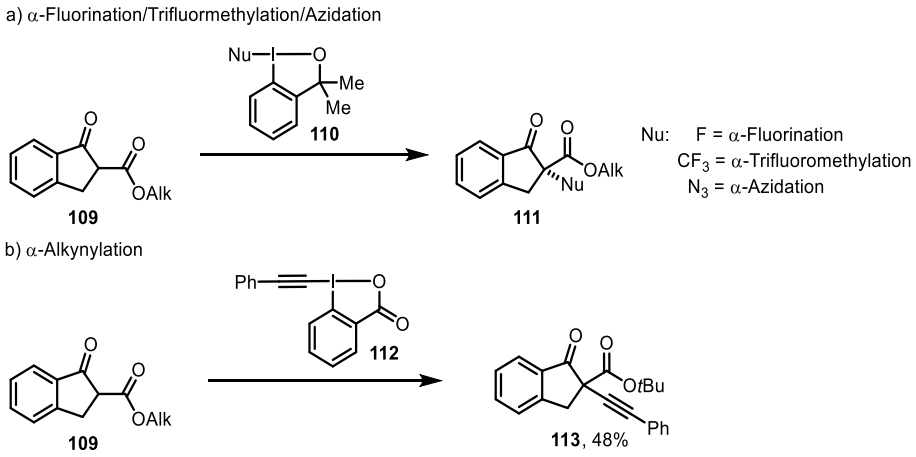

*Scheme 13: Overview of α-functionalizations of 1,3- dicarbonyl compound **109** with cyclic λ³-iodanes **110** and **112**.*

Cyclic λ^3-iodanes **110** on the other hand have recently started to show their potential in the α-functionalization of 1,3-dicarbonylic structures **109** (scheme 13). These highly nucleophilic carbonyls can be readily transformed to the respective compounds **111** in an α-fluorination,[90] α-trifluoromethylation[91] or α-azidation[92] reaction depending on the respective nucleophile in the used hypervalent iodane **110**. Even α-alkynylation[93] of these highly reactive β-ketoester **109** to product **113** was achieved with reagent **112**.

A major drawback of these transformations is the general need of the desired nucleophile to be incorporated into the hypervalent iodane scaffold in order to transfer it into the α-position of the respective ketones. This is a limiting factor for the nucleophiles that can be utilized to form stable and isolable iodanes.

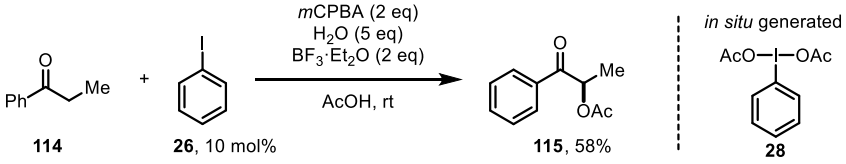

*Scheme 14: Catalytic α-acetoxylation of ketone **114**.*

Ochiai *et al.*[40] realized that the reduction of the λ^3-iodane to the univalent aryliodine constitutes the driving force for the oxidation reactions and that when stoichiometric amounts of λ^3-iodanes were used, equimolecular amounts of aryl iodines were produced as waste. They hypothesized that if aryliodine **26** can be reoxidized to the hypervalent aryl-λ^3-iodane **28** during the reaction, only a catalytic amount of the expensive aryl λ^3-iodane or aryl iodine would be needed. They established a protocol for the *in situ* generation of PIDA (**28**) from phenyliodine **26** using *m*-chloroperoxybenzoic acid (*m*CPBA) as the sacrificial oxidant (for catalytic cycle see figure 6b, Introduction) and successfully employed this approach in the catalytic α-acetoxylation of ketone **114** (scheme 14). This concept proved to be not only the door opener for catalytic reactions but more importantly improved the applicability of

enantioselective reactions. Since no isolation of the reactive hypervalent iodane species is needed, complex chiral aryliodine structures could be employed without the need for tedious pre-synthesis, advancing the enantioselective approaches greatly.

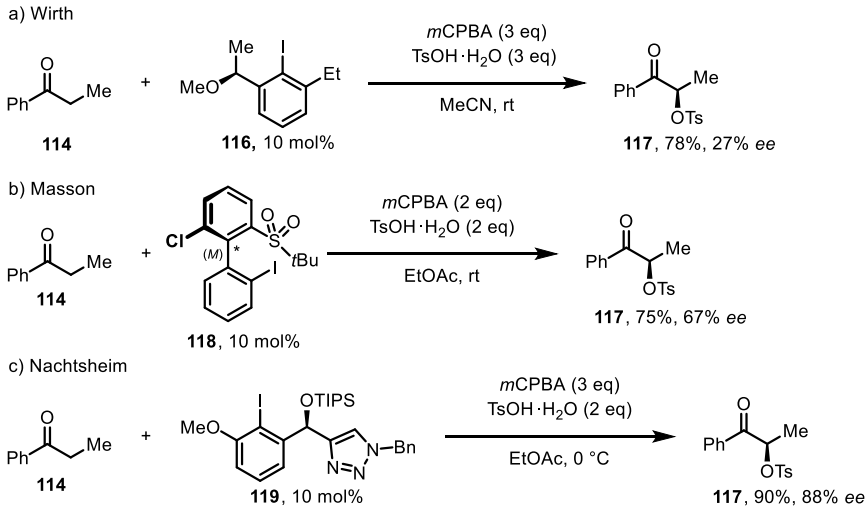

*Scheme 15: Catalytic and enantioselective α-tosylations of ketone **114**.*

The first catalytic and enantioselective α-functionalization of ketones with hypervalent iodane mediators was achieved by the Wirth group (scheme 15a).[94] By installing a chiral side chain in vicinity to the iodine center of compound **116** they were able to induce enantioselectivity into the tosylation reaction to obtain product **117** in 27% enantiomeric excess (*ee*). The *in situ* generation of the reactive hypervalent species improved the applicability of the chiral catalyst immensely, as the pre-synthesis of the oxidized Koser's-reagent-type derivative of aryliodine **116** is rather demanding.[95] Masson *et al.*[96] took another path and utilized the axial chirality of aryliodine **118** to improve the *ee* to 67% (scheme 15b). They were also able to α-phosphoryloxylate ketones enantioselectively under similar condition with similar *ee*, although stoichiometric amounts of the iodoarene **118** were needed. Nachtsheim *et al.*[97] concluded the race for higher enantiomeric purity by developing the triazole substituted aryl iodide **119**, which was not only able to give the desired product **117** in an excellent yield of 90% and an *ee* of 88% (scheme 15c), but could further be used in enantioselective phenol dearomatizations, intramolecular oxygenations of ketones and oxidative rearrangement of allylic alcohols.

The *in situ* oxidation is an elegant way to circumvent the difficulties of isolating the hypervalent iodane species for the reactions. Nonetheless, the desired nucleophile still must be incorporated into the λ^3-iodane at some point during the reaction.

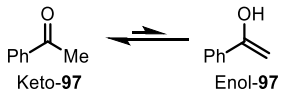

*Scheme 16: Keto enol tautomerism of acetophenone **97**.*

The presence of a protic hydrogen in α-position to the carbonyl function enables the formation of the enol tautomer enol-**97** in small quantities.[98] As this enol is the reactive species necessary for the α-functionalization, trapping the enol form as a silyl enol ether increases the reactivity and by choosing a silyl group with a nucleophilic moiety, nucleophiles can be delivered in an intramolecular fashion.[99]

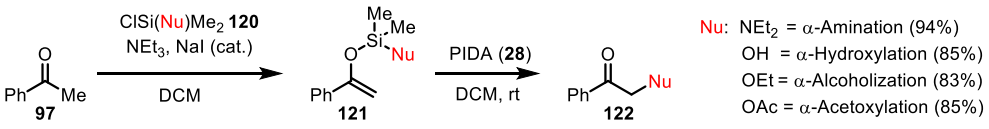

*Scheme 17: α-Functionalization of simple ketone **97** via intramolecular nucleophile delivery.*

Mizar and Wirth[100] adapted this concept for the use in hypervalent iodine chemistry. By transforming ketone **97** to the nucleophile bearing silyl enol ether **121** under basic conditions, they were able to carry out α-aminations, α-hydroxylations, α-alcoholizations and α-acetoxylations (**122**) for a variety of different ketones using just one hypervalent iodane reagent, PIDA (**28**) for all transformations (scheme 17). Furthermore, substituting PIDA (**28**) with a chiral hypervalent iodane reagent led to stereoselective conversion of selected ketones.

Even though nucleophiles can be introduced into the ketone with this method without having to be incorporated into the hypervalent iodane scaffold, the synthesis of the silyl-nucleophile species **120** is not facile and only an intramolecular nucleophile delivery was possible. Nonetheless, preformation of the enol species turned out to be a breakthrough approach for the direct introduction of external and advanced nucleophiles into ketone scaffolds.

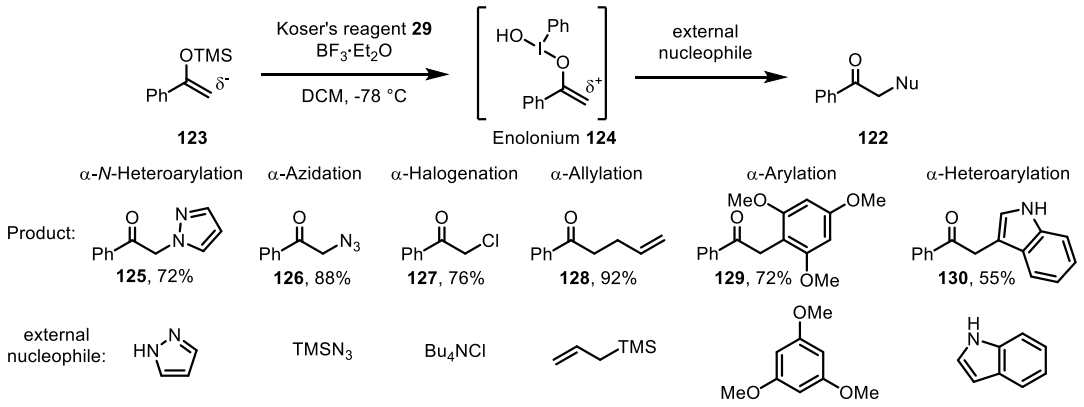

Scheme 18: Approach by Szpilman et al. to introduce external nucleophiles.

Szpilman *et al.* were responsible for a significant advance in recent years in this field. With their in-depth analysis of the conversion of silyl enol ether **123** with Koser's reagent **29** they were the first to characterize the long expected, reactive enolonium species **124** *via* NMR spectroscopy (scheme 18),[101] that was till then only identified by computational studies.[102] This discovery proved, that the addition of the linear hypervalent iodanes to the silyl enol ether go through an oxygen bound hypervalent iodane intermediate rather than through an α-carbon bound species. The immense reactivity of the silyl enol ether with hypervalent iodanes had to be counteracted by lowering the reaction temperature in most reactions to reduce unwanted overoxidation. But once the activity was under control, selective α-functionalizations became possible that were previously inaccessible from simple ketones. With the optimal conditions for the formation of the enolonium species **124** in hand, they were able to introduce a wide variety of external nucleophiles to obtain the ketones **122** in a two-step-one-pot synthesis. α-*N*-heteroarylations (**125**), α-azidations (**126**),[103] α-halogenations (**127**), α-allylations (**128**),[101] α-arylations (**129**) and α-heteroarylations (**130**)[104] were achieved with this method.

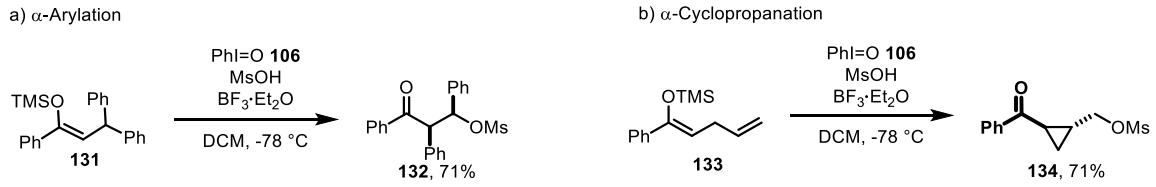

Scheme 19: Examples of intramolecular nucleophiles in the approach with silyl enol ethers.

Maulide *et al.* on the other hand disclosed an intramolecular α-arylation[105] starting from TMS-enol ether (**131**, scheme 19). The reaction of the *in situ* generated mesyl-iodane **99** from iodosobenzene **106** and methanesulfonic acid with the TMS-enol **131** leads to an Umpolung of the polarity at the α-carbon. The subsequent intramolecular, nucleophilic attack at the α-position by the phenyl furnishes a spirocyclic cyclopropane carbocationic derivative that is opened by the mesyl nucleophile to obtain **132**. The reaction of silyl enol ether **133** is similar except that the nucleophilic attack at the α-position is performed by the allylic moiety to furnish the cyclopropane **134** after the nucleophilic ring opening by the mesyl nucleophile.[106]

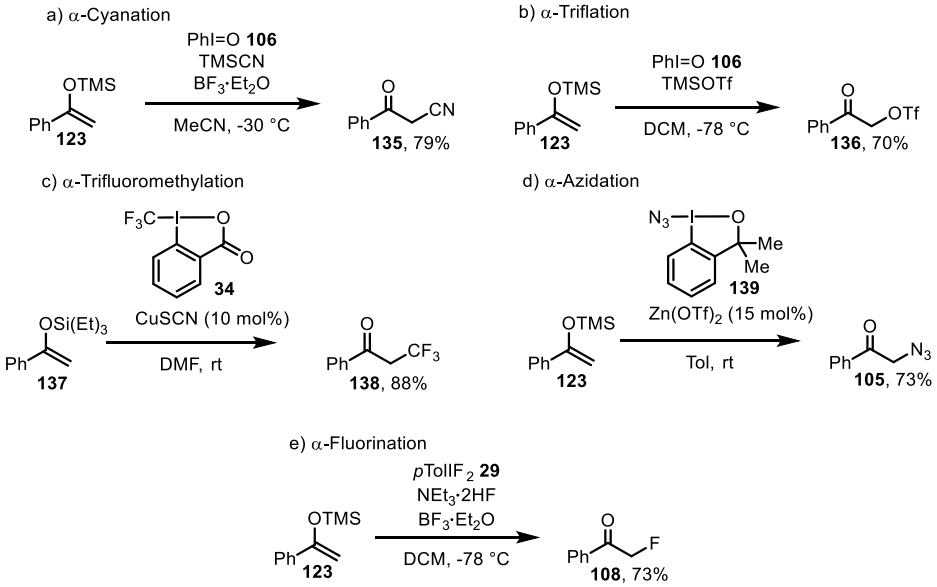

*Scheme 20: Introduction of further nucleophiles into the α-position of silyl enol ether **123**.*

Additionally, α-functionalizations can be carried out with silyl enol ether that were previously inaccessible from simple ketones (scheme 20). The direct α-cyanation[107] as well as the α-triflation[108] was accomplished by *in situ* generation of the needed hypervalent iodane species from iodosobenzene **106** and TMSCN or TMSOTf respectively and the silyl enol ether **123** converted to the ketones **135** and **136**. Furthermore, direct α-trifluoromethylations (**138**),[109] α-azidations (**105**),[92] and α-fluorinations (**108**)[110] became accessible with this concept under mild conditions.

In conclusion, simple ketones can be directly α-functionalized with a small selection of hypervalent λ^3-iodane mediators and preforming the respective silyl enol ether further opened the door for a broad scope of external or intramolecular nucleophiles to be introduced in a mild and selective manner. Nonetheless, preformation of the silyl enol ether and the careful selection of ketones with only one accessible α-position are still considerable limitations for the introduction of nucleophiles.

2.3 Non-Covalent Coordination in λ^3-Iodanes

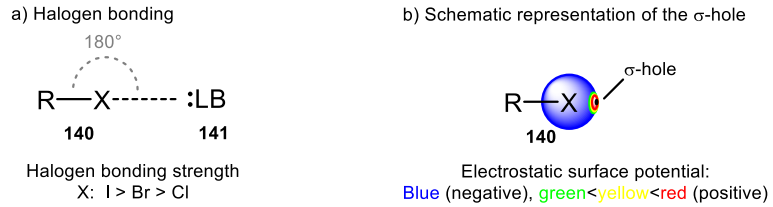

Figure 10: Schematic representations of a) halogen bonding and b) the σ-hole in halogen-containing molecules.

Halogen-containing molecules (**140**, figure 10a) demonstrate a rather interesting effect in combination with Lewis bases (**141**, LB). There appears to be a non-covalent attraction between the negative polarized halogen X and the electron donating molecule.[111] The strength of this halogen bonding is dependent on the respective halogen and increases from chlorine to bromine to iodine. Furthermore, it possesses an almost perfect 180° directionality from the molecule-halogen σ-bond. Extensive computational studies[112] established the source of the unexpected interaction to be an area of positive electrostatic potential on the outer surface of the halogen while the rest of the halogen surface is negative (figure 10b). This σ-hole is located on the extension of the molecule-halogen σ-bond, explaining the high directionality.[112-113]

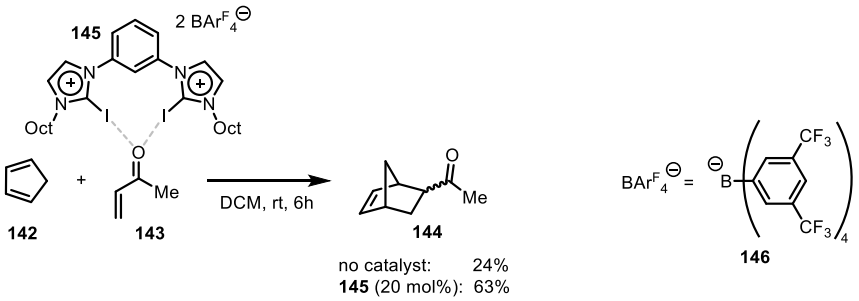

Scheme 21: Halogen bonding catalyzed Diels-Alder reaction.

Uses of halogen bonding in organo-catalysis are scarce, but have experienced an increase in interest in recent years.[114] One application was discovered by Huber *et al*.[115] in the catalyzation of a Diels-Alder reaction between cyclopentadiene (**142**, scheme 21) and methyl vinyl ketone **143**. The carbonyl compound **143** is activated through halogen bonding of the oxygen to the two iodine atoms of a dicationic imidazolium-based catalyst **145**. The yield of product **144** increased significantly to 63% when the catalyst **145** was present compared to 24% yield without any catalyst. Since halogen bonding is a rather weak interaction similar to hydrogen bonding, they had to use a bulky, non-coordinating counterion **146** and carried out multiple control experiments to confirm, that the activation was in fact caused by an oxygen-iodine coordination. They were also able to exploit this approach in the catalyzation of a Michael-addition.[116] Furthermore, Huber *et al*. demonstrated that halogen bonding is not exclusive to monovalent halogenated molecules **140** by applying the hypervalent diaryl iodonium compound (**147**, figure 11a) as an organocatalyst for the activation of the carbonyl **143** in the Diels-Alder reaction.[117]

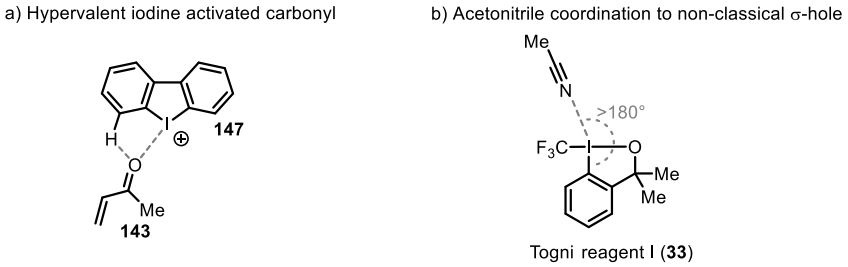

Figure 11: Examples of halogen bonding in hypervalent iodane compounds.

Lüthi *et al.* focused their DFT calculations on λ^3-iodanes and discovered that they also possess a σ-hole located in the plane defined by the 3-center 4-electron bond.[118] However, its location is not restricted to the extension of the σ-bond between the aromatic ligand and the iodine and heavily influenced by the present ligands.[119] Based on these deviations, they are called non-classical σ-holes. The strength of the coordination to these non-classical σ-holes by solvent molecules, as shown in the non-covalent interaction of acetonitrile to Togni reagent I (**33**, figure 11b) or nucleophiles can be linked to the reactivity of the respective λ^3-iodanes.[120] While studies into these electrostatic interactions were done mostly by computational methods, Togni *et al.* were able to support this concept by NMR-spectroscopic findings.[121]

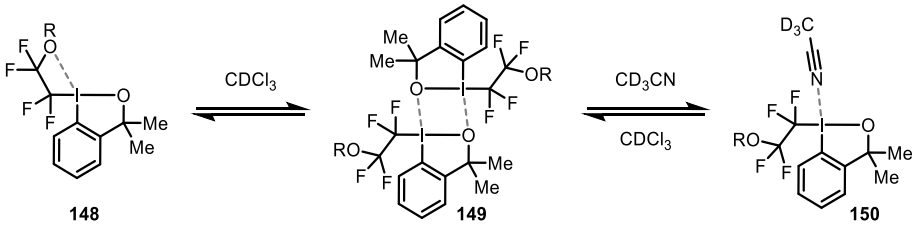

*Scheme 22: Suggested solvent-dependent equilibria of perfluoroalkylated cyclic hypervalent iodane **148**.*

The conformation of the perfluoroalkylated cyclic hypervalent iodane (**148**, scheme 22) is heavily influenced by the present solvent. The NMR-spectroscopic data suggests an equilibrium between the intramolecular coordinated structure **148**, confirmed by crystal structure, the dimeric **149** in the non-nucleophilic solvent chloroform, similar to the by Legault observed crystal structure of the *F*-iodane **35**,[51] and the intermolecularly ligated form **150** in acetonitrile.

Besides these σ-hole interactions, non-covalent coordination of pyridine in hypervalent iodanes has been known and utilized for quite some time. Weiss and Seubert discovered in 1994[122] that the pyridyl-complex (**151**, scheme 23a), now known as Weiss' reagent can be obtained by letting PIDA (**28**) react with TMS triflate and pyridine **1**. Experimental and computational studies carried out by the Dutton group gave a deeper insight into the present bonding between the N and I in reagent **151**. Their conclusion was, that the bond is best described by a coordinative, dative bond between the pyridine ligands and the iodine center with a formal charge of +2.[123] This result suggests a strong affiliation of Weiss' reagent (**151)** to transition metal complexes compared to the previously presented λ^3-iodanes with covalent ligand bonds.[124] It is therefore not surprising that the main application of reagent **151** is as a strong oxidant and not as a nucleophile deliverer.

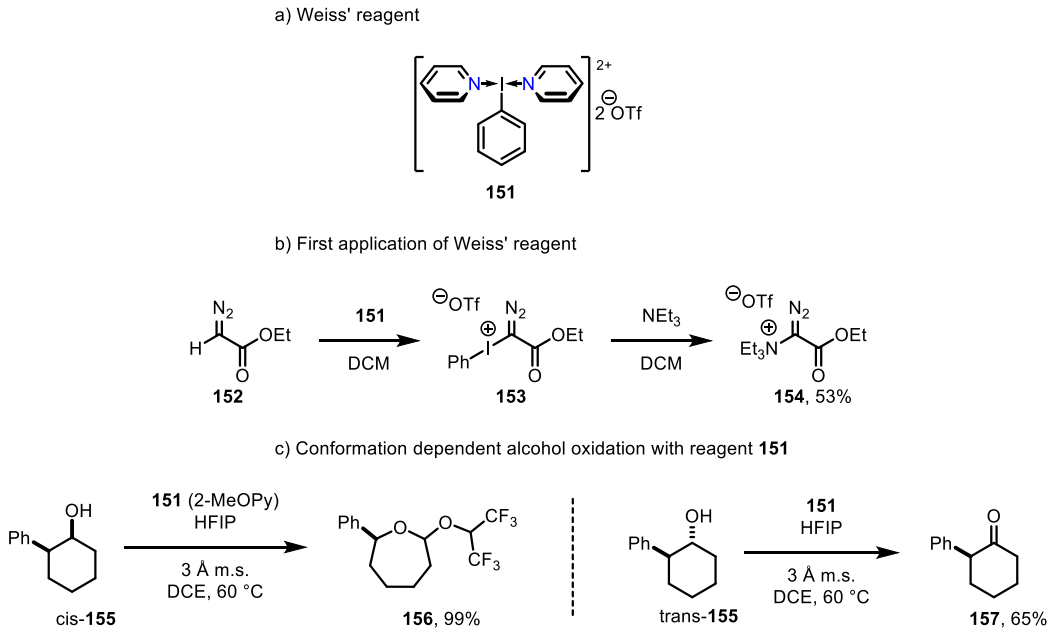

*Scheme 23: Weiss' reagent (**151**) and selected applications in organic synthesis.*

The first use of Weiss' reagent (**151**) was the α-functionalization of diazo compounds **152** (scheme 23b).[125] The electrophilic iodine center is attacked by the diazocarbon to form the α-aryliodonium diazo compound **153**. A nucleophilic attack to substitute the highly nucleofuge aryliodonium moiety leads to the respective salt **154**. Since a formal nucleophile-nucleophile reaction took place, it can once again be classified as an Umpolung reaction. Zhdankin *et al.*[126] discovered that this method is not exclusive to diazo compounds and demonstrated the use of reagent **151** to functionalize phosphonium ylides in a similar reaction pattern. Although there have been further examples of pyridine ligated hypervalent iodine complexes, e.g. the use of a 4-DMAP ligated derivative of **151** as competent oxidants for hetero and homo azo coupling reactions by the Huber group,[127] applications in organic synthesis were still scarce until Wengryniuk *et al*. realized that the absence of a competing nucleophile and the relatively high oxidation potential[128] of reagent **151** render it a suitable reagent for selective and mild oxidation of alcohols in ring expansion reactions or to ketones (scheme 23c). Depending on the conformation of the secondary alcohols **155**, either an oxidative ring-expansion reaction to product **156** was achieved with an adapted 2-MeO-pyridine ligated derivative of reagent **151** starting from alcohol cis-**155**, or an oxidation to the ketone **157** with Weiss' reagent **151** and alcohol trans-**155**.[129] They also expanded the scope of Weiss' reagent (**151**) in additional alcohol oxidation reactions.[130]

Furthermore, Weiss' reagent (**151**) and its derivatives have found applications in inorganic and organometallic chemistry. In contrast to its employment in organic synthesis, transfer of the respective pyridine ligands in combination with an oxidation of the metallic center is here the main mode of reactivity.[131]

The cyclic hypervalent iodine complex (**158**, figure 12) was synthesized by Zhdankin *et al.* in 2002,[132] confirming that the nitrogen ligand coordination concept can be transferred to cyclic hypervalent iodanes.

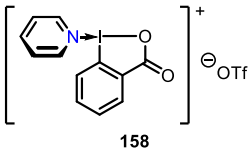

*Figure 12: Structure of the cyclic hypervalent iodine pyridine complex **158**.*

Although charged complexes with pyridine were achieved and used in various oxidation approaches, utilizing a non-covalent interaction between a pyridine and a neutral hypervalent iodane species remained severely underexplored. There are only two examples to our knowledge, where a coordination between the pyridine and an λ^3-iodane might occur and influence the reactivity (scheme 24).

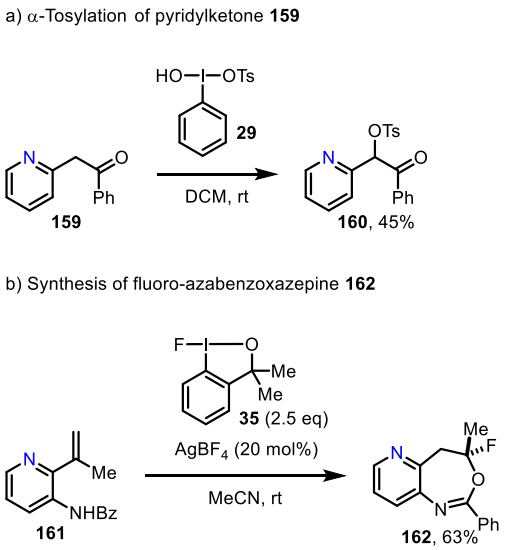

Scheme 24: Reactions with possible coordination between pyridine and the hypervalent iodane reagent.

The susceptibility of pyridylketones **159** towards oxidation and functionalization by hypervalent iodane reagents was shown by the Wells group in 1994.[133] They were able to α-tosylate pyridylketone **159** with Koser's reagent (**29**) to ketone **160** (scheme 24a). Their attempts with PIDA and PIFA led to a substantial over-oxidation and the respective diketones were obtained. The scope of successful reactions was severely limited, as they only employed carbonyls with one accessible α-position and were exclusively able to introduce the nucleophile ligand of the hypervalent iodane. Nonetheless, they observed the importance of an unblocked interaction of the pyridine moiety with the λ^3-iodanes. The second example is the conversion of the styrene derivative **161** to the fluoro-azabenzoxazepine **162** (scheme 24b) disclosed by our group.[134] Not only was there the need to activate the *F*-iodane **35** with $AgBF_4$ but more interestingly, 2.5 equivalents of the hypervalent iodane **35** had to be added to give good yields. This finding gave way to the hypothesis, that the Lewis basic nitrogen of the pyridine interacts with the λ^3-iodane **35** and suppresses its reactivity. Although it is a drawback in this approach, a concept to harness this apparent coordination was deemed worthwhile.

3. Goals & Motivation

Hypervalent λ^3-iodanes have proven to be mild and selective oxidizing agents for a wide variety of substrates.[43, 45a] Their application in the α-functionalization of ketones has been extensively studied and the scope of introducible nucleophiles is quite broad.[80] To directly functionalize simple ketones however, the nucleophile must be incorporated into the reactive hypervalent iodane species, which is accompanied by additional synthetic effort and limits the acceptable nucleophiles. The preformation of silyl enol ethers from the ketones made the introduction of external nucleophiles facile, but the usable ketones had to be specifically chosen and the enol formation meant one additional synthetic step. Furthermore, the occurrence of constitutional isomers when converting ketones with two accessible α-positions is still an issue, whose solution has been underdeveloped and new approaches are worth exploring.

One of the most fascinating, new hypervalent λ^3-iodanes is the fluorobenziodoxole (**35**, scheme 25a), discovered in 2012 by Legault and Prévost.[51] Our group has participated in the race for new applications of this easy-to-handle fluorination reagent by demonstrating its chemoselectivity in the conversion of styrene[41] and pyridylstyrene[134] derivatives. The potential of the mild, moisture and air insensitive oxidizing reagent was far from being exploited to completion and so, in contrast to our previous endeavors, the main emphasis of this work was the development of a non-covalent pre-coordination concept to gain control for the selective introduction of external nucleophiles into the desired α-position of ketones. Because pyridine has already demonstrated its affinity towards hypervalent iodane centers[131] and the synthesis of the respective pyridylketones **163** is straightforward and facile[135], it was selected as the suitable Lewis basic directing group for the regioselective α-functionalization of ketones. The hypothesis, that the pyridine of ketone **163** coordinates to the hypervalent iodane **164** and leads to the selective oxidation of the α-position instead of α'-position (**165**) had to be evaluated (scheme 25b). The anticipated subsequent step is the substitution of the highly nucleofuge iodine moiety by an external nucleophile, furnishing the selectively functionalized ketone **166.**

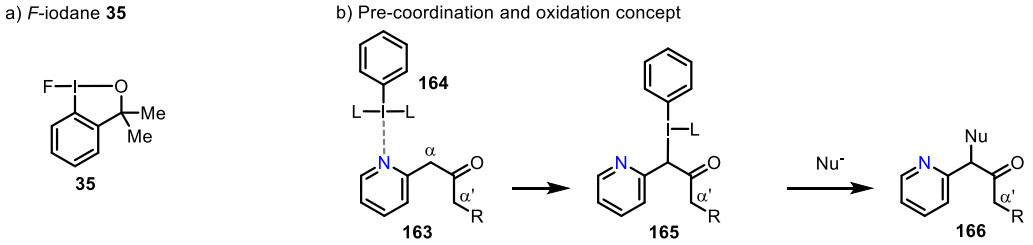

*Scheme 25: a) Structure of F-iodane **35** and b) pre-coordination concept for selective oxidation and nucleophile introduction.*

Within this endeavor the following milestones need to be addressed:

- Transferring the hypothesis of Lewis acid/Lewis base interactions to the hypervalent iodane mediated α-functionalization of ketones
- Evaluation of suitable ketone substrates for pre-coordination concept
- Evaluation of chemoselectivity towards desired α-position
- Execution of experiments for the verification of the hypothesized mechanism

Furthermore, our recently developed method to furnish fluoro-azabenzoxazepines **168** from styrenes **167**[134] offers the possibility for an additional assessment of the applicability of this approach in the selective α-functionalization of ketones. Since the cyclic fluoro-azabenzoxazepines **168** can be opened to the respective ketones **169** and transformed to the indoles **170** in two separate steps, inquiries into intercepting the ketone **169** and subsequently converting it to the α-functionalized ketone **171** are of high interest and would validate the hypothesized pre-coordination concept for selective oxidation and nucleophile introduction using pyridine and *F*-iodane **35**.

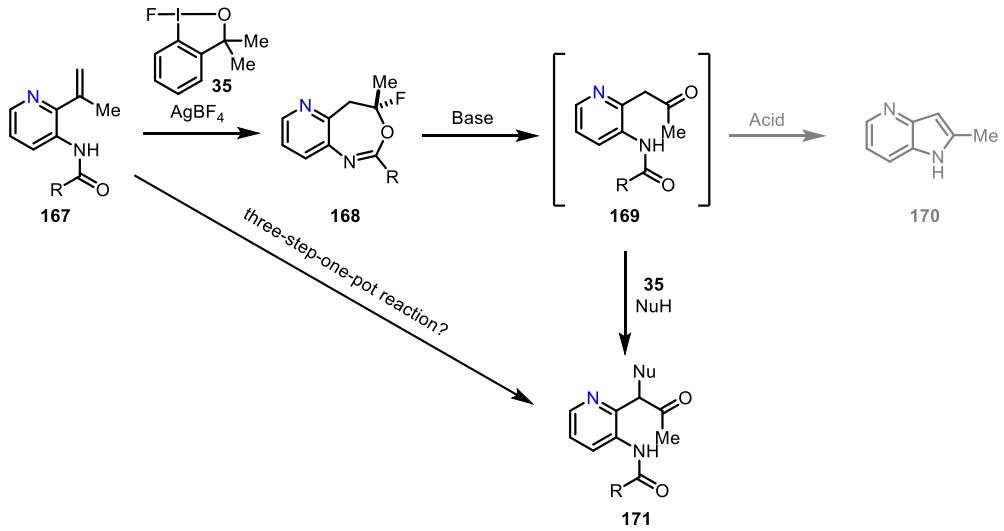

*Scheme 26: Theoretical, synthetic pathway to the desired α-functionalized product **171** starting from pyridylstyrene **167**.*

The following goals are emphasized:

- Evaluation of the transferability of the pre-coordination concept to pyridylstyrenes **167**
- Development of one-pot method for the introduction of nucleophiles into the ketone scaffolds
- Uncovering the mechanistic pathway present by executing the approach step by step
- In depth analysis of substrate dependent reactivity

II. Results & Discussion

1. Hypervalent Iodane Triggered Umpolung of Ketones

G. M. Kiefl, T. Gulder, α-Functionalization of Ketones via a Nitrogen Directed Oxidative Umpolung; *J. Am. Chem. Soc.* **2020**, *142*, 20577-20582.[136]

The hypervalent λ^3-*F*-iodane **35** has seen a great interest in recent years with fluorinations, fluorocyclizations and traceless directing approaches being disclosed [41, 53, 58, 60-68, 70-73, 90, 134, 137] showing its fascinating and unique reactivity and selectivity. Especially the uncovering of the hypervalent fluoroiodane-triggered synthesis of fluoro-azabenzoxazepines and azaindoles[134] by our group drew the focus on the apparent non-covalent interaction of Lewis basic pyridines with the hypervalent iodane **35**. Realizing that applying a pre-coordination concept in the α-functionalization of ketones via hypervalent iodane mediation could potentially combat the problem of regioisomerism, an intricate investigation was carried out. The Wells group had already done preliminary work on the oxidation of substituted pyridines with hypervalent iodane reagents in 1994[133] but were limited to internal nucleophiles and had serious problems with overoxidation.

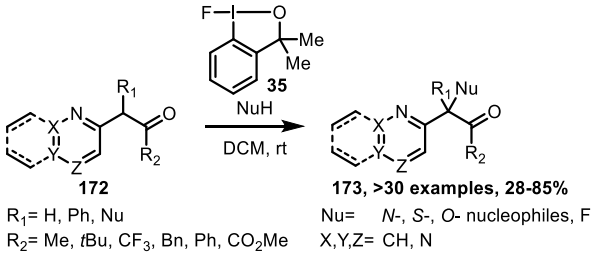

*Scheme 27: General reaction scheme for the nitrogen directed oxidative Umpolung of ketones **172**.*

The exchange of the polar acetonitrile, previously the solvent of choice in our group for reactions with *F*-iodane **35**, to dichloromethane (DCM) resolved the issue of the competitive solvent coordination with the hypervalent iodane **35**, that suppressed the reaction completely at first. Using a small excess of ketone (**172**, scheme 27) and 3 equivalents of a nucleophile turned out to be the optimum conditions for the selective introduction of a wide variety of external, protic *N*-, *S*-, *O*- nucleophiles such as triazoles, thiols, sulfonic and carboxylic acids into the α-position of 2-pyridylketones **172** to furnish the α-functionalized ketones **173**. The room temperature and moisture insensitive procedure was established for a plethora of ketones **172** with various substitution patterns. A nitrogen in the ortho-position of the aromatic moiety was preconditional, but the enamide as carbonyl surrogate was well tolerated and no enol-preformation was necessary for the successful conversion. Furthermore, direct fluorination was achieved after overcoming the instability and decomposition problem of α-mono-fluorinated ketones with an additional acidic proton in the α-position. Reducing the ketones to the respective alcohols *in situ* or using α-disubstituted substrates was the key to obtain stable and isolable fluoro products. First mechanistic investigations suggest an essential electrostatic interaction between the pyridine and the *F*-iodane **35**.

JACS
JOURNAL OF THE AMERICAN CHEMICAL SOCIETY
pubs.acs.org/JACS
Communication

α-Functionalization of Ketones via a Nitrogen Directed Oxidative Umpolung

Gabriel M. Kiefl and Tanja Gulder*

Cite This: J. Am. Chem. Soc. 2020, 142, 20577−20582
Read Online
ACCESS | Metrics & More | Article Recommendations | Supporting Information

ABSTRACT: Reversing the polarity in molecules is a versatile tool for expanding the boundaries of structural space. Despite a manifold of different umpolung methods available today, overcoming the inherent reactivity still remains a constant challenge in organic chemistry. The oxidative α-functionalization of ketones by external nucleophiles constitute such an example. Herein, we present a hypervalent *F*-iodane mediated umpolung of pyridyl ketones triggered by Lewis base/Lewis acid noncovalent interactions. A wide variety of external nucleophiles are introduced with high regioselectivity applying this substrate-directing concept.

The α-functionalization of ketones **1** builds a cornerstone in organic synthesis with electrochemical,[1] photoredox,[2] and organocatalytic[3] approaches leading to important recent advances. The intrinsic polarization of ketones **1**, however, offers a nucleophilic (blue, Scheme 1) center at the α-position that determines the inherent reactivity and thus limits the addressable transformations of reactions employing electrophiles (red, Scheme 1a). The umpolung concept (Scheme 1b), originally coined by Seebach and Corey for reversing the reactivity at acyl C atoms,[4] has led to a tremendous expansion of the reaction scope entering new structural territory not accessible with conventional methods. Reversing the polarity of carbonyl compounds[5] can be accomplished with the help of various mediators, such as simple halogens,[6] hypervalent iodanes,[7] Lewis acids,[8] and transition-metal catalysts.[9]

The first hypervalent iodane triggered umpolung of ketones **1** was described already in 1978 by Mizukami et al.[10] Applying this concept, a multitude of functional groups[11,12] have been transferred ranging from acetoxylations[10] to azidations[11f] and halogenations[11e] to date. However, when using ketones **1**, the nucleophile must be bound directly to the hypervalent iodane reagent in most cases. This is associated with an enormous synthetic effort and restricts the scope of this method to the transfer of a few selected nucleophiles that are able to form chemically stable and isolable λ^3-hypervalent iodane reagents **2**. The preformation of the enol species as a silyl enol ether or Ir enolate **3** proved to be an elegant solution to this limitation and opened the door for applying external nucleophiles. α-Aminations,[13] cyanations,[14] azidations,[15] (hetero)arylation,[16] and cyclopropanation[17] of premodified ketones have thus become available (Scheme 1b).

Despite this tremendous progress, specific enol formation, no matter whether in situ or beforehand, constitutes still a limiting factor, as regiocontrol is difficult to achieve if more than one enolizable C atoms are present.[12a] The Martín-Matute group recently reported on an elegant attempt to overcome this issue by generating an Ir-enolate via isomerization of ally alcohols.[18]

Given our interest in λ^3-hypervalent *F*-iodane mediated reactions together with the use of fluorine atoms as traceless

Scheme 1. General Concepts for the Oxidative α Functionalization of Carbonyls

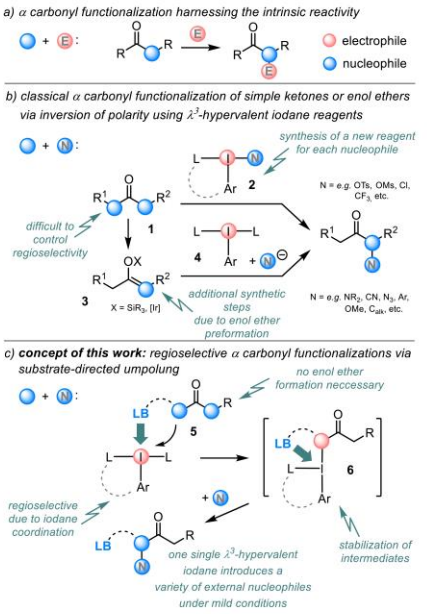

Received: October 8, 2020
Published: November 24, 2020

https://dx.doi.org/10.1021/jacs.0c10700
J. Am. Chem. Soc. 2020, 142, 20577−20582

directing groups to trigger unusal reactivity,[19] we were wondering if the problem of regioisomerism in the α-functionalization of ketones can be overcome by precoordination of the hypervalent iodane to a specific site of the substrate. The substrate-directed, now intramolecular nucleophilic addition of the enol to the electrophilic iodane furnishes regioselectively intermediate **6** which exhibits a reversed polarity compared to **5**. Displacement of the hypervalent iodane hyperfug by an external nucleophile yields the target compound in a proximity driven reaction/intermediate stabilization event. In particular fluorine containing iodanes, such as **16** and **17**, show significant secondary bonding between the iodine atom and intra- **7** and intermolecular nucleophiles **8** (Scheme 2).[20]

Scheme 2. Literature Examples of Inter- and Intramolecular Noncovalent Interactions of Lewis Basic Groups and λ^3-Hypervalent Iodane Reagents[19,21]

Inspired by the preliminary work of the Wells group in 1994,[21] we chose pyridines as the Lewis-basic, directing element in our investigations. Its coordinating characteristics with hypervalent iodane atoms is impressively exemplified by the Weiss reagent (**9**).[22] In addition, the pyridyl ring is among the most important structural motifs in bioactive compounds,[23] making the exploration of new functionalization pathways highly desirable.

We set out to explore our substrate-directing λ^3-hypervalent iodane mediated umpolung of pyridyl ketones **10** that is devoid of any enol preformation and allows the application of external nucleophiles. The model reaction was performed in the noncoordinating solvent DCM in order to avoid competitive interactions. Screening of several λ^3-hypervalent iodane reagents **13**–**17** (Table 1) disclosed both the linear **16** and the cyclic *F*-iodane **17**[24] as superior. Product **12a** was formed as a single regioisomer in 53% and 55% yield, respectively. The reagents **13**–**15** which have previously been the gold standard in such umpolung reactions failed. PIFA (**13**) and Koser's reagent (**14**) led to an instantaneous decomposition even at lower temperatures, while the less oxidative PIDA (**15**) gave a 1:2 mixture of the target compound **12a** and the corresponding acetoxy derivative **12g**. Since **17** is, in general, easier to handle than **16**, all further optimizations were carried out with the cyclic *F*-benziodoxole **17**. Variations of the reaction conditions, such as changing the temperature or the solvent, did not improve the reaction outcome (cf. the Supporting Information (SI)). Adjusting the ratio of **17** (0.91 equiv) and **11** (3 equiv) abolished the formation of *N*,*N*-disubstituted product and thus increased the yield to 72% (66% isolated yield).

It is noteworthy that the use of MeCN (Table 1, entry 7), which has been the optimum medium in all fluoro functionalizations employing **17** hitherto reported by our group,[19] failed completely. This supports our hypothesis of a noncovalent interaction between the pyridyl ketone **10a** and the electron-deficient iodine atom in **17** being decisive for a successful conversion. With MeCN another, yet competitive Lewis basic compound was added in huge quantities to the reaction mixture and thus significantly inhibits pyridine-**17** coordination by forming an MeCN-**17** complex instead. Their

Table 1. Optimization of the Reaction Conditions[a]

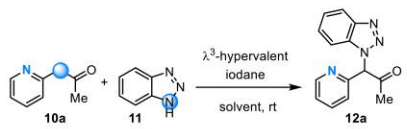

entry	iodane	equiv of **11**	solvent	yield **12a**[b]
1	**13**	1.1	DCM	<5%
2	**14**	1.1	DCM	<5%
3	**15**	1.1	DCM	25%[c]
4	**16**	1.1	DCM	53%
5	**17**	1.1	DCM	55%
6	**17**	3.0	DCM	72%/66%[c]
7	**17**	1.1	MeCN	<5%

[a]**12a** was isolated as a 1:99 mixture of ketone and enol form. [b]Yield determined from the ^{1}H NMR spectrum. [c]Isolated yield.

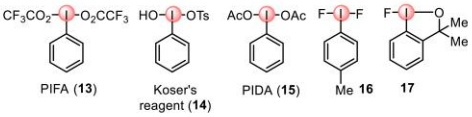

existence has been described by Togni and Lüthi for other *F*-benziodoxole compounds (see **8** in Scheme 2).[20]

Our mechanistic proposal was further verified by positioning the interacting nucleophilic entity at the *meta* **10b** or *para* position **10c** of the pyridine ring or using the benzyl analog **18** devoid of the strong Lewis basic site (Scheme 3). In all cases no

Scheme 3. Preliminary Studies on the Role of the Pyridyl Nitrogen

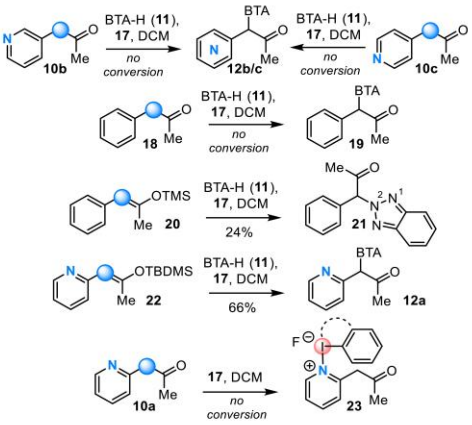

conversion was detected. Only the activated benzyl silyl enol ether **20** showed some turnover. Interestingly, here BAT-H (**11**) solely attacked with its N-2 and not with the N-1 atom as observed for all pyridyl ketones **10**. The corresponding N-2 addition product **21** was isolated in 24% yield. In contrast, when using the *o*-pyridyl enol ether **22** no difference in the chemical yield of the obtained addition product **12a** was detected (66%). Overall, these preliminary mechanistic studies emphasize the

https://dx.doi.org/10.1021/jacs.0c10700
J. Am. Chem. Soc. 2020, 142, 20577−20582

importance of the presence and the position of the Lewis basic nitrogen atom *ortho* to the acidic *C*−*H* functionality and thus corroborate its role as a directing (**5**, see Scheme 1c) and intermediate stabilizing group (**6**, Scheme 1c). A reaction proceeding via an in situ formed pyridinium species such as **23** can be ruled out as treating ketone **10a** solely with **17** delivered almost quantitatively untouched starting materials **10a** and **17**.

Scheme 4. (a) α Functionalizations of Pyridyl Ketone 10a with Varying External Nucleophiles and (b) Ligand Exchange Forming 24 versus H-Bonding Interactions of 11 and 17[a]

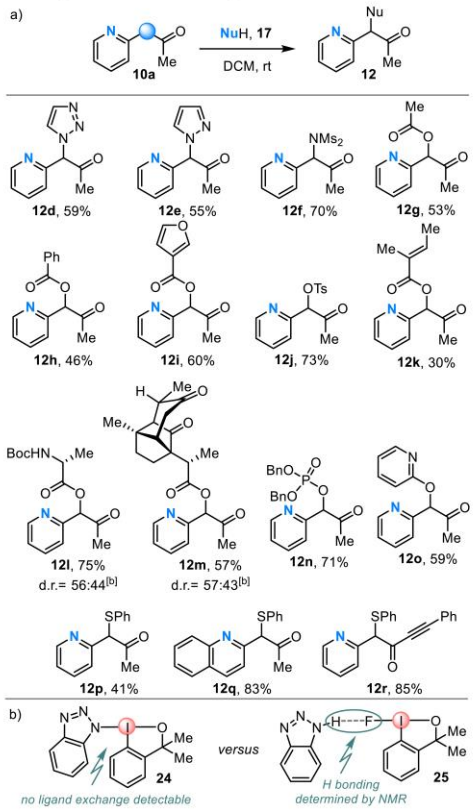

[a]**10a** (0.11 mmol), **17** (0.10 mmol), and NuH (0.30 mmol) were stirred in distilled DCM (0.2 M). **12d,e,j** were isolated in both tautomeric forms, the ketone and the enol. [b]d.r. was determined from the ^{1}H NMR spectrum of the crude mixture.

Next, we turned our attention to the versatility of our developed procedure. The method showed a remarkably broad variety in the external nucleophile (Scheme 4). Besides different *N*-nucleophiles, such as heterocycles (→ **12d** and **12e**) and sulfonamides (→ **12f**), a wide range of structurally different *O*- and *S*-nucleophiles were selectively installed giving the products **12g**−**12r** in good to excellent 30−85% yields. The mildness of the method accounted for the tolerance of multiple, even oxidation sensitive functional groups such as alkenes, alkynes, furans, carbamates and phosphates. The method can also be extended to structurally more complex and/or chiral structures as showcased by the amino acid alanine (→**12l**) and santonic acid (→**12m**). No racemization of the existing stereogenic centers occurred and even extra acidic C−H groups were well accepted.

To our surprise, we found out that only nucleophiles exhibiting an acidic proton were successfully implemented in this transformation (for failed nucleophiles, see the SI). NMR spectra obtained from the titration of iodane **17** with increasing amounts of BTA-H (**11**) showed a significant upfield shift of the *N*-1 proton signal in **11** and simultaneously a downfield shift of the *F* resonance in **17** (cf. SI for spectra). Both observations provide evidence for an H-bonding interaction like **25** which activates the BTA-H nucleophile (**11**) and at the same time the iodine(III) atom in **17**. Basic aqueous workup of these mixtures led to the recovery of both substrates **11** and **17** in quantitative yields thus excluding a likewise possible umpolung of the BTA moiety by generating a BTA-benziodoxole **24** in situ via ligand exchange (Scheme 4b).

Thorough analysis of the crude reaction mixture revealed that small amounts (5−14%) of α fluorinated side products were built if carboxylic acids served as external nucleophiles (cf. in Scheme 4). Since fluorinated compounds are, in general, extremely valuable substances whose applications range from pharmacy,[25] medical diagnostics,[26] agrochemistry[27] to materials science,[28] we thought changing our protocol to yield selectively the fluorinated ketones **12** would be worthwhile. Addition of pyridine HF to increase the concentration of fluoride and at the same time activate the F-iodane **17** via H-bonding gave the optimum conditions for forming the *F*-ketones. Their isolation, however, was impossible due to decomposition if an acidic proton was present in α-position.[29] Changing the substrate to α-disubstituted ketones **10s**−**10v** solved this problem and furnished the target compounds **12s**−**12v** in 56%−68%. Equipping the pyridine with substituents adjacent to the Lewis basic pyridine nitrogen proved to be an excellent approach, too. The synthesis of the desired fluorinated products, which were isolated as the alcohols **26a** and **26b** due to the chemical instability of the corresponding ketones in 47% and 70% yield

Scheme 5. α Fluorinations of Pyridyl Ketones 10

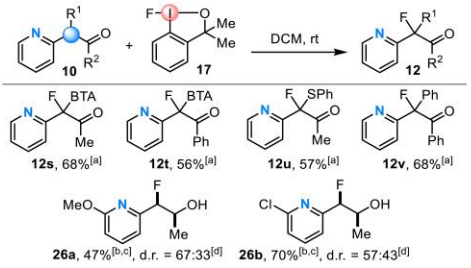

[a]**10** (0.20 mmol), **17** (0.20 mmol), and pyridine HF (0.60 mmol) were stirred in anhydrous DCM (0.2 M) in a Teflon vial. [b]**10** (0.20 mmol) and **17** (0.20 mmol) were stirred in anhydrous DCM (0.2 M). 1.00 mL MeOH and $NaBH_4$ (1.00 mmol) were added. [c]Yield over two steps. [d]d.r. was determined from the ^{1}H NMR spectrum of the crude mixture.

https://dx.doi.org/10.1021/jacs.0c10700
J. Am. Chem. Soc. 2020, 142, 20577−20582

(over two steps) was accomplished even without additional HF (Scheme 5).

The method also turned out to be highly flexible upon structural variations at the ketone **10**. In all cases, oxidative functionalization of **10** proceeded regio- and chemoselectively with up to 81% yield (Scheme 6), with preconditional a N atom

Scheme 6. Oxidative α Functionalizations of Various Ketones 10[a]

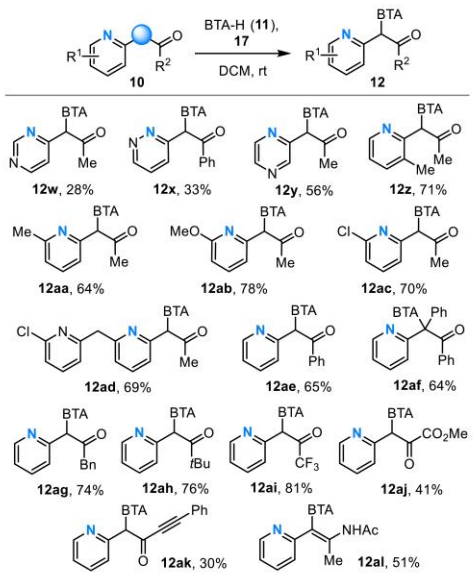

[a]**10** (0.11 mmol), **17** (0.10 mmol), and **11** (0.30 mmol) were stirred in distilled DCM (0.2 M). **12y,z,ab,ac,ae,ah** were isolated in both tautomeric forms, the ketone and the enol.

in the *ortho* position. Besides other *N*-heterocycles, different substituents at the pyridine were equally well accepted. Here again, the reaction clearly benefited from an increase of the electron density at the pyridine nitrogen evidenced by a significant rate acceleration. The range of tolerated substituents at the other site of the carbonyl (R^2) span from alkyl, aryl, and even benzyl portions to alkynyl and electron-withdrawing fragments, such as CF_3 or esters. The enamide **10al** was converted to product **12al** as well indicating that carbonyl surrogates are likewise applicable.

In summary, we established an as yet unprecedented and efficient synthetic strategy for the oxidative umpolung of ketones **10**. To realize our goal, we combined the unusual reactivity triggered by hypervalent *F*-iodanes[30] and the directing, activating, and stabilizing properties of the pyridine moiety. The addition of nucleophiles to the α-position of ketones **10** only takes place with 2-pyridyl substrates, in the presence of the hypervalent fluoro iodane **17**. Preliminary mechanistic investigations unambiguously showed that the pyridine ring in **10** and the λ^3-fluoro iodane **17** are causally related and this relationship can, most likely, be attributed to a noncovalent electrostatic interaction (halogen bonding). The power of this concept was demonstrated by the synthesis of over 30 α-functionalized ketones **12** with no relevant background reactions observed. Further investigations on the underlying complex principles operative here and the extension of this concept to other reaction types are currently underway in our laboratory.

■ ASSOCIATED CONTENT

Supporting Information

The Supporting Information is available free of charge at https://pubs.acs.org/doi/10.1021/jacs.0c10700.

NMR spectra of compounds **12a−al**, **21**, and **26a,b** (PDF)

Additional studies, experimental procedures, and compound characterization (PDF)

■ AUTHOR INFORMATION

Corresponding Author

Tanja Gulder − *Department of Chemistry, Technical University Munich, 85748 Garching, Germany; Institute of Organic Chemistry, Leipzig University, 04103 Leipzig, Germany;* orcid.org/0000-0003-4870-2266; Email: tanja.gulder@uni-leipzig.de

Author

Gabriel M. Kiefl − *Department of Chemistry, Technical University Munich, 85748 Garching, Germany*

Complete contact information is available at: https://pubs.acs.org/10.1021/jacs.0c10700

Notes

The authors declare no competing financial interest.

■ ACKNOWLEDGMENTS

This work was funded by the Emmy-Noether (GU 1134/3) and Heisenberg program (GU 1134/4) of the DFG and is in memory of Prof. Kilian Muñiz.

■ REFERENCES

(1) Liang, S.; Xu, K.; Zeng, C.-C.; Tian, H.-Y.; Sun, B.-G. Recent Advances in the Electrochemical α-C−H Bond Functionalization of Carbonyl Compounds. *Adv. Synth. Catal.* **2018**, *360*, 4266−4292.

(2) Liu, Y.; Dong, W. Functionalization of Carbonyl Compounds via Photoredox Organocatalysis. *Chin. J. Chem.* **2017**, *35*, 1491−1500.

(3) (a) Guillena, G. α-Heteroatom Functionalization of Carbonyl Compounds. In *Comprehensive Enantioselective Organocatalysis*; Dalko, P. I., Ed.; 2013; pp 757−790. (b) Lee, H.-E.; Kim, D.; You, A.; Park, M. H.; Kim, M.; Kim, C. Transition Metal-Catalyzed α-Position Carbon−Carbon Bond Formations of Carbonyl Derivatives. *Catalysts* **2020**, *10*, 861.

(4) (a) Seebach, D.; Corey, E. J. Generation and synthetic applications of 2-lithio-1,3-dithianes. *J. Org. Chem.* **1975**, *40*, 231−237. (b) Seebach, D. Methods of Reactivity Umpolung. *Angew. Chem., Int. Ed. Engl.* **1979**, *18*, 239−258.

(5) Miyata, O.; Miyoshi, T.; Ueda, M. Umpolung reaction at the α-carbon position of carbonyl compounds. *ARKIVOC* **2013**, *2013*, 60−81.

(6) Erian, A. W.; Sherif, S. M.; Gaber, H. M. The Chemistry of α-Haloketones and Their Utility in Heterocyclic Synthesis. *Molecules* **2003**, *8*, 793−865.

(7) (a) Merritt, E.; Olofsson, B. α-Functionalization of Carbonyl Compounds Using Hypervalent Iodine Reagents. *Synthesis* **2011**, *2011*, 517−538. (b) Hyatt, I. F. D.; Dave, L.; David, N.; Kaur, K.; Medard, M.; Mowdawalla, C. Hypervalent iodine reactions utilized in carbon-carbon bond formations. *Org. Biomol. Chem.* **2019**, *17*, 7822−7848. (c) Dong,

https://dx.doi.org/10.1021/jacs.0c10700
J. Am. Chem. Soc. 2020, 142, 20577−20582

D.-Q.; Hao, S.-H.; Wang, Z.-L.; Chen, C. Hypervalent iodine: a powerful electrophile for asymmetric α-functionalization of carbonyl compounds. *Org. Biomol. Chem.* **2014**, *12*, 4278−4289. (d) Yoshimura, A.; Zhdankin, V. V. Advances in Synthetic Applications of Hypervalent Iodine Compounds. *Chem. Rev.* **2016**, *116*, 3328−3435. (e) Zhdankin, V. V.; Stang, P. J. Chemistry of Polyvalent Iodine. *Chem. Rev.* **2008**, *108*, 5299−5358. (f) Hari, D. P.; Caramenti, P.; Waser, J. Cyclic Hypervalent Iodine Reagents: Enabling Tools for Bond Disconnection via Reactivity Umpolung. *Acc. Chem. Res.* **2018**, *51*, 3212−3225.

(8) (a) Wu, Y.-K.; Dunbar, C. R.; McDonald, R.; Ferguson, M. J.; West, F. G. Experimental and Computational Studies on Interrupted Nazarov Reactions: Exploration of Umpolung Reactivity at the α-Carbon of Cyclopentanones. *J. Am. Chem. Soc.* **2014**, *136*, 14903−14911. (b) Miyoshi, T.; Miyakawa, T.; Ueda, M.; Miyata, O. Nucleophilic α-Arylation and α-Alkylation of Ketones by Polarity Inversion of N-Alkoxyenamines: Entry to the Umpolung Reaction at the α-Carbon Position of Carbonyl Compounds. *Angew. Chem., Int. Ed.* **2011**, *50*, 928−931.

(9) Xu, Z.; Chen, H.; Wang, Z.; Ying, A.; Zhang, L. One-Pot Synthesis of Benzene-Fused Medium-Ring Ketones: Gold Catalysis-Enabled Enolate Umpolung Reactivity. *J. Am. Chem. Soc.* **2016**, *138*, 5515−5518.

(10) Mizukami, F.; Ando, M.; Tanaka, T.; Imamura, J. The Acetoxylation of p-Substituted Acetophenones and β-Diketones with (Diacetoxyiodo)benzene. *Bull. Chem. Soc. Jpn.* **1978**, *51*, 335−336.

(11) (a) Lodaya, J. S.; Koser, G. F. Direct α-mesyloxylation of ketones and.beta.-dicarbonyl compounds with [hydroxy(mesyloxy)iodo]-benzene. *J. Org. Chem.* **1988**, *53*, 210−212. (b) Koser, G. F.; Lodaya, J. S.; Ray, D. G.; Kokil, P. B. Direct α-phosphoryloxylation of ketones and (phosphoryloxy)lactonization of pentenoic acids with [hydroxy-[(bis(phenyloxy)phosphoryl)oxy]iodo]benzene. *J. Am. Chem. Soc.* **1988**, *110*, 2987−2988. (c) Koser, G. F.; Relenyi, A. G.; Kalos, A. N.; Rebrovic, L.; Wettach, R. H. One-step α-tosyloxylation of ketones with [hydroxy(tosyloxy)iodo]benzene. *J. Org. Chem.* **1982**, *47*, 2487−2489. (d) Moriarty, R. M.; Hu, H.; Gupta, S. C. Direct α-hydroxylation of ketones using iodosobenzene. *Tetrahedron Lett.* **1981**, *22*, 1283−1286. (e) Geary, G. C.; Hope, E. G.; Singh, K.; Stuart, A. M. Preparation of iodonium ylides: probing the fluorination of 1,3-dicarbonyl compounds with a fluoroiodane. *RSC Adv.* **2015**, *5*, 16501−16506. (f) Lee, J. C.; Kim, S.; Shin, W. C. An Effective Synthesis of α-Azido Ketones From Ketones. *Synth. Commun.* **2000**, *30*, 4271−4275. (g) Kieltsch, I.; Eisenberger, P.; Togni, A. Mild Electrophilic Trifluoromethylation of Carbon- and Sulfur-Centered Nucleophiles by a Hypervalent Iodine-(III)−CF_3 Reagent. *Angew. Chem., Int. Ed.* **2007**, *46*, 754−757.

(12) For selected examples on catalytic variants, see: (a) Ochiai, M.; Takeuchi, Y.; Katayama, T.; Sueda, T.; Miyamoto, K. Iodobenzene-Catalyzed α-Acetoxylation of Ketones. In Situ Generation of Hypervalent (Diacyloxyiodo)benzenes Using m-Chloroperbenzoic Acid. *J. Am. Chem. Soc.* **2005**, *127*, 12244−12245. (b) Richardson, R. D.; Page, T. K.; Altermann, S.; Paradine, S. M.; French, A. N.; Wirth, T. Enantioselective α-Oxytosylation of Ketones Catalysed by Iodoarenes. *Synlett* **2007**, *2007*, 0538−0542. (c) Levitre, G.; Dumoulin, A.; Retailleau, P.; Panossian, A.; Leroux, F. R.; Masson, G. Asymmetric α-Sulfonyl- and α-Phosphoryl-Oxylation of Ketones by a Chiral Hypervalent Iodine(III). *J. Org. Chem.* **2017**, *82*, 11877−11883. (d) Abazid, A. H.; Nachtsheim, B. J. A Triazole-Substituted Aryl Iodide with Omnipotent Reactivity in Enantioselective Oxidations. *Angew. Chem., Int. Ed.* **2020**, *59*, 1479−1484.

(13) Mizar, P.; Wirth, T. Flexible stereoselective functionalizations of ketones through umpolung with hypervalent iodine reagents. *Angew. Chem., Int. Ed.* **2014**, *53*, 5993−5997.

(14) Shen, H.; Li, J.; Liu, Q.; Pan, J.; Huang, R.; Xiong, Y. Umpolung Strategy for Synthesis of β-Ketonitriles through Hypervalent Iodine-Promoted Cyanation of Silyl Enol Ethers. *J. Org. Chem.* **2015**, *80*, 7212−7218.

(15) Vita, M. V.; Waser, J. Azidation of β-Keto Esters and Silyl Enol Ethers with a Benziodoxole Reagent. *Org. Lett.* **2013**, *15*, 3246−3249.

(16) (a) More, A. A.; Pathe, G. K.; Parida, K. N.; Maksymenko, S.; Lipisa, Y. B.; Szpilman, A. M. α-N-Heteroarylation and α-Azidation of Ketones via Enolonium Species. *J. Org. Chem.* **2018**, *83*, 2442−2447. (b) Li, J.; Bauer, A.; Di Mauro, G.; Maulide, N. α-Arylation of Carbonyl Compounds through Oxidative C−C Bond Activation. *Angew. Chem., Int. Ed.* **2019**, *58*, 9816−9819. (c) Maksymenko, S.; Parida, K. N.; Pathe, G. K.; More, A. A.; Lipisa, Y. B.; Szpilman, A. M. Transition-Metal-Free Intermolecular alpha-Arylation of Ketones via Enolonium Species. *Org. Lett.* **2017**, *19*, 6312−6315. (d) Arava, S.; Kumar, J. N.; Maksymenko, S.; Iron, M. A.; Parida, K. N.; Fristrup, P.; Szpilman, A. M. Enolonium Species-Umpoled Enolates. *Angew. Chem., Int. Ed.* **2017**, *56*, 2599−2603.

(17) Bauer, A.; Di Mauro, G.; Li, J.; Maulide, N. An α-Cyclopropanation of Carbonyl Derivatives by Oxidative Umpolung. *Angew. Chem., Int. Ed.* **2020**, *59*, 18208−18212.

(18) Sanz-Marco, A.; Martinez-Erro, S.; Pauze, M.; Gómez-Bengoa, E.; Martín-Matute, B. An umpolung strategy to react catalytic enols with nucleophiles. *Nat. Commun.* **2019**, *10*, 5244.

(19) (a) Andries-Ulmer, A.; Brunner, C.; Rehbein, J.; Gulder, T. Fluorine as a Traceless Directing Group for the Regiodivergent Synthesis of Indoles and Tryptophans. *J. Am. Chem. Soc.* **2018**, *140*, 13034−13041. (b) Brunner, C.; Andries-Ulmer, A.; Kiefl, G. M.; Gulder, T. Hypervalent Fluoroiodane-Triggered Synthesis of Fluoro-Azabenzoxazepines and Azaindoles. *Eur. J. Org. Chem.* **2018**, *2018*, 2615−2621. (c) Ulmer, A.; Brunner, C.; Arnold, A. M.; Pöthig, A.; Gulder, T. A Fluorination/Aryl Migration/Cyclization Cascade for the Metal-Free Synthesis of Fluoro-Benzoxazepines. *Chem. - Eur. J.* **2016**, *22*, 3660−3664.

(20) (a) Matoušek, V.; Václavík, J.; Hájek, P.; Charpentier, J.; Blastik, Z. E.; Pietrasiak, E.; Budinská, A.; Togni, A.; Beier, P. Expanding the Scope of Hypervalent Iodine Reagents for Perfluoroalkylation: From Trifluoromethyl to Functionalized Perfluoroethyl. *Chem. - Eur. J.* **2016**, *22*, 417−424. (b) Pinto de Magalhães, H.; Togni, A.; Lüthi, H. P. Importance of Nonclassical σ-Hole Interactions for the Reactivity of λ3-Iodane Complexes. *J. Org. Chem.* **2017**, *82*, 11799−11805.

(21) Andrews, I. P.; Lewis, N. J.; McKillop, A.; Wells, A. S. Oxidation of Substituted Pyridines $PyrCH_2X$ (X = H, COOH, COC_6H_5) with Hypervalent Iodine Reagents. *Heterocycles* **1994**, *38*, 713−717.

(22) (a) Weiss, R.; Seubert, J. Electrostatic Activation of Hypervalent Organo-Iodine Compounds: Bis(onio)-Substituted Aryliodine(III) Salts. *Angew. Chem., Int. Ed. Engl.* **1994**, *33*, 891−893. (b) Corbo, R.; Dutton, J. L. Weiss' Reagents: A synthetically useful class of iodine(III) coordination compounds. *Coord. Chem. Rev.* **2018**, *375*, 69−79.

(23) Vitaku, E.; Smith, D. T.; Njardarson, J. T. Analysis of the structural diversity, substitution patterns, and frequency of nitrogen heterocycles among U.S. FDA approved pharmaceuticals. *J. Med. Chem.* **2014**, *57*, 10257−74.

(24) (a) Legault, C. Y.; Prevost, J. 1-Fluoro-3,3-dimethyl-1,3-dihydro-1λ3-benzo[d][1,2]iodoxole. *Acta Crystallogr., Sect. E: Struct. Rep. Online* **2012**, *68*, o1238. (b) Geary, G. C.; Hope, E. G.; Singh, K.; Stuart, A. M. Electrophilic fluorination using a hypervalent iodine reagent derived from fluoride. *Chem. Commun.* **2013**, *49*, 9263−9265. (c) Matoušek, V.; Pietrasiak, E.; Schwenk, R.; Togni, A. One-Pot Synthesis of Hypervalent Iodine Reagents for Electrophilic Trifluoromethylation. *J. Org. Chem.* **2013**, *78*, 6763−6768.

(25) (a) Gillis, E. P.; Eastman, K. J.; Hill, M. D.; Donnelly, D. J.; Meanwell, N. A. Applications of Fluorine in Medicinal Chemistry. *J. Med. Chem.* **2015**, *58*, 8315−8359. (b) Wang, J.; Sanchez-Rosello, M.; Acena, J. L.; del Pozo, C.; Sorochinsky, A. E.; Fustero, S.; Soloshonok, V. A.; Liu, H. Fluorine in Pharmaceutical Industry: Fluorine-Containing Drugs Introduced to the Market in the Last Decade (2001−2011). *Chem. Rev.* **2014**, *114*, 2432−2506. (c) Purser, S.; Moore, P. R.; Swallow, S.; Gouverneur, V. Fluorine in medicinal chemistry. *Chem. Soc. Rev.* **2008**, *37*, 320−330.

(26) (a) Tredwell, M.; Gouverneur, V. ^{18}F Labeling of Arenes. *Angew. Chem., Int. Ed.* **2012**, *51*, 11426−11437. (b) Miller, P. W.; Long, N. J.; Vilar, R.; Gee, A. D. Synthesis of ^{11}C, ^{18}F, ^{15}O, and ^{13}N radiolabels for positron emission tomography. *Angew. Chem., Int. Ed.* **2008**, *47*, 8998−9033.

(27) (a) Fujiwara, T.; O'Hagan, D. Successful fluorine-containing herbicide agrochemicals. *J. Fluorine Chem.* **2014**, *167*, 16−29.

https://dx.doi.org/10.1021/jacs.0c10700
J. Am. Chem. Soc. 2020, 142, 20577−20582

(b) Jeschke, P. The unique role of halogen substituents in the design of modern agrochemicals. *Pest Manage. Sci.* **2010**, *66*, 10−27.
(28) Berger, R.; Resnati, G.; Metrangolo, P.; Weber, E.; Hulliger, J. Organic fluorine compounds: a great opportunity for enhanced materials properties. *Chem. Soc. Rev.* **2011**, *40*, 3496−3508.
(29) López-Alvarado, P.; Avendaño, C.; Menéndez, J. C. A General Synthesis of Quinoline-2,5,8(1H)-triones via Acylation of 2,5-Dimethoxyaniline with *S*-tert-Butyl Thioacetates by Application of the Knorr Cyclization. *Synthesis* **1998**, *1998*, 186−194.
(30) Kohlhepp, S. V.; Gulder, T. Hypervalent iodine(III) fluorinations of alkenes and diazo compounds: new opportunities in fluorination chemistry. *Chem. Soc. Rev.* **2016**, *45*, 6270−6288.

https://dx.doi.org/10.1021/jacs.0c10700
J. Am. Chem. Soc. 2020, 142, 20577−20582

2. Synthesis of α-Functionalized Ketones and Imidazo[1,5-*a*]pyridines starting from Pyridylstyrenes

2.1. Three-Step-One-Pot Synthesis of α-Functionalized Ketones 179

After the successful demonstration of a novel α-functionalization of ketones **172** via a nitrogen directed oxidative Umpolung, investigations into further utilizations of this concept were carried out. The recently by our group developed method for the hypervalent fluoroiodane-triggered synthesis of fluoro-azabenzoxazepines **175** (scheme 28)[134] represented an optimal opportunity to test the Umpolung strategy in a more complex synthetic environment. The fluoro-azabenzoxazepines **175**, obtained from pyridylstyrenes **174**, can be opened under relatively harsh conditions with 6 M NaOH at 80 °C to the ketones **176**. These ketones **176** can subsequently be transformed to the respective indoles **177** in excellent yields.

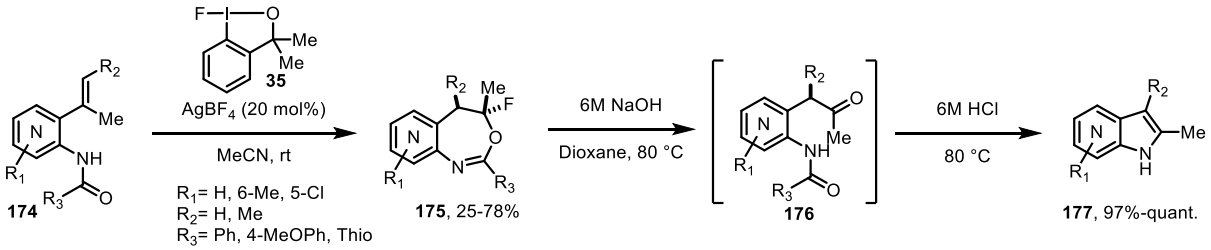

*Scheme 28: The fluoroiodane-triggered synthesis of fluoro-azabenzoxazepines **175** and follow up reaction to the indoles **177**.*

Since the ketones **176** exhibit the necessary characteristics to be suitable ketones for the implemented method described in the previous chapter, an endeavor to intercept these ketones **176** and directly functionalize them in a three-step-one-pot reaction was carried out.

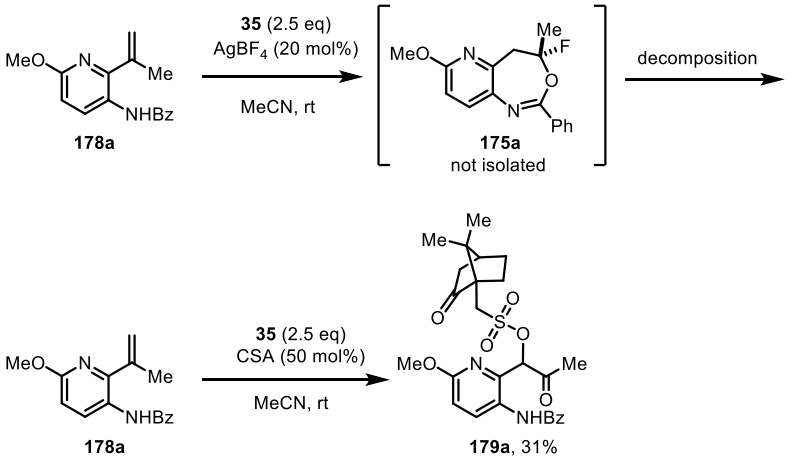

*Scheme 29: Preliminary experiments on the conversion of pyridylstyrene **178a**.*

The methoxy substituted pyridylstyrene **178a** was chosen as the standard substrate, although the respective fluoro-azabenzoxazepines **175a** could not be isolated. It was hypothesized that compound **175a** is too reactive under oxidative conditions because it decomposes to an unidentifiable mixture of compounds rather quickly when using $AgBF_4$ as a catalyst (scheme 29). The considerable electron donating effect of the methoxy substituent increases the electron density at the benzylic position, making it more susceptible to follow-up reactions. An approach to exploit the apparent low stability of

fluoro-azabenzoxazepine **175a** and directly functionalize it with a nucleophile to obtain the respective ketone was devised and the catalyst $AgBF_4$ exchanged to camphorsulfonic acid (CSA). The sulfonic acid was chosen, because it can act as a mild, protic activator for the *F*-iodane **35**, as already established for the conversion of styrenes **72** (scheme 7)[41b] and as a nucleophile in the desired α-functionalization. The preliminary experiment with 50 mol% CSA showed already great promise and pyridylstyrene **178a** was directly converted to ketone **179a** in 31% isolated yield.

Encouraged by this unprecedented finding that confirmed our hypothesis, a thorough investigation for the optimal reaction conditions was carried out. *Para*-toluenesulfonic acid mono hydrate ($TsOH{\cdot}H_2O$) was chosen as the nucleophile and protic activator for simplification reasons as the purification of the crude mixtures turned out to be more conclusive and reproducible compared to experiments with CSA. As the product **179a** appears to be a follow up product of the fluoro-azabenzoxazepines **175**, the amount of 2.5 equivalents of *F*-iodane **35** was unaltered at first and optimization attempts focused on the amount of added nucleophile and the reaction temperature. The method with a small excess of nucleophile gave the desired product **179b** already in a surprisingly good yield of 49% considering the number of steps necessary for the formation (table 1, entry 1).

*Table 1: Optimization of the reaction conditions for the conversion of styrene **178a** to ketone **179b**.*

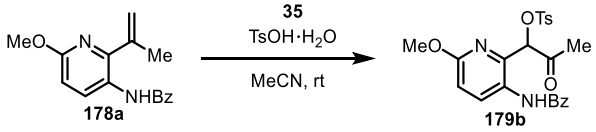

Entry	Equiv. $TsOH{\cdot}H_2O$	Equiv. **35**	Solvent	Time	Yield
1	1.1	2.5	MeCN	1 h	49%
2	2.5	2.5	MeCN	1 h	45%
3	3.0	2.5	MecN	1 h	46%
4[a]	1.1	2.5	MeCN	2 h	44%
5	1.1	2.5	MeCN	15 min	46%
6	1.1	3.0	MeCN	1 h	47%
7	1.1	1.1	MeCN	1 h	27%
8	1.1	2.5	DCM	2 h	<5%

Reactions were carried out with styrene **178a** (0.1 mmol), *F*-iodane **35** and $TsOH{\cdot}H_2O$ in solvent (0.5 mL). The mixture was stirred until no styrene **178a** was detected by TLC and the solvent removed under reduced pressure. The product **179a** was obtained after column chromatography on silica gel. [a] at 0 °C.

A further increase in nucleophile loading (entries 2-3) did not lead to an improved yield and the lowering of the reaction temperature from room temperature to 0 °C prolonged the reaction time to two hours till full consumption of the styrene **178a** was achieved and the product was obtained in a slightly lower yield (entry 4). Working up the reaction after 15 minutes (entry 5) gave the product in a similar but

lower yield compared to after one hour (entry 1) demonstrating that most of the product formation takes place in the beginning of the reaction. This result corresponds to the observation, that no intermediate, for example the fluoro-azabenzoxazepine **175** was ever observed by TLC or after thorough analysis of the obtained column chromatography fractions. Despite the rather complex mechanism, buildup of the product **179b** seems to be the kinetically favored pathway. The increase of *F*-iodane **35** to 3 equivalents did not result in a higher yield (entry 6) but the decrease to 1.1 equiv. reduced the outcome drastically (entry 7). The solvent was exchanged to dichloromethane as a control experiment to evaluate if the acetonitrile suppresses the interaction between the pyridine and the *F*-iodane **35** as discussed in the previous chapter on the Umpolung of ketones. Interestingly, in this reaction the opposite effect seems to occur as no product was obtained with DCM (entry 8). The last two results are in alignment with the previously disclosed results in the hypervalent fluoroiodane-triggered synthesis of fluoro-azabenzoxazepines and azaindoles[134] where 2.5 equivalents of *F*-iodane **35** gave the highest yield and no conversion of the styrene was observed in DCM. Consequently, although it might be the optimal solvent for the Umpolung reactions it is entirely unsuitable for the cascade reaction of styrene **178a** to ketone **179b**.

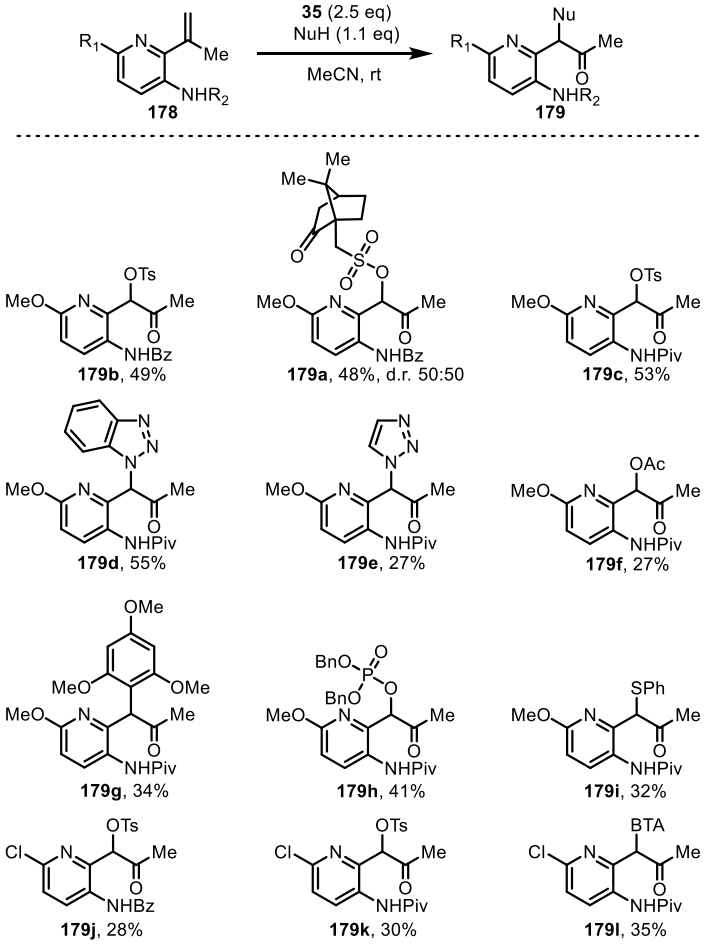

*Scheme 30: Scope for the functionalization of pyridylstyrenes **178**.*

With the optimal reaction conditions in hand, a wide variety of nucleophiles were selectively introduced into the α-position of the ketone scaffold (scheme 30). The improved conditions lead to an increase in yield of ketone **179a** to 48% for the reaction with CSA compared to the preliminary experiment that started this investigation (scheme 29). There was no induction of diastereoselectivity as the ketone **179a** was obtained with a diastereomeric ratio (d.r.) of 50:50. Changing the amide moiety from a benzoyl to a pivaloyl substituted scaffold led to a slight increase in yield of product **179c**. This seemingly unsignificant result is highly interesting when viewed in the context, that for the synthesis of fluoro-azabenzoxazepines **175**, alkyl moieties were not tolerated as substituents at the amide (scheme 28). As the pivaloyl substituted styrene led to a higher amount of product, further experiments were carried out using this substrate. 1*H*-Benzotriazole (BTA-H), the standard nucleophile used in the Umpolung of ketones, was readily accepted in the reaction and furnished ketone **179d** in 55%. Attempts with 1,2,3-triazole or acetic acid converted the styrene into the respective α-functionalized ketones **179e** and **179f** in 27% yield. Up to this point, the suitable nucleophiles are in accordance with the previously used protic compounds but using this method, it is furthermore possible to build up new *C-C* bonds using the nucleophilic 1,3,5-trimethoxybenzene. The functionalized ketone **179g** was obtained in 34% yield with no double or triple substituted side products observed. Products **179h** and **179i** with dibenzyl phosphate and thiophenol respectively complete the scope for various nucleophiles. *S*-, *N*-, *O*- and *C*-nucleophiles can be introduced in a mild, selective, and unprecedented fashion utilizing this method. So far, only the highly activated methoxy-substrate **178** was converted with various nucleophiles and attempts to use the unsubstituted or methyl substituted styrenes **178** (R_1= H, Me) did not show any sign of product formation independent from the amide substitution (R_2). Similar to the previous chapter where the methoxy and chloro substituted pyridyl ketones were the only suitable substrates for the direct mono-fluorination, as they possess an elevated affinity towards the hypervalent iodane **35**, chloro-substituted styrenes **178** (R_1= Cl) were the only other substrate that was suitable in this method. Benzoyl as well as pivaloyl amide moieties R_2 were well tolerated, furnishing the ketones **179j** and **179k** with $TsOH{\cdot}H_2O$ in 28% and 30% yield, respectively. Additionally, the introduction of BTA into the ketone scaffold **179l** was achieved in 35% yield. Although the overall yields for the α-functionalized ketones **179** are only in the range between 27 - 55%, the complexity and multitude of steps necessary for the formation cannot be disregarded. Several control experiments were carried out trying to obtain insight into the exact mechanistic pathway for this unprecedented cascade reaction.

Mechanistical investigations into the formation of the α-functionalized ketones 179

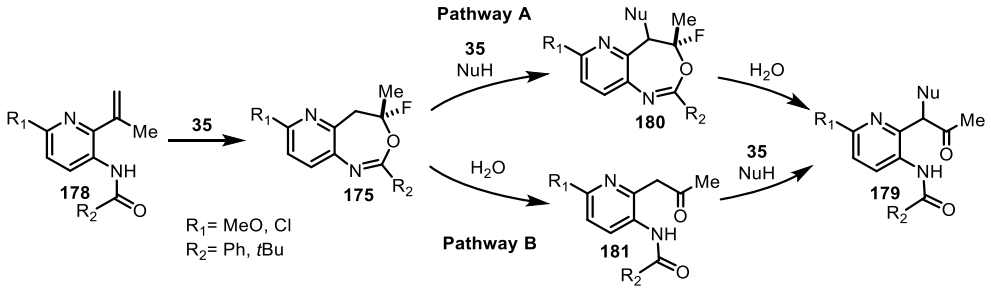

*Scheme 31: Possible mechanistic pathways for the conversion of pyridylstyrenes **178**.*

Two plausible reaction pathways are shown in scheme 31. The conversion of styrene **178** to the azabenzoxazepine **175** was shown in our previous work[134] and can be assumed as certain, because no other reasonable mechanism to obtain the linear alkyl chain present in the product **179** is known. The addition of the nucleophile to give the cyclic intermediate **180** with the hydrolysis and ring opening as a subsequent step is described as **pathway A**. Following **pathway B** with the ring opening as the first step results in intermediate **181** with a strong resemblance of the pyridylketones **172** used in the Umpolung of ketones and so the following addition of the nucleophile would be in greater accordance with the previously disclosed work.

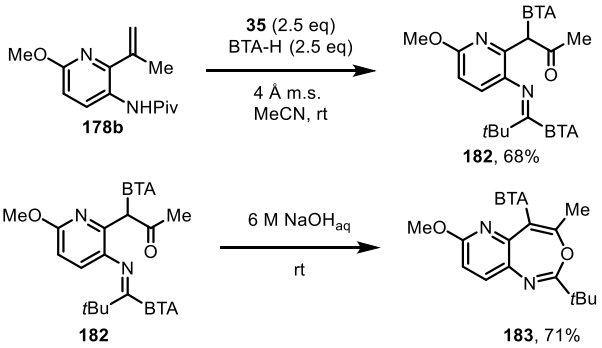

Scheme 32: Control experiments for the two possible mechanistic pathways A and B.

To determine the correct pathway, water was removed from the solvent with molecular sieve (scheme 32) to obtain intermediate **180** (pathway **A**) or stop the reaction at the fluoro-azabenzoxazepine **175** (pathway **B**). The resulting product **182** (68% yield) is a clear indicator for reaction pathway **A** as the nucleophile BTA-H replaced the unavailable water in the ring opening step. This also confirms the initial assumption, that fluoro-azabenzoxazepine **175** must be furnished as an intermediate because no other pathway could explain the introduction of the nucleophile BTA-H at the amide portion of the molecule.

Product **182** is quite instable and was readily converted in a basic, aqueous environment to the azabenzoxazepine **183** in 71% yield. This compound can be formally derived from the hypothetical intermediate **180** after an elimination of HF and it was transformed to the ketone **178d** in quantitative yield after stirring in "wet" acetonitrile. These results strengthen the argument for pathway **A** as the alleged mechanistic pathway.

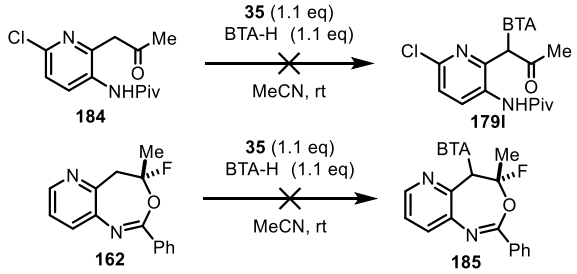

Scheme 33:Control experiments to gain insight into the present mechanistic pathway.

To further corroborate this hypothesis, ketone **184**, obtained as a minor side product in an unsuccessful conversion of the chloro-substituted styrene **178**, was employed in an attempt to introduce BTA-H into the ketone scaffold mediated by *F*-iodane **35** (scheme 33). Interestingly, the expected product **179l** was not observed and only minor decomposition of the starting material occurred, therefore providing a definite proof, that pathway **B** can be disregarded. Considering these results, a similar pathway to pathway **A** can be expected as the mechanism with a benzylic-oxidation-type step to the intermediate **180** present in this type of functionalization. The verification of this essential step meant the isolation of the methoxy or chloro substituted fluoro-azabenzoxazepine **175**, which was unfortunately not achieved due to their apparent affinity to react further. The reaction of the already established, stable fluoro-azabenzoxazepine **162** to the oxidized product **185** was not successful with no conversion of the starting material apparent, demonstrating the necessity for activating substituents at the aromatic scaffold for this cascade reaction.

Overall, there is strong evidence that suggests that a pathway similar to pathway **A** is the underlying mechanistic pathway of the disclosed cascade reaction to transform pyridylstyrenes **178** to the α-functionalized ketones **179**.

2.2. Novel Synthetic Pathway towards Imidazo[1,5-*a*]pyridines 187

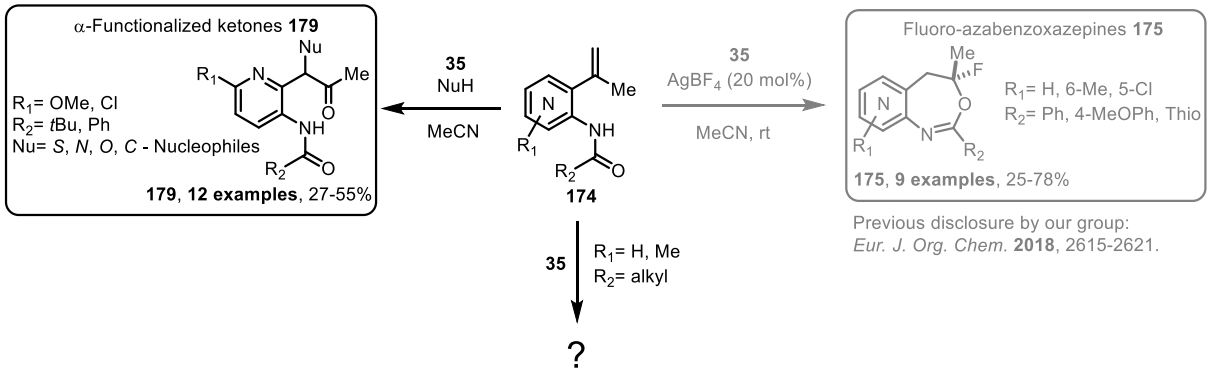

*Scheme 34: General substrate dependent product selectivity for the pyridylstyrenes **174**.*

Taking a closer look at the substrate scopes for the α-functionalized ketones **179** and the fluoro-azabenzoxazepines **175** revealed an astonishing fact concerning the composition and substitution pattern of the respective pyridylstyrenes (**174**, scheme 34). There is no apparent overlap between these two reactions, suggesting that a substrate dependent product selectivity is present. Solely activated, methoxy or chloro (R_1) substituted styrenes **174** with alkyl or aromatic (R_2) amide moieties can be converted to α-functionalized ketones **179** and unsubstituted, methyl and chloro (R_1) substituted pyridylstyrenes **174** possessing an aromatic (R_2) moiety can be transformed in a $AgBF_4$ catalyzed reaction to the seven-membered fluoro-azabenzoxazepines **175**. This discovery leaves only one class of pyridylstyrene substrates **174** with unknown reactivity. The question, if non activated substrates **174** with an alkyl (R_2) rest can be transformed with *F*-iodane **35** and towards what kind of product, needed to be addressed.

The unsubstituted styrene (**186a**, table 2) was chosen as the standard substrate and a search for suitable conversion conditions was carried out. Since acetonitrile has proven to be the optimal solvent for the other two reaction pathways, it was determined to be the solvent of choice in this case as well. The first attempt, carried out by my colleague Anna Andries-Ulmer with the established catalyst $AgBF_4$ showed already promise and led to the formation of compound **187a** in 31% isolated yield (table 2, entry 1). This heterocyclic structure with a condensed five and six-membered ring belongs to the class of imidazo[1,5-*a*]pyridines. For the furnishing of the five-membered ring, acetonitrile was introduced into the scaffold as the nucleophilic species with a subsequent ring-closure. This result was highly unexpected as such a synthetic route towards the imidazopyridines was completely unprecedented. Encouraged by this fascinating discovery, an additive screening was carried out to find the optimal catalyst. The silver salts $AgSbF_6$ and $AgPF_6$ gave similar yields (entries 2-3) while silver triflimide (entries 4-5) showed an increased yield of 45% after 19 h and 40% after 16 h in a higher concentrated attempt. Unfortunately, this catalyst is relatively expensive and the reaction time left room for improvement. Copper salts have already demonstrated to be suitable catalysts for the furnishing of imidazo[1,5-*a*]pyridines[138] and copper triflate was therefore chosen for further screening efforts. The first attempt using the standard conditions without deviation (entry 6) led to the desired product **187a** in a substantial shorter time and an even higher yield of 46%.

*Table 2: Additive screening for the synthesis of imidazo[1,5-a]pyridine **187a**.*

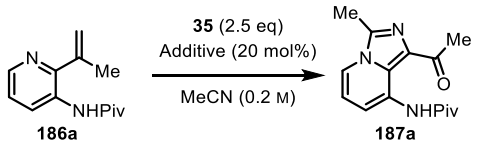

Entry	Additive	Time	Yield (isolated)
1[a]	$AgBF_4$	20 h	(31 %)
2[a]	$AgSbF_6$	19 h	35 %
3[a]	$AgPF_6$	19 h	32 %
4[a]	$AgN(SO_2CF_3)_2$	19 h	45 %
5[ab]	$AgN(SO_2CF_3)_2$	16 h	40 %
6	$Cu(OTf)_2$	4 h	46 % (44%)
7[c]	$Cu(OTf)_2$	4.5 h	33 %
8[d]	$Cu(OTf)_2$	6 h	37 %
9[de]	$Cu(OTf)_2$	6 h	24 %
10[df]	$Cu(OTf)_2$	6 h	31 %
11[g]	$Cu(OTf)_2$	5 h	30 %
12[h]	$Cu(OTf)_2$	20 h	27 %
13[i]	$Cu(OTf)_2$	20 h	30 % (29 %)
14[j]	$Cu(OTf)_2$	20 h	40 %
15	$Cu(MeCN)_4PF_6$	20 h	39 %
16[k]	Cu(salan) 2TfOH	18 h	39 %
17	$Cu(OAc)_2\,H_2O$	48 h	< 5 %
18	CuOAc	19 h	< 5 %
19	CuI	19 h	< 5 %
20	$Bi(OTf)_3$	18 h	32 %
21	$Zn(OTf)_2$	3 h	26 % (23 %)
22[a]	NaOTf	8 h	24 % (19 %)
23[a]	Tf_2O	3 h	32 %
24[a]	TfOH	18 h	33 %
25[a]	40 °C	72 h	32 %

For the reaction, styrene **186a** (0.1 mmol) was dissolved in MeCN (0.5 mL) and *F*-iodane **35** (0.25 mmol) added. The respective additive (20 mol%) was added and the reaction was monitored by TLC. The mixture was washed through a silica plug to quench the reaction and the solvent evaporated under reduced pressure. Mesitylene (~ 0.1 mmol) was added as an internal standard and the crude mixture analyzed by ^{1}H NMR spectroscopy. [a] no silica plug; [b] 0.4 M in MeCN; [c] 0.05 M in MeCN; [d] in DCM:MeCN 1:1, 0.2 M; [e] $Cu(OTf)_2$ (5 mol%); [f] $Cu(OTf)_2$ (50 mol%); [g] BHT (0.1 mmol) added; [h] $NaHCO_3$ (2.5 mmol) added; [i] at 40 °C; [j] at 0 °C; [k] in situ from $Cu(OTf)_2$ and salan-ligand.

In all screening experiments so far, minor precipitation occurred in acetonitrile caused by the low solubility of the product **187a**. The dilution of the reaction to a 0.05 M solution (entry 7) as well as the use of a 1:1 mixture of dichloromethane and acetonitrile (entry 8) did not lead to an increased yield although the precipitation was not observed anymore in both cases. Neither the decrease to 5 mol% (entry 9) nor the increase to 50 mol% (entry 10) of $Cu(OTf)_2$ improved the reaction outcome but rather gave lower yields. The addition of butylated hydroxytoluene (BHT) as a radical scavenger (entry 11) to exclude the possibility of a radical mechanism did not suppress the reaction, as did the addition of the weak base $NaHCO_3$ (entry 12). Variation of the reaction temperature to 40 °C (entry 13) lead to 30% product yield. This decrease can be assigned to the instability of the product in an oxidative environment that is magnified by the increased temperature. Conversely, executing the reaction at 0 °C (entry 14) led to the imidazo[1,5-*a*]pyridine **187a** in 40% yield, which is an improvement compared to the reaction at 40 °C but is still lower than at room temperature. Different Cu(II)-salts (entries 15-16) gave the product in 39%, but copper acetates, both $Cu(OAc)_2$ and CuOAc (entries 17 -18) completely suppressed product formation although there was full substrate consumption. The same applies to CuI (entry 19) confirming the preceding findings that the counter ion to the metals in the additives play an essential role. The need for a weak-nucleophilic counter ion is evident as silver and copper salts with tetrafluoroborate, hexafluoroantimonate, hexafluorophosphate, triflimide and triflate were successfully employed as additives for the synthesis of **187a** while acetate and iodide failed. The utilization of bismuth (entry 20), zinc (entry 21) and sodium (entry 22) triflates to produce **187a** in moderate yields further supported this hypothesis. Since the influence of the metallic ion is relatively insignificant, attempts without a metal were carried out and successful reactions achieved with trifluoromethanesulfonic anhydride (entry 23) and trifluoromethanesulfonic acid (entry 24) in similar but lower product yields. Last but not least, an elevated temperature of 40 °C without any further additive (entry 25) gave the product **187a** in 32% yield but after an overly prolonged reaction time of 72 h compared to the optimal reaction conditions with $Cu(OTf)_2$ at room temperature (entry 6), that furnished the desired imidazo[1,5-*a*]pyridine **187a** in 46% ^{1}H NMR-yield and 44% isolated yield after just 4 h.

As the previously disclosed conversions of pyridylstyrenes **174** worked best with 2.5 equivalents of *F*-iodane **35**, it can be assumed that it does in the formation of imidazo[1,5-*a*]pyridines **187a** as well. Nevertheless, in the scientific world certainty is worth much more than assumptions and so, an *F*-iodane **35** equivalent screening was carried out once more. Unlike the previous screenings, gas chromatography (GC) was chosen instead of ^{1}H-NMR-spectroscopy and intermediate measurements were executed to give a detailed insight into the kinetic of the reaction.

The overall GC-yield measured after 4 h reaction time showed significant deviations. Using 1.0 equivalents of *F*-iodane **35** led to the product **187a** in 15% yield (table 3, entry 1), while 2.0 equiv. (entry 2) and 2.2 equiv. (entry 3) gave the product **187a** in more than twice the yield, with 38%.

Yet, the maximum yield was once again obtained with 2.5 equiv. of *F*-iodane **35** (entry 4) at 41%. The further increase in equivalents led to a steady decrease in yield as 3.0 equiv. (entry 5) gave the product

in 36% yield and the attempt with an even higher excess of *F*-iodane **35**, 5.0 equiv. (entry 6) gave an even lower yield of 30% for **187a**. These results confirmed the assumption made in the beginning, that 2.5 equivalents of *F*-iodane **35** is the optimal amount of hypervalent iodane reagent for these type of styrene conversions.

*Table 3: Equivalent screening for the optimal amount of F-iodane **35** for the formation of product **187a**.*

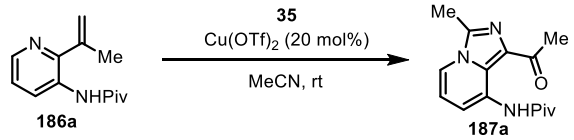

Entry	Equiv. **35**	Yield (4h)
1	1.0	15 %
2	2.0	38 %
3	2.2	38 %
4	2.5	41 %
5	3.0	36 %
6	5.0	30 %

Yield measured by GC with an internal standard.

The selection of GC as the mode of measurement turned out to be helpful, because of the possibility to take small aliquots of the crude reaction mixtures without having to interfere in the reaction. The results from these intermediate measurements are graphically shown in figure 13 and figure 14.

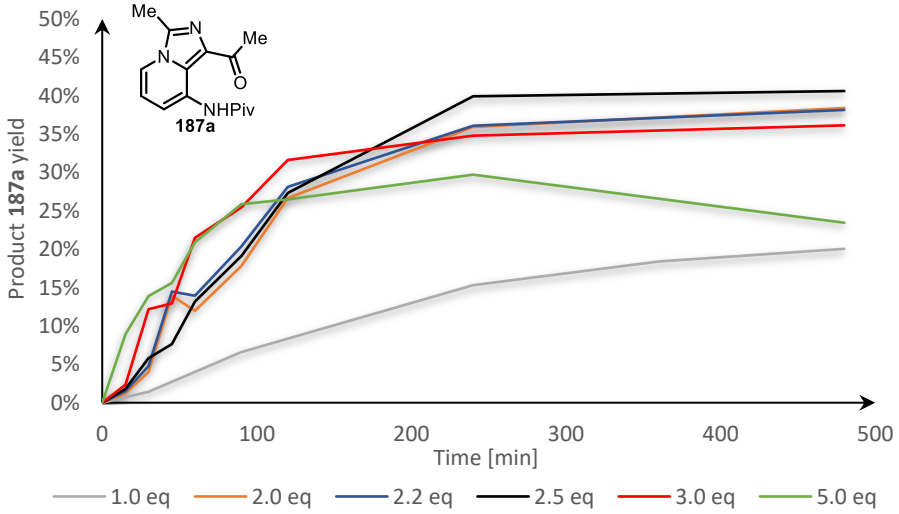

*Figure 13: Product **187a** formation over time for reactions with different equivalents of F-iodane **35**.*

The reactions with 2.0 (orange, figure 13), 2.2 (blue) and 2.5 (black) equivalents of *F*-iodane **35** showcase a very similar product **187a** formation rate and are solely distinguishable in the slightly higher yield in the case of 2.5 equivalents. 3.0 (red) and 5.0 (green) equivalents demonstrated an increased product formation during the first 100 minutes of the reaction but stopped at a lower yield.

Interestingly, decomposition of the product was observed in the reaction with 5.0 equivalents of *F*-iodane **35**, as the product yield began to decrease from 30% after 240 minutes to 24% after 480

minutes. As expected, 1.0 (grey) equiv. of *F*-iodane **35** displayed the slowest product formation rate that topped out at a yield of 20% after 480 minutes (8h). A control measurement after 23 h revealed neither an increase nor a decrease in product yield.

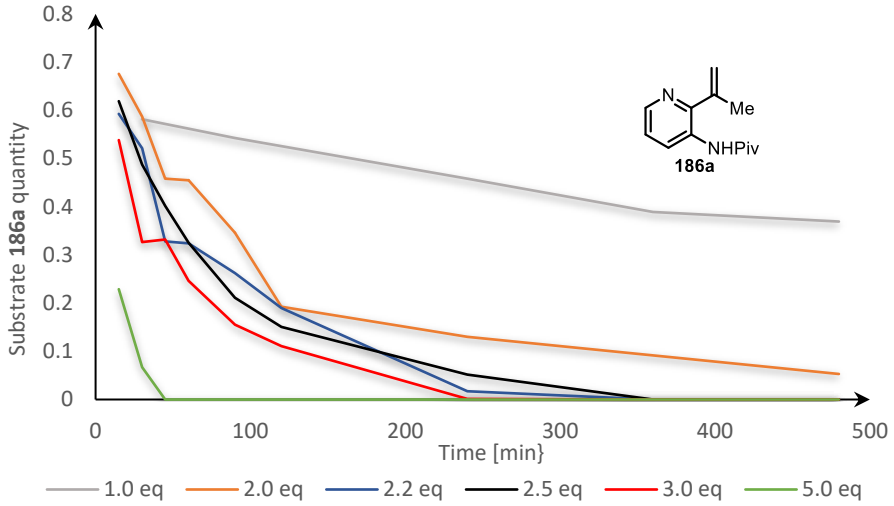

*Figure 14: Relative substrate **186a** consumption over time for reactions with different equivalents of F-iodane **35**.*

In figure 14, the relative substrate consumption is displayed. The decrease in substrate **186a** for 5.0 (green), 3.0 (red), 2.5 (black), 2.2 (blue) and 2.0 (orange) equivalents of *F*-iodane **35** showed the expected correlation between substrate **186a** consumption and product **187a** formation, but the attempt with 1.0 (grey) equivalents gave a highly interesting result. The GC-measurements revealed, that around half of the substrate **186a** is not converted. This indicates that the reaction pathway for the formation of **187a** is kinetically favored and that the occurring intermediates possess a higher affinity towards the *F*-iodane **35** compared to the styrene **186a**. Otherwise, complete substrate consumption should have occurred and no or only a small amount of product **187a** been furnished.

With the optimal reaction conditions in hand, it was time to explore the scope of the reaction. Several styrenes **186** with varying alkyl moieties (R_2) and substituents (R_1) at the aromatic portion were synthesized and converted with alkyl nitriles R_3CN in a $Cu(OTf)_2$ catalyzed cascade reaction to obtain the novel imidazo[1,5-*a*]pyridines **187** (scheme 35).

Deuterated acetonitrile was readily introduced to give the bicycle **187b** in 44% yield. The reaction was successful as well for the alkylnitriles (R_3CN) propionitrile, isobutyronitrile and pivalonitrile, furnishing the imidazopyridines **187c-e** in 41%, 28% and 17% yield respectively. This steady decrease in yield can be explained by the increase in steric hindrance as well as the reduced electrophilicity of the carbon center of the cyano-group needed for the ring closure, caused by the increasingly stronger electron donating effect of the alkyl-moieties when going from ethyl to *tert*butyl.

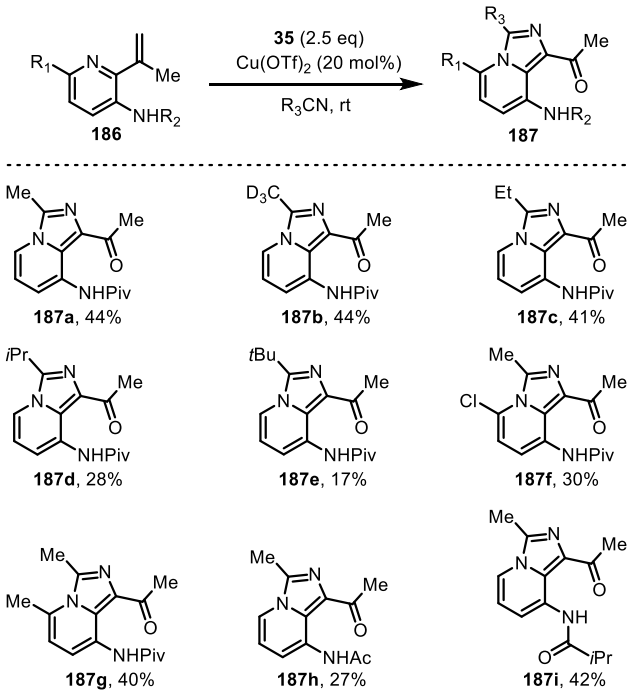

*Scheme 35: Scope for the imidazo[1,5-a]pyridines **187**.*

Chloro and methyl substituents (R_1) were tolerated and products **187f** and **187g** were obtained in 30%, respectively 40% yield. The lower yield for the chloro-substituted styrene might be derived from the increased susceptibility towards decomposition for the activated styrene, already acknowledged in previous chapters. Finally, R_2 was varied from the pivaloyl group and products **187h** and **187i** obtained in 27%, respectively 42% yield. In conclusion, pyridylstyrenes **186** with H, Me or Cl as R_1 and an alkyl moiety for R_2 can be transformed with alkylnitriles R_3CN to form imidazo[1,5-*a*]pyridines **187** in good yields.

So far, the only substituent that is tolerated in all three different types of conversion (fluoro-azabenzoxazepines **175**, α-functionalized ketones **179** and imidazo[1,5-*a*]pyridines **187**) is a chloro-substituent at the aromatic portion. Attempts to expand the substrate scope by transforming the methoxy substituted styrene **178b** using the optimized conditions did not lead to any observable product **187j** (scheme 36) and the benzoyl substituted styrene **161** was converted to the fluoro-azabenzoxazepine **162** in 64% yield. These results vividly demonstrate the substrate dependent product selectivity.

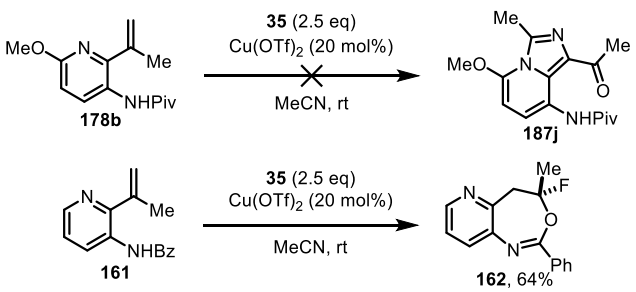

Scheme 36: Substrate dependent selectivity for the optimized reaction conditions.

3. Conclusion & Perspective

The excellent properties of λ^3-*F*-iodane **35** have led to a multitude of fascinating publications attending to its applications in organic synthesis [41, 51, 53, 58, 60-62, 64-68, 70-73, 90, 134, 137, 139] and computational studies on activation and the complex mechanisms involved.[59, 63, 69, 124, 140] This shows the immense interest in this novel oxidizing reagent, considering the relatively short period of time since its discovery in 2012. Our group previously contributed by demonstrating selective styrene conversions triggered by *F*-iodane **35** in the facile and straightforward synthesis of fluoro-benzoxazepines **67**,[41a] fluoro-azabenzoxazepines **162**[134] and subsequent follow up reactions towards indoles **76** and **77**, ketones **75**[41b] and azaindoles **177**.[134]

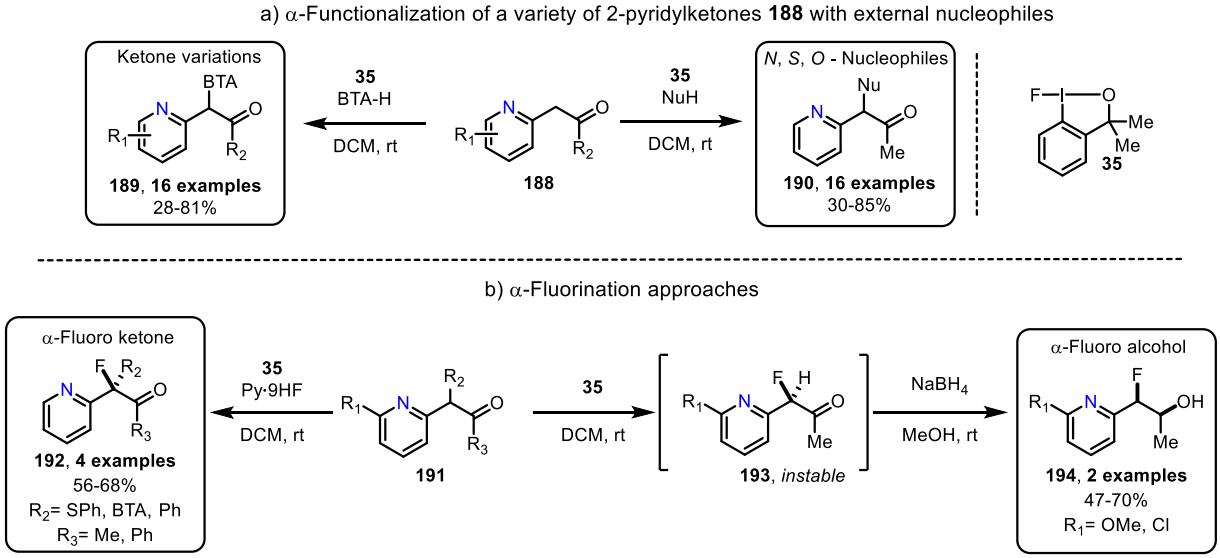

*Scheme 37: Overview of the successful α-functionalizations of 2-pyridylketones **188** and **191** with F-iodane **35**.*

Departing from styrene substrates, in this work an unprecedented α-functionalization of ketones **188** via a nitrogen directed oxidative Umpolung with *F*-iodane **35** as the oxidative mediator was presented (scheme 37).[136] The reactions can be carried out without the need for the careful preparation of a moisture and air free environment and ambient temperatures are sufficient. The developed procedure was exploited to furnish over 30 novel, α-functionalized ketones **189** and **190** with a variety of protic, external *N*-, *S*- and *O*-nucleophiles in a regio- and chemoselective fashion in good to excellent yields. Furthermore, α-fluorination was achieved after the preliminary difficulties to purify the instable α-fluoro ketones **193** were overcome. The *in situ* reduction of the ketone **193** to the respective alcohol as well as choosing suitable α-disubstituted substrates **191** gave way to two novel α-fluoro alcohols **194** and four quaternary α-fluoro ketones **192** in good yields.

Preliminary mechanistic experiments showed a causal attraction between the nitrogen of the aromatic moiety and the λ^3-fluoro iodane **35** and that this can be most likely attributed to a non-covalent electrostatic interaction. The stabilizing and activating effects of the pyridine are essential to the reactivity, demonstrating that the developed concept could potentially be a powerful tool in organic synthesis.

Another objective was the evaluation of the established concept in a more complex synthetic environment. The substrate class of the pyridylstyrenes **174**, previously employed in the λ^3-fluoro iodane **35** mediated synthesis of fluoro-azabenzoxazepines **175**[134], turned out to be the ideal starting point for the thorough investigation into a substrate dependent product formation (scheme 38).

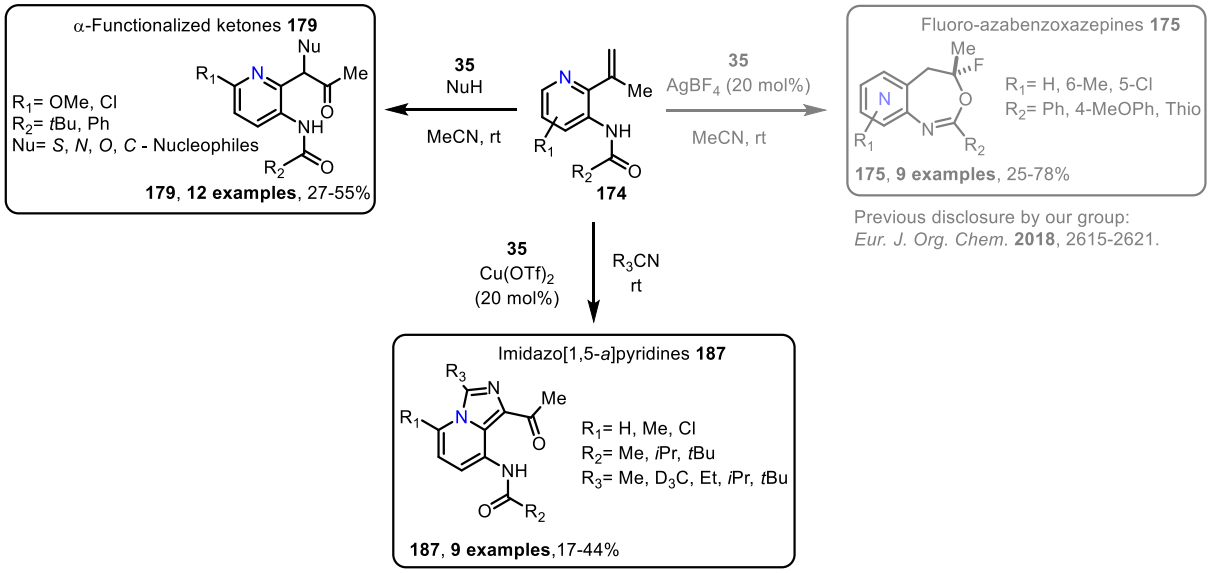

*Scheme 38: Substrate dependent product formation for the conversion of pyridylstyrenes **174** with F-iodane **35**.*

Activated pyridylstyrenes **174** with methoxy and chloro substituents (R_1) were transformed to 12 novel α-functionalized ketones **179** with various *S*-, *N*-, *O*-, and *C*-nucleophiles in a straightforward manner. The substitution at the amide moiety (R_2) played a minor role, as alkyl and aryl groups were tolerated. Surprisingly, mechanistic experiments suggest, that the intermediatory fluoro-azabenzoxazepine **175** is functionalized in a benzylic-oxidation type reaction rather than an α-functionalization of the possible ketone intermediate, which would have been more in alignment to the preceding concept.

Pyridylstyrenes **174** bearing an alkyl group at the amide portion (R_2) were converted under adapted reaction conditions in the respective alkyl nitrile solvent (R_3CN) with copper triflate as the catalyst to directly obtain 9 novel imidazo[1,5-*a*]pyridines **187**.

By carefully selecting the substitution pattern for the pyridyl styrenes **174**, complete control over the product formation is gained. Under the optimal conditions for each product, none of the other two possible products was ever observed, showing a perfect substrate dependent product selectivity.

In conclusion, further valuable contributions were made for the application of the still relatively new hypervalent iodane reagent **35**, demonstrating its immense synthetic utility for a wide variety of reactions.

A key role for future applications of the Lewis base directed oxidative Umpolung concept developed in this work is going to be having a better understanding of the exact mechanism of the reaction. Computational studies have proven themselves to be helpful tools and when accompanied with conscientiously selected experiments can give rather quickly profound insights into the mechanistic pathways and potential electrostatic interactions between the reacting partners. Fortunately, we were able to commence a collaboration with the groups of Professor Huber and Professor Legault and preliminary calculations are already being implemented. With their advice on further suitable Lewis bases and requirements for the hypervalent iodane reagents to carry out the directed Umpolung reactions, rapid improvements should be made in the development of novel procedures.

A major improvement for the nitrogen directed oxidative Umpolung of ketones would be the introduction of *C*-nucleophiles into the structures. This situation could be remedied by derivatives of *F*-iodane **35**. Two variants have surfaced quite recently, and first applications were disclosed (scheme 39). The phenyl substituted λ^3-*F*-iodane **35a** was used to furnish unsymmetrical diaryliodonium salts **196** with aryls **195** having an electron donating group.[139] Derivative **35b** with two CF_3-groups in combination with $BF_3{\cdot}OEt_2$ on the other hand showed potential in the iodo(III)etherification of alkynes **197** in ethereal solvents to obtain compound **198**.[141] Both λ^3-*F*-iodanes show exceptional affinity towards carbon structures and might show promise as the oxidative mediator for the introduction of *C*-nucleophiles in the presented pre-coordination concept.

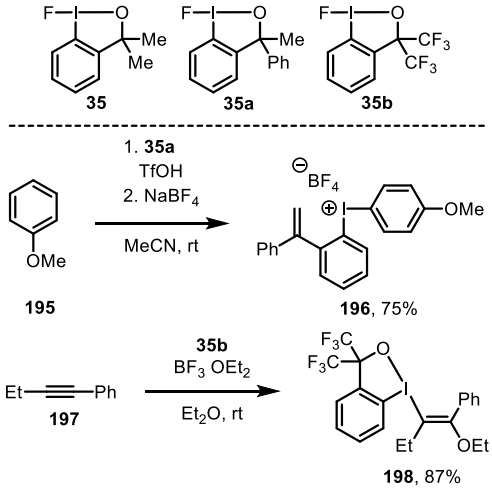

*Scheme 39: Derivatives **35a** and **35b** and their applications.*

Furthermore, substituents at the aromatic moiety of *F*-iodane **35** could be used to optimize the interaction of the electrophilic iodane center with the Lewis base and various Lewis bases, e.g. phenols, furans, tested under similar reaction conditions.

4. Zusammenfassung & Ausblick

Die exzellenten Eigenschaften des λ^3-*F*-iodans **35** haben zu einer Vielzahl von faszinierenden Veröffentlichungen geführt, die sich mit dessen Anwendung in der organischen Synthese[41, 51, 53, 58, 60-62, 64-68, 70-73, 90, 134, 137, 139] und mit Berechnungen zur Aktivierung und den zugrundeliegenden, komplexen Mechanismen befasst haben.[59, 63, 69, 124, 140] Dies verdeutlicht das große Interesse an diesem neuartigen Oxidationsreagenz, wenn man die kurze Zeit seit seiner Entdeckung im Jahr 2012 bedenkt. Unsere Arbeitsgruppe beteiligte sich an der Erforschung dieses Reagenzes durch die Veröffentlichungen zweier durch das *F*-Iodan **35** ermöglichten, selektiven Styrolderivat-Umsetzungen in der direkten Synthese von fluorierten Benzoxazepinen **67**,[41a] fluorierten Azabenzoxazepinen **162**[134] und deren Folgereaktionen zu Indolen **76** und **77**, Ketonen **75**[41b] und Azaindolen **177**.[134]

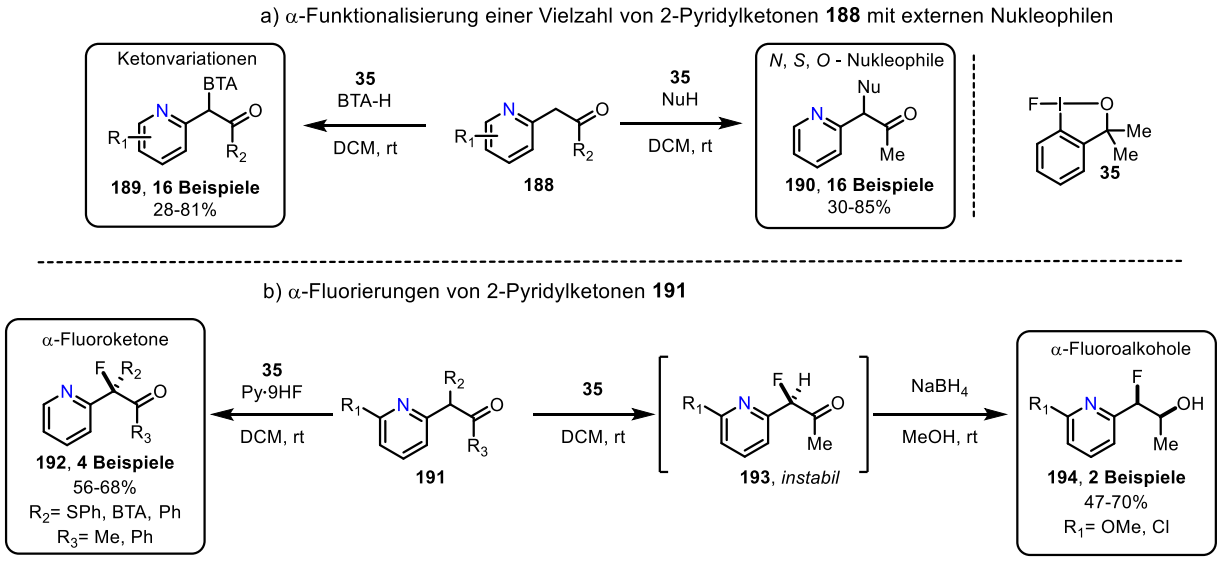

*Schema 40: Überblick über die erfolgreichen α-Funktionalisierungen von 2-Pyridylketonen **188** und **191** mit dem F-Iodan **35**.*

Die vorliegende Arbeit beschäftigte sich mit einer neuartigen α-Funktionalisierung von 2-Pyridylketonen **188** mittels einer Stickstoff dirigierten, oxidativen Umpolung mit dem *F*-Iodan **35** als oxidativem Mittelsmann (Schema 40a).[136] Die Reaktionen konnten bei Raumtemperatur durchgeführt werden, ohne dass auf eine feuchtigkeits- oder luftfreie Umgebung geachtet werden musste. Die hier entwickelte Methode wurde benutzt, um über 30 neuartige, α-funktionalisierte Ketone **189** und **190** herzustellen, welche durch die Umsetzung mit einer Vielzahl an protischen, externen *N*-, *S*- und *O*-Nukleophilen in einer regio- und chemoselektiven Reaktion in guten bis exzellenten Ausbeuten erhalten wurden. Desweiteren konnten α-Fluorierungen (Schema 40b) erfolgreich durchgeführt werden, nachdem das Problem der Aufreinigung der instabilen α-Fluoroketone **193** gelöst wurde. Eine *in situ* Reduktion der Ketone **193** zu den jeweiligen Alkoholen **194**, als auch die Wahl von α-disubstituierten Substraten **191** führten zu zwei neuen α-Fluoroalkoholen **194** und vier quartären α-Fluoroketonen **192** in guten Ausbeuten.

Erste mechanistische Experimente deuten darauf hin, dass eine kausale Koordination zwischen dem Stickstoff des Aromaten und dem λ^3-Fluoroiodan **35** vorliegt und dass dies sehr wahrscheinlich einer nicht-kovalenten, elektrostatischen Wechselwirkung zuzuschreiben ist. Die Stabilisierungs- und Aktivierungseigenschaften des Pyridins sind essenziell für die Reaktivität und zeigen anschaulich, dass das entwickelte Konzept ein wertvolles Werkzeug in der organischen Synthese sein könnte.

Als weiteres Ziel dieser Arbeit sollte das Konzept in einer anspruchsvolleren, synthetischen Umgebung getestet werden. Die Pyridin-basierten Styrole **174**, welche bereits für die Synthese von fluorierten Azabenzoxazepinen **175**[134] verwendet wurden, stellten sich dabei als ideale Substratklasse heraus, um eine Substrat-abhängige Produktformation zu untersuchen (Schema 41).

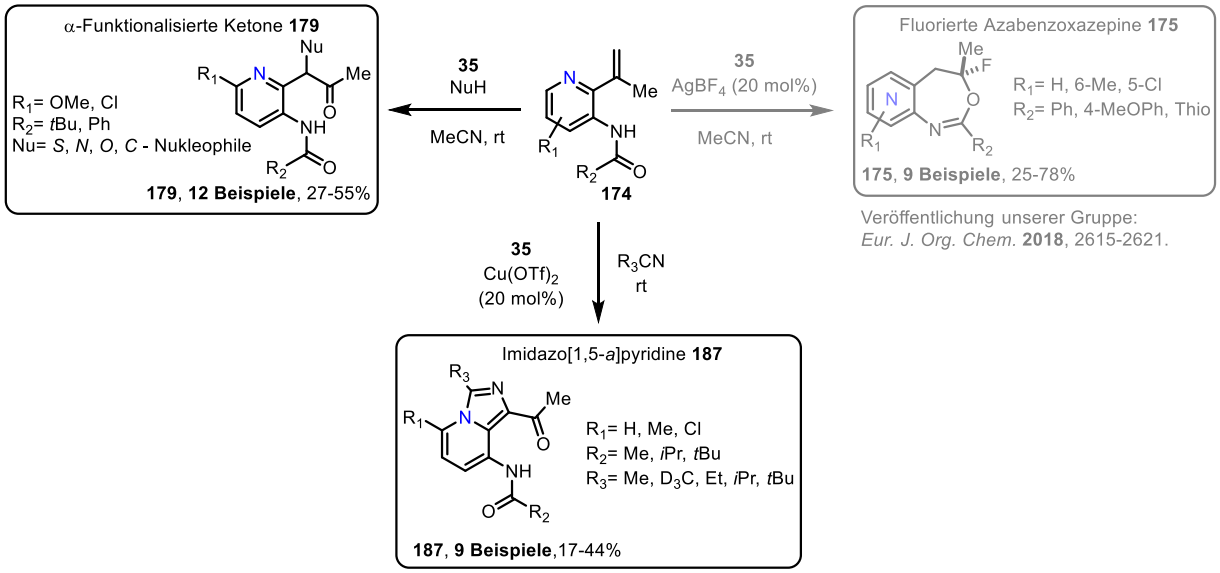

*Schema 41: Substrat-abhängige Produktformation der Umsetzung von Pyridylstyrolen **174** mit dem F-*Iodan **35**.

Aktivierte Pyridylstyrole **174** mit Methoxy- oder Chlor-Substituenten (R_1) wurden zu 12 neuartigen, α-funktionalisierten Ketonen **179** mit unterschiedlichen *S*-, *N*-, *O*-, und *C*-Nukleophilen in einer Eintopf-Reaktion umgesetzt. Der Rest (R_2) an der Amidbindung spielte hierbei eine Nebenrolle, weil sowohl Alkyl als auf aromatische Gruppen akzeptiert wurden. Überraschenderweise suggerieren mechanistische Experimente, dass das fluorierte Azabenzoxazepin **175** Zwischenprodukt in einer benzylischen Oxidationsreaktion funktionalisiert wird und nicht ein Keton Zwischenprodukt, was besser mit dem vorher erarbeiteten Konzept übereingestimmt hätte.

Des Weiteren wurden Pyridylstyrole **174** mit einer Alkyl-Gruppe (R_2) an der Amidbindung unter angepassten Reaktionsbedingungen in einer Alkyl-Nitril (R_3CN) Lösung mit Kupfertriflat Katalysator umgesetzt und so neun, neuartige Imidazo[1,5-*a*]pyridine **187** synthetisiert.

Durch die sorgfältige Auswahl der Substituenten der jeweiligen Pyridylstyrole **174** kann somit die Produktformation perfekt gesteuert werden und unter den optimalen Reaktionsbedingungen wurde stets nur das gewünschte Produkt erhalten.

Zusammenfassend kann gesagt werden, dass durch diese Arbeit weitere, wertvolle Anwendungsbeispiele des immer noch neuen hypervalenten Iod Reagenzes **35** gezeigt wurden und ein erstes Beispiel für ein Substrat-dirigierendes Konzept in der hypervalenten Iodchemie entwickelt wurde.

Eine wichtige Rolle in der weiteren Verwendung des Lewis Basen dirigierten, oxidativen Umpolung Konzeptes wird das bessere Verständnis des vorliegenden Mechanismus spielen. Computerberechnungen, zusammen mit passenden Experimenten haben sich schon oft als äußerst hilfreich herausgestellt und können tiefe Einblicke in den Mechanismus und eventuell vorliegende, elektrostatische Wechselwirkungen geben. Glücklicherweise konnten wir bereits Kooperationen mit den Gruppen von Professor Huber und Professor Legault starten und erste Berechnungen werden bereits durchgeführt. Mithilfe ihrer Erkenntnisse zu weiteren, nutzbaren Lewis Basen und Anforderungen an die hypervalenten Iod Reagenzien für die Durchführung der Umpolungsreaktionen können bald Weiterentwicklungen erwartet werden.

Eine wichtige Verbesserung des entwickelten Konzeptes wäre zudem die Möglichkeit, *C*-Nukleophile in die Moleküle einbauen zu können. Dieses Problem könnte durch das Einsetzen von Derivaten des *F*-iodans **35** gelöst werden. Zwei vielversprechende Reagenzien wurden erst vor kurzem entwickelt und erste Anwendungen veröffentlicht (Schema 42). Das Phenyl-substituierte λ^3-*F*-iodan **35a** wurde verwendet, um das unsymmetrische Diaryliodonium Salz **196** aus dem Aromaten **195** mit einer Elektronendonor-Gruppe herzustellen.[139] Derivat **35b** mit zwei CF_3-Gruppen auf der anderen Seite, zeigte sein Potential in der Iod(III)veretherung von Alkin **197** zu der Verbindung **198**.[141] Beide λ^3-*F*-iodane besitzen eine außergewöhnliche Affinität zu Kohlenstoff-Verbindungen und könnten sich als erfolgreiche Oxidationsreagenzien für die Einführung von *C*-Nukleophilen in dem gezeigten Koordinationskonzept beweisen.

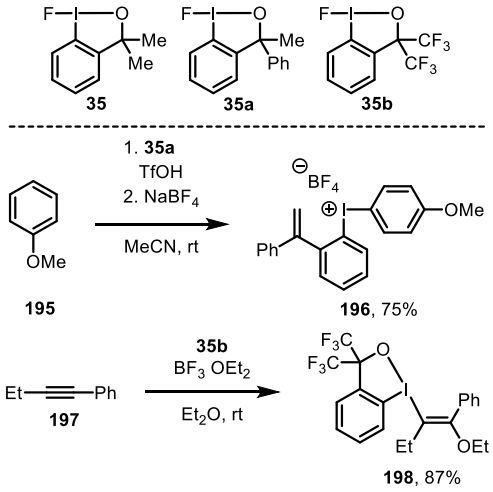

*Schema 42: Derivate **35a** und **35b** und deren Anwendungen.*

Des Weiteren könnte durch die Einführung von aromatischen Substituenten, das *F*-iodan **35** optimal auf die gewünschte Wechselwirkung mit einer Eletronendonor-Gruppe eingestellt werden und weitere Lewis Basen, wie z.B. Phenole oder Furane in den Substraten ausprobiert werden.

III. Methods & Experimental Procedures

1. General Methods

1.1. Preliminary Remarks

Schlenk flasks were dried under vacuum at 250 °C and all air or moisture sensitive reactions carried out under an argon atmosphere utilizing the Schlenk techniques.[142]
Solvent and eluent mixtures are understood as volume / volume (v/v).
Chemicals and reagents, if not otherwise noted, were purchased at the highest purity commercially available (*abcr, Acros Organics, Alfa Aesar, Carbolution, Fisher Scientific, Merck, Sigma Aldrich, Strem Chemicals, TCI)* and used without further purification.

1.2. Solvents

Dichloromethane (DCM), diethyl ether (Et_2O) and tetrahydrofuran (THF) were purified and dried for use under argon atmosphere through a solvent purification system (SPS-800) from M. Braun GmbH *via* the following phases:

Dichloromethane:	2 × MB-KOL-A (alumina)
Diethyl ether:	1 × MB-KOL-A (alumina), 1× MB-KOL-M Type 2 (molecular sieve 3 Å)
Tetrahydrofuran:	2 × MB-KOL-M Type 2 (molecular sieve 3Å)

HPLC grade solvents (acetonitrile, *n*-hexan, *iso*-propanol) and analytical grade ethyl acetate were purchased from *Fisher Scientific.* Solvents for column chromatography, thin layer chromatography (TLC) and for moisture and air insensitive reactions (aceton, chloroform, dichloromethane, diethyl ether, *n*-hexan, methanol, *n*-pentan) were purified by simple distillation.

1.3 Analytical Methods

Chromatography

Thin-layer chromatography (TLC) for reaction monitoring was carried out with aluminum precast plates from *Merck* (aluminum, silica gel 60, F_{254}). Substances were visualized by fluorescence detection under UV light with the wavelengths λ = 254 nm and λ = 366 nm, or stained by derivatization depending on the functional groups present in staining solutions with subsequent heat treatment:

Potassium permanganate solution ($KMnO_4$):	$KMnO_4$ (4.00 g) and $NaHCO_3$ (2.00 g) in H_2O (100 mL)
Phosphomolybdic acid (PMA):	$12MoO_3 \cdot H_3PO_4$ (10.00 g) in Ethanol (200 mL)

Retardation factor (R_f) values were obtained by applying following equation to the measured distances on the respective TLC:

$$R_f = \frac{migration\ distance\ of\ substance}{migration\ distance\ of\ solvent\ front}$$

Silica gel 60 (230-400 mesh ASTM, pore size: 40-63 μm) from *Acros Organics* was used for the purification by column chromatography.

High-pressure liquid chromatography (HPLC)

High-pressure liquid chromatography (HPLC) for analytical separation was carried out on a CHROMASTER system from *Hitachi* (autosampler 5210, pumping system 5110, diode array detector 5430 and column oven 5310). System control and evaluation of the measurements were carried out with the software EZCHROM ELITE. The mobile phase acetonitrile, water, *iso*-propanol and *n*-hexane were used in HPLC grade with acidic additive (0.01% trifluoroacetic acid).

Nuclear magnetic resonance (NMR)

NMR spectra were recorded on *Bruker* AV300, *Bruker* AV400, *Bruker* AV500, or *Bruker* AV500-cryo spectrometers. The spectra were calibrated using residual undeuterated solvent as an internal reference (^{1}H-NMR: $CDCl_3$ δ = 7.26 ppm, D_3COD δ = 3.31 ppm; ^{13}C-NMR $CDCl_3$ δ = 77.16 ppm, D_3COD δ = 49 ppm). The following abbreviations, or combinations thereof were used to explain the multiplicities: s = singlet, d = doublet, dd = doublet of doublets, t = triplet, dt = doublet of triplets, q = quartet, p = pentet, quint = quintet (with 1:2:3:2:1 intensity), hept = heptet, m = multiplet, br = broad.

The reported coupling constants *J* correspond to the mean values of the experimentally found values in Hertz (Hz).

Gas Chromatography (GC)

Gas chromatographies (GC) were conducted on an *Agilent* 6890 gas chromatograph (carrier gas: hydrogen, standard method: 60 °C 3 min, 15 °C/min → 250 °C, 250 °C 5 min) on a column HP5 (5%-phenyl)-methylpolysiloxane).

Mass Spectrometry (MS)

Electron ionization (EI) mass spectroscopies were conducted on an *Agilent* 5973 Network Mass Selective Detector (70 eV) after an *Agilent* 6890 gas chromatograph (carrier gas: Helium, standard method: 60 °C 3 min, 15 °C/min → 250 °C, 250 °C 5 min) on a column HP5 (30 m, 95% dimethylpolysiloxan, 5% diphenylpolysiloxan, layer thickness 25 – 50 μm).

Electrospray ionization (ESI) mass spectra were recorded on an *Advion* Mass Express™ Compact mass spectrometer or on a *Finnigan* LCQ™ classic.

Intensities of the peaks were given in relation to the basis peak (I = 100%).

High resolution mass spectra (HRMS) were recorded *via* electrospray ionization (ESI) on an LTQ-ORBITRAP XL spectrometer from *ThermoFisher Scientific*.

Infrared spectroscopy (IR)

Infrared spectroscopy spectra were recorded on a *JASCO* FT/IR-spectrometer by ATR technique and are reported in terms of frequency of absorption (cm^{-1}).

Melting Points (M.p.)

Melting points were measured on a *Büchi* 510 and are not calibrated. Solvents from which the solid crystallized were reported in parenthesis.

2. Synthetic Procedures & Analytical Data

2.1 Synthetic Procedures

General Procedure for the Synthesis of Pyridylstyrenes 178 and 186:

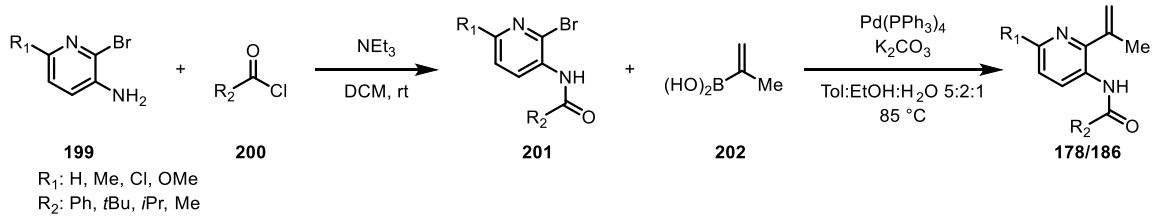

Pyridylamine **199** (1.0 equiv.) was dissolved in dry DCM (0.5 M) and triethylamine (1.2 equiv.) and the respective acid chloride **200** (1.2 equiv.) added slowly. The mixture was stirred overnight, H_2O (30 mL) added afterwards, and the mixture extracted with DCM (3x30 mL). The combined organic phases were washed with brine, dried over Na_2SO_4, filtered and the filtrate evaporated under reduced pressure. The crude mixture was purified by column chromatography on silica gel if necessary (purity checked by TLC).

Next, pyridylamide **201** (1.0 equiv.) was dissolved in a solvent mixture of toluene:ethanol:water 5:2:1 (0.1 M) and the crude mixture degassed under argon atmosphere. Boronic acid **202** (1.5 equiv.), K_2CO_3 (4 equiv.) and $Pd(PPh_3)_4$ (0.1 equiv.) were added and the crude mixture stirred at 85 °C overnight. After cooling to room temperature, H_2O (30 mL) was added, and the mixture extracted with Et_2O (3x30 mL). The combined organic phases were dried over Na_2SO_4, filtered and the filtrate evaporated under reduced pressure. The crude mixture was purified by column chromatography on silica gel.

General Procedure A (GPA) for the Synthesis of α-functionalized Ketones 179:

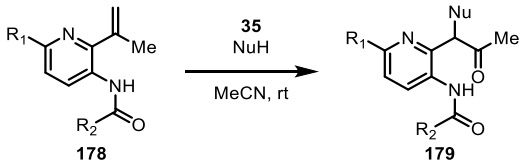

Pyridylstyrene **178** (0.20 mmol, 1.00 equiv.) and NuH (0.22 mmol, 1.10 equiv.) were dissolved in 1 mL MeCN (0.2 M). *F*-iodane **35** (140 mg, 0.50 mmol, 2.50 equiv.) was added and the reaction mixture stirred at rt until full consumption of the styrene (TLC). The solvent was evaporated under reduced pressure and the crude mixture purified by column chromatography on silica gel.

General Procedure B (GPB) for the Synthesis of Imidazo[1,5-*a*]pyridines 187:

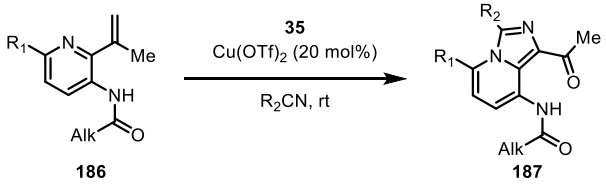

Pyridylstyrene **186** (0.20 mml, 1.00 equiv.) and *F*-iodane **35** (140 mg, 0.50 mmol, 2.50 equiv.) were dissolved in 1 mL R_2CN (0.2 M). $Cu(OTf)_2$ (14.5 mg, 20.0 mol%) was added and the reaction mixture stirred at rt until full consumption of the styrene (TLC). The solvent was evaporated under reduced pressure and the crude mixture purified by column chromatography on silica gel.

Procedure for the Equivalent Screening of *F*-iodane 35 in the conversion towards compound 187a:

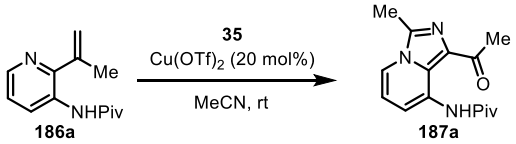

Pyridylstyrene **186a** (21.8 mg, 0.10 mml), *F*-iodane **35** (1.0 - 5.0 equiv.) and the internal standard mesitylene (0.80 - 1.56 equiv.) were dissolved in 1 mL MeCN (0.2 M). $Cu(OTf)_2$ (7.2 mg, 20 mol%) was added and the reaction mixture stirred at room temperature. 10 µl aliquots were taken at allotted times, filtered through a silica plug and diluted with EtOAc (1 mL). A GC measurement was performed of the samples and the product yield obtained. The relative response factor of the product to the internal standard was calculated by separate measurements of known amounts of product and internal standard.

2.2 Analytical Data

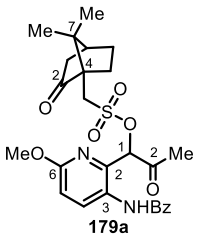

179a

1-(3-benzamido-6-methoxypyridin-2-yl)-2-oxopropyl ((1*S*,4*S*)-7,7-dimethyl-2-oxobicyclo[2.2.1]heptan-1-yl)methanesulfonate (179a):

Following **GPA** using **178a** (53.7 mg, 0.20 mmol), product **179a** was isolated after 30 min as a light-yellow oil (49.0 mg, 95.2 µmol, 48% yield, d.r. = 50:50).

R_f = 0.35 (EtOAc/hexanes 33:67);

^{1}H NMR (300 MHz, $CDCl_3$) diastereomeric mixture δ = 8.75 (d, *J* = 15.8 Hz, 1H), 8.23 (d, *J* = 8.9 Hz, 1H), 8.08 – 7.95 (m, 2H), 7.64 – 7.45 (m, 3H), 6.88 (d, *J* = 8.9 Hz, 1H), 6.24 (d., s, 1H), 6.21 (d., s, 1H), 3.91 (d., s, 3H), 3.90 (d., s, 3H), 3.70 (d., d, *J* = 15.1 Hz, 1H), 3.60 (d., d, *J* = 14.9 Hz, 1H), 3.18 (d., d, *J* = 14.9 Hz, 1H), 3.16 (d., d, *J* = 15.1 Hz, 1H), 2.44 – 2.28 (m, 2H), 2.26 (d., s, 3H), 2.26 (d., s, 3H), 2.16 – 2.04 (m, 1H), 2.10 – 1.94 (m, 1H), 1.90 (dd, *J* = 18.6, 9.4 Hz, 1H), 1.82 – 1.65 (m, 1H), 1.49 – 1.35 (m, 1H), 1.04 (d., s, 3H), 1.03 (d., s, 3H), 0.83 (d., s, 3H), 0.80 (d., s, 3H) ppm;

^{13}C NMR (76 MHz, $CDCl_3$) diastereomeric mixture δ = 214.2, 214.1, 200.3, 200.2, 166.4, 166.3, 161.2, 161.1, 140.8, 137.8, 137.7, 133.6, 133.6, 132.4, 132.3, 128.9, 128.4, 128.2, 127.6, 113.30, 113.27, 82.83, 82.64, 58.26, 58.14, 54.00, 53.97, 49.53, 49.33, 48.29, 48.28, 42.88, 42.82, 42.57, 27.24, 27.17, 27.01, 27.99, 25.32, 25.06, 19.79, 19.76, 19.70 ppm;

IR (ATR): $\tilde{\upsilon}_{max}$ = 3346, 2961, 1744, 1488, 1355, 1272, 1172, 1039, 956, 850, 711 cm^{-1};

MS (EI, positive): *m*/*z* (%) = 282 (22) $[M\text{-}CSA\text{-}H]^+$, 105 (100);

HRMS (ESI, positive) calcd. for $C_{26}H_{31}N_2O_7S$ $[M+H]^+$ 515.1846, found 515.1846.

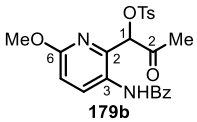

179b

1-(3-benzamido-6-methoxypyridin-2-yl)-2-oxopropyl 4-methylbenzenesulfonate (179b):

Following **GPA** using **178a** (53.7 mg, 0.20 mmol), product **179b** was isolated after 30 min as a light-yellow oil (44.8 mg, 98.6 µmol, 49% yield, keto/enol: 90:10 in $CDCl_3$).

R_f = 0.46 (EtOAc/hexanes 33:67);

^{1}H NMR (400 MHz, $CDCl_3$) δ = 8.70 (s, 1H), 8.25 (d, *J* = 8.9 Hz, 1H), 8.03 – 7.94 (m, 2H), 7.74 – 7.66 (m, 2H), 7.61 – 7.55 (m, 1H), 7.55 – 7.46 (m, 2H), 7.21 (d, *J* = 8.1 Hz, 2H), 6.77 (d, *J* = 8.9 Hz, 1H), 6.08 (s, 1H), 3.83 (s, 3H), 2.39 (s, 3H), 2.23 (s, 3H) ppm;

^{13}C NMR (101 MHz, $CDCl_3$) δ = 200.6, 165.9, 160.6, 145.7, 139.4, 136.8, 133.6, 132.6, 132.4, 129.9, 128.9, 128.3, 128.1, 127.5, 112.8, 82.98, 53.83, 27.24, 21.79 ppm;

IR (ATR): $\tilde{\upsilon}_{max}$ = 1743, 1663, 1489, 1270, 1175, 956, 709, 676 cm^{-1};

MS (ESI, positive): *m*/*z* (%) = 455 (100) $[M+H]^+$, 283 (100) $[M\text{-}OTs]^+$;

HRMS (ESI, positive) calcd. for $C_{16}H_{15}N_2O_3$ $[M\text{-}OTs]^+$ 283.1083, found 283.1081.

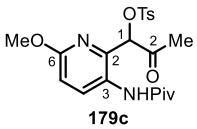

179c

1-(6-methoxy-3-pivalamidopyridin-2-yl)-2-oxopropyl 4-methylbenzenesulfonate (179c):

Following **GPA** using **178b** (49.7 mg, 0.20 mmol), product **179c** was isolated after 45 min as a light-yellow oil (46.0 mg, 106 µmol, 53% yield).

R_f = 0.41 (EtOAc/hexanes 25:75);

^{1}H NMR (300 MHz, $CDCl_3$) δ = 8.08 (d, *J* = 8.9 Hz, 1H), 8.00 (s, 1H), 7.75 – 7.65 (m, 2H), 7.27 – 7.22 (m, 2H), 6.69 (d, *J* = 8.9 Hz, 1H), 5.97 (s, 1H), 3.80 (s, 3H), 2.40 (s, 3H), 2.19 (s, 3H), 1.31 (s, 9H) ppm;

^{13}C NMR (75 MHz, $CDCl_3$) δ = 200.2, 177.8, 160.4, 145.6, 139.0, 136.7, 132.8, 129.9, 128.4, 128.2, 112.4, 83.67, 53.75, 39.75, 27.49, 27.04, 21.76 ppm;

IR (ATR): $\tilde{\upsilon}_{max}$ = 2972, 1753, 1622, 1175, 1121, 1034, 1010, 817, 682 cm^{-1};

MS (ESI, positive): *m*/*z* (%) = 435 (24) $[M+H]^+$, 263 (100) $[M\text{-}OTs]^+$;

HRMS (ESI, positive) calcd. for $C_{14}H_{19}N_2O_3$ $[M\text{-}OTs]^+$ 263.1396, found 263.1392.

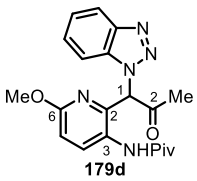

179d

***N*-(2-(1-(1*H*-benzo[*d*][1,2,3]triazol-1-yl)-2-oxopropyl)-6-methoxypyridin-3-yl)-pivalamide (179d):**

Following **GPA** using **178b** (49.7 mg, 0.20 mmol), product **179d** was isolated after 24 h as a light-yellow solid (41.9 mg, 110 µmol, 55% yield).

M.p. = 71 °C (DCM);

R_f = 0.15 (EtOAc/hexanes 25:75);

^{1}H NMR (400 MHz, $CDCl_3$) δ = 8.31 (s, 1H), 8.01 (d, *J* = 8.4 Hz, 1H), 7.91 (d, *J* = 8.8 Hz, 1H), 7.54 (d, *J* = 8.4 Hz, 1H), 7.47 – 7.41 (m, 1H), 7.39 – 7.31 (m, 1H), 6.88 – 6.77 (m, 2H), 3.94 (s, 3H), 2.33 (s, 3H), 1.31 (s, 9H) ppm;

^{13}C NMR (101 MHz, $CDCl_3$) δ = 198.7, 178.3, 161.0, 146.1, 142.9, 138.7, 133.4, 128.2, 128.2, 124.6, 120.1, 112.8, 111.3, 71.24, 54.07, 39.64, 27.82, 27.51 ppm;

IR (ATR): $\tilde{\upsilon}_{max}$ = 2967, 1734, 1665, 1479, 1263, 1036, 824, 746 cm^{-1};

MS (ESI, positive): *m*/*z* (%) = 382 (100) $[M+H]^+$, 263 (52) $[M\text{-}N_3C_6H_4]^+$;

HRMS (ESI, positive) calcd. for $C_{20}H_{24}N_5O_3$ $[M+H]^+$ 382.1874, found 382.1881.

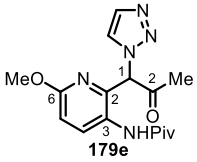

179e

***N*-(6-methoxy-2-(2-oxo-1-(1*H*-1,2,3-triazol-1-yl)propyl)pyridin-3-yl)pivalamide (179e):**

Following **GPA** using **178b** (49.7 mg, 0.20 mmol), product **179e** was isolated after 4 h as a yellow oil (17.9 mg, 45.0 µmol, 27% yield).

R_f = 0.19 (EtOAc/hexanes 33:67);

^{1}H NMR (300 MHz, $CDCl_3$) δ = 8.34 (s, 1H), 7.90 (d, *J* = 8.9 Hz, 1H), 7.84 (d, *J* = 1.1 Hz, 1H), 7.71 (d, *J* = 1.1 Hz, 1H), 6.82 (d, *J* = 8.8 Hz, 1H), 6.59 (s, 1H), 3.88 (s, 3H), 2.25 (s, 3H), 1.34 (s, 9H) ppm;

^{13}C NMR (101 MHz, $CDCl_3$) δ = 198.3, 178.4, 161.3, 143.1, 138.8, 134.0, 128.0, 125.0, 112.9, 70.58, 53.97, 39.65, 27.80, 27.58 ppm;

IR (ATR): $\tilde{\upsilon}_{max}$ = 2964, 1737, 1664, 1481, 1263, 1032, 736 cm^{-1};

MS (ESI, positive): *m*/*z* (%) = 332 (54) $[M+H]^+$, 263 (100) $[M\text{-}N_3C_2H_2]^+$;

HRMS (ESI, positive) calcd. for $C_{14}H_{19}N_2O_3$ $[M\text{-}C_2H_2N_3]^+$ 263.1396, found 263.1395.

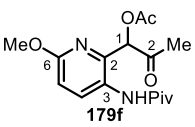

179f

1-(6-methoxy-3-pivalamidopyridin-2-yl)-2-oxopropyl acetate (179f):
Following **GPA** using **178b** (49.7 mg, 0.20 mmol), product **179f** was isolated after 18 h as a light-yellow oil (17.2 mg, 53.3 µmol, 27% yield).

R_f = 0.53 (EtOAc/hexanes 25:75);

^{1}H NMR (300 MHz, $CDCl_3$) δ = 8.34 (d, *J* = 9.0 Hz, 1H), 8.30 (br. s, 1H), 6.77 (d, *J* = 9.0 Hz, 1H), 6.14 (s, 1H), 3.90 (s, 3H), 2.21 (s, 3H), 2.18 (s, 3H), 1.33 (s, 9H) ppm;

^{13}C NMR (75 MHz, $CDCl_3$) δ = 201.2, 177.4, 169.7, 160.3, 138.6, 135.7, 129.0, 112.1, 81.48, 53.80, 39.85, 27.54, 26.93, 20.75 ppm;

IR (ATR): $\tilde{\upsilon}_{max}$ = 3345, 2966, 1731, 1479, 1262, 1220, 1034, 917, 829 cm^{-1};

MS (EI): *m*/*z* (%) = 322 (9) [M], 280 (25), 262 (10), 237 (66);

HRMS (ESI, positive) calcd. for $C_{16}H_{23}N_2O_5$ $[M+H]^+$ 323.1601, found 323.1604.

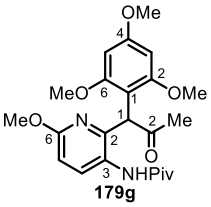

179g

***N*-(6-methoxy-2-(2-oxo-1-(2,4,6-trimethoxyphenyl)propyl)pyridin-3-yl)pivalamide (179g):**
Following **GPA** using **178b** (49.7 mg, 0.20 mmol), product **179g** was isolated after 2 h 30 min as a colorless oil (29.5 mg, 68.5 µmol, 34% yield).

R_f = 0.10 (EtOAc/hexanes 17:83);

^{1}H NMR (500 MHz, $CDCl_3$) δ = 7.87 (d, *J* = 8.7 Hz, 1H), 7.38 (s, 1H), 6.59 (d, *J* = 8.7 Hz, 1H), 6.15 (s, 2H), 5.31 (s, 1H), 3.82 (s, 3H), 3.66 (s, 6H), 3.65 (s, 3H), 2.23 (s, 3H), 1.18 (s, 9H) ppm;

^{13}C NMR (101 MHz, $CDCl_3$) δ = 207.7, 177.1, 161.2, 159.9, 159.3, 147.8, 135.8, 126.6, 108.6, 106.4, 91.09, 55.90, 55.50, 53.73, 53.17, 39.33, 29.13, 27.49 ppm;

IR (ATR): $\tilde{\upsilon}_{max}$ = 3406, 2961, 1705, 1677, 1592, 1459, 1257, 1149, 1117, 1034, 816, 734 cm^{-1};

MS (ESI, positive): *m*/*z* (%) = 431 (100) $[M+H]^+$;

HRMS (ESI, positive) calcd. for $C_{23}H_{31}N_2O_6$ $[M+H]^+$ 431.2177, found 431.2185.

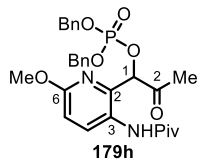

179h

Dibenzyl (1-(6-methoxy-3-pivalamidopyridin-2-yl)-2-oxopropyl) phosphate (179h): Following **GPA** using **178b** (49.7 mg, 0.20 mmol), product **179h** was isolated after 1 h as a yellow oil (43.6 mg, 80.6 µmol, 41% yield).

R_f = 0.45 (EtOAc/hexanes 33:67);

^{1}H NMR (500 MHz, $CDCl_3$) δ = 8.71 (s, 1H), 8.10 (d, *J* = 8.9 Hz, 1H), 7.37 – 7-30 (m, 5H), 7.28 – 7.24 (m, 3H), 7.18 – 7.09 (m, 2H), 6.75 (d, *J* = 8.9 Hz, 1H), 5.79 (d, *J* = 8.3 Hz, 1H), 5.14 (d, *J* = 8.1 Hz, 2H), 4.92 – 4.82 (m, 2H), 3.83 (s, 3H), 2.08 (s, 3H), 1.30 (s, 9H) ppm;

^{13}C NMR (101 MHz, $CDCl_3$) δ = 200.6 (d, *J* = 6.3 Hz), 178.1, 160.6, 141.1 (d, *J* = 3.6 Hz), 137.3, 135.4 (d, *J* = 7.3 Hz), 135.1 (d, *J* = 7.0 Hz), 128.9, 128.7, 128.6, 128.6, 128.1, 127.9, 112.6, 81.44 (d, *J* = 5.3 Hz), 70.16 (d, *J* = 5.7 Hz), 69.79 (d, *J* = 5.7 Hz), 53.72, 39.66, 27.47, 26.77 ppm;

^{31}P NMR (162 MHz, $CDCl_3$) δ = -1.41 (h, *J* = 8.1, 7.5 Hz) ppm;

IR (ATR): $\tilde{\upsilon}_{max}$ = 2963, 1739, 1679, 1478, 1263, 1007, 736, 696 cm^{-1};

MS (ESI, positive): *m*/*z* (%) = 541 (100) $[M+H]^+$, 563 (37) $[M+Na]^+$, 263 (50) $[M\text{-}O_2P(OBn)_2]^+$;

HRMS (ESI, positive) calcd. for $C_{28}H_{34}N_2O_7P$ $[M+H]^+$ 541.2098, found 541.2112.

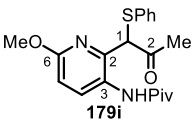

179i

***N*-(6-methoxy-2-(2-oxo-1-(phenylthio)propyl)pyridin-3-yl)pivalamide (179i):** Following **GPA** using **178b** (24.8 mg, 0.10 mmol), product **179i** was isolated after 5 h as a light-yellow oil (11.8 mg, 31.7 µmol, 32% yield).

R_f = 0.31 (EtOAc/hexanes 17:83);

^{1}H NMR (400 MHz, $CDCl_3$) δ = 8.18 (s, 1H), 8.06 (d, *J* = 8.8 Hz, 1H), 7.35 – 7.29 (m, 2H), 7.26 – 7.19 (m, 3H), 6.68 (d, *J* = 8.8 Hz, 1H), 5.19 (s, 1H), 3.81 (s, 3H), 2.27 (s, 3H), 1.32 (s, 9H) ppm;

^{13}C NMR (75 MHz, $CDCl_3$) δ = 204.3, 177.5, 160.3, 142.7, 136.7, 133.0, 132.2, 129.2, 128.1, 127.5, 110.7, 64.64, 53.83, 39.72, 28.12, 27.63 ppm;

IR (ATR): $\tilde{\upsilon}_{max}$ = 2965, 1682, 1477, 1262, 1150, 1037, 747, 691 cm^{-1};

MS (ESI, positive): *m*/*z* (%) = 373 (100) $[M+H]^+$;

HRMS (ESI, positive) calcd. for $C_{20}H_{25}N_2O_3S$ $[M+H]^+$ 373.1580, found 373.1577.

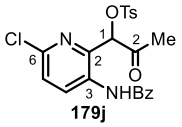

179j

1-(3-benzamido-6-chloropyridin-2-yl)-2-oxopropyl 4-methylbenzenesulfonate (179j):

Following **GPA** using **178c** (54.5 mg, 0.20 mmol), product **179j** was isolated after 1h as a light-yellow oil (26.0 mg, 56.7 µmol, 28% yield, keto/enol: 88:12 in $CDCl_3$).

R_f = 0.35 (EtOAc/hexanes 33:67);

^{1}H NMR (500 MHz, $CDCl_3$) δ = 9.03 (s, 1H), 8.68 (d, *J* = 8.7 Hz, 1H), 8.01 – 7.98 (m, 2H), 7.70 – 7.65 (m, 2H), 7.63 – 7.58 (m, 1H), 7.56 – 7.49 (m, 2H), 7.29 (d, *J* = 8.8 Hz, 1H), 7.22 (d, *J* = 8.1 Hz, 2H), 6.13 (s, 1H), 2.40 (s, 3H), 2.30 (s, 3H) ppm;

^{13}C NMR (101 MHz, $CDCl_3$) δ = 200.8, 165.7, 145.9, 145.3, 140.3, 133.9, 133.8, 133.3, 132.8, 132.4, 130.0, 129.1, 128.1, 127.5, 125.7, 84.41, 27.46, 21.83 ppm;

IR (ATR): $\tilde{\upsilon}_{max}$ = 3316, 1739, 1487, 1175, 814, 707, 672 cm^{-1};

MS (EI): *m*/*z* (%) = 286 (7) [M-TsOH], 243 (100);

HRMS (ESI, positive) calcd. for $C_{22}H_{20}ClN_2O_5S$ $[M+H]^+$ 459.0776, found 459.0779.

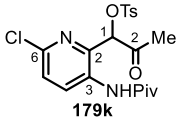

179k

1-(6-chloro-3-pivalamidopyridin-2-yl)-2-oxopropyl 4-methylbenzenesulfonate (179k):

Following **GPA** using **178d** (50.3 mg, 0.20 mmol), product **179k** was isolated after 30 min as a colorless oil (26.0 mg, 59.2 µmol, 30% yield).

R_f = 0.40 (EtOAc/hexanes 17:83);

^{1}H NMR (300 MHz, $CDCl_3$) δ = 8.51 (d, *J* = 8.8 Hz, 1H), 8.38 (s, 1H), 7.76 – 7.61 (m, 2H), 7.28 – 7.24 (m, 2H), 7.22 (d, *J* = 8.8 Hz, 1H), 6.01 (s, 1H), 2.41 (s, 3H), 2.24 (s, 3H), 1.31 (s, 9H) ppm;

^{13}C NMR (101 MHz, $CDCl_3$) δ = 200.0, 177.9, 146.0, 144.9, 140.0, 133.9, 133.8, 132.4, 130.0, 128.3, 125.4, 84.89, 40.21, 27.36, 27.30, 21.81 ppm;

IR (ATR): $\tilde{\upsilon}_{max}$ = 2972, 1765, 1565, 1160, 1122, 1009, 816, 683 cm^{-1};

MS (ESI, positive): *m*/*z* (%) = 267 (100) $[M\text{-OTs}]^+$;

HRMS (ESI, positive) calcd. for $C_{20}H_{24}ClN_2O_5S^+$ $[M+H]^+$ 439.1089, found 439.1089.

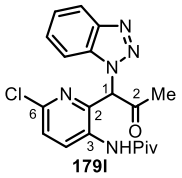

179l

***N*-(2-(1-(1*H*-benzo[*d*][1,2,3]triazol-1-yl)-2-oxopropyl)-6-chloropyridin-3-yl)pivalamide (179l):**

Following **GPA** using **178d** (50.2 mg, 0.20 mmol), product **179l** was isolated after 24 h as a light yellow oil (27.0 mg, 70.0 µmol, 35% yield).

R_f = 0.24 (EtOAc/hexanes 25:75);

^{1}H NMR (300 MHz, $CDCl_3$) δ = 9.21 (s, 1H), 8.26 (d, *J* = 8.6 Hz, 1H), 8.08 (dt, *J* = 8.4, 1.0 Hz, 1H), 7.62 – 7.47 (m, 2H), 7.47 – 7.36 (m, 2H), 6.71 (s, 1H), 2.26 (s, 3H), 1.31 (s, 9H) ppm;

^{13}C NMR (101 MHz, $CDCl_3$) δ = 197.9, 178.4, 146.4, 145.8, 145.4, 137.5, 133.9, 133.6, 128.8, 126.1, 125.0, 120.4, 110.3, 71.93, 39.95, 27.50, 27.35 ppm;

IR (ATR): $\tilde{\upsilon}_{max}$ = 2968, 1738, 1675, 1493, 1451, 1141, 747 cm^{-1};

MS (ESI, positive): *m*/*z* (%) = 388/386 (32/100) $[M+H]^+$;

HRMS (ESI, positive) calcd. for $C_{19}H_{21}ClN_5O_2$ $[M+H]^+$ 386.1378, found 386.1382.

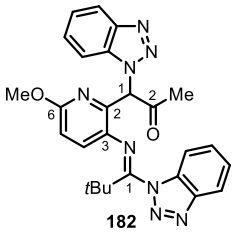

182

1-(3-((1-(1*H*-benzo[*d*][1,2,3]triazol-1-yl)-2,2-dimethylpropylidene)amino)-6-methoxy-pyridin-2-yl)-1-(1*H*-benzo[*d*][1,2,3]triazol-1-yl)propan-2-one (182):

Following **GPA** using **178b** (50.4 mg, 203 µmol) and 3 pieces of 4 Å molecular sieve, product **182** was isolated after 3 h 30 min as a colorless oil (63.8 mg, 132 µmol, 65% yield).

R_f = 0.17 (EtOAc/hexanes 17:83);

^{1}H NMR (400 MHz, $CDCl_3$) δ = 8.17 – 8.09 (m, 1H), 7.83 (d, *J* = 8.5 Hz, 1H), 7.72 (s, 1H), 7.69 – 7.59 (m, 1H), 7.44 – 7.34 (m, 2H), 7.00 (t, *J* = 7.7 Hz, 1H), 6.26 (d, *J* = 13.2 Hz, 1H), 6.22 (s, 1H), 6.18 (d, *J* = 8.9 Hz, 1H), 3.81 (s, 3H), 2.35 (s, 3H), 1.45 (s, 9H) ppm;

^{13}C NMR (101 MHz, $CDCl_3$) δ = 199.3, 161.4, 159.6, 146.7, 144.4, 143.8, 135.1, 133.7, 131.6, 131.1, 128.5, 127.7, 124.4, 124.2, 120.0, 119.7, 112.8, 112.6, 108.9, 70.15, 54.06, 41.94, 28.16, 27.80 ppm;

IR (ATR): $\tilde{\upsilon}_{max}$ = 2971, 1734, 1653, 1596, 1473, 1273, 1035, 979, 844, 744 cm^{-1};

MS (ESI, positive): *m*/*z* (%) = 505 (40) $[M+Na]^+$, 364 (100) $[M-N_3C_6H_4]^+$, 336 (85) $[M-N_3C_6H_4-N_2]^+$;

HRMS (ESI, positive) calcd. for $C_{26}H_{27}N_8O_2^+$ $[M+H]^+$ 483.2251, found 483.2251.

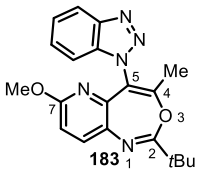

5-(1*H*-benzo[*d*][1,2,3]triazol-1-yl)-2-(tert-butyl)-7-methoxy-4-methylpyrido-[3,2-*d*][1,3]-oxazepine (183):

Compound **182** (62.9 mg, 130 µmol) was dissolved in 6 M $NaOH_{aq}$ (5 mL), and the mixture stirred at room temperature for 15 h. DCM (5 mL) was added and the mixture extracted with DCM (3x10 mL). The combined organic phases were dried over Na_2SO_4, filtered and the solvent evaporated under reduced pressure. The crude mixture was purified by column chromatography on silica gel to obtain product **183** as a colorless crystallin solid (33.6 mg, 92.5 µmol, 71%).

M.p. = 136 °C (DCM);

R_f = 0.67 (EtOAc/hexanes 25:75);

^{1}H NMR (300 MHz, $(CD_3)_2CO$) δ = 8.08 (dt, *J* = 8.3, 0.9 Hz, 1H), 7.62 – 7.51 (m, 2H), 7.49 (d, *J* = 8.6 Hz, 1H), 7.43 (ddd, *J* = 8.1, 6.2, 1.7 Hz, 1H), 6.64 (d, *J* = 8.6 Hz, 1H), 3.02 (s, 3H), 2.02 (s, 3H), 1.41 (s, 9H) ppm;

^{13}C NMR (75 MHz, $(CD_3)_2CO$) δ = 166.1, 161.3, 160.8, 146.3, 143.9, 139.6, 136.1, 135.4, 128.7, 124.6, 123.8, 120.3, 111.6, 111.5, 53.08, 39.75, 28.20, 18.76 ppm;

IR (ATR): $\tilde{\upsilon}_{max}$ = 2960, 1682, 1474, 1264, 1070, 834, 754 cm^{-1};

MS (ESI, positive): *m*/*z* (%) = 364 (100) $[M+H]^+$, 321 (28);

HRMS (ESI, positive) calcd. for $C_{20}H_{22}N_5O_2$ $[M+H]^+$ 364.1768, found 364.1766.

***N*-(6-chloro-2-(2-oxopropyl)pyridin-3-yl)pivalamide (184):**

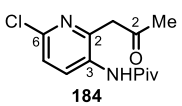

Following **GPA** using **178d** (50.2 mg, 0.20 mmol) and 1,3-indandione (32.2 mg, 0.22 mmol) as the nucleophile, product **184** was obtained after 12 h as an off-white solid (5.7 mg, 21.2 µmol, 21% yield).

M.p. = 76 °C ($CDCl_3$);

R_f = 0.43 (EtOAc/hexanes 33:67);

^{1}H NMR (300 MHz, $CDCl_3$) δ = 8.88 (s, 1H), 8.27 (d, *J* = 8.6 Hz, 1H), 7.25 (d, *J* = 8.5 Hz, 1H), 3.95 (s, 2H), 2.38 (s, 3H), 1.34 (s, 9H) ppm;

^{13}C NMR (101 MHz, $CDCl_3$) δ = 208.5, 178.0, 145.6, 145.4, 134.9, 133.5, 123.6, 50.28, 39.88, 31.36, 27.64 ppm;

IR (ATR): $\tilde{\upsilon}_{max}$ = 2923, 2853, 1698, 1501, 1439, 1137 cm^{-1};

MS (ESI, positive): *m*/*z* (%) = 271/269 (32/100) $[M+H]^+$, 185 (24);

HRMS (ESI, positive) calcd. for $C_{13}H_{18}ClN_2O_2^+$ $[M+H]^+$ 269.1051, found 269.1053.

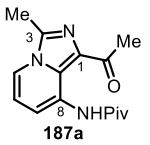

187a

***N*-(1-acetyl-3-methylimidazo[1,5-*a*]pyridin-8-yl)pivalamide (187a):**

Following **GPB** using **186a** (43.7 mg, 0.20 mmol), product **187a** was isolated after 4 h as a yellow solid (24.3 mg, 88.9 µmol, 44% yield).

M.p. = 140 °C (DCM, decomposition);

R_f = 0.27 (EtOAc/hexanes 33:67);

^{1}H NMR (400 MHz, $CDCl_3$) δ = 12.50 (s, 1H), 8.58 (dd, *J* = 7.8, 0.8 Hz, 1H), 7.54 (dd, *J* = 6.8, 0.8 Hz, 1H), 6.91 (dd, *J* = 7.8, 6.7 Hz, 1H), 2.76 (s, 3H), 2.67 (s, 3H), 1.40 (s, 9H) ppm;

^{13}C NMR (101 MHz, $CDCl_3$) δ = 195.9, 179.5, 136.5, 132.5, 129.7, 129.3, 116.4, 116.1, 112.0, 40.79, 27.43, 27.28, 13.09 ppm;

IR (ATR): $\tilde{\upsilon}_{max}$ = 2923, 1671, 1533, 1474, 1424, 1316, 1140, 934, 763, 736 cm^{-1};

MS (ESI, positive): *m*/*z* (%) = 274 (100) $[M+H]^+$, 275 (18);

HRMS (ESI, positive) calcd. for $C_{15}H_{20}N_3O_2$ $[M+H]^+$ 274.1550, found 274.1550.

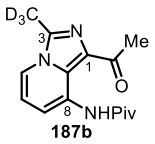

187b

***N*-(1-acetyl-3-(methyl-*d*$_3$)imidazo[1,5-*a*]pyridin-8-yl)pivalamide (187b):**

Following **GPB** using **186a** (43.7 mg, 0.20 mmol), product **187b** was isolated after 3 h 15 min as a yellow solid (24.2 mg, 87.6 µmol, 44% yield).

M.p. = 205 °C (DCM, decomposition);

R_f = 0.24 (EtOAc/hexanes 33:67);

^{1}H NMR (500 MHz, $CDCl_3$) δ = 12.50 (s, 1H), 8.59 – 8.54 (m, 1H), 7.55 – 7.50 (m, 1H), 6.93 – 6.85 (m, 1H), 2.74 (s, 3H), 1.39 (s, 9H) ppm;

^{13}C NMR (126 MHz, $CDCl_3$) δ = 195.9, 179.5, 136.5, 132.5, 129.7, 129.3, 116.4, 116.1, 112.0, 40.76, 27.40, 27.26, 12.37 (hept, *J* = 19.5 Hz) ppm;

IR (ATR): $\tilde{\upsilon}_{max}$ = 2967, 2919, 1673, 1531, 1473, 1426, 1316, 1152, 951, 761, 734 cm^{-1};

MS (ESI, positive): *m*/*z* (%) = 277 (100) $[M+H]^+$, 278 (16);

HRMS (ESI, positive) calcd. for $C_{15}H_{17}D_3N_3O_2$ $[M+H]^+$ 277.1738, found 277.1740.

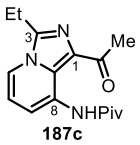

187c

***N*-(1-acetyl-3-ethylimidazo[1,5-*a*]pyridin-8-yl)pivalamide (187c):**
Following **GPB** using **186a** (43.7 mg, 0.20 mmol), product **187c** was isolated after 6 h as a yellow solid (23.7 mg, 82.5 µmol, 41% yield).

M.p. = 143 °C (DCM, decomposition);

R_f = 0.52 (EtOAc/hexanes 33:67);

^{1}H NMR (400 MHz, $CDCl_3$) δ = 12.52 (s, 1H), 8.54 (d, *J* = 7.7 Hz, 1H), 7.56 (d, *J* = 6.8 Hz, 1H), 6.87 (t, *J* = 7.3 Hz, 1H), 2.97 (q, *J* = 7.5 Hz, 2H), 2.75 (s, 3H), 1.44 (t, *J* = 7.5 Hz, 4H), 1.39 (s, 9H) ppm;

^{13}C NMR (101 MHz, $CDCl_3$) δ = 196.1, 179.5, 141.1, 132.6, 129.8, 129.3, 116.2, 116.0, 112.0, 40.76, 27.34, 27.26, 20.30, 10.87 ppm;

IR (ATR): $\tilde{\upsilon}_{max}$ = 2971, 1673, 1616, 1529, 1422, 1271, 1195, 947, 758, 735 cm^{-1};

MS (ESI, positive): *m*/*z* (%) = 288 (100) $[M+H]^+$, 289 (16);

HRMS (ESI, positive) calcd. for $C_{16}H_{21}N_3NaO_2$ $[M+Na]^+$ 310.1531, found 310.1525.

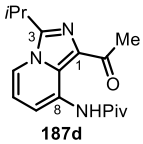

187d

***N*-(1-acetyl-3-isopropylimidazo[1,5-*a*]pyridin-8-yl)pivalamide (187d):**
Following **GPB** using **186a** (43.7 mg, 0.20 mmol), product **187d** was isolated after 23 h as a light-yellow solid (16.7 mg, 55.4 µmol, 28% yield).

M.p. = 95 °C (DCM)

R_f = 0.62 (EtOAc/hexanes 17:83);

^{1}H NMR (400 MHz, $CDCl_3$) δ = 12.55 (s, 1H), 8.53 (d, *J* = 7.7 Hz, 1H), 7.62 (d, *J* = 6.8 Hz, 1H), 6.86 (dd, *J* = 7.7, 6.8 Hz, 1H), 3.28 (hept, *J* = 6.8 Hz, 1H), 2.76 (s, 3H), 1.45 (d, *J* = 6.8 Hz, 6H), 1.39 (s, 9H) ppm;

^{13}C NMR (101 MHz, $CDCl_3$) δ = 196.4, 179.5, 144.7, 132.7, 129.9, 129.3, 116.1, 116.1, 111.9, 40.78, 27.28, 26.29, 20.26 ppm;

IR (ATR): $\tilde{\upsilon}_{max}$ = 2971, 1690, 1620, 1542, 1422, 1296, 1197, 956, 737 cm^{-1};

MS (ESI, positive): *m*/*z* (%) = 302 (100) $[M+H]^+$, 303 (18);

HRMS (ESI, positive) calcd. for $C_{17}H_{23}N_3NaO_2$ $[M+Na]^+$ 324.1688, found 324.1680.

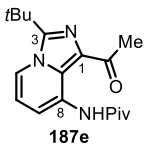

187e

***N*-(1-acetyl-3-(tert-butyl)imidazo[1,5-*a*]pyridin-8-yl)pivalamide (187e):**
Following **GPB** using **186a** (38.5 mg, 0.18 mmol), product **187e** was isolated after 3 h 30 min as a white solid (9.6 mg, 30.4 µmol, 17% yield).

M.p. = 143 °C (DCM, decomposition);

R_f = 0.70 (EtOAc/hexanes 50:50);

^{1}H NMR (300 MHz, $CDCl_3$) δ = 12.58 (s, 1H), 8.52 (dd, *J* = 7.7, 0.6 Hz, 1H), 7.92 (dd, *J* = 7.0, 0.6 Hz, 1H), 6.82 (dd, *J* = 7.7, 7.0 Hz, 1H), 2.76 (s, 3H), 1.56 (s, 9H), 1.39 (s, 9H) ppm;

^{13}C NMR (101 MHz, $CDCl_3$) δ = 196.6, 179.5, 146.3, 132.8, 130.9, 128.5, 118.6, 115.4, 111.7, 40.79, 33.72, 28.23, 27.33, 27.28 ppm;

IR (ATR): $\tilde{\upsilon}_{max}$ = 2972, 1691, 1543, 1475, 1397, 1224, 1105, 952, 738 cm^{-1};

MS (ESI, positive): *m*/*z* (%) = 316 (100) $[M+H]^+$, 317 (20);

HRMS (ESI, positive) calcd. for $C_{18}H_{26}N_3O_2$ $[M+H]^+$ 316.2020, found 316.2015.

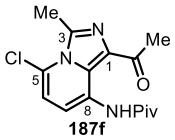

187f

***N*-(1-acetyl-5-chloro-3-methylimidazo[1,5-*a*]pyridin-8-yl)pivalamide (187f):**
Following **GPB** using **186b** (50.5 mg, 0.20 mmol), product **187f** was isolated after 5 h as a yellow solid (18.5 mg, 60.1 µmol, 30% yield).

M.p. = 193 °C (DCM, decomposition);

R_f = 0.67 (EtOAc/hexanes 25:75);

^{1}H NMR (400 MHz, $CDCl_3$) δ = = 12.50 (s, 1H), 8.41 (d, *J* = 8.2 Hz, 1H), 6.80 (d, *J* = 8.2 Hz, 1H), 3.05 (s, 3H), 2.75 (s, 3H), 1.37 (s, 9H) ppm;

^{13}C NMR (101 MHz, $CDCl_3$) δ = = 196.6, 179.4, 138.4, 132.7, 131.4, 129.2, 118.8, 117.6, 112.8, 40.82, 27.81, 27.22, 19.21 ppm;

IR (ATR): $\tilde{\upsilon}_{max}$ = 2967, 1682, 1468, 1364, 1201, 946, 752 cm^{-1};

MS (ESI, positive): *m*/*z* (%) = 310/308 (34/100) $[M+H]^+$;

HRMS (ESI, positive) calcd. for $C_{15}H_{19}ClN_3O_2$ $[M+H]^+$ 308.1160, found 308.1159.

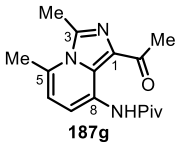

187g

***N*-(1-acetyl-3,5-dimethylimidazo[1,5-*a*]pyridin-8-yl)pivalamide (187g):**
Following **GPB** using **186c** (46.5 mg, 0.20 mmol), product **187g** was isolated after 16 h as a colorless solid (23.0 mg, 80.0 µmol, 40% yield).

M.p. = 222 °C (EtOAc);

R_f = 0.46 (EtOAc/hexanes 40:60);

^{1}H NMR (500 MHz, $CDCl_3$) δ = 12.50 (s, 1H), 8.36 (d, *J* = 7.8 Hz, 1H), 6.52 (d, *J* = 7.8 Hz, 1H), 2.97 (s, 3H), 2.82 (s, 4H), 2.74 (s, 3H), 1.37 (s, 9H) ppm;

^{13}C NMR (101 MHz, $CDCl_3$) δ = 196.0, 179.3, 137.9, 132.1, 130.9, 128.5, 128.3, 117.5, 113.4, 40.72, 27.64, 27.31, 20.77, 18.78 ppm;

IR (ATR): $\tilde{\upsilon}_{max}$ = 2926, 1779, 1685, 1636, 1508, 1363, 1277, 1137, 1057, 942, 840 cm^{-1};

MS (EI, 70 eV): *m*/*z* (%) = 287 (64) $[M+H]^+$, 230 (100) $[M-tBu]^+$;

HRMS (ESI, positive) calcd. for $C_{16}H_{22}N_3O_2^+$ $[M+H]^+$ 288.1707, found 288.1708.

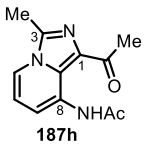

187h

***N*-(1-acetyl-3-methylimidazo[1,5-*a*]pyridin-8-yl)acetamide (187h):**
Following **GPB** using **186d** (35.2 mg, 0.20 mmol), product **187h** was isolated after 6 h 40 min as a light-yellow solid (12.5 mg, 54.1 µmol, 27% yield).

M.p. = 195 °C (DCM, decomposition);

R_f = 0.13 (EtOAc/hexanes 50:50);

^{1}H NMR (400 MHz, $CDCl_3$) δ = 12.90 (s, 1H), 8.41 (d, *J* = 7.7 Hz, 1H), 7.54 (d, *J* = 6.8 Hz, 1H), 6.91 (t, *J* = 7.2 Hz, 1H), 2.75 (s, 3H), 2.67 (s, 3H), 2.31 (s, 3H) ppm;

^{13}C NMR (101 MHz, $CDCl_3$) δ = 196.5, 170.3, 136.7, 131.9, 129.9, 129.1, 116.6, 116.3, 111.5, 27.41, 25.08, 13.01 ppm;

IR (ATR): $\tilde{\upsilon}_{max}$ = 2920, 1688, 1578, 1428, 1302, 932, 779, 748 cm^{-1};

MS (ESI, positive): *m*/*z* (%) = 232 (29) $[M+H]^+$, 190 (100);

HRMS (ESI, positive) calcd. for $C_{12}H_{14}N_3O_2$ $[M+H]^+$ 232.1081, found 232.1073.

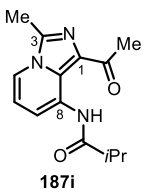

187i

***N*-(1-acetyl-3-methylimidazo[1,5-*a*]pyridin-8-yl)isobutyramide (187i):**

Following **GPB** using **186e** (40.9 mg, 0.20 mmol), product **187i** was isolated after 4 h 45 min as a light-green solid (21.7 mg, 83.7 µmol, 42% yield).

M.p. = 160 °C (DCM, decomposition);

R_f = 0.33 (EtOAc/hexanes 50:50);

^{1}H NMR (400 MHz, $CDCl_3$) δ = 12.81 (s, 1H), 8.46 (dd, *J* = 7.7, 0.8 Hz, 1H), 7.53 (dd, *J* = 6.7, 0.8 Hz, 1H), 6.90 (dd, *J* = 7.7, 6.8 Hz, 1H), 2.80 (hept, *J* = 6.9 Hz, 1H), 2.75 (s, 3H), 2.66 (s, 3H), 1.29 (d, *J* = 6.9 Hz, 6H) ppm;

^{13}C NMR (101 MHz, $CDCl_3$) δ = 196.4, 177.7, 136.6, 132.2, 129.9, 129.2, 116.6, 116.2, 111.6, 37.22, 27.42, 19.53, 13.01 ppm;

IR (ATR): $\tilde{\upsilon}_{max}$ = 2924, 1686, 1536, 1424, 1279, 1197, 936, 762 cm^{-1};

MS (ESI, positive): *m*/*z* (%) = 260 (62) $[M+H]^+$, 190 (100);

HRMS (ESI, positive) calcd. for $C_{14}H_{17}N_3NaO_2$ $[M+Na]^+$ 282.1218 found, 282.1205.

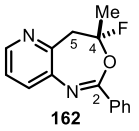

162

4-Fluoro-4-methyl-2-phenyl-4,5-dihydro-6*N*-pyridooxazepine (162):

Following **GPB** using **161** (47.7 mg, 0.20 mmol), product **162** was isolated after 3 h as a colorless oil (32.8 mg, 128 µmol) in 64 % yield.

R_f = 0.65 (EtOAc/hexanes, 65:35);

^{1}H NMR (500 MHz, $CDCl_3$) δ = 8.38 (d, *J* = 4.7 Hz, 1 H), 8.19 (d, *J* = 7.7 Hz, 2 H), 7.61 (d, *J* = 7.9 Hz, 1 H), 7.50–7.55 (m, 1 H), 7.49–7.42 (m, 2 H), 7.31 (dd, *J* = 8.1, 4.6 Hz, 1 H), 3.52–3.41 (m, 2 H), 1.78 (d, *J* =17.8 Hz, 3 H) ppm;

^{19}F NMR (471 MHz, $CDCl_3$) δ = –73.51 (dtd, *J* = 24.0, 17.7, 8.9 Hz) ppm.

The physical and spectroscopic data is in accordance to those reported in the literature.[134]

3. Supporting Information

3.1 α-Functionalization of Ketones via a Nitrogen Directed Oxidative Umpolung

– SUPPORTING INFORMATION –

α-Functionalization of Ketones via a Nitrogen Directed Oxidative Umpolung

Gabriel M. Kiefl,[a] and Tanja Gulder[a,b]*

[a]*Biomimetic Catalysis, Department of Chemistry, Technical University Munich, Lichtenbergstrasse 4, 85747 Garching, Germany*

[b] *Institute of Organic Chemistry, Leipzig University, Johannisallee 29, 04103 Leipzig, Germany*

*corresponding author: tanja.gulder@uni-leipzig.de

Content

1. General Information

Solvents used in reactions were p.A. grade. Solvents for chromatography were technical grade and distilled prior to use. For transformations following GP A and GP B, dichloromethane technical grade was employed and distilled prior to use. The anhydrous dichloromethane used for reactions following GP C and GP D was obtained from a MBraun MB-SPS 800 solvent purification system. The λ^3-Iodane reagents PIFA **13** (Alfa Aesar), Koser's reagent **14** (Carbolution), PIDA **15** (Fluorochem) and *F*-iodane **17** (Fluorochem) were purchased with the highest purity commercially available and used without further purification. λ^3-Iodane reagents **16**, **S1** and **S2** were synthesized following literature procedures.[1] Pyridine·9HF was purchased from Sigma-Aldrich. The reagent was clear in color and used as received. *According to safety, precautions should be taken when handling HF reagents, such as working in a well ventilated fumehood, quenching of excess reagents and keeping calcium gluconate lotion close by at all times!*

Yields refer to chromatographically and spectroscopically (^{1}H-NMR) homogeneous materials, unless otherwise stated. Reactions were monitored by thin layer chromatography (TLC) carried out on Merck silica gel aluminium plates with F-254 indicator using UV light as the visualizing agent (UV), basic potassium permanganate solution (KMnO4), ceric ammonium molybdate (CAN), and heat as developing agents. Silica gel Merck 60 (particle size 40–63µm) was used for flash column chromatography. Solvent mixtures are understood as volume/volume. NMR spectra were recorded on Bruker AV300, Bruker AV400, Bruker AV500, or Bruker AV500-cryo spectrometers. The spectra were calibrated using residual undeuterated solvent as an internal reference ($CDCl_3$ @ 7.26 ppm, D_3COD @ 3.31 ppm ^{1}H-NMR, $CDCl_3$ @ 77.16ppm, D_3COD @ 49ppm ^{13}C-NMR).The following abbreviations (or combinations thereof) were used to explain the multiplicities: s = singlet, d = doublet, dd = doublet of doublets, t = triplet, dt = doublet of triplets, q = quartet, p = pentet, quint = quintet (with 1:2:3:2:1 intensity), hept = heptet, m = multiplet, br = broad. In addition, the following abbreviations were used: EtOAc = ethyl acetate, MeCN = acetonitrile, Et_2O = diethylether, DCM = dichloromethane, HFIP = Hexafluoroisopropanol, MeOH = Methanol, Ts = tosyl, Ms = mesyl, Bn = benzyl, BTA-H = 1*H*-1,2,3-benzotriazole, TLC = thin layer chromatography, rt = room temperature, sat. = saturated, m.p. = melting point, d.p. = decomposition point, d.r. = diastereomeric ratio. The ratio of keto and enol form was determined from the ^{1}H-NMR spectrum. Melting points were measured on a Büchi 510 and are not calibrated. IR spectra were recorded on a JASCO FT-IR-4100 (ATR) and are reported in terms of frequency of absorption (cm^{-1}). Mass spectra were conducted on a Finnigan MAT SSQ 7000 (MS-EI, 70 eV; CI, 100 eV), or a Thermo Scientific LTQ-FT ultra and ThermoFisher Scientific LTQ Orbitrap XL spectrometer (ESI HRMS).

2. Optimization of reaction conditions

Table S1: Evaluation of the optimum reaction conditions.

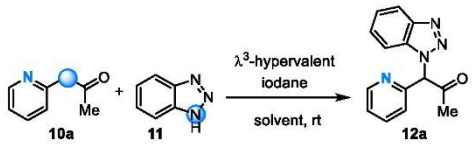

entry	λ³-iodane	Eq. λ³- iodanes	Eq. **11**	solvent	yield[]
1[a]	**17**	1.1	1.1	MeCN	<5%
2[a]	**17**	1.1	1.1	HFIP	32%
3[a]	**17**	1.1	1.1	DCM	55%
4[a]	**17**	1.1	1.1	toluene	54%
5[a]	**17**	1.1	1.1	$CHCl_3$	55%
6[a]	**17**	1.1	1.1	Et_2O	30%
7[a]	**17**	1.1	1.1	THF	<5%
8[a]	**13**	1.1	1.1	DCM	<5%
9[a]	**14**	1.1	1.1	DCM	<5%
10[a]	**15**	1.1	1.1	DCM	25%[i]
11[a]	**16**	1.1	1.1	DCM	53%
12[a]	**S1**	1.1	1.1	DCM	<5%
13[a]	**S2**	1.1	1.1	DCM	<5%
14[b]	**17**	1.5	2.5	DCM	43%
15[c]	**17**	2.0	2.5	DCM	38%
16[d]	**17**	2.5	2.5	DCM	31%
17[a][e]	**17**	1.1	1.1	DCM	54%
18[f]	**17**	0.9	2.0	DCM	65%
19[f]	**17**	0.9	5.0	DCM	70%
20[f]	**17**	0.9	3.0	DCM	72%, 66%[h]

[a]ketone **10a** (0.1 mmol), iodane (0.11 mmol) and BTA-H (**11**, 0.11 mmol) were stirred at rt for 1h in 0.2 M solvent [b]**10a** (0.10 mmol), **17** (0.15 mmol) and **11** (0.25 mmol) were stirred at rt in DCM (0.2 M) [c]**10a** (0.10 mmol), **17** (0.20 mmol) and **11** (0.25 mmol) were stirred at rt in DCM (0.2 M) [d]**10a** (0.10 mmol), **17** (0.25 mmol) and **11** (0.30 mmol) were stirred at rt in DCM (0.2 M) [e]at 0°C, stirred for 2 h [f]**10a** (0.11 mmol), **17** (0.10 mmol) and **11** were stirred at rt in DCM (0.2 M) [g]yield determined from the crude ^{1}H-NMR spectrum using an internal standard [h]isolated yield.

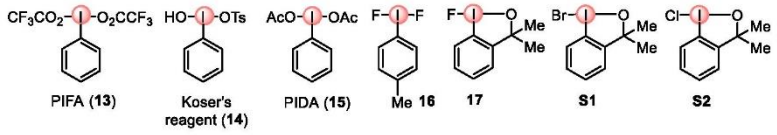

3. General Procedures

General Procedure A (GPA):

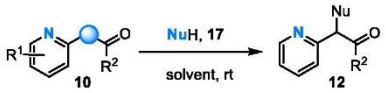

Substrate **10** (0.11 mmol) was dissolved in 0.50 mL DCM and the nucleophile (NuH, 0.30 mmol) together with the F-iodane **17** (28.0 mg, 0.10 mmol) were added. The reaction mixture was stirred at rt until no starting material was observed by TLC. The crude reaction mixture was directly purified by column chromatography on silica gel.

General Procedure B (GPB; 1 mmol scale):

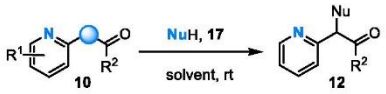

Substrate **10** (1.10 mmol) was dissolved in 5.0 mL DCM and the nucleophile (3.00 mmol) together with the F-iodane **17** (280 mg, 1.00 mmol) were added. the reaction mixture was stirred at rt until no starting material was observed by TLC. The solvent of the crude reaction mixture was evaporated under reduced pressure and subsequently purified by column chromatography on silica gel.

General Procedure C (GPC):

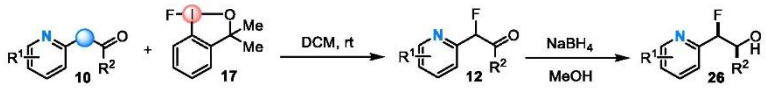

Ketone **10** (0.20 mmol) and F-iodane **17** (56.0 mg, 0.20 mmol) were dissolved in anhydrous DCM (1.00 mL) and stirred until full consumption of the starting material. The reaction mixture was diluted with MeOH (1.00 mL) and $NaBH_4$ (38.0 mg, 1.00 mmol) was added in portions. After the gas development seized, the solvent was evaporated under reduced pressure and the crude mixture purified by column chromatography on silica gel.

General Procedure D (GPD):

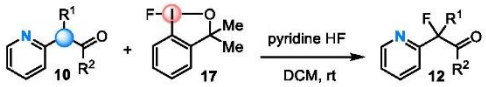

A disubstituted pyridyl ketone **10** (0.20 mmol) was dissolved in anhydrous DCM (1.00 mL) under argon atmosphere in a teflon vial. F-iodane **17** (56.0 mg, 0.20 mmol) and pyridine 9HF (2 drops) were added and the reaction mixture stirred until full consumption of starting material (monitored by TLC). The crude reaction mixture was directly purified by column chromatography.

The iodoarene **S3** was recovered in pure form in 70 - 80% yield (depending on the substrate used in the transformation) and was converted to the *F*-iodane **17** following the literature procedure by Stuart et al.[1b]

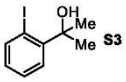

2-(2-iodophenyl)propan-2-ol (S3): ^{1}H NMR (400 MHz, CD_2Cl_2) δ = 7.97 (dd, *J* = 7.8, 1.4 Hz, 1H), 7.65 (dd, *J* = 7.9, 1.7 Hz, 1H), 7.34 (ddd, *J* = 8.0, 7.3, 1.4 Hz, 1H), 6.91 (td, *J* = 7.6, 1.7 Hz, 1H), 2.46 (br s, 1H), 1.73 (s, 6H) ppm.

4. External Nucleophiles failed in the α-Functionalization of Ketones 10

External nucleophiles **S4** – **S14** were treated under the optimized conditions of **GP A** using substrate **10a** but did not yield the corresponding product **12**.

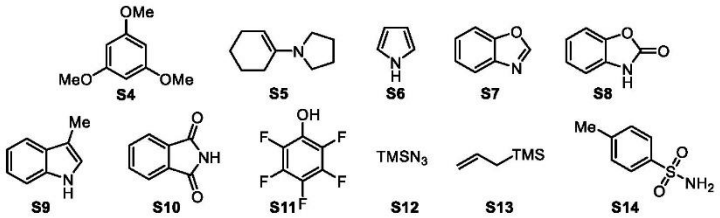

5. Investigation on the Interaction of BTA-H (11) with *F*-Iodane 17

In order to test the influence of the nucleophile and the λ^3-iodane **17** on the reactivity, increasing equivalents of **11** were added to **17** (0.1 M in $CDCl_3$), followed by subsequent ^{19}F- and 1-H-NMR measurements.

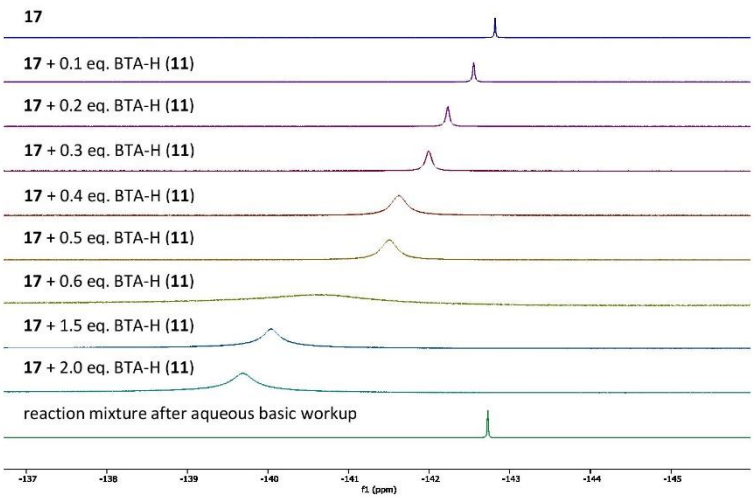

Figure S1: ^{19}F shift of **17** (0.1 M in $CDCl_3$) upon addition of various equivalents of BTA-H (**11**) and after basic extraction, recorded at 300 K with 376 MHz.

The resonance of the fluorine atom in **17** was gradually shifted from - 142.8 ppm to a broadened peak at - 139.7 ppm (**17** + 2.0 eq. BTA-H (**11**)) by increasing the equivalents of **11.** This hints at a strong and dynamic interaction (Figure **S1**). The downfield shift signifies a decrease in electron density at the fluorine.

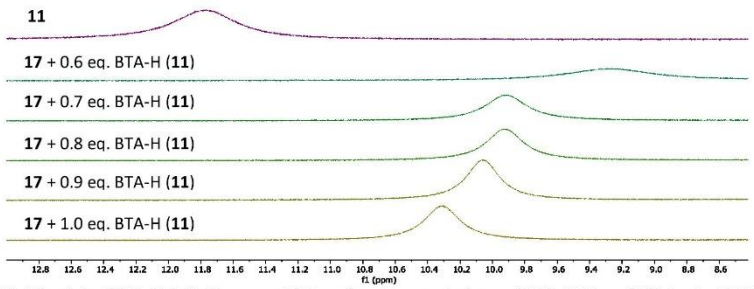

Figure S2: ^{1}H shift of the NH in BTA-H **11** upon addition of various equivalents of BTA-H **11** to **17** (0.1 M in $CDCl_3$), recorded with 400 MHz.

At the same time the chemical shift of the *N*-1 proton in BTA-H (**11**) changes from 11.8 ppm (pure **11**) to 9.27 ppm up-field upon addition of increasing amounts of **11** reaching its maximum in the 0.6 to 1.0

complex of **11** to **17** (0.1 M in $CDCl_3$, Figure **S2**) accounting for an increase in electron density at the *N*-1-*H* bond. The mutual down-field shift of the fluorine in **17** ($\Delta\delta > 3$ ppm with 2 eq. **11**) and the up-field shift of the *N*-1 hydrogen in **11** ($\Delta\delta = 2.5$ ppm with 0.6 eq. **11**) indicates a strong hydrogen bonding between the two structural entities, such as exemplifies in **25**.

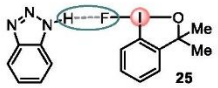

25

Figure S3: Possible H bonding interaction responsible for the activation of the nucleophile **11** and the electrophile **17**

Upon aqueous basic workup of the reaction mixtures (1 mL of a sat. aq. $NaHCO_3$ solution was added to the reaction mixture and after thorough mixing, the organic phase was separated, dried over Na_2SO_4, filtered, and evaporated under reduced pressure. The residue was dissolved in $CDCl_3$ (0.5 mL) and a ^{19}F-NMR spectrum was measured (figure **S1**, bottom), the F atom resonated again at – 142.8 ppm as a sharp signal, which corresponds to the chemical shift of untreated **17**. This corroborates the assumption of a non-covalent interaction between **11** and **17** and excludes the in-situ formation of a BTA-benziodoxole **24** via ligand exchange (Scheme S1).

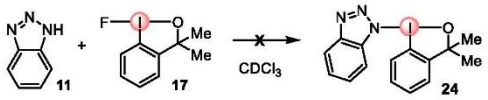

11 **17** **24**

Scheme S4: Formation of a λ^3-hypervalent BTA-iodane **24** upon ligand exchange.

6. Physical and Spectroscopic Data of Products 12a-12al, 21, 26a-b

1-(1*H*-Benzo[*d*][1,2,3]triazol-1-yl)-1-(pyridin-2-yl)propan-2-one (12a): Following **GPA** using **10a** (14.9 mg, 0.11 mmol), product **12a** was isolated after 30 min as a yellow solid (16.7 mg, 66.2 µmol, 66% yield; keto:enol = 1:99 in $CDCl_3$).

Following **GPB** using **10a** (149 mg, 1.10 mmol), product **12a** was isolated after 30 min as a yellow solid (169 mg, 0.67 mmol, 67% yield, keto:enol = 1:99 in $CDCl_3$).

M.p. = 103 °C (EtOAc); **Rf** = 0.30 (EtOAc/hexanes 35:65); **^{1}H NMR** (400 MHz, $CDCl_3$) δ = 8.18 (ddd, *J* = 5.5, 1.7, 1.0 Hz, 1H), 8.15 (dt, *J* = 8.2, 1.0 Hz, 1H), 7.52 – 7.39 (m, 3H), 7.36 (dt, *J* = 8.2, 1.0 Hz, 1H), 6.97 (ddd, *J* = 7.4, 5.5, 1.1 Hz, 1H), 5.95 (dt, *J* = 8.5, 1.1 Hz, 1H), 1.75 (s, 3H) ppm; **^{13}C NMR** (101 MHz, $CDCl_3$) δ = 175.7, 155.3, 146.0, 141.0, 138.9, 134.9, 128.3, 124.4, 120.4, 117.9, 116.7, 109.9, 104.2, 20.56 ppm; **IR** (ATR) $\tilde{\nu}_{max}$ = 2922, 2358, 1632, 1455, 1397, 1064 cm^{-1}; **MS** (EI, 70 eV): *m/z* (%) = 252 (35) $[M]^+$, 210 (100); **HRMS** (ESI) calcd. for $C_{14}H_{13}N_4O$ $[M+H]^+$ 253.1084, found 253.1083.

1-(Pyridin-2-yl)-1-(1*H*-1,2,3-triazol-1-yl)propan-2-one (12d): Following **GPA** using **10a** (14.9 mg, 0.11 mmol), product **12d** was isolated after 45 min as a yellow oil (12.0 mg, 59.3 µmol, 59% yield, keto:enol = 9:91 in $CDCl_3$).

Rf = 0.24 (EtOAc/hexanes 50:50); **^{1}H NMR** (500 MHz, $CDCl_3$) δ = 8.17 (d, *J* = 5.3 Hz, 1H), 7.90 (s, 1H), 7.64 (s, 1H), 7.56 (ddd, *J* = 8.7, 7.3, 1.7 Hz, 1H), 6.99 (ddd, *J* = 6.8, 5.5, 1.1 Hz, 1H), 6.11 (d, *J* = 8.5 Hz, 1H), 1.81 (s, 3H) ppm; **^{13}C NMR** (101 MHz, $CDCl_3$) δ = 173.2, 155.5, 141.5, 138.8, 134.4, 127.6, 118.3, 116.6, 107.0, 20.06 ppm; **IR** (ATR) $\tilde{\nu}_{max}$ = 3121, 1734, 1633, 1559, 1458, 1314, 1228, 1028, 946 cm^{-1}; **MS** (EI, 70 eV): *m/z* (%) = 173 (14) $[M-N_2]$, 105 (100); **HRMS** (ESI) calcd. for $C_{10}H_{11}N_4O$ $[M+H]^+$ 203.0927, found 203.0927.

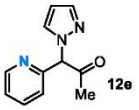

1-(1*H*-Pyrazol-1-yl)-1-(pyridin-2-yl)propan-2-one (12e): Following **GPA** using **10a** (14.9 mg, 0.11 mmol), product **12e** was isolated after 1 h 10 min as a yellow solid (11.0 mg, 54.7 µmol, 55% yield, keto:enol = 9:91 in $CDCl_3$).

M.p. = 102 °C (EtOAc); **Rf** = 0.19 (EtOAc/hexanes 35:65); **^{1}H NMR** (400 MHz, $CDCl_3$) δ = 16.00 (s, 1H), 8.18 (ddd, *J* = 5.4, 1.7, 0.9 Hz, 1H), 7.73 (d, *J* = 1.5 Hz, 1H), 7.55 – 7.48 (m, 1H), 7.45 (dd, *J* = 2.2, 0.7 Hz, 1H), 6.95 (ddd, *J* = 7.4, 5.4, 1.1 Hz, 1H), 6.43 (t, *J* = 2.1 Hz, 1H), 6.18 (dt, *J* = 8.5, 1.1 Hz, 1H), 1.83 (s, 3H) ppm; **^{13}C NMR** (101 MHz, $CDCl_3$) δ = 171.5, 157.1, 142.2, 141.2, 138.3, 133.1, 118.2, 117.2, 110.9, 106.6, 19.46 ppm; **IR** (ATR) $\tilde{\nu}_{max}$ = 3133, 1719, 1631, 1598, 1510, 1366, 1314, 928, 779, 755 cm^{-1}; **MS** (EI, 70 eV): *m/z* (%) = 201 (17) [M], 158 (100) $[M-C_2H_3O]$; **HRMS** (ESI) calcd. for $C_{11}H_{12}N_3O$ $[M+H]^+$ 202.0975, found 202.0975.

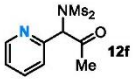

***N*-(Methylsulfonyl)-*N*-(2-oxo-1-(pyridin-2-yl)propyl)methanesulfonamide (12f):** Following **GP A** using **10a** (14.8 mg, 0.11 mmol), product **12f** was isolated after 3h 15 min as a pale-yellow solid (21.5 mg, 70.1 µmol, 70% yield, keto:enol = 1:99 in $CDCl_3$).

M.p. = 111 °C (EtOAc); **Rf** = 0.23 (EtOAc/hexanes 50:50); **^{1}H NMR** (300 MHz, $CDCl_3$) δ = 8.04 (ddd, *J* = 5.6, 1.7, 0.9 Hz, 1H), 7.73 (ddd, *J* = 8.9, 7.3, 1.7 Hz, 1H), 7.23 (dt, *J* = 8.7, 1.0 Hz, 1H), 6.97 (ddd, *J* = 7.3, 5.6, 1.1 Hz, 1H), 3.43 (s, 6H), 2.26 (s, 3H) ppm; **^{13}C NMR** (75 MHz, $CDCl_3$) δ = 182.4, 156.4, 139.7, 139.1, 117.8, 117.3, 101.6, 44.20, 22.86 ppm; **IR** (ATR) $\tilde{\nu}_{max}$ = 3016, 2933, 1626, 1549, 1358, 1341, 1319, 1152 cm^{-1}; **MS** (EI, 70 eV): *m/z* (%) = 207 (1), 183 (2), 147 (4), 105 (100), 78 (18); **HRMS** (ESI) calcd. for $C_{10}H_{15}N_2O_5S_2$ $[M+H]^+$ 307.0417 found 307.0416.

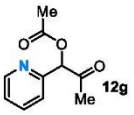

2-Oxo-1-(pyridin-2-yl)propyl acetate (12g): Following **GPA** using **10a** (14.8 mg, 0.11 mmol), product **12g** was isolated after 2 h 30 min as a colorless oil (10.2 mg, 52.8 µmol, 53% yield, keto:enol = 99:1 in $CDCl_3$).

Rf = 0.44 (EtOAc/hexanes 50:50); **^{1}H NMR** (500 MHz, $CDCl_3$) δ = 8.61 (ddd, *J* = 4.9, 1.9, 1.0 Hz, 1H), 7.74 (td, *J* = 7.7, 1.8 Hz, 1H), 7.46 (dt, *J* = 7.8, 1.1 Hz, 1H), 7.29 (ddd, *J* = 7.6, 4.8, 1.2 Hz, 1H), 6.13 (s, 1H), 2.25 (s, 3H), 2.22 (s, 3H) ppm; **^{13}C NMR** (101 MHz, $CDCl_3$) δ = 201.6, 170.1, 153.7, 149.8, 137.4, 123.9, 122.7, 81.73, 27.13, 20.80 ppm; **IR** (ATR) $\tilde{\nu}_{max}$ = 2926, 1730, 1226, 1056, 763 cm^{-1}; **MS** (ESI, 70 eV): *m/z* (%) = 194 (100) $[M+H]^+$, 152 (20); **HRMS** (ESI) calcd. for $C_{10}H_{12}NO_3$ $[M+H]^+$ 194.0812, found 194.0812.

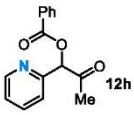

2-Oxo-1-(pyridin-2-yl)propyl benzoate (12h): Following **GPA** using **10a** (14.8 mg, 0.11 mmol), product **12h** was isolated after 3h as a pale yellow oil (11.7 mg, 45.8 µmol, 46% yield, keto:enol = 99:1 in $CDCl_3$).

Rf = 0.21 (EtOAc/hexanes 20:80); **^{1}H NMR** (400 MHz, $CDCl_3$) δ = 8.64 (ddd, *J* = 4.9, 1.8, 0.9 Hz, 1H), 8.18 – 8.10 (m, 2H), 7.79 (td, *J* = 7.7, 1.8 Hz, 1H), 7.63 – 7.57 (m, 2H), 7.47 (dd, *J* = 8.4, 7.0 Hz, 2H), 7.32 (ddd, *J* = 7.7, 4.8, 1.2 Hz, 1H), 6.38 (s, 1H), 2.37 (s, 3H) ppm; **^{13}C NMR** (101 MHz, $CDCl_3$) δ = 201.7, 165.6, 154.0, 149.7, 137.5, 133.7, 130.1, 129.3, 128.6, 124.0, 122.7, 81.90, 27.33 ppm; **IR** (ATR) $\tilde{\nu}_{max}$ = 3062, 1717, 1267, 1108, 709 cm^{-1}; **MS** (ESI): *m/z* (%) = 256 (100) $[M+H]^+$, 105 (30); **HRMS** (ESI) calcd. for $C_{15}H_{14}NO_3$ $[M+H]^+$ 256.0968 found 256.0968.

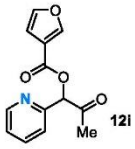

2-Oxo-1-(pyridin-2-yl)propyl furan-3-carboxylate (12i): Following **GPA** using **10a** (14.8 mg, 0.11 mmol), product **12i** was isolated after 3h as a pale yellow oil (14.7 mg, 59.9 µmol, 60% yield, keto:enol = 99:1 in $CDCl_3$).

Rf = 0.42 (EtOAc/hexanes 35:65); **^{1}H NMR** (400 MHz, $CDCl_3$) δ = 8.67 – 8.62 (m, 1H), 8.12 (d, *J* = 29.1 Hz, 1H), 7.77 (td, *J* = 7.7, 1.9 Hz, 1H), 7.53 (d, *J* = 7.8 Hz, 1H), 7.45 (t, *J* = 1.7 Hz, 1H), 7.32 (dd, *J* = 7.8, 5.0 Hz, 1H), 6.79 (dt, *J* = 18.4, 1.0 Hz, 1H), 6.31 (s, 1H), 2.33 (s, 3H) ppm; **^{13}C NMR** (101 MHz, $CDCl_3$) δ = 201.7, 162.0, 153.9, 149.8, 148.6, 144.1, 137.4, 124.0, 122.7, 118.5, 110.1, 81.58, 27.30 ppm; **IR** (ATR) $\tilde{\nu}_{max}$ = 1720, 1589, 1573, 1306, 1159, 1078 cm^{-1}; **MS** (EI, 70 eV): *m/z* (%) = 245 (2) $[M]^+$, 203 (38), 150 (5) $[M\text{-}C_5H_3O_2]^+$, 108 (100); **HRMS** (ESI) calcd. for $C_{13}H_{12}NO_4$ $[M+H]^+$ 246.0761 found 246.0760.

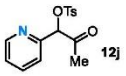

2-Oxo-1-(pyridin-2-yl)propyl-4-methylbenzenesulfonate (12j): Following **GPA** with molecular sieve 3Å (2 pellets) using **10a** (14.9 mg, 0.11 mmol), product **12j** was isolated after 1h 40 min as a yellow oil (22.3 mg, 73.0 µmol, 73% yield, keto:enol = 88:12 in $CDCl_3$).

Rf = 0.26 (EtOAc/hexanes 35:65); **^{1}H NMR** (400 MHz, $CDCl_3$) δ = 8.48 (ddd, *J* = 5.0, 1.8, 0.9 Hz, 1H), 7.77 – 7.71 (m, 2H), 7.67 (td, *J* = 7.8, 1.8 Hz, 1H), 7.33 (dt, *J* = 7.9, 1.2 Hz, 1H), 7.28 – 7.21 (m, 3H), 5.84 (s, 1H), 2.37 (s, 3H), 2.21 (s, 3H) ppm; **^{13}C NMR** (75 MHz, $CDCl_3$) δ = 200.6, 152.7, 149.1, 145.5, 137.9, 132.9, 130.0, 128.2, 124.3, 122.8, 84.79, 26.81, 21.75 ppm; **IR** (ATR) $\tilde{\nu}_{max}$ = 3060, 1735, 1594, 1362, 1225, 1175, 1009, 814, 679 cm^{-1}; **MS** (ESI, 70 eV): *m/z* (%) = 306 (100) $[M+H]^+$, 267 (80), 150 (70); **HRMS** (ESI) calcd. for $C_{15}H_{16}NO_4S$ $[M+H]^+$ 306.0795, found 306.0794.

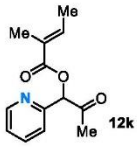

2-Oxo-1-(pyridin-2-yl)propyl (*E*)-2-methylbut-2-enoate (12k): Following **GPA** using **10a** (14.8 mg, 0.11 mmol), product **12k** was isolated after 3h as a colorless oil (7.00 mg, 30.0 µmol, 30% yield, keto:enol = 99:1 in $CDCl_3$).

Rf = 0.60 (EtOAc/hexanes 20:80); **^{1}H NMR** (300 MHz, $CDCl_3$) δ = 8.61 (ddd, *J* = 4.9, 1.8, 0.9 Hz, 1H), 7.75 (td, *J* = 7.7, 1.8 Hz, 1H), 7.50 (dt, *J* = 8.0, 1.2 Hz, 1H), 7.29 (ddd, *J* = 7.6, 4.9, 1.2 Hz, 1H), 7.05 (qq, *J* = 7.0, 1.4 Hz, 1H), 6.18 (s, 1H), 2.31 (s, 3H), 1.90 (dq, *J* = 1.2, 1.2 Hz, 3H)), 1.83 (dq, *J* = 7.1, 1.2 Hz, 3H) ppm; **^{13}C NMR** (75 MHz, $CDCl_3$) δ = 202.3, 167.0, 154.2, 149.5, 139.4, 137.5, 127.8, 123.8, 122.6, 81.47, 27.36, 14.69, 12.21 ppm; **IR** (ATR) $\tilde{\nu}_{max}$ = 2360, 2343, 1717, 1261, 1132, 905, 726 cm^{-1}; **MS** (EI, 70 eV): *m/z* (%) = 233 (1) [M], 150 (7) [M – C_5H_7O], 108 (100) $[M\text{–}C_7H_{11}O_2]$; **HRMS** (ESI) calcd. for $C_{13}H_{16}NO_3$ $[M+H]^+$ 234.1125, found 234.1124.

2-Oxo-1-(pyridin-2-yl)propyl (tert-butoxycarbonyl)-L-alaninate (12l): Following **GPA** using **10a** (14.8 mg, 0.11 mmol), product **12l** was isolated after 3h 15 min as a pale yellow oil (24.2 mg, 75.0 µmol, 75% yield, keto:enol = 99:1 in $CDCl_3$, d.r. = 56:44).

Rf = 0.42 (EtOAc/hexanes 35:65); **^{1}H NMR** (400 MHz, $CDCl_3$) *major diastereomer* δ = 8.66 – 8.54 (m, 1H), 7.80 – 7.67 (m, 1H), 7.47 – 7.40 (m, 1H), 7.33 – 7.22 (m, 1H), 6.17 (s, 1H), 5.15 – 5.01 (m, 1H), 4.58 – 4.37 (m, 1H), 2.24 (s, 3H), 1.54 (d, J = 7.3 Hz, 3H), 1.41 (s, 9H) ppm; *minor diastereomer* δ = 8.66 – 8.54 (m, 1H), 7.80 –7.67 (m, 1H), 7.47 – 7.40 (m, 1H), 7.33 – 7.22 (m, 1H), 6.13 (s, 1H), 5.15 – 5.01 (m, 1H), 4.58 –4.37 (m, 1H), 2.27 (s, 3H), 1.44 (d, J = 7.2 Hz, 3H), 1.40 (s, 9H) ppm; **^{13}C NMR** (101 MHz, $CDCl_3$) *maj. + min. d.* δ = 201.3, 200.9, 172.7, 172.4, 155.2, 153.5, 153.3, 149.7, 137.4, 137.3, 124.0, 123.9, 122.7, 122.5, 81.98, 81.96, 80.05, 49.47, 49.23, 28.40, 27.12, 27.07, 18.69, 18.50 ppm; **IR** (ATR) $\tilde{\nu}_{max}$ = 2978, 1712, 1590, 1509, 1436, 1365, 1159, 1069 cm^{-1}; **MS** (EI, 70 eV): *m/z* (%) = 322 (1) $[M]^+$, 249 (12), 145 (50), 108 (100); **HRMS** (ESI) calcd. for $C_{16}H_{23}N_2O_5$ $[M+H]^+$ 323.1601 found 323.1604.

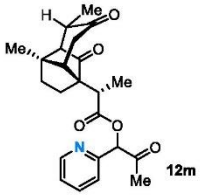

2-Oxo-1-(pyridin-2-yl)propyl(2*S*)-2-((1*R*,3a*S*,4*R*,5*S*,7a*S*)-3a,5-dimethyl-6,8-dioxooctahydro-1*H*-1,4-methanoinden-1-yl)propanoate (12m): Following **GPA** using **10a** (14.8 mg, 0.11 mmol), product **12m** was isolated after 16 h as a colorless oil (22.7 mg, 57.1 µmol, 57% yield, keto/enol in 99:1, $CDCl_3$, d.r. = 57:43).

Rf = 0.43 (EtOAc/hexanes 50:50); **^{1}H NMR** (400 MHz, $CDCl_3$) *major diastereomer* δ = 8.62 – 8.56 (m, 1H), 7.80 – 7.70 (m, 1H), 7.47 – 7.39 (m, 1H), 7.34 – 7.25 (m, 1H), 6.06 (s, 1H), 3.02 – 2.91 (m, 1H), 2.88 (dd, *J* = 18.2, 2.1 Hz, 1H), 2.76 – 2.57 (m, 2H), 2.39 – 2.32 (m, 1H), 2.25 (s, 3H), 2.23 – 2.16 (m, 1H), 2.11 – 2.03 (m, 1H), 1.85 – 1.71 (m, 1H), 1.66 – 1.50 (m, 2H), 1.39 (d, *J* = 7.1 Hz, 3H), 1.37 (s, 3H), 1.14 (d, *J* = 6.7 Hz, 3H, major) ppm; *minor diastereomer* δ = 8.62 – 8.56 (m, 1H), 7.80 – 7.70 (m, 1H), 7.47 – 7.39 (m, 1H), 7.34 – 7.25 (m, 1H), 6.09 (s, 1H), 3.02 – 2.91 (m, 1H), 2.76 – 2.57 (m, 2H), 2.42 (dd, *J* = 18.2, 4.8 Hz, 1H), 2.28 (dd, *J* = 12.1, 5.0 Hz, 1H), 2.25 (s, 3H), 2.15 – 2.10 (m, 1H), 2.11 – 2.03 (m, 1H), 1.85 – 1.71 (m, 1H), 1.66 – 1.50 (m, 2H), 1.46 (d, *J* = 7.1 Hz, 3H), 1.32 (s, 3H), 1.11 (d, *J* = 6.7 Hz, 3H) ppm; **^{13}C NMR** (101 MHz, $CDCl_3$) *maj. d.* δ = 216.1, 210.1, 201.4, 173.7, 153.3, 149.7, 137.5, 124.0, 122.6, 82.10, 62.89, 61.43, 51.77, 44.59, 44.49, 38.25, 37.10, 33.42, 27.30, 25.21, 16.78, 13.69, 12.57 ppm; *min. d.* δ = 216.1, 209.5, 201.3, 173.2, 153.5, 149.7, 137.4, 123.9, 122.6, 81.74, 63.03, 61.33, 51.50, 44.70, 44.25, 37.95, 37.67, 33.41, 27.27, 26.23, 16.72, 13.46, 12.57 ppm; **IR** (ATR) $\tilde{\nu}_{max}$ = 2939, 2878, 1728, 1708, 1150, 730 cm^{-1}; **MS** (ESI, 70 eV): *m/z* (%) = 398 (100) $[M+H]^+$, 265 (19); **HRMS** (ESI) calcd. for $C_{23}H_{28}NO_5$ $[M+H]^+$ 398.1962, found 398.1965.

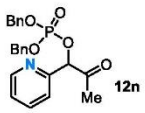

Dibenzyl (2-oxo-1-(pyridin-2-yl)propyl) phosphate (12n): Following **GPA** using **10a** (14.9 mg, 0.11 mmol), product **12n** was isolated after 45 min as a yellow oil (29.1 mg, 70.7 µmol, 71% yield, keto:enol = 99:1 in $CDCl_3$).

Rf = 0.19 (EtOAc/hexanes 50:50); **^{1}H NMR** (400 MHz, $CDCl_3$) δ = 8.56 (ddd, *J* = 4.9, 1.8, 0.9 Hz, 1H), 7.67 (td, *J* = 7.8, 1.8 Hz, 1H), 7.40 – 7.18 (m, 12H), 5.80 (d, *J* = 8.3 Hz, 1H), 5.14 (d, *J* = 8.1 Hz, 2H), 4.98 (dd, *J* = 8.3, 1.5 Hz, 2H), 2.20 (s, 3H) ppm; **^{13}C NMR** (101 MHz, $CDCl_3$) δ = 202.0 (d, *J* = 4.7 Hz), 154.4 (d, *J* = 6.5 Hz), 149.6, 137.3, 135.7 (d, *J* = 7.1 Hz), 135.6 (d, *J* = 6.9 Hz), 128.7, 128.6, 128.2, 128.0, 127.1, 123.9, 122.4, 83.77 (d, *J* = 5.2 Hz), 69.94 (d, *J* = 5.6 Hz), 69.71 (d, *J* = 5.7 Hz), 26.69 ppm; **^{31}P NMR** (162 MHz, $CDCl_3$) δ = -1.97 (h, *J* = 8.3 Hz) **IR** (ATR) $\tilde{\nu}_{max}$ = 3033, 1718, 1700, 1455, 1243, 1001, 739, 696 cm^{-1}; **MS** (ESI, 70 eV): *m/z* (%) = 434 (100) $[M+Na]^+$, 412 (80) $[M+H]^+$; **HRMS** (ESI) calcd. for $C_{22}H_{23}NO_5P$ $[M+H]^+$ 412.1308, found 412.1306.

1-(Pyridin-2-yl)-1-(pyridin-2-yloxy)propan-2-one (12o): Following **GPA** using **10a** (14.8 mg, 0.11 mmol), product **12o** was isolated after 45 min as a yellow oil (13.4 mg, 58.7 µmol, 59% yield, keto:enol= 99:1 in $CDCl_3$).

Rf = 0.59 (EtOAc/hexanes 50:50); **^{1}H NMR** (400 MHz, $CDCl_3$) δ = 8.62 (ddd, *J* = 4.9, 1.8, 0.9 Hz, 1H), 8.09 (ddd, *J* = 5.0, 2.0, 0.8 Hz, 1H), 7.74 (td, *J* = 7.7, 1.8 Hz, 1H), 7.66 – 7.57 (m, 2H), 7.27 (ddd, *J* = 7.5, 4.9, 1.2 Hz, 1H), 6.96 (dt, *J* = 8.3, 0.9 Hz, 1H), 6.90 (ddd, *J* = 7.1, 5.1, 0.9 Hz, 1H), 6.41 (s, 1H), 2.36 (s, 3H) ppm; **^{13}C NMR** (101 MHz, $CDCl_3$) δ = 204.7, 162.2, 155.3, 149.6, 146.8, 139.1, 137.2, 123.5, 122.6, 117.8, 111.3, 82.58, 27.27 ppm; **IR** (ATR) $\tilde{\nu}_{max}$ = 1732, 1590, 1571, 1469, 1432. 1272, 778 cm^{-1}; **MS** (EI, 70 eV): *m/z* (%) = 228 (1) [M], 169 (100); **HRMS** (ESI) calcd. for $C_{13}H_{13}N_2O_2$ $[M+H]^+$ 229.0972, found 229.0970.

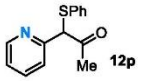

1-(Phenylthio)-1-(pyridin-2-yl)propan-2-one (12p): Following **GPA** using **10a** (14.9 mg, 0.11 mmol), product **12p** was isolated after 15 min as a yellow solid (9.9 mg, 40.7 µmol, 41% yield, keto:enol = 1:99 in $CDCl_3$).

M.p. = 52 °C (DCM); **Rf** = 0.55 (EtOAc/hexanes 35:65); **^{1}H NMR** (400 MHz, $CDCl_3$) δ = 8.04 (d, *J* = 5.5 Hz, 1H), 7.67 (d, *J* = 8.6 Hz, 1H), 7.63 – 7.53 (m, 1H), 7.25 – 7.17 (m, 2H), 7.16 – 7.10 (m, 2H), 7.11 – 7.02 (m, 1H), 6.91 (ddd, *J* = 7.0, 5.5, 1.2 Hz, 1H), 2.41 (s, 3H) ppm; **^{13}C NMR** (101 MHz, $CDCl_3$) δ = 185.6, 158.7, 139.4, 139.2, 138.8, 129.0, 124.7, 120.4, 116.9, 90.92, 24.33 ppm; **IR** (ATR) $\tilde{\nu}_{max}$ = 3056, 2919, 1580, 1475, 1154, 997 cm^{-1}; **MS** (EI, 70 eV): *m/z* (%) = 243 (21) [M], 200 (60) [M-C_2H_3O], 167 (100); **HRMS** (ESI) calcd. for $C_{14}H_{14}NOS$ $[M+H]^+$ 244.0791, found 244.0790.

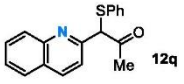

1-(Phenylthio)-1-(quinolin-2-yl)propan-2-one (12q): Following **GPA** using **10q** (20.4 mg, 0.11 mmol), product **12q** was isolated after 5 min as a yellow solid (24.3 mg, 82.8 µmol, 83% yield, keto:enol = 1:99 in $CDCl_3$).

M.p. = 108 °C (Pentan); **Rf** = 0.64 (EtOAc/hexanes 35:65); **^{1}H NMR** (400 MHz, $CDCl_3$) δ = 7.75 (q, *J* = 9.4 Hz, 2H), 7.64 – 7.55 (m, 2H), 7.53 (d, *J* = 8.1 Hz, 1H), 7.33 (ddd, *J* = 8.1, 6.9, 1.2 Hz, 1H), 7.25 – 7.18 (m, 2H), 7.17 – 7.11 (m, 2H), 7.10 – 7.03 (m, 1H), 2.46 (s, 3H) ppm; **^{13}C NMR** (101 MHz, $CDCl_3$) δ = 198.1, 156.4, 139.9, 138.0, 137.1, 131.5, 129.1, 127.8, 124.7, 124.5, 123.2, 120.5, 118.3, 89.79, 27.94 ppm; **IR** (ATR) $\tilde{\nu}_{max}$ = 3054, 1624, 1578, 1513, 1369, 1312, 1148, 737 cm^{-1}; **MS** (EI, 70 eV): *m/z* (%) = 293 (33) [M], 250 (64) [M-C_2H_3O], 217 (100); **HRMS** (ESI) calcd. for $C_{18}H_{16}NOS$ $[M+H]^+$ 294.0947, found 294.0946.

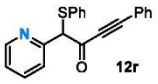

4-Phenyl-1-(phenylthio)-1-(pyridin-2-yl)but-3-yn-2-one (12r): Following **GPA** using **10r** (24.3 mg, 0.11 mmol), product **12r** was isolated after 20 min as a yellow green solid (28.0 mg, 85.0 µmol, 85% yield, keto:enol = 1:99 in $CDCl_3$).

D.p. = 120 °C (EtOAc); **Rf** = 0.49 (EtOAc/hexanes 50:50); **^{1}H NMR** (400 MHz, $CDCl_3$) δ = 8.08 (ddd, *J* = 5.7, 1.7, 1.0 Hz, 1H), 7.74 (dt, *J* = 8.7, 1.1 Hz, 1H), 7.66 (ddd, *J* = 8.7, 7.1, 1.7 Hz, 1H), 7.48 – 7.41 (m, 2H), 7.36 – 7.18 (m, 7H), 7.12 – 7.06 (m, 1H), 6.98 (ddd, *J* = 7.1, 5.7, 1.3 Hz, 1H) ppm; **^{13}C NMR** (101 MHz, $CDCl_3$) δ = 166.7, 157.9, 139.5, 138.9, 138.7, 132.5, 129.3, 129.0, 128.3, 125.8, 125.1, 122.1, 121.9, 117.7, 97.30, 93.48, 87.60 ppm; **IR** (ATR) $\tilde{\nu}_{max}$ = 3056, 2197, 1622, 1578, 1489, 1374, 1152, 738, 689 cm^{-1}; **MS** (ESI): *m/z* (%) = 330 (100) $[M+H]^+$, 222 (70); **HRMS** (ESI) calcd. for $C_{21}H_{16}NOS$ $[M+H]^+$ 330.0947 found 330.0949.

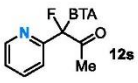

1-(1*H*-Benzo[*d*][1,2,3]triazol-1-yl)-1-fluoro-1-(pyridin-2-yl)propan-2-one (12s): Following **GPD** using **12a** (54.7 mg, 0.22 mmol), product **12s** was isolated after 30 min as a colorless solid (39.9 mg, 148 µmol, 68% yield).

M.p. = 110 °C (DCM); **Rf** = 0.35 (EtOAc/hexanes 35:65); **^{1}H NMR** (400 MHz, $CDCl_3$) δ = 8.66 (ddt, *J* = 4.8, 1.8, 0.9 Hz, 1H), 8.15 – 8.06 (m, 1H), 7.95 (td, *J* = 7.8, 1.8 Hz, 1H), 7.83 (dq, *J* = 8.0, 1.2 Hz, 1H), 7.49 (ddd, *J* = 7.6, 4.8, 1.2 Hz, 1H), 7.36 (dddd, *J* = 15.0, 8.4, 7.1, 1.3 Hz, 2H), 6.63 (dt, *J* = 7.7, 1.0 Hz, 1H), 2.57 (d, *J* = 2.5 Hz, 3H) ppm; **^{13}C NMR** (101 MHz, $CDCl_3$) δ = 195.7 (d, *J* = 28.6 Hz), 151.4 (d, *J* = 31.0 Hz), 149.8 (d, *J* = 2.1 Hz), 146.3, 137.9, 132.47 (d, *J* = 1.9 Hz), 128.7, 125.6, 124.9, 122.7 (d, *J* = 5.9 Hz), 120.7, 111.3, 101.9 (d, *J* = 218.5 Hz), 26.57 ppm; **^{19}F NMR** (376 MHz, $CDCl_3$) δ -125.19 ppm; **IR** (ATR) $\tilde{\nu}_{max}$ = 3062, 1745, 1219, 782, 796, 744 cm^{-1}; **MS** (ESI): *m/z* (%) = 271 (100) $[M+H]^+$, 223 (60), 251 (50); **HRMS** (ESI) calcd. for $C_{14}H_{12}FN_4O$ $[M+H]^+$ 271.0990, found 271.0989.

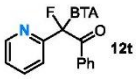

12t

2-(1*H*-Benzo[*d*][1,2,3]triazol-1-yl)-2-fluoro-1-phenyl-2-(pyridin-2-yl)ethan-1-one (12t): Following **GPD** using **12ae** (59.2 mg, 0.19 mmol), product **12t** was isolated after 45 min as a colorless oil (35.5 mg, 107 µmol, 56% yield).

Rf = 0.35 (EtOAc/hexanes 25:75); **^{1}H NMR** (400 MHz, $CDCl_3$) δ = 8.63 (d, *J* = 4.9 Hz, 1H), 8.13 – 8.08 (m, 1H), 8.00 – 7.91 (m, 3H), 7.88 (dd, *J* = 8.0, 1.2 Hz, 1H), 7.58 – 7.48 (m, 1H), 7.49 – 7.34 (m, 5H), 7.22 – 7.14 (m, 1H) ppm; **^{13}C NMR** (101 MHz, $CDCl_3$) δ = 188.4 (d, *J* = 30.2 Hz), 152.6 (d, *J* = 27.8 Hz), 149.3 (d, *J* = 1.7 Hz), 146.3, 137.6, 133.9, 133.3 (d, *J* = 2.7 Hz), 132.8 (d, *J* = 2.0 Hz), 130.7, 130.7, 128.4, 125.3, 124.7, 123.0 (d, *J* = 4.3 Hz), 120.5, 111.6 (d, *J* = 1.9 Hz), 103.5 (d, *J* = 215.7 Hz) ppm; **^{19}F NMR** (376 MHz, $CDCl_3$) δ = -117.70 ppm; **IR** (ATR) $\tilde{\nu}_{max}$ = 3061, 1707, 1589, 1450, 745, 691 cm^{-1}; **MS** (ESI): *m/z* (%) = 355 (46) $[M+Na]^+$, 333 (100) $[M+H]^+$, 285 (80); **HRMS** (ESI) calcd. for $C_{19}H_{14}FN_4O$ $[M+H]^+$ 333.1146 found 333.1145.

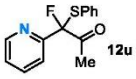

12u

1-Fluoro-1-(phenylthio)-1-(pyridin-2-yl)propan-2-one (12u): Following **GPD** using **12p** (24.3 mg, 0.10 mmol), product **12u** was isolated after 2 h and 30 min as a colorless oil (15.0 mg, 57.4 µmol, 57% yield).

Rf = 0.12 (EtOAc/hexanes 50:50); **^{1}H NMR** (400 MHz, $CDCl_3$) δ = 8.66 (ddt, *J* = 4.8, 1.7, 0.8 Hz, 1H), 7.70 (td, *J* = 7.8, 1.8 Hz, 1H), 7.56 – 7.50 (m, 2H), 7.47 (dq, *J* = 8.0, 1.1 Hz, 1H), 7.39 – 7.26 (m, 4H), 2.19 (d, *J* = 2.9 Hz, 3H) ppm; **^{13}C NMR** (101 MHz, $CDCl_3$) δ = 199.23 (d, *J* = 29.0 Hz), 154.45 (d, *J* = 27.3 Hz), 149.40 (d, *J* = 1.7 Hz), 137.2, 135.98 (d, *J* = 1.6 Hz), 129.8, 129.2, 128.5, 124.2, 121.33 (d, *J* = 5.9 Hz), 109.10 (d, *J* = 233.3 Hz), 26.32 ppm; **^{19}F NMR** (376 MHz, $CDCl_3$) δ = -132.23 (d, *J* = 2.7 Hz) ppm; **IR** (ATR) $\tilde{\nu}_{max}$ = 3058, 1731, 1585, 1433, 1195, 747 cm^{-1}; **MS** (ESI): *m/z* (%) = 262 (74) $[M+H]^+$, 242 (100); **HRMS** (ESI) calcd. for $C_{14}H_{13}FNOS$ $[M+H]^+$ 262.0696, found 262.0696.

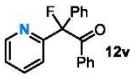

12v

2-Fluoro-1,2-diphenyl-2-(pyridin-2-yl)ethan-1-one (12v): Following **GPD** using **10v** (54.7 mg, 0.20 mmol), product **12v** was isolated after 24 h as a colorless oil (39.9 mg, 137 µmol, 68%).

Rf = 0.59 (EtOAc/hexanes 17:83); **^{1}H NMR** (400 MHz, $CDCl_3$) δ = 8.61 (dd, *J* = 4.9, 1.7 Hz, 1H), 7.91 (dt, *J* = 8.6, 1.6 Hz, 2H), 7.77 (td, *J* = 7.8, 1.8 Hz, 1H), 7.54 – 7.47 (m, 4H), 7.44 – 7.33 (m, 5H), 7.27 (dd, *J* = 7.3, 4.6 Hz, 1H) ppm; **^{13}C NMR** (101 MHz, $CDCl_3$) δ = 195.56 (d, *J* = 28.4 Hz), 158.95 (d, *J* = 24.7 Hz), 149.06, 137.98 (d, *J* = 23.0 Hz), 137.24, 135.02 (d, *J* = 3.5 Hz), 133.04, 130.51 (d, *J* = 5.0 Hz), 128.79 (d, *J* = 1.6 Hz), 128.31, 128.25, 126.66 (d, *J* = 8.3 Hz), 123.56 (d, *J* = 1.6 Hz), 121.65 (d, *J* = 5.5 Hz), 102.21 (d, *J* = 187.6 Hz) ppm; **^{19}F NMR** (376 MHz, $CDCl_3$) δ = -146.98 ppm; **IR** (ATR) $\tilde{\nu}_{max}$ = 3060, 1692, 1448, 1247, 748, 695 cm^{-1}; **MS** (ESI, 70 eV): *m/z* (%) = 292 (100) $[M+H]^+$, 272 (14); **HRMS** (ESI) calcd. for $C_{19}H_{14}NO$ $[M-F]^+$ 272.1075, found 272.1068.

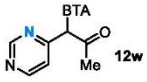

1-(1*H*-Benzo[*d*][1,2,3]triazol-1-yl)-1-(pyrimidin-4-yl)propan-2-one (12w): Following **GPA** using **10w** (14.9 mg, 0.11 mmol), product **12w** was isolated after 2 h 15 min as a yellow solid (7.0 mg, 27.6 µmol, 28% yield, keto:enol = 1:99 in $CDCl_3$).

M.p. = 177 °C (EtOAc); **Rf** = 0.28 (EtOAc/hexanes 25:75); **^{1}H NMR** (400 MHz, $CDCl_3$) δ = 15.82 (s, 1H), 8.80 (d, *J* = 1.4 Hz, 1H), 8.24 (d, *J* = 6.0 Hz, 1H), 8.18 (dt, *J* = 8.3, 1.0 Hz, 1H), 7.54 (ddd, *J* = 8.1, 6.9, 1.1 Hz, 1H), 7.46 (ddd, *J* = 8.1, 7.0, 1.1 Hz, 1H), 7.35 (dt, *J* = 8.2, 1.0 Hz, 1H), 5.88 (dd, *J* = 6.0, 1.4 Hz, 1H), 1.80 (s, 3H) ppm; **^{13}C NMR** (101 MHz, $CDCl_3$) δ = 181.4, 158.3, 156.3, 152.1, 146.0, 134.5, 128.8, 124.7, 120.7, 112.3, 109.5, 104.1, 21.37 ppm; **IR** (ATR) $\tilde{\nu}_{max}$ = 2924, 1630, 1582, 1558, 1522, 1380, 1268, 1074 cm^{-1}; **MS** (EI, 70 eV): *m/z* (%) = 254 (100) $[M+H]^+$; **HRMS** (ESI) calcd. for $C_{13}H_{12}N_5O$ $[M+H]^+$ 254.1036 found 254.1036.

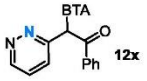

2-(1*H*-Benzo[*d*][1,2,3]triazol-1-yl)-1-phenyl-2-(pyridazin-3-yl)ethan-1-one (12x): Following **GPA** using **10x** (21.8 mg, 0.11 mmol), product **12x** was isolated after 15 min as a yellow solid (10.5 mg, 33.3 µmol, 33% yield, keto:enol = 1:99 in $CDCl_3$).

D.p. = 131 °C (DCM); **Rf** = 0.12 (EtOAc/hexanes 25:75); **^{1}H NMR** (500 MHz, $CDCl_3$) δ = 8.33 (dd, *J* = 4.3, 1.6 Hz, 1H), 8.02 (d, *J* = 8.2 Hz, 1H), 7.36 – 7.27 (m, 2H), 7.20 – 7.14 (m, 4H), 7.14 – 7.09 (m, 1H), 7.06 – 6.99 (m, 2H), 6.40 (dd, *J* = 9.4, 1.6 Hz, 1H) ppm; **^{13}C NMR** (101 MHz, $CDCl_3$) δ = 185.1, 154.1, 145.9, 143.5, 138.1, 135.1, 130.2, 129.5, 128.4, 128.1, 126.9, 125.4, 124.3, 120.1, 109.8, 99.86 ppm; **IR** (ATR) $\tilde{\nu}_{max}$ = 2090, 1619, 1556, 1518, 1327, 1028, 749, 709 cm^{-1}; **MS** (ESI): *m/z* (%) = 316 (100) $[M+H]^+$, 288 (14) $[M+H-N_2]^+$; **HRMS** (ESI) calcd. for $C_{18}H_{14}N_5O$ $[M+H]^+$ 316.1193 found 316.1193.

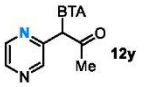

1-(1*H*-Benzo[*d*][1,2,3]triazol-1-yl)-1-(pyrazin-2-yl)propan-2-one (12y): Following **GPA** using **10y** (14.9 mg, 0.11 mmol), product **12y** was isolated after 2 h as a yellow solid (14.1 mg, 55.6 µmol, 56% yield, keto:enol = 4:96 in $CDCl_3$).

M.p. = 90 °C (DCM); **Rf** = 0.42 (EtOAc/hexanes 50:50); **^{1}H NMR** (300 MHz, $CDCl_3$) δ = 14.59 (s, 1H), 8.41 – 8.32 (m, 2H), 8.19 (dt, *J* = 8.1, 1.0 Hz, 1H), 7.59 – 7.42 (m, 2H), 7.42 – 7.33 (m, 2H), 1.80 (s, 3H) ppm; **^{13}C NMR** (75 MHz, $CDCl_3$) δ = 170.5, 151.3, 145.9, 140.5, 139.8, 138.6, 134.5, 128.7, 124.6, 120.5, 109.4, 104.8, 18.63 ppm; **IR** (ATR) $\tilde{\nu}_{max}$ = 2923, 1634, 1067, 853, 760 cm^{-1}; **MS** (ESI): *m/z* (%) = 254 (100) $[M+H]^+$; **HRMS** (ESI) calcd. for $C_{13}H_{12}N_5O$ $[M+H]^+$ 254.1036 found 254.1037.

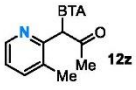

12z

1-(1*H*-benzo[*d*][1,2,3]triazol-1-yl)-1-(3-methylpyridin-2-yl)propan-2-one (12z): Following **GPA** using **10z** (16.4 mg, 0.11 mmol), product **12z** was isolated after 1 h as a yellow oil (18.9 mg, 71.0 µmol, 71% yield, keto:enol = 77:23 in $CDCl_3$).

Rf = 0.56 (EtOAc/hexanes 50:50); **^{1}H NMR** (400 MHz, $CDCl_3$) keto δ = 8.54 (dd, *J* = 5.0, 1.7 Hz, 1H), 8.00 (ddd, *J* = 7.2, 3.1, 1.2 Hz, 1H), 7.53 – 7.49 (m, 1H), 7.30 – 7.24 (m, 4H), 7.19 (s, 1H), 2.34 (s, 3H), 2.23 (s, 3H) ppm; **^{13}C NMR** (101 MHz, $CDCl_3$) keto + enol δ = 199.9, 181.9, 153.2, 151.6, 146.9, 146.5, 145.7, 142.2, 139.5, 137.1, 135.9, 134.7, 133.3, 128.7, 128.5, 127.6, 127.4, 127.1, 124.7, 124.3, 124.0, 120.3, 119.8, 116.8, 112.2, 110.3, 102.1, 71.71, 65.43, 28.43, 21.93, 18.27 ppm; **IR** (ATR) $\tilde{\nu}_{max}$ = 2923, 1732, 1452, 1141, 876, 746 cm^{-1}; **MS** (EI, 70 eV): *m/z* (%) = 266 (2) [M], 238 (18) [M-N_2], 223 (25) [M-C_2H_3O], 195 (100) [M-N_2-C_2H_3O]; **HRMS** (ESI) calcd. for $C_{15}H_{15}N_4O$ $[M+H]^+$ 267.1240, found 267.1239.

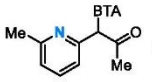

12aa

1-(1*H*-Benzo[*d*][1,2,3]triazol-1-yl)-1-(6-methylpyridin-2-yl)propan-2-one (12aa): Following **GPA** using **10aa** (16.7 mg, 0.11 mmol), product **12aa** was isolated after 40 min as a colorless solid (17.0 mg, 63.8 µmol, 64% yield, keto:enol = 1:99 in $CDCl_3$).

M.p. = 109 °C (EtOAc); **Rf** = 0.58 (EtOAc/hexanes 35:65); **^{1}H NMR** (400 MHz, $CDCl_3$) δ = 8.14 (dt, *J* = 8.2, 1.0 Hz, 1H), 7.48 (ddd, *J* = 8.1, 6.9, 1.1 Hz, 1H), 7.41 (ddd, *J* = 8.1, 6.9, 1.2 Hz, 1H), 7.38 – 7.32 (m, 2H), 6.74 (dt, *J* = 7.6, 0.8 Hz, 1H), 5.75 (dt, *J* = 8.4, 0.8 Hz, 1H), 2.57 (s, 3H), 1.74 (s, 3H) ppm; **^{13}C NMR** (101 MHz, $CDCl_3$) δ = 178.6, 154.5, 149.5, 146.0, 139.5, 135.0, 128.2, 124.3, 120.3, 116.7, 113.5, 110.0, 103.0, 21.85, 21.49 ppm; **IR** (ATR) $\tilde{\nu}_{max}$ = 2923, 1734, 1645, 1592, 1568, 1305, 1267 cm^{-1}; **MS** (EI, 70 eV): *m/z* (%) = 267 (1) $[M+H]^+$, 195 (100); **HRMS** (ESI) calcd. for $C_{15}H_{15}N_4O$ $[M+H]^+$ 267.1240, found 267.1240.

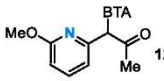

12ab

1-(1*H*-Benzo[*d*][1,2,3]triazol-1-yl)-1-(6-methoxypyridin-2-yl)propan-2-one (12ab): Following **GPA** using **10ab** (18.2 mg, 0.11 mmol), product **12ab** was isolated after 20 min as a colorless oil (21.9 mg, 77.6 µmol, 78% yield, keto:enol = 9:91 in $CDCl_3$).

Rf = 0.72 (EtOAc/hexanes 35:65); **^{1}H NMR** (400 MHz, $CDCl_3$) enol δ = 14.96 (s, 1H), 8.15 (dt, *J* = 8.2, 1.0 Hz, 1H), 7.53 – 7.46 (m, 1H), 7.45 – 7.34 (m, 2H), 6.55 (d, *J* = 8.3 Hz, 1H), 5.54 (dd, *J* = 7.7, 0.7 Hz, 1H), 4.03 (s, 3H), 1.73 (s, 3H) ppm; **^{13}C NMR** (101 MHz, $CDCl_3$) enol δ = 166.1, 161.8, 153.8, 145.8, 140.6, 134.8, 128.3, 124.4, 120.3, 109.9, 109.3, 107.6, 107.2, 54.01, 18.28 ppm; **IR** (ATR) $\tilde{\nu}_{max}$ = 2922, 1593, 1567, 1273, 1063 cm^{-1}; **MS** (EI, 70 eV): *m/z* (%) = 282 (1) $[M]^+$, 239 (100) $[M-CH_3CO]^+$; **HRMS** (ESI) calcd. for $C_{15}H_{15}N_4O_2$ $[M+H]^+$ 283.1190, found 283.1189.

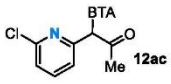

1-(1*H*-Benzo[*d*][1,2,3]triazol-1-yl)-1-(6-chloropyridin-2-yl)propan-2-one (12ac): Following **GPA** using **10ac** (25.2 mg, 0.10 mmol), product **12ac** was isolated after 15 min as a colorless oil (20.0 mg, 69.8 µmol, 70% yield, keto:enol = 5:95 in $CDCl_3$).

M.p. = 96 °C (DCM); **Rf** = 0.45 (EtOAc/hexanes 20:80); **^{1}H NMR** (500 MHz, $CDCl_3$) δ = 14.28 (s, 1H), 8.17 (dt, *J* = 8.4, 1.0 Hz, 1H), 7.51 (ddd, *J* = 8.1, 6.9, 1.1 Hz, 1H), 7.49 – 7.41 (m, 2H), 7.35 (dt, *J* = 8.2, 1.1 Hz, 1H), 7.10 (d, *J* = 7.9 Hz, 1H), 5.89 (d, *J* = 8.1 Hz, 1H), 1.76 (s, 3H) ppm; **^{13}C NMR** (75 MHz, $CDCl_3$) δ = 168.3, 157.0, 147.9, 145.9, 140.4, 134.7, 128.6, 124.6, 120.5, 115.2, 109.8, 106.5, 18.52 ppm; **IR** (ATR) $\tilde{\nu}_{max}$ = 3100, 1642, 1583, 1444, 1063, 888, 745, 732 cm^{-1}; **MS** (ESI): *m/z* (%) = 289/287 (34/100) $[M+H]^+$, 227 (15); **HRMS** (ESI) calcd. for $C_{14}H_{12}ClN_4O$ $[M+H]^+$ 287.0694, found 287.0694.

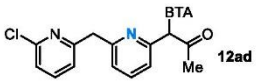

1-(1*H*-Benzo[*d*][1,2,3]triazol-1-yl)-1-(6-((6-chloropyridin-2-yl)meth-yl) pyr-idin-2-yl)propan-2-one (12ad): Following **GPA** using **10ad** (28.7 mg, 0.11 mmol), product **12ad** was isolated after 15 min as a yellow solid (25.9 mg, 68.5 µmol, 69% yield, keto:enol = 1:99 in $CDCl_3$).

M.p. = 131 °C (DCM); **Rf** = 0.48 (EtOAc/hexanes 33:67); **^{1}H NMR** (300 MHz, $CDCl_3$) δ = 8.14 (dt, *J* = 8.0, 1.1 Hz, 1H), 7.74 – 7.64 (m, 1H), 7.53 – 7.31 (m, 4H), 7.27 (d, *J* = 7.8 Hz, 2H), 6.99 (d, *J* = 7.6 Hz, 1H), 5.82 (d, *J* = 8.3 Hz, 1H), 4.30 (s, 2H), 1.70 (d, *J* = 1.3 Hz, 3H) ppm; **^{13}C NMR** (75 MHz, $CDCl_3$) δ = 172.2, 158.4, 155.8, 152.9, 151.5, 145.9, 139.7, 139.2, 134.8, 128.3, 124.4, 122.9, 122.3, 120.3, 119.0, 114.8, 110.0, 105.3, 45.01, 19.59 ppm; **IR** (ATR) $\tilde{\nu}_{max}$ = 3071, 1641, 1559, 750 cm^{-1}; **MS** (ESI): *m/z* (%) = 400 (62) $[M+Na]^+$ 378 (100) $[M+H]^+$, 350 (84) $[M+H-N_2]^+$; **HRMS** (ESI) calcd. for $C_{20}H_{17}ClN_5O$ $[M+H]^+$ 378.1116, found 378.1116.

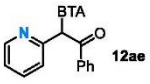

2-(1*H*-Benzo[*d*][1,2,3]triazol-1-yl)-1-phenyl-2-(pyridin-2-yl)ethan-1-one (12ae): Following **GPA** using **10ae** (21.7 mg, 0.11 mmol), product **12ae** was isolated after 2 h 45 min as a yellow solid (20.4 mg, 64.9 µmol, 65% yield, keto:enol = 11:89 in $CDCl_3$).

M.p. = 139 °C (EtOAc); **Rf** = 0.43 (EtOAc/hexanes 35:65); **^{1}H NMR** (400 MHz, $CDCl_3$) δ = 8.29 (ddd, *J* = 5.5, 1.7, 0.9 Hz, 1H), 8.06 – 8.02 (m, 1H), 7.54 (ddd, *J* = 8.6, 7.4, 1.7 Hz, 1H), 7.35 – 7.27 (m, 2H), 7.22 – 7.17 (m, 3H), 7.15 – 7.02 (m, 4H), 6.14 (dt, *J* = 8.5, 1.0 Hz, 1H) ppm; **^{13}C NMR** (75 MHz, $CDCl_3$) δ = 172.5, 156.1, 145.9, 141.3, 139.1, 135.9, 135.0, 129.8, 128.1, 128.1, 127.2, 124.2, 120.1, 118.8, 117.7, 110.0, 104.3 ppm; **MS** (EI, 70 eV): *m/z* (%) = 315 (80) $[M+H]^+$, 305 (100).

The analytical data obtained was in agreement with that reported in the literature.[2]

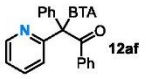

2-(1*H*-Benzo[*d*][1,2,3]triazol-1-yl)-1,2-diphenyl-2-(pyridin-2-yl)ethan-1-one (12af): Following **GPA** using **10v** (27.3 mg, 0.10 mmol), product **12af** was isolated after 21 h as a colorless solid (24.9 mg, 63.7 µmol, 64% yield).

M.p. = 75 °C (Et_2O); **Rf** = 0.42 (EtOAc/hexanes 25:75); **^{1}H NMR** (500 MHz, $CDCl_3$) δ = 8.52 (dd, *J* = 4.9, 1.8 Hz, 1H), 7.99 (d, *J* = 8.1 Hz, 1H), 7.72 (td, *J* = 7.8, 1.8 Hz, 1H), 7.56 (dt, *J* = 8.5, 1.6 Hz, 3H), 7.32 – 7.19 (m, 7H), 7.19 – 7.12 (m, 2H), 7.08 (t, *J* = 7.9 Hz, 2H), 6.91 (d, *J* = 8.2 Hz, 1H) ppm; **^{13}C NMR** (101 MHz, $CDCl_3$) δ = 192.9, 158.0, 148.2, 146.3, 137.5, 136.7, 136.1, 134.1, 132.3, 130.2, 129.4, 128.6, 128.2, 127.8, 127.5, 126.8, 124.1, 123.5, 120.1, 113.0, 82.13 ppm; **IR** (ATR) $\tilde{\nu}_{max}$ = 3063, 1706, 1272, 747 cm^{-1}; **MS** (ESI): *m/z* (%) = 391 (100) $[M+H]^+$, 227 (15); **HRMS** (ESI) calcd. for $C_{25}H_{19}N_4O$ $[M+H]^+$ 391.1553, found 391.1553.

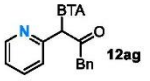

1-(1*H*-Benzo[*d*][1,2,3]triazol-1-yl)-3-phenyl-1-(pyridin-2-yl)propan-2-one (12ag): Following **GPA** using **10ag** (23.2 mg, 0.11 mmol), product **12ag** was isolated after 30 min as a yellow solid (24.2 mg, 73.7 µmol, 74% yield, keto:enol = 1:99 in $CDCl_3$).

M.p. = 146 °C (EtOAc); **Rf** = 0.27 (EtOAc/hexanes 35:65); **^{1}H NMR** (400 MHz, $CDCl_3$) δ = 8.20 – 8.14 (m, 1H), 8.08 (d, *J* = 5.3 Hz, 1H), 7.46 – 7.40 (m, 3H), 7.25 – 7.20 (m, 1H), 7.18 – 7.11 (m, 3H), 7.03 – 6.98 (m, 2H), 6.93 (ddd, *J* = 7.1, 5.6, 1.1 Hz, 1H), 5.92 (dt, *J* = 8.7, 1.0 Hz, 1H), 3.33 (d, *J* = 14.5 Hz, 1H), 3.25 (d, *J* = 14.5 Hz, 1H) ppm; **^{13}C NMR** (101 MHz, $CDCl_3$) δ = 178.3, 155.0, 146.0, 139.9, 139.1, 136.1, 135.2, 129.2, 128.4, 128.3, 126.7, 124.4, 120.3, 117.6, 117.0, 110.0, 103.2, 40.65 ppm; **IR** (ATR) $\tilde{\nu}_{max}$ = 3027, 1629, 1583, 1556, 1453, 1398, 1274, 1155, 1060 cm^{-1}; **MS** (EI, 70 eV): *m/z* (%) = 329 (100) $[M+H]^+$; **HRMS** (ESI) calcd. for $C_{20}H_{17}N_4O$ $[M+H]^+$ 329.1397 found 329.1396.

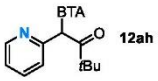

1-(1*H*-Benzo[*d*][1,2,3]triazol-1-yl)-3,3-dimethyl-1-(pyridin-2-yl)butan-2-one (12ah): Following **GPA** using **10ah** (19.5 mg, 0.11 mmol), product **12ah** was isolated after 1h 45 min as a yellow solid (22.3 mg, 75.7 µmol, 76% yield, keto:enol = 71:29 in $CDCl_3$).

M.p. = 144 °C (EtOAc); **Rf** = 0.56 (EtOAc/hexanes 35:65); **^{1}H NMR** (400 MHz, $CDCl_3$) keto δ = 8.64 (ddd, *J* = 4.9, 1.8, 1.0 Hz, 1H), 8.05 – 7.96 (m, 1H), 7.65 (td, *J* = 7.7, 1.8 Hz, 1H), 7.48 (s, 1H) 7.39 – 7.26 (m, 4H), 7.19 (d, *J* = 7.9 Hz, 1H), 1.24 (s, 9H) ppm; enol δ = 8.18 (br d, *J* = 5.2 Hz, 1H), 8.14 (dt, *J* = 8.2, 1.0 Hz, 1H), 7.52 – 7.44 (m, 1H), 7.44 – 7.39 (m, 1H), 7.38 – 7.26 (m, 2H), 6.96 (ddd, *J* = 7.4, 5.4, 1.1 Hz, 1H), 5.51 (dt, *J* = 8.6, 1.0 Hz, 1H), 0.95 (s, 9H) ppm; **^{13}C NMR** (101 MHz, $CDCl_3$) keto + enol δ = 207.8, 183.3, 157.0, 154.3, 149.5, 146.6, 145.9, 141.2, 138.6, 137.5, 136.3, 133.2, 128.3, 127.7, 124.3, 124.1, 124.0, 123.9, 120.3, 119.9, 118.4, 116.9, 112.3, 110.5, 68.10, 45.06, 39.96, 28.58, 26.62 ppm; **IR** (ATR) $\tilde{\nu}_{max}$ = 2967, 2360, 2248, 1720, 1590, 906 cm^{-1}; **MS** (EI, 70 eV): *m/z* (%) = 209 (23) [M-*t*BuCO]$^+$, 181 (100); **HRMS** (ESI) calcd. for $C_{17}H_{19}N_4O$ $[M+H]^+$ 295.1553, found 295.1551.

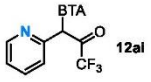

12ai

3-(1*H*-Benzo[*d*][1,2,3]triazol-1-yl)-1,1,1-trifluoro-3-(pyridin-2-yl)propane-2-one (12ai): Following **GPA** using **10ai** (20.9 mg, 0.11 mmol), product **12ai** was isolated after 1.5 h as a yellow oil (24.7 mg, 80.6 µmol, 81% yield, diol/enol: 99:1 in $CDCl_3$).

Rf = 0.59 (EtOAc/hexanes 35:65); **^{1}H NMR** (400 MHz, $CDCl_3$) δ = 8.50 (ddd, *J* = 4.9, 1.8, 1.0 Hz, 1H), 7.99 (dt, *J* = 8.4, 1.0 Hz, 1H), 7.60 (d, *J* = 8.4 Hz, 1H), 7.49 (ddd, *J* = 8.2, 6.9, 1.0 Hz, 1H), 7.36 (ddd, *J* = 8.2, 7.0, 1.0 Hz, 1H), 7.25 (td, *J* = 7.7, 1.7 Hz, 1H), 7.11 (ddd, *J* = 7.7, 4.8, 1.2 Hz, 1H), 6.48 (dt, *J* = 7.9, 1.1 Hz, 1H), 5.14 (s, 1H) ppm; **^{13}C NMR** (101 MHz, $CDCl_3$) δ = 149.7, 149.6, 145.2, 136.7, 133.4, 129.2, 125.0, 124.5, 121.0 (q, *J* = 281.0 Hz) 120.4, 120.2, 110.0, 69.72 (q, *J* = 42.8 Hz), 61.66 (d, *J* = 1.7 Hz) ppm; **^{19}F NMR** (376 MHz, $CDCl_3$) δ – 76.58 (s) ppm; **IR** (ATR) $\tilde{\nu}_{max}$ = 3067, 1590, 1455, 1289, 1200, 1174, 1142, 744 cm^{-1}; **MS** (EI, 70 eV): *m/z* (%) = 277 (10), 249 (100), 209 (39) $[M\text{-}CF_3CO]^+$; **HRMS** (ESI) calcd. for $C_{14}H_{10}F_3N_4O$ $[M+H]^+$ 307.0801, found 307.0803.

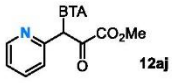

12aj

Methyl 3-(1*H*-benzo[*d*][1,2,3]triazol-1-yl)-2-oxo-3-(pyridin-2-yl)propanoate (12aj): Following **GPA** using **10aj** (19.7 mg, 0.11 mmol), product **12aj** was isolated after 2 h as a yellow solid (12.1 mg, 40.8 µmol, 41% yield, keto:enol = 1:99 in $CDCl_3$).

M.p. = 134 °C (EtOAc); **Rf** = 0.15 (EtOAc/hexanes 65:35); **^{1}H NMR** (400 MHz, $CDCl_3$) δ = 8.25 (ddd, *J* = 5.9, 1.7, 0.9 Hz, 1H), 8.17 – 8.10 (m, 1H), 7.65 (ddd, *J* = 8.8, 7.3, 1.6 Hz, 1H), 7.54 – 7.46 (m, 1H), 7.44 – 7.36 (m, 2H), 7.13 (ddd, *J* = 7.2, 5.9, 1.1 Hz, 1H), 6.25 (dt, *J* = 8.7, 1.0 Hz, 1H), 3.44 (s, 3H) ppm; **^{13}C NMR** (101 MHz, $CDCl_3$) δ = 166.9, 163.5, 154.2, 145.8, 140.7, 138.1, 135.6, 128.3, 124.3, 120.3, 118.7, 118.6, 110.0, 103.6, 52.53 ppm; **IR** (ATR) $\tilde{\nu}_{max}$ = 1733, 1628, 1588, 1559, 1219, 1163, 775, 749, 668 cm^{-1}; **MS** (EI, 70 eV): *m/z* (%) = 297 (80) $[M+H]^+$, 259 (100); **HRMS** (ESI) calcd. for $C_{15}H_{13}N_4O_3$ $[M+H]^+$ 279.0982, found 297.0980.

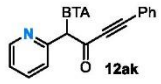

12ak

1-(1*H*-Benzo[*d*][1,2,3]triazol-1-yl)-4-phenyl-1-(pyridin-2-yl)but-3-yn-2-one (12ak): Following **GPA** using **10ak** (24.3 mg, 0.11 mmol), product **12ak** was isolated after 30 min as a yellow green oil (10.3 mg, 30.4 µmol, 30% yield, keto:enol = 1:99 in $CDCl_3$).

Rf = 0.36 (EtOAc/hexanes 50:50); **^{1}H NMR** (400 MHz, $CDCl_3$) δ = 8.23 – 8.16 (m, 2H), 7.60 (ddd, *J* = 8.8, 7.3, 1.6 Hz, 1H), 7.54 – 7.48 (m, 2H), 7.44 (ddd, *J* = 8.1, 4.8, 3.2 Hz, 1H), 7.26 – 7.17 (m, 1H), 7.14 – 7.08 (m, 2H), 7.05 (ddd, *J* = 7.1, 5.7, 1.1 Hz, 1H), 6.80 – 6.72 (m, 2H), 6.36 (d, *J* = 8.7 Hz, 1H) ppm; **^{13}C NMR** (101 MHz, $CDCl_3$) δ = 159.1, 154.3, 145.8, 139.7, 139.4, 135.1, 132.2, 129.7, 128.2, 128.2, 124.2, 120.7, 120.2, 118.1, 118.1, 110.6, 108.6, 95.22, 84.00 ppm; **IR** (ATR) $\tilde{\nu}_{max}$ = 3058, 2931, 2830, 2203, 1628, 1582, 1546, 1490, 1401 cm^{-1}; **MS** (EI, 70 eV): *m/z* (%) = 339 (90) $[M+H]^+$, 259 (100); **HRMS** (ESI) calcd. for $C_{21}H_{15}N_4O$ $[M+H]^+$ 339.1240 found 339.1240.

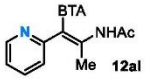

***N*-(1-(1*H*-Benzo[*d*][1,2,3]triazol-1-yl)-1-(pyridin-2-yl)prop-1-en-2-yl)acetamide (12al):** Following **GPA** using **10al** (19.4 mg, 0.11 mmol), product **12al** was isolated after 15 min as a yellow solid (15.0 mg, 51.1 µmol, 51% yield, imin/enamin: 1:99 in $CDCl_3$).

M.p. = 74 °C (DCM); **Rf** = 0.29 (EtOAc/hexanes 25:75); **^{1}H NMR** (400 MHz, $CDCl_3$) δ = 13.93 (s, 1H), 8.60 (ddd, *J* = 5.0, 1.9, 0.9 Hz, 1H), 8.18 (dt, *J* = 8.2, 1.0 Hz, 1H), 7.54 – 7.40 (m, 3H), 7.34 (dt, *J* = 8.2, 1.1 Hz, 1H), 7.11 (ddd, *J* = 7.5, 4.9, 1.1 Hz, 1H), 5.90 (dt, *J* = 8.3, 1.0 Hz, 1H), 2.31 (s, 3H), 2.07 (s, 3H) ppm; **^{13}C NMR** (101 MHz, $CDCl_3$) δ = 169.8, 155.8, 147.1, 146.8, 145.8, 137.8, 134.8, 128.6, 124.6, 120.9, 120.5, 119.7, 111.9, 109.9, 25.91, 16.77 ppm; **IR** (ATR) $\tilde{\nu}_{max}$ = 2928, 1711, 1662, 1590, 1499, 1345, 1255, 1066, 780, 748 cm^{-1}; **MS** (ESI): *m/z* (%) = 294 (100) $[M+H]^+$, 224 (22); **HRMS** (ESI) calcd. for $C_{16}H_{16}N_5O$ $[M+H]^+$ 294.1349 found 294.1350.

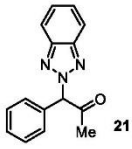

1-(2*H*-Benzo[*d*][1,2,3]triazol-2-yl)-1-phenylpropan-2-one (21): Following **GPA** using the TMS-enolether **20** (22.7 mg, 0.11 mmol), product **21** was isolated after 90 min as a colorless solid (6.1 mg, 24 µmol, 24% yield, keto:enol = 99:1 in $CDCl_3$).

M.p. = 55 °C ($CDCl_3$); **Rf** = 0.33 (EtOAc/hexanes 9:91); **^{1}H NMR** (300 MHz, $CDCl_3$) δ = 7.94 – 7.81 (m, 2H), 7.62 – 7.55 (m, 2H), 7.50 – 7.42 (m, 3H), 7.42 – 7.35 (m, 2H), 6.66 (s, 1H), 2.23 (s, 3H) ppm; **^{13}C NMR** (75 MHz, $CDCl_3$) δ = 199.8, 144.7, 132.6, 129.9, 129.8, 129.2, 126.9, 118.5, 78.76, 27.69 ppm; **IR** (ATR) $\tilde{\nu}_{max}$ = 3073, 2919, 1702, 1265, 1214, 938, 747, 713 cm^{-1}; **MS** (EI, 70 eV): *m/z* (%) = 251 (11) $[M]^+$, 209 (100), 180 (100), 152 (60); **HRMS** (ESI) calcd. for $C_{15}H_{12}N_3O$ $[M-H]^-$ 250.0980, found 250.0974.

1-Fluoro-1-(6-methoxypyridin-2-yl)propan-2-ol (26a): Following **GPC** using **10ab** (33.0 mg, 0.20 mmol), the major diastereomer of **23a** was isolated after 4 h as a colorless oil (11.3 mg, 61.0 µmol, 31% yield, d.r. = 67:33).

Rf = 0.61 (EtOAc/hexanes 25:75); **^{1}H NMR** (400 MHz, D_3COD) δ = 7.68 (dd, *J* = 8.3, 7.3 Hz, 1H), 7.04 (d, *J* = 7.3 Hz, 1H), 6.71 (d, *J* = 8.3 Hz, 1H), 5.31 (dd, *J* = 48.2, 3.6 Hz, 1H), 4.29 (dqd, *J* = 20.7, 6.6, 3.7 Hz, 1H), 1.13 (dd, *J* = 6.5, 1.1 Hz, 3H) ppm; **^{13}C NMR** (126 MHz, D_3COD) δ = 164.94 (d, *J* = 2.7 Hz), 156.08 (d, *J* = 24.5 Hz), 140.5, 114.52 (d, *J* = 7.5 Hz), 111.0, 97.64 (d, *J* = 177.6 Hz), 69.99 (d, *J* = 22.3 Hz), 53.77, 16.63 (d, *J* = 6.3 Hz) ppm; **^{19}F NMR** (376 MHz, $CDCl_3$) δ = -199.74 (dd, *J* = 48.6, 21.2 Hz) ppm **IR** (ATR) $\tilde{\nu}_{max}$ = 3381 (br), 2980, 1579, 1469, 1262, 1029, 989, 810 cm^{-1}; **MS** (ESI): *m/z* (%) = 187/186 (10/100) $[M+H]^+$; **HRMS** (ESI) calcd. for $C_9H_{13}FNO_2$ $[M+H]^+$ 186.0925, found 186.0926.

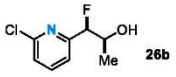

26b

1-(6-Chloropyridin-2-yl)-1-fluoropropan-2-ol (26b): Following **GPC** using **10ac** (33.9 mg, 0.20 mmol), product **26b** was isolated after 5 h as a colorless oil (26.5 mg, 140 µmol, 70% yield, d.r. = 57:43).

Rf = 0.22 (EtOAc/hexanes 17:83); **^{1}H NMR** (400 MHz, D_3COD) maj. d. δ = 7.85 (t, *J* = 7.8 Hz, 1H), 7.47 (d, *J* = 7.7 Hz, 1H), 7.40 (d, *J* = 7.9 Hz, 1H), 5.33 (dd, *J* = 47.6, 4.0 Hz, 1H), 4.30 – 4.11 (m, 1H), 1.13 (dd, *J* = 6.5, 1.4 Hz, 3H) ppm; min. d. δ = 7.84 (t, *J* = 7.8 Hz, 1H), 7.47 (d, *J* = 7.7 Hz, 1H), 7.40 (d, *J* = 7.9 Hz, 1H), 5.23 (dd, *J* = 47.0, 4.0 Hz, 1H), 4.30 – 4.11 (m, 1H), 1.24 (d, *J* = 6.6 Hz, 3H) ppm; **^{13}C NMR** (126 MHz, D_3COD) maj. d. δ = 159.27 (d, *J* = 24.8 Hz), 151.63 (d, *J* = 2.3 Hz), 141.1, 125.0, 121.21 (d, *J* = 6.6 Hz), 97.34 (d, *J* = 178.0 Hz), 69.76 (d, *J* = 23.6 Hz), 17.03 (d, *J* = 6.1 Hz) ppm; min. d. δ = 159.80 (d, *J* = 25.7 Hz), 151.69 (d, *J* = 2.6 Hz), 141.1, 125.0, 121.18 (d, *J* = 6.5 Hz), 97.67 (d, *J* = 177.8 Hz), 69.75 (d, *J* = 19.9 Hz), 18.97 (d, *J* = 5.6 Hz) ppm; **^{19}F NMR** (376 MHz, $CDCl_3$) maj. d. δ = -197.22 (dd, *J* = 47.6, 19.1 Hz) ppm, min. d. δ = -200.41 (dd, *J* = 47.0, 22.7 Hz) ppm **IR** (ATR) $\tilde{\nu}_{max}$ = 3376 (br), 2981, 1565, 1441, 1166, 989, 790 cm^{-1}; **MS** (ESI): *m/z* (%) = 192/190 (34/100) $[M+H]^+$, 172 (15); **HRMS** (ESI) calcd. for $C_8H_9ClFNNaO$ $[M+Na]^+$ 212.0254, found 212.0249.

7. References:

[1] a) C. Ye, B. Twamley, J. M. Shreeve, *Org. Lett.* **2005**, *7*, 3961-3964; b) G. C. Geary, E. G. Hope, K. Singh, A. M. Stuart, *Chem. Commun.* **2013**, *49*, 9263-9265; c) J. P. Brand, C. Chevalley, R. Scopelliti, J. Waser, *Chem. Eur. J.* **2012**, *18*, 5655-5666.

[2] A. R. Katritzky, G. Yao, S. Rachwal, *J. Heterocyclic Chem.* **1994**, 757–763.

– SUPPORTING INFORMATION –

α-Functionalization of Ketones via a Nitrogen Directed Oxidative Umpolung

Gabriel M. Kiefl, [a] and Tanja Gulder[a,b]*

[a]*Biomimetic Catalysis, Department of Chemistry, Technical University Munich, Lichtenbergstrasse 4, 85747 Garching, Germany*

[b] *Institute of Organic Chemistry, Leipzig University, Johannisallee 29, 04103 Leipzig, Germany*

**corresponding author: tanja.gulder@uni-leipzig.de*

NMR spectra of compounds 12a-al, 21, 26a-b

Those ^{1}H-NMR spectra showing the product as a mixture of its ketone and enol form, the signals of both species have been picked and the signals of the minor tautomer was labelled with a *.

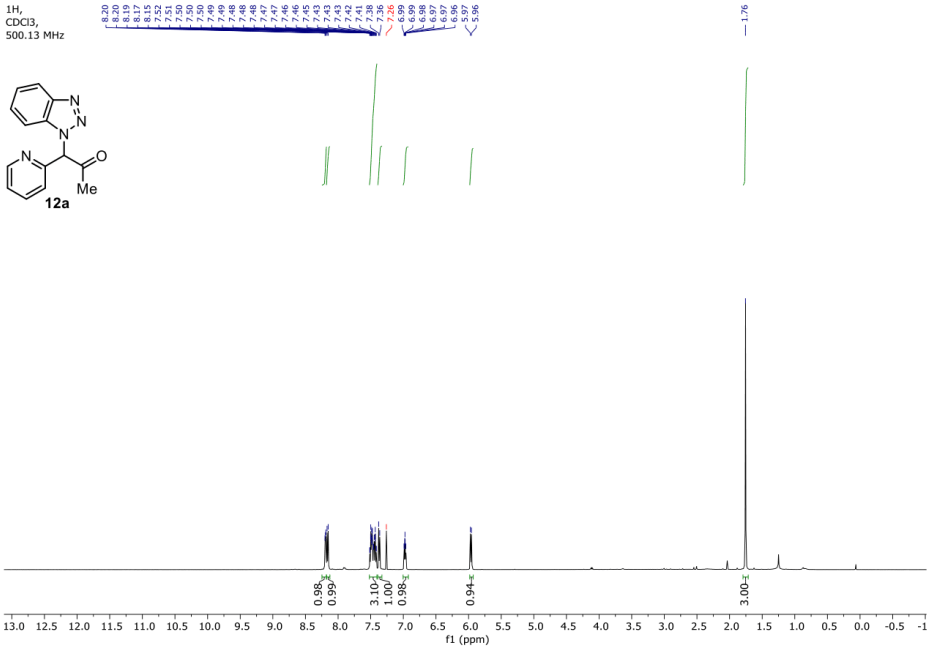
1H,
CDCl3,
500.13 MHz
12a
f1 (ppm)

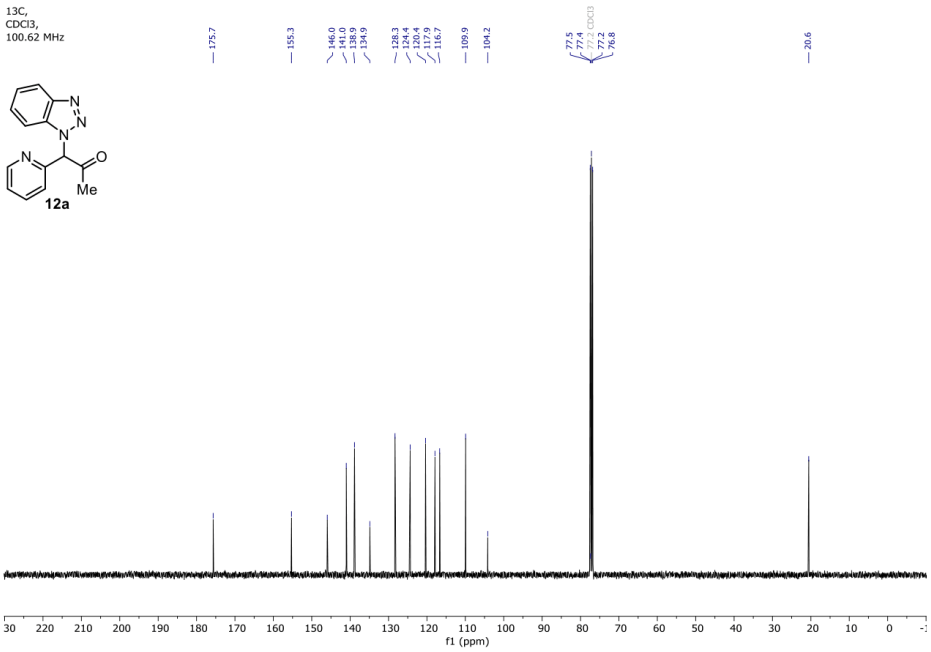
13C,
CDCl3,
100.62 MHz
12a
f1 (ppm)

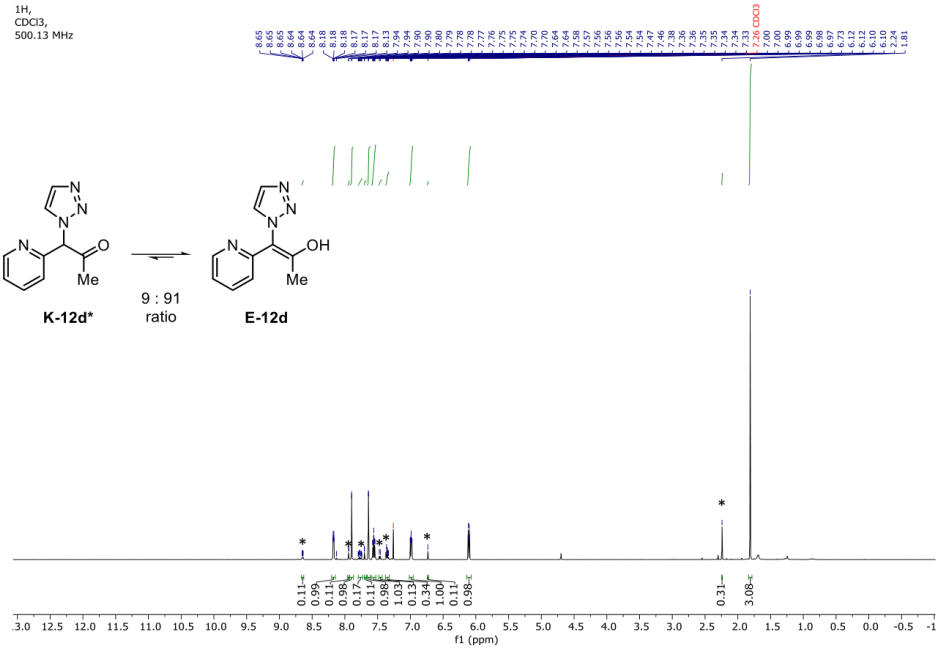
1H,
CDCl3,
500.13 MHz
Me
K-12d*
9 : 91
ratio
OH
Me
E-12d
f1 (ppm)

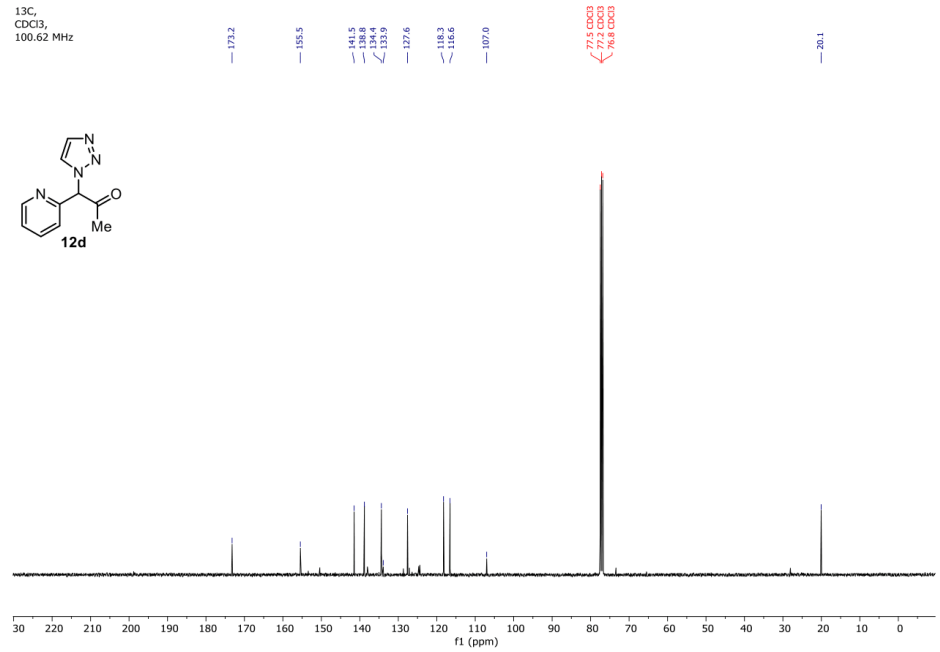
13C,
CDCl3,
100.62 MHz
Me
12d
f1 (ppm)

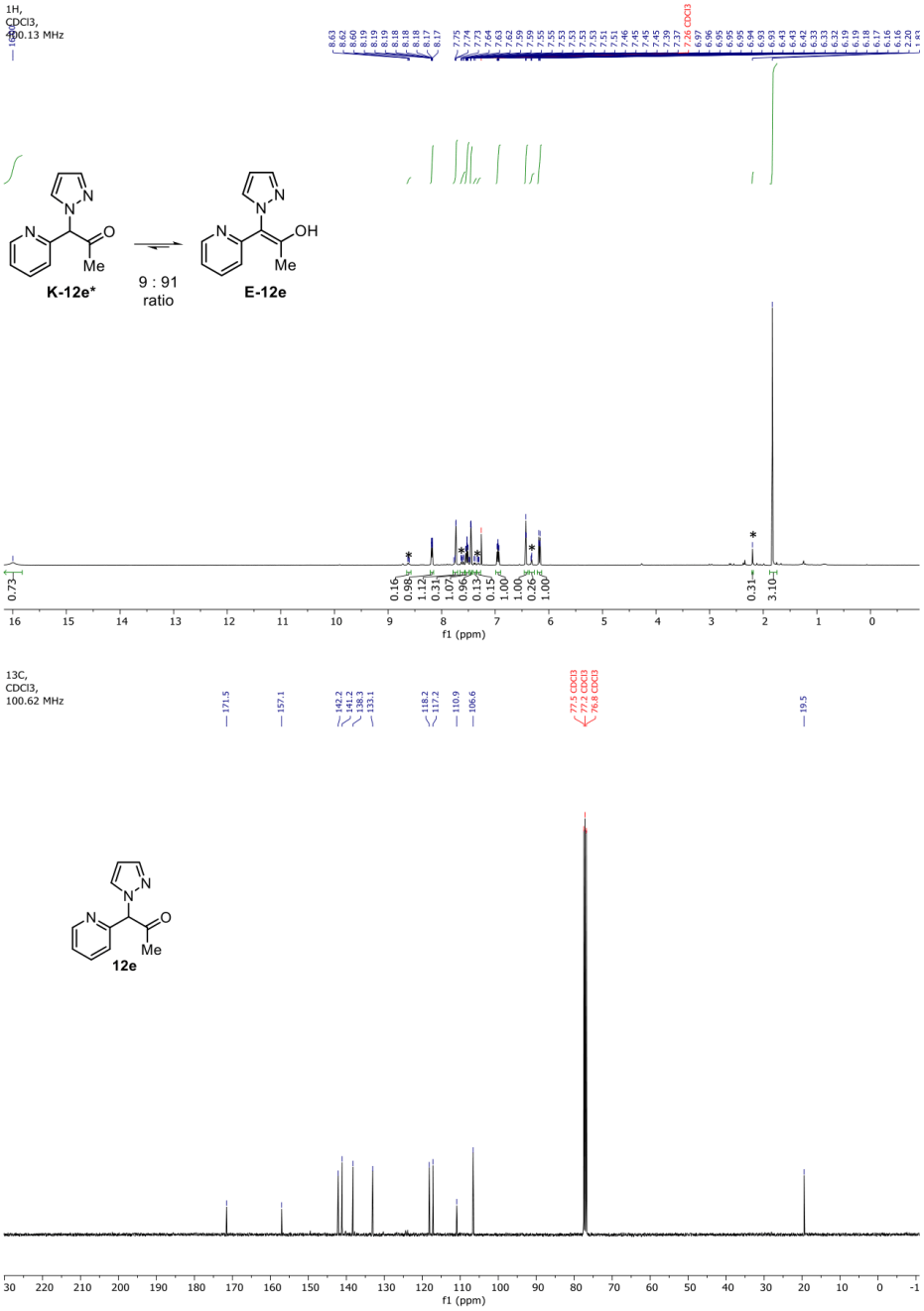
1H,
CDCl3,
400.13 MHz
K-12e*
9 : 91
ratio
E-12e
f1 (ppm)
13C,
CDCl3,
100.62 MHz
12e
f1 (ppm)

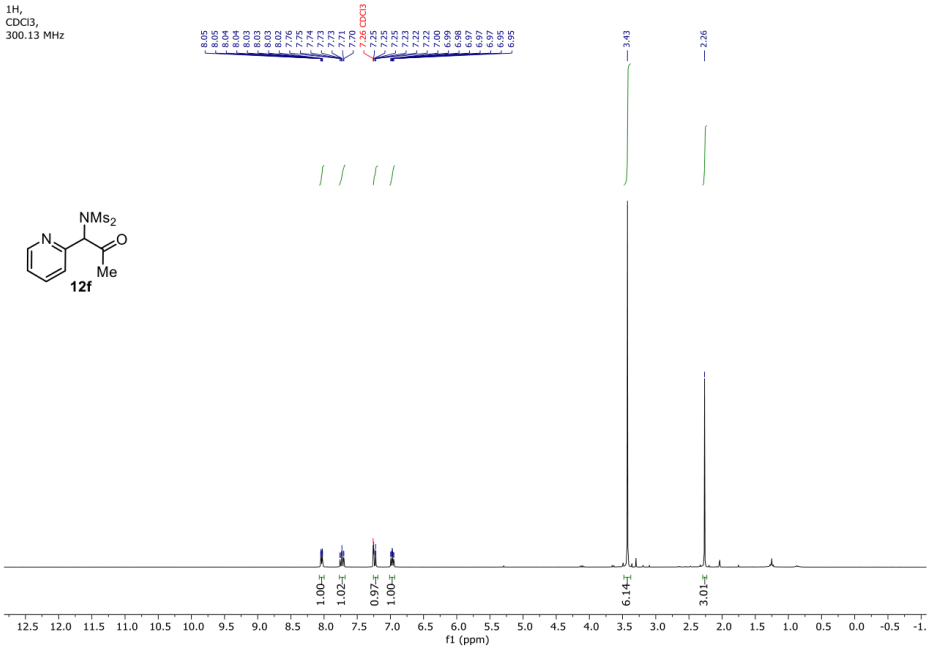
1H,
CDCl3,
300.13 MHz
NMs2
Me
12f
f1 (ppm)

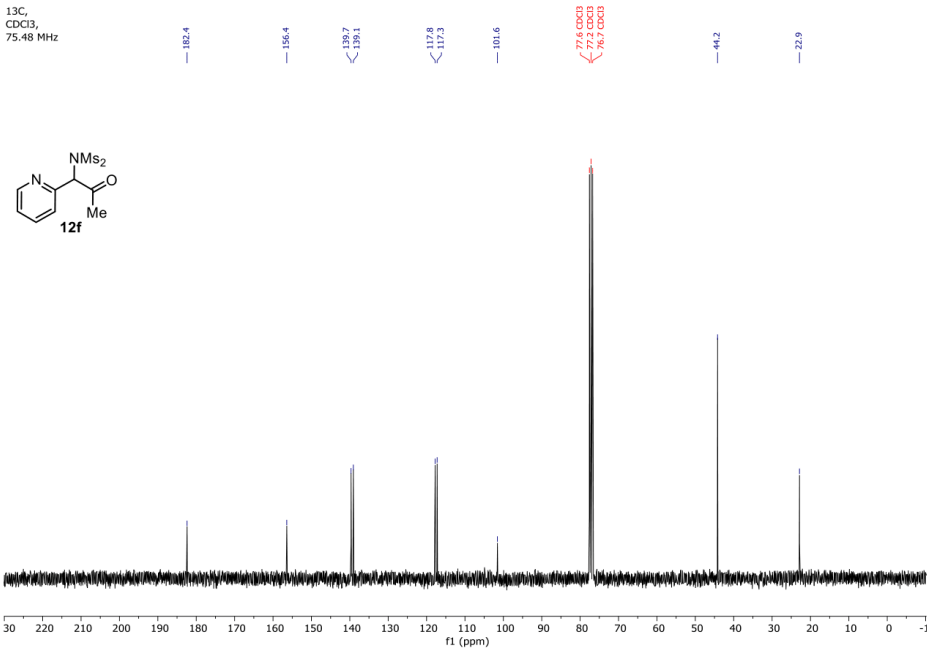
13C,
CDCl3,
75.48 MHz
NMs2
Me
12f
f1 (ppm)

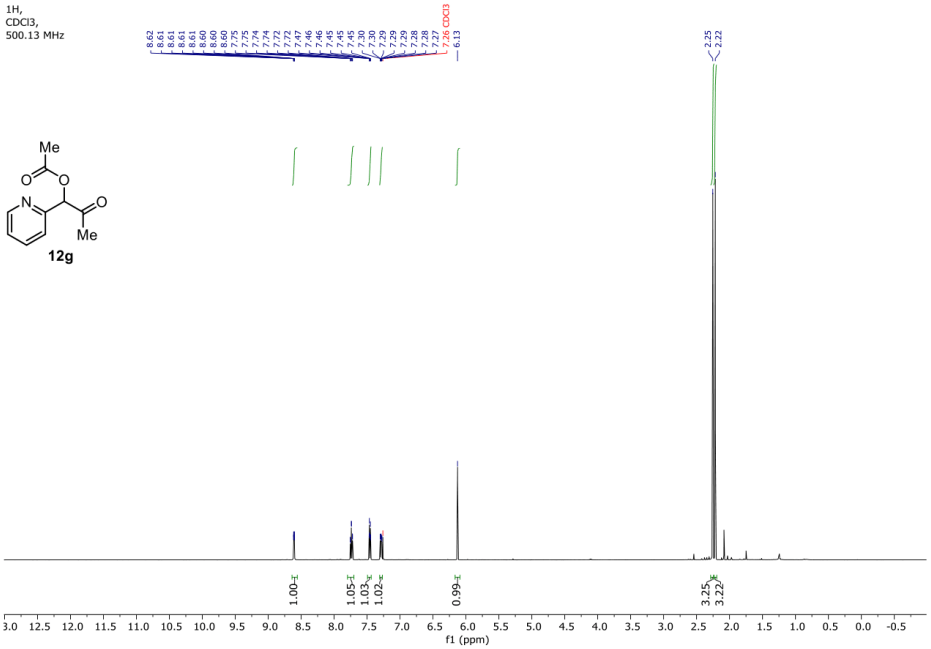
1H,
CDCl3,
500.13 MHz
Me
Me
12g
f1 (ppm)

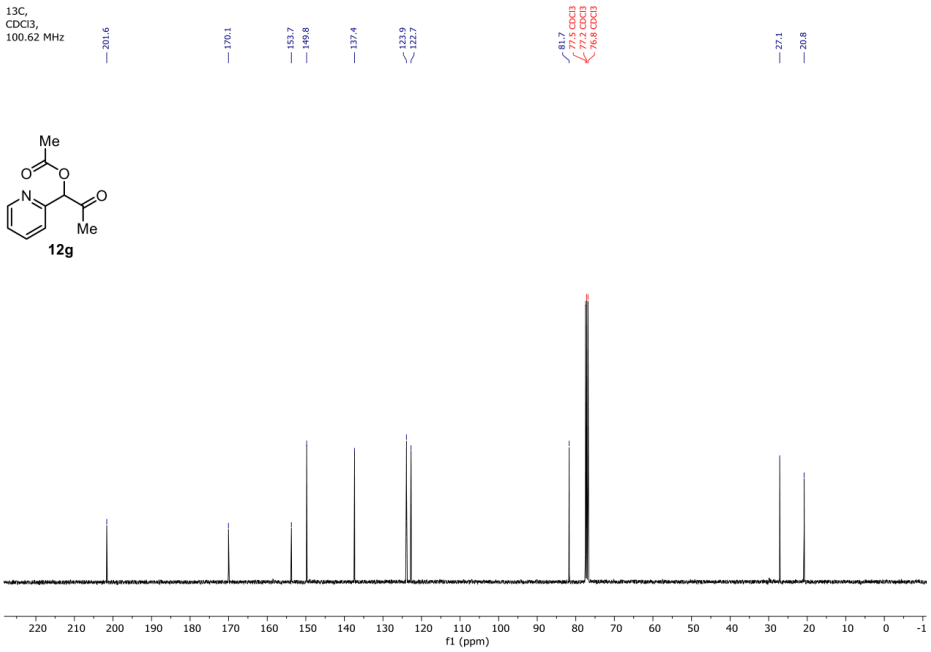
13C,
CDCl3,
100.62 MHz
Me
Me
12g
f1 (ppm)

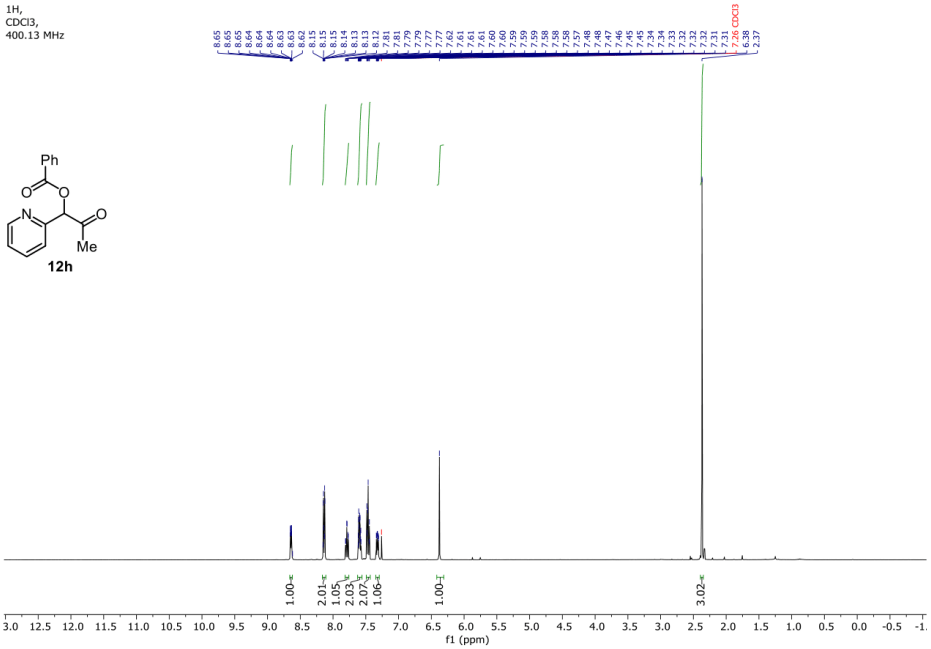
1H,
CDCl3,
400.13 MHz
Ph
O
O
N
O
Me
12h
f1 (ppm)

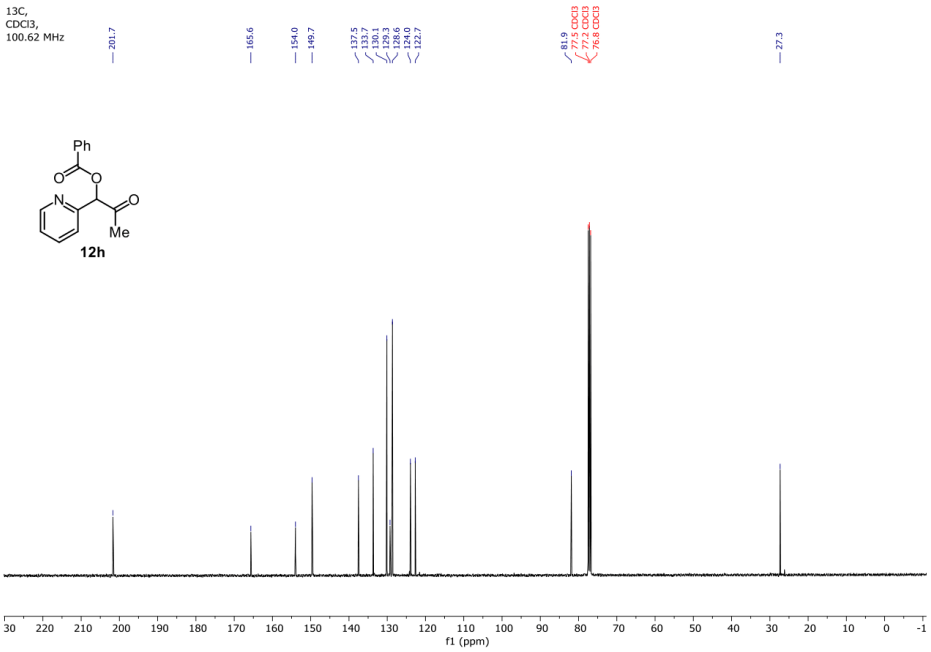
13C,
CDCl3,
100.62 MHz
Ph
O
O
N
O
Me
12h
f1 (ppm)

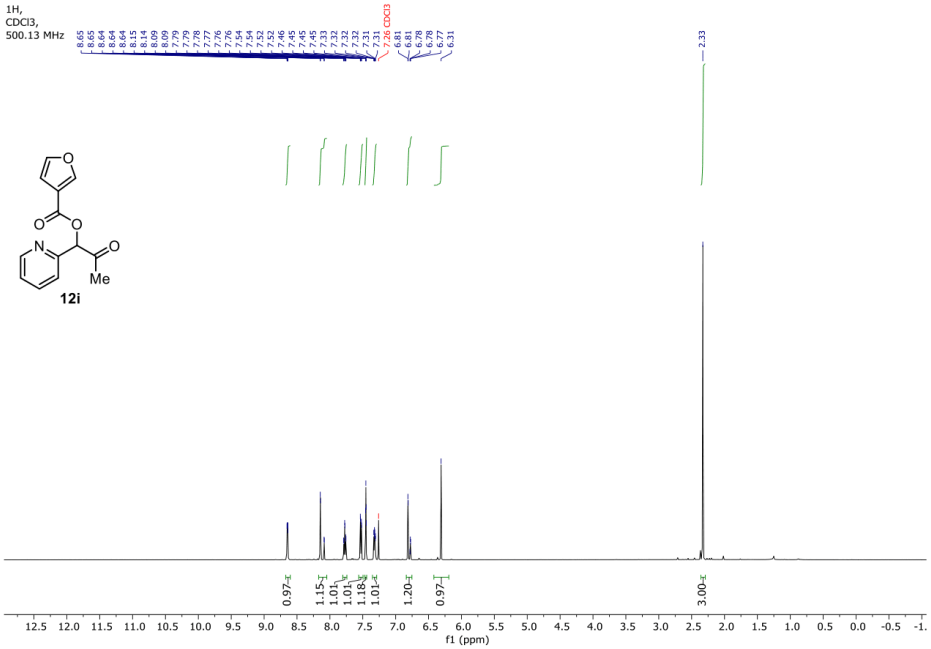
1H,
CDCl3,
500.13 MHz
12i
f1 (ppm)

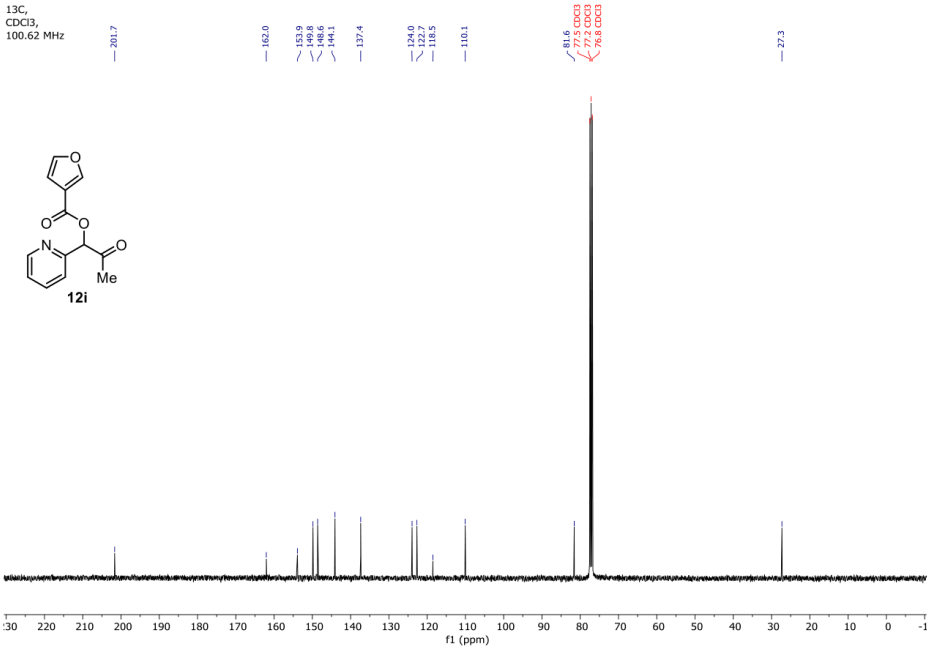
13C,
CDCl3,
100.62 MHz
12i
f1 (ppm)

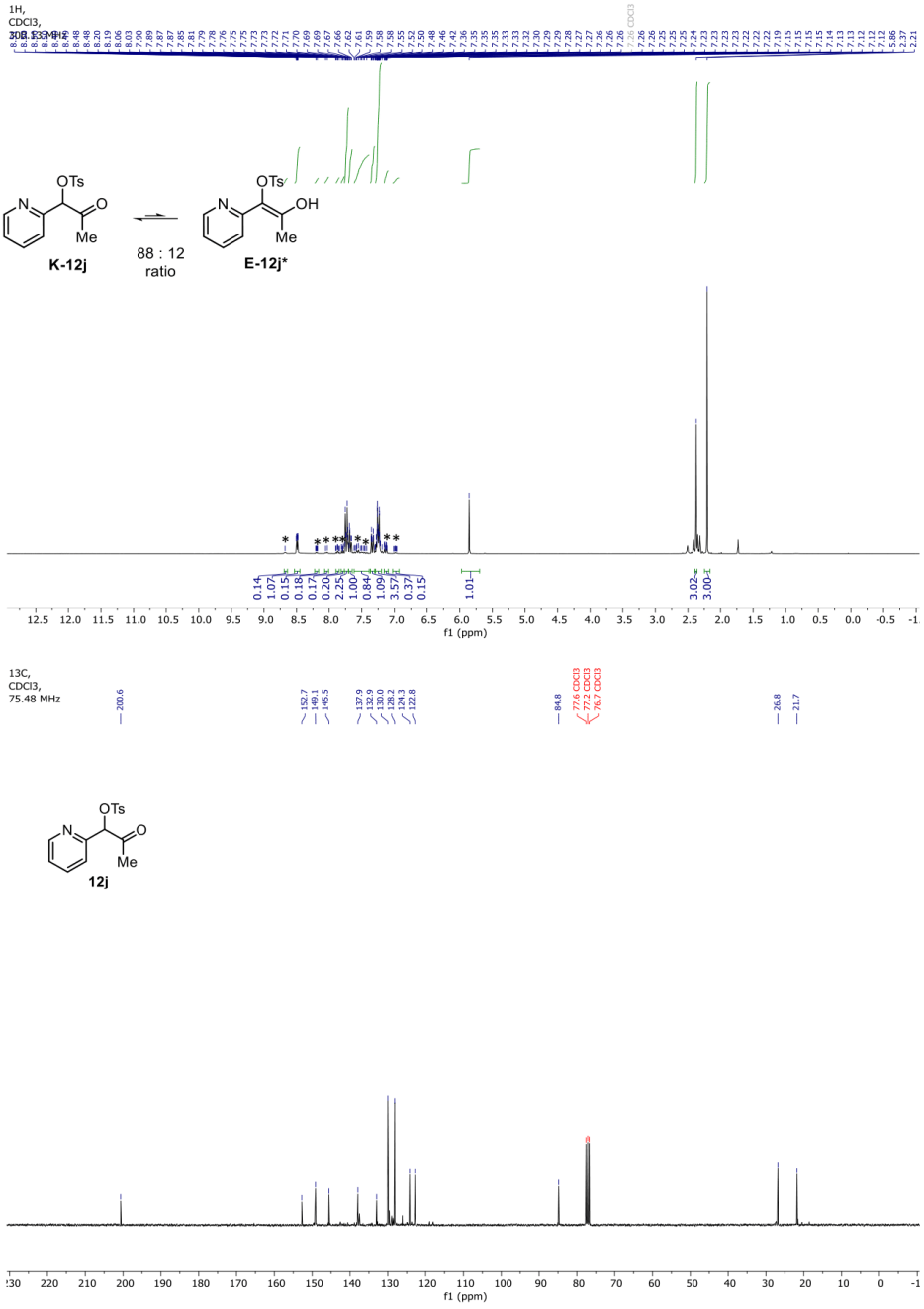
1H,
CDCl3,
OTs
N
O
Me
K-12j
88 : 12
ratio
OTs
N
OH
Me
E-12j*
f1 (ppm)
13C,
CDCl3,
75.48 MHz
77.6 CDCl3
77.2 CDCl3
76.7 CDCl3
OTs
N
O
Me
12j
f1 (ppm)

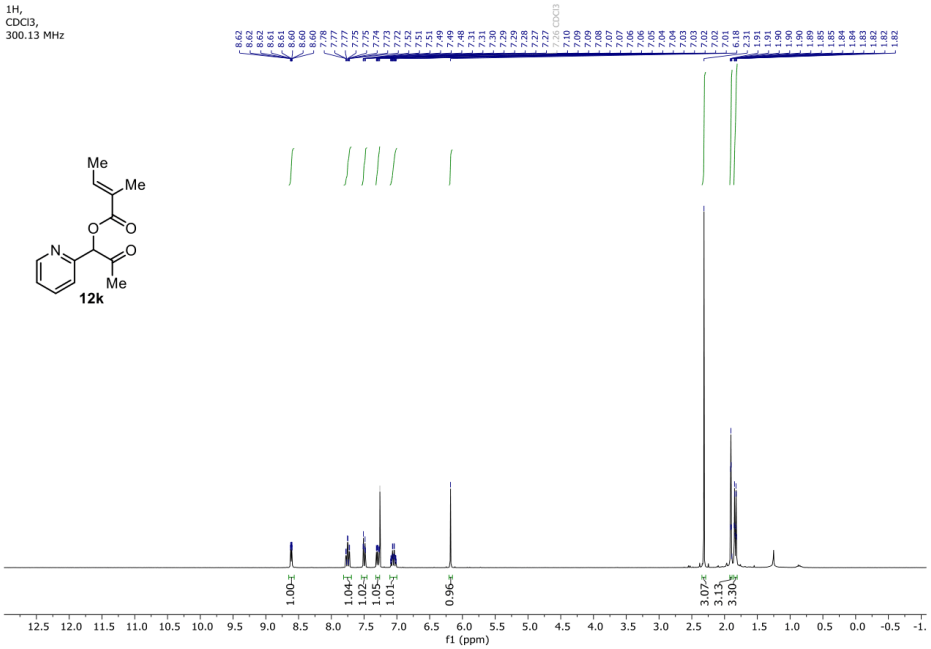
1H,
CDCl3,
300.13 MHz
Me
Me
O
O
N
O
Me
12k
1.00
1.04
1.02
1.05
1.01
0.96
3.07
3.13
3.30
f1 (ppm)

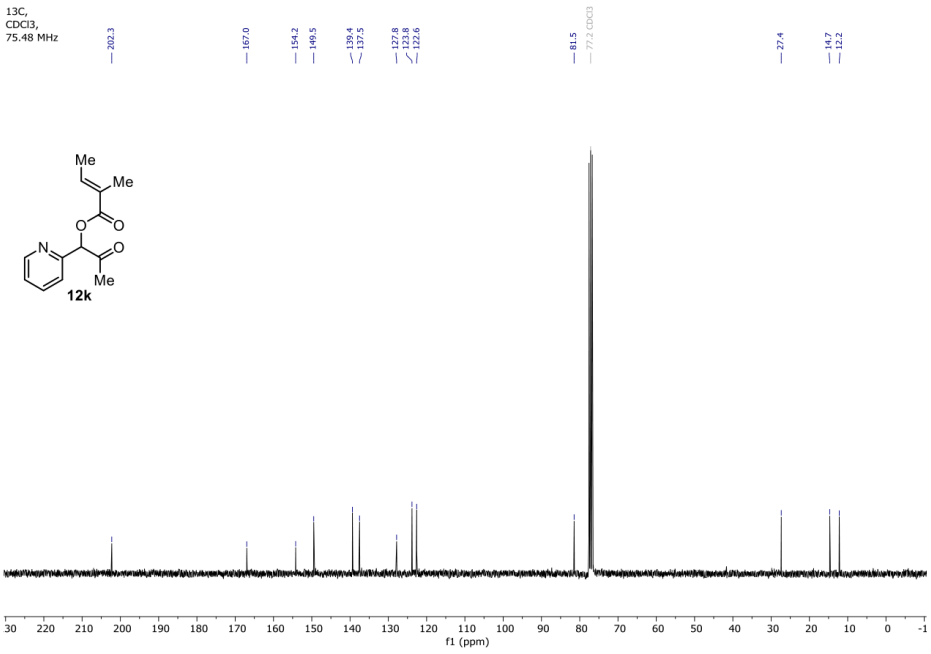
13C,
CDCl3,
75.48 MHz
202.3
167.0
154.2
149.5
139.4
137.5
127.8
123.8
122.6
81.5
77.2 CDCl3
27.4
14.7
12.2
Me
Me
O
O
N
O
Me
12k
f1 (ppm)

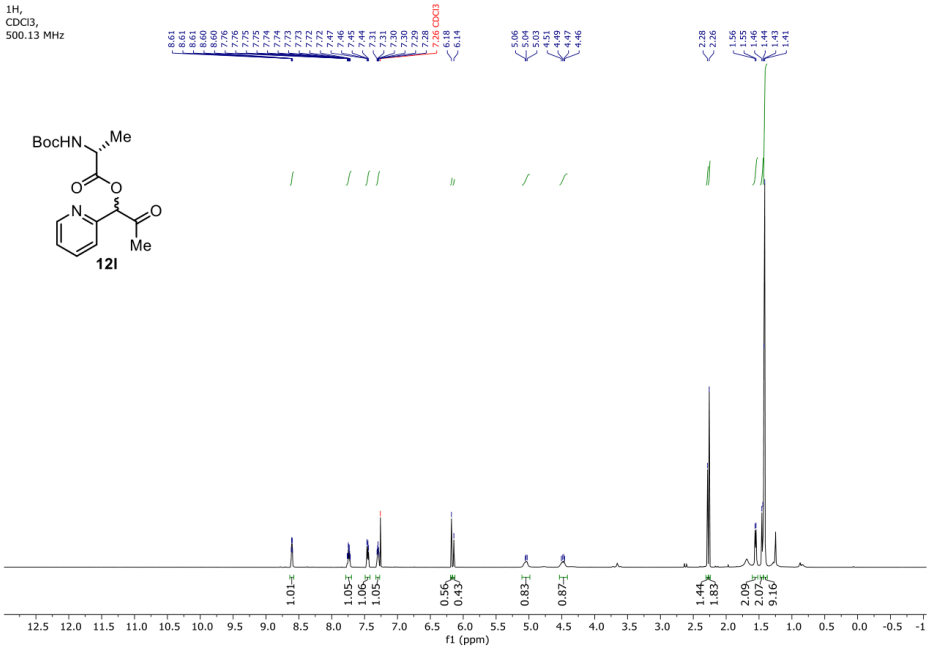
1H,
CDCl3,
500.13 MHz
BocHN
Me
O
O
N
O
Me
12l
f1 (ppm)

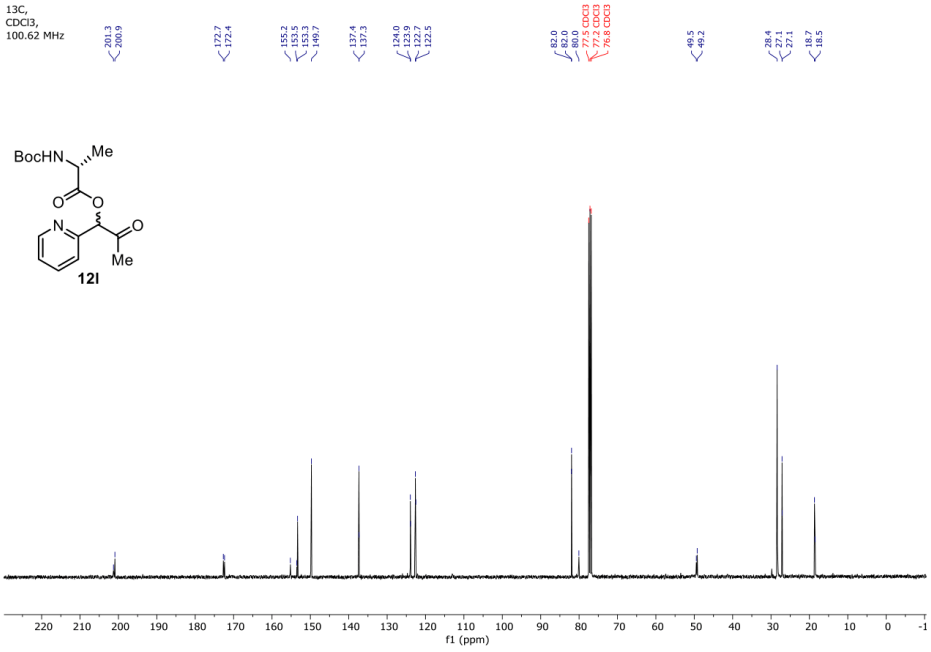
13C,
CDCl3,
100.62 MHz
BocHN
Me
O
O
N
O
Me
12l
f1 (ppm)

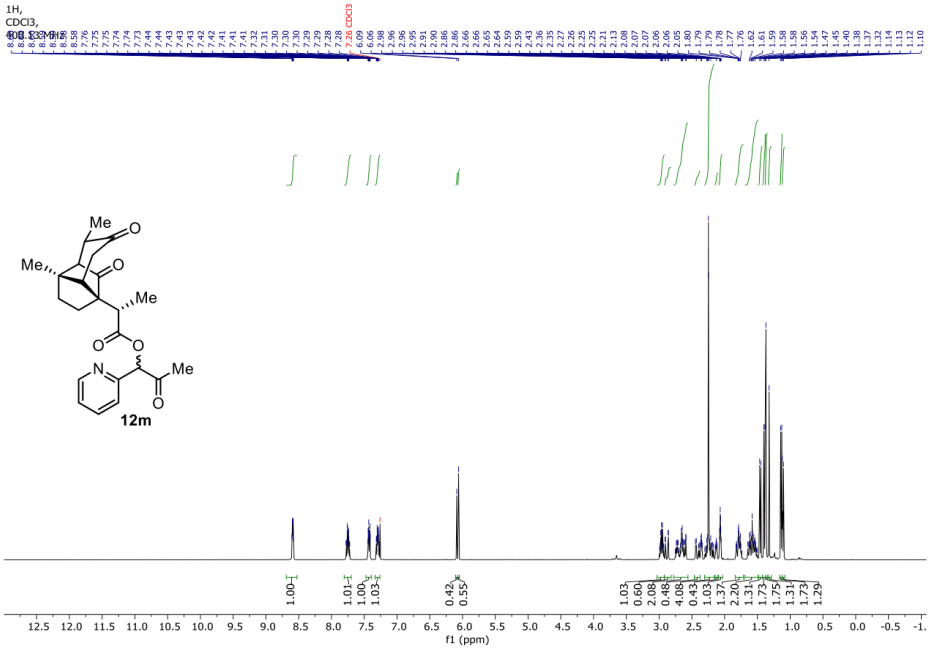
1H,
CDCl3,
12m
f1 (ppm)

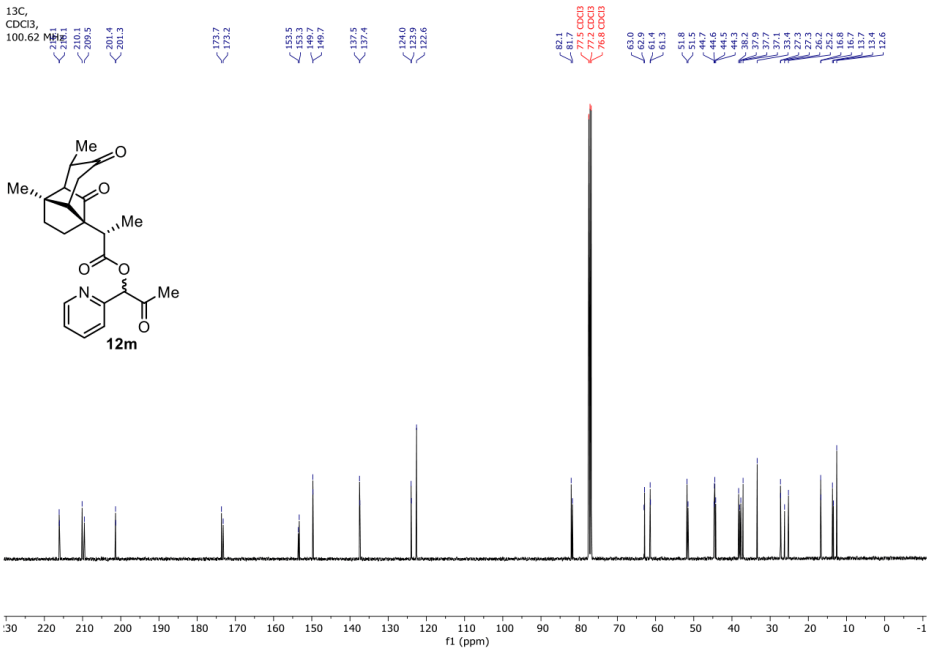
13C,
CDCl3,
12m
f1 (ppm)

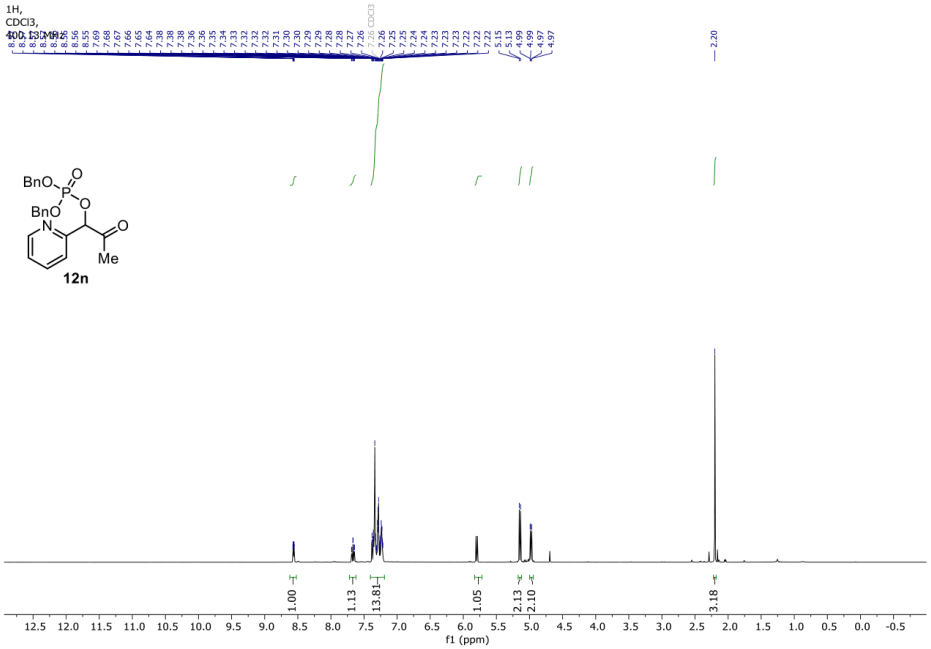
1H,
CDCl3,
12n
f1 (ppm)

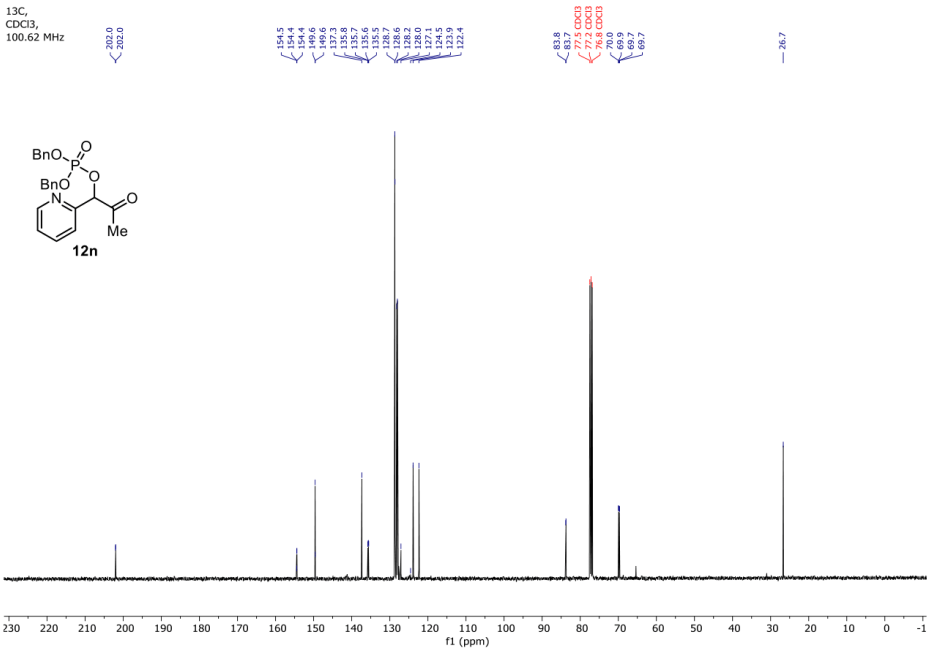
13C,
CDCl3,
100.62 MHz
12n
f1 (ppm)

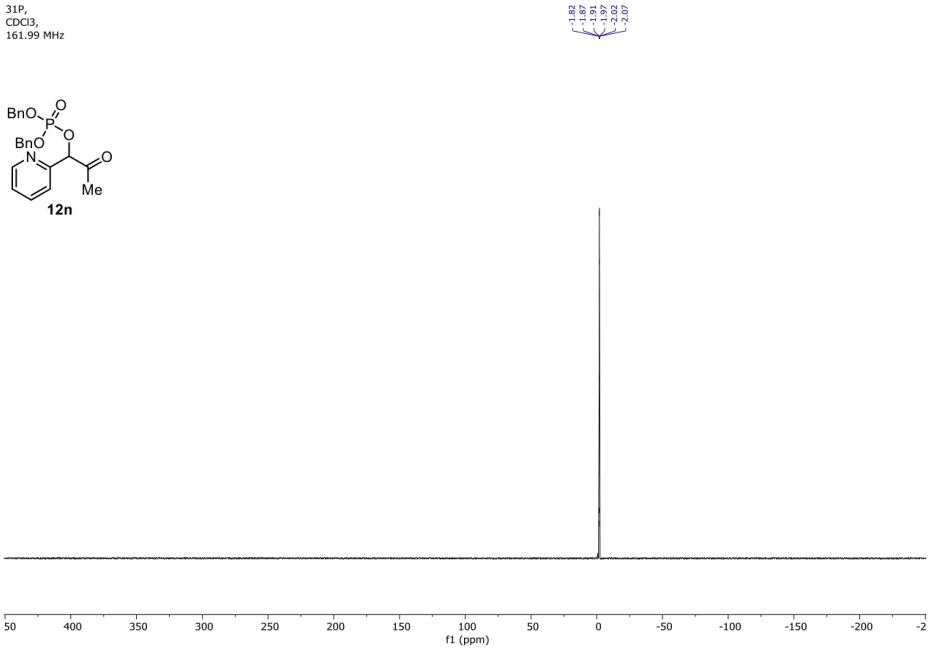
31P,
CDCl3,
161.99 MHz
-1.82
-1.87
-1.92
-1.97
-2.02
-2.07
BnO
O
P
O
BnO
N
O
Me
12n
50
400
350
300
250
200
150
100
50
0
-50
-100
-150
-200
-2
f1 (ppm)

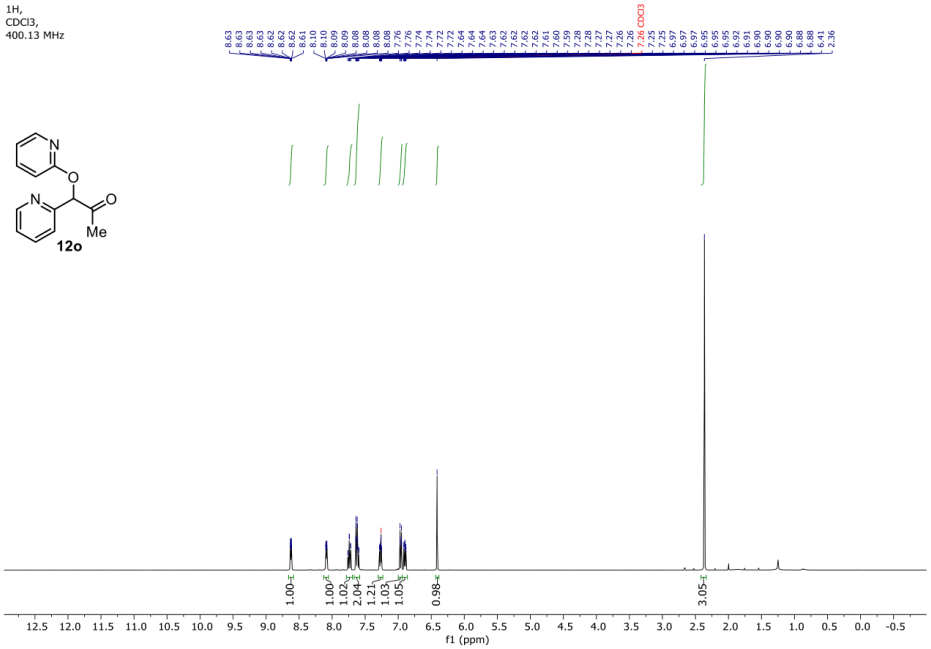
1H,
CDCl3,
400.13 MHz
12o
f1 (ppm)

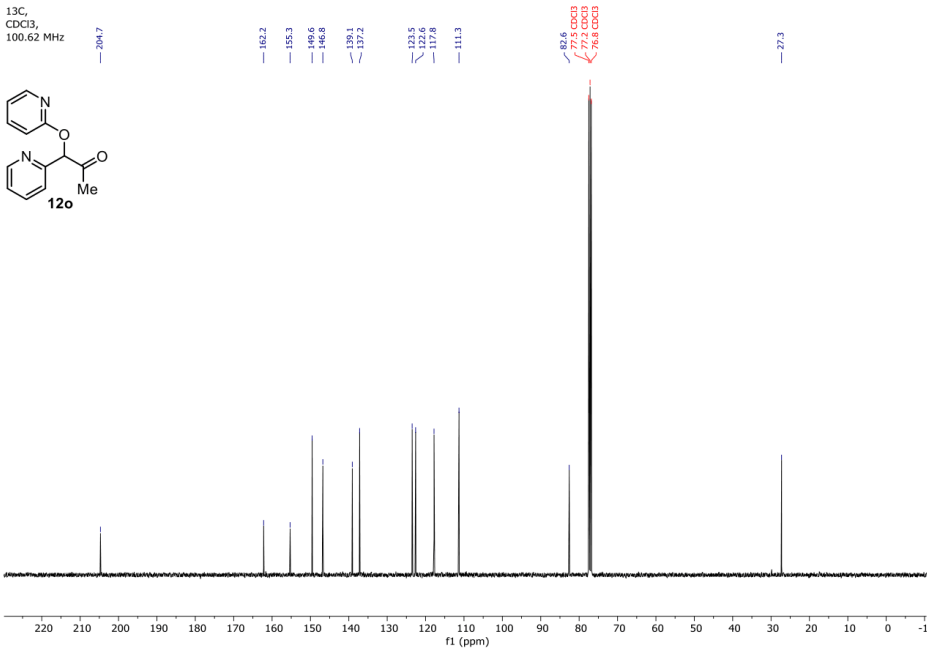
13C,
CDCl3,
100.62 MHz
12o
f1 (ppm)

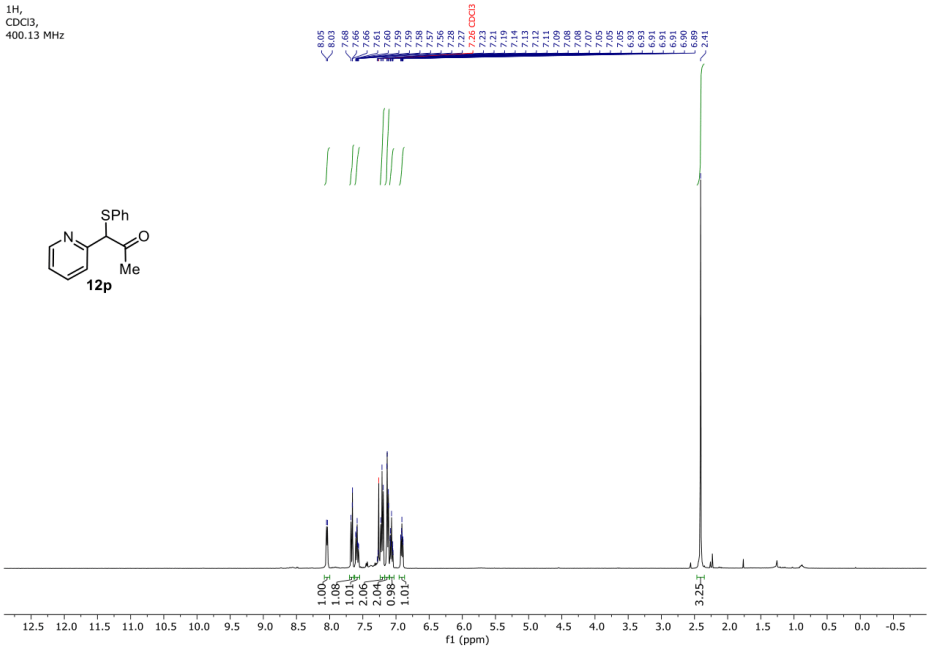
1H,
CDCl3,
400.13 MHz
SPh
N
O
Me
12p
f1 (ppm)

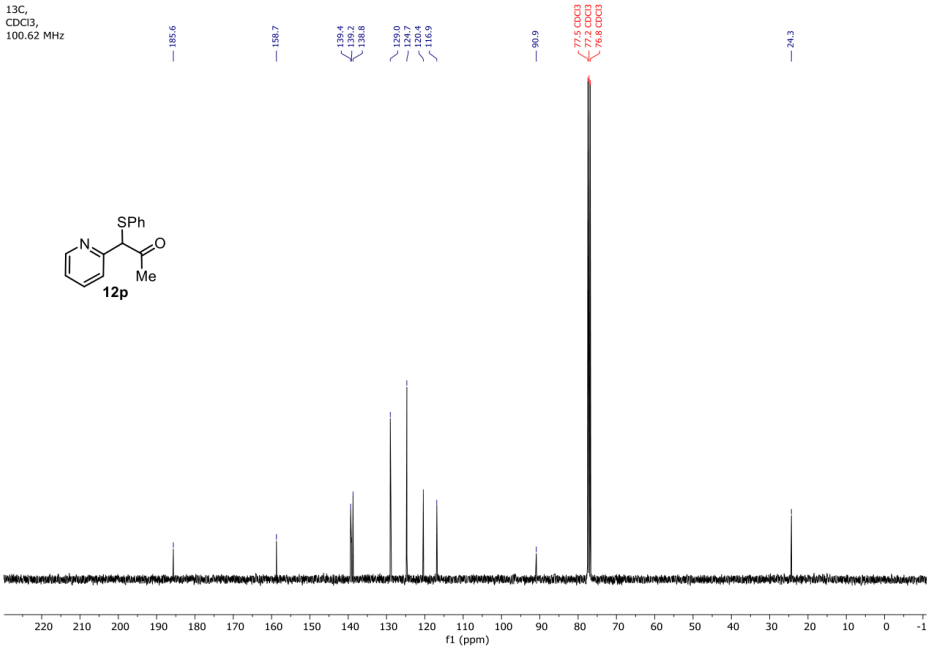
13C,
CDCl3,
100.62 MHz
SPh
N
O
Me
12p
f1 (ppm)

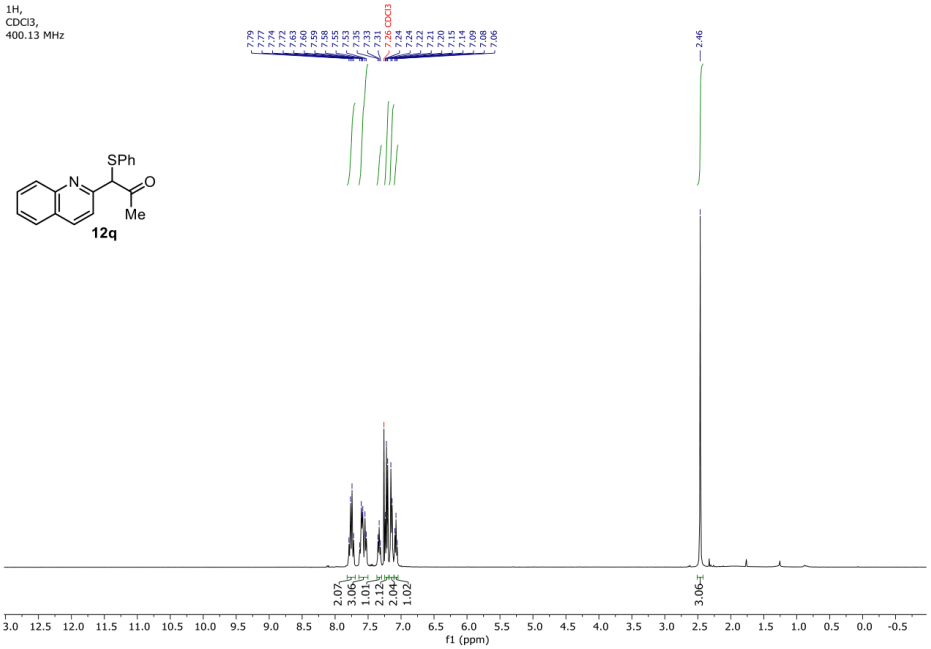
1H,
CDCl3,
400.13 MHz
SPh
N
O
Me
12q
7.79
7.77
7.74
7.72
7.63
7.60
7.59
7.58
7.55
7.53
7.35
7.33
7.31
7.26 CDCl3
7.24
7.22
7.21
7.20
7.15
7.14
7.09
7.08
7.06
2.46
2.07
3.06
1.01
2.12
2.04
1.02
3.06
f1 (ppm)

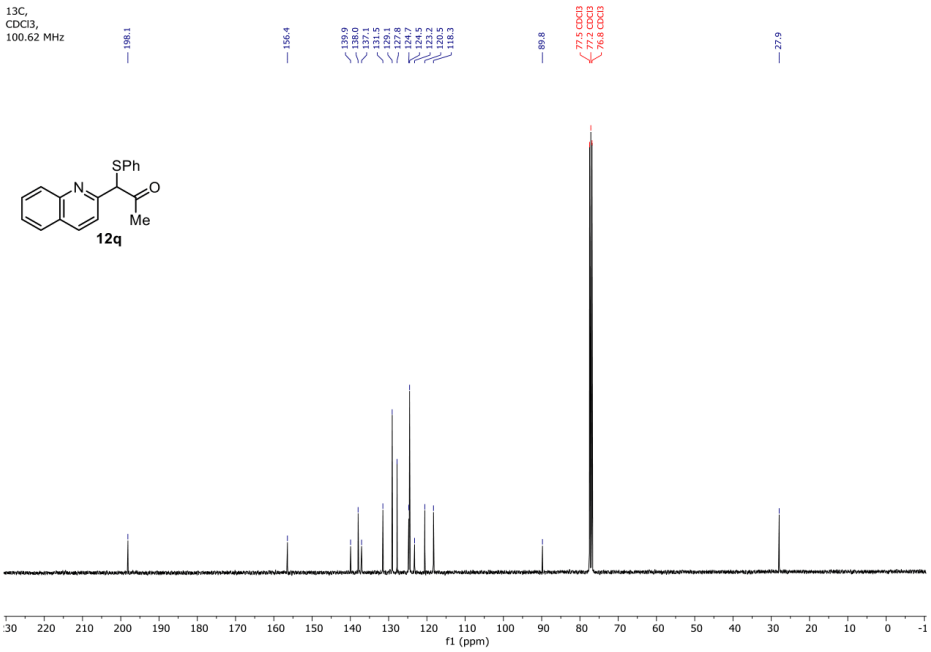
13C,
CDCl3,
100.62 MHz
198.1
156.4
139.9
138.0
137.1
131.5
129.1
127.8
124.7
124.5
123.2
121.5
118.3
89.8
77.5 CDCl3
77.2 CDCl3
76.8 CDCl3
27.9
SPh
N
O
Me
12q
f1 (ppm)

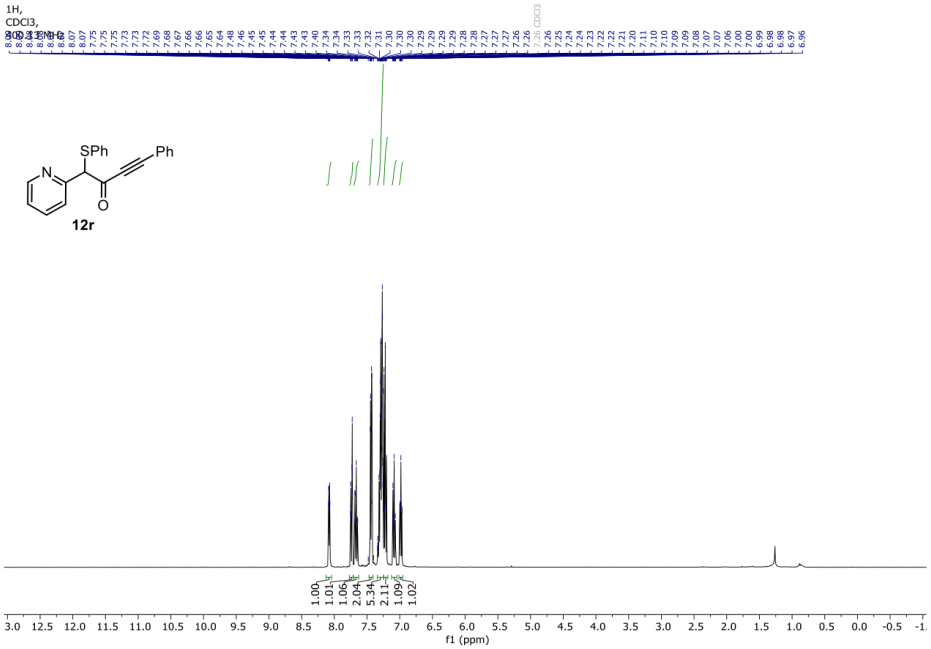
1H,
CDCl3,
SPh
Ph
N
O
12r
1.00
1.01
1.06
2.04
5.34
2.11
1.09
1.02
f1 (ppm)

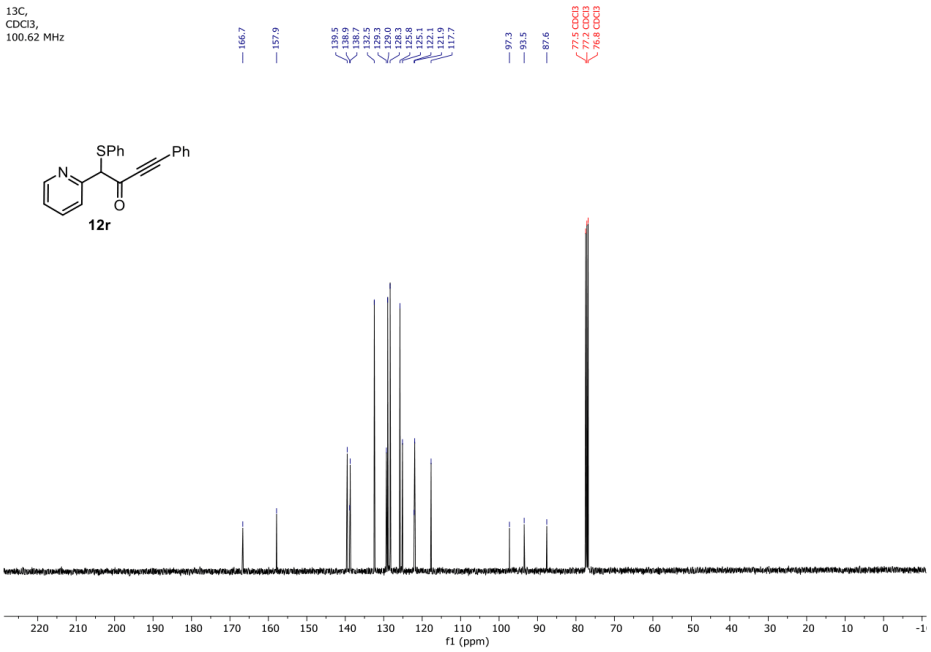
13C,
CDCl3,
100.62 MHz
166.7
157.9
139.5
138.9
138.7
132.5
129.3
129.0
128.3
125.8
125.1
122.1
121.9
117.7
97.3
93.5
87.6
77.5 CDCl3
77.2 CDCl3
76.8 CDCl3
SPh
Ph
N
O
12r
f1 (ppm)

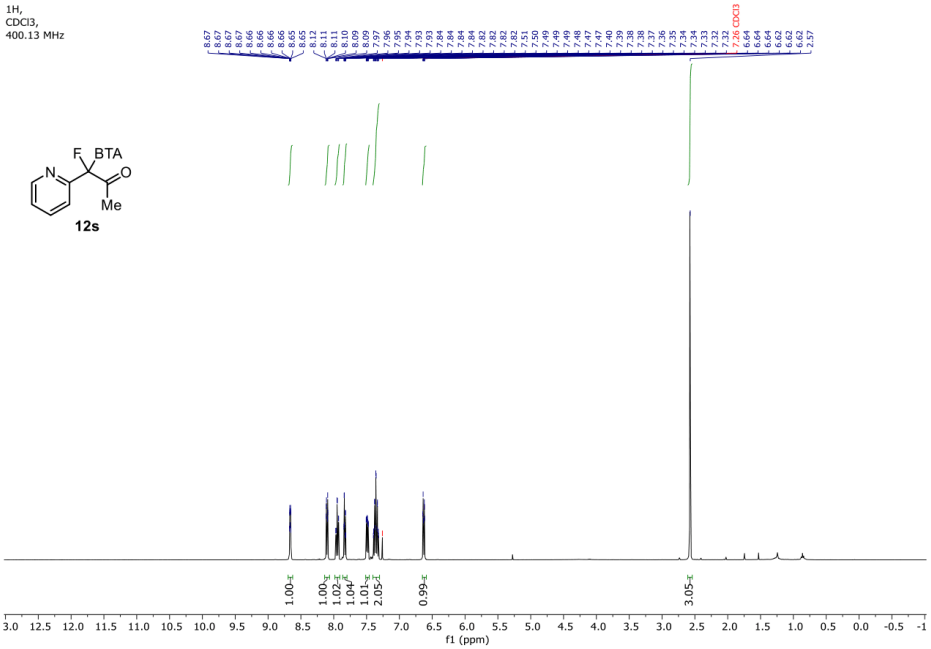
1H,
CDCl3,
400.13 MHz
F
BTA
N
O
Me
12s
1.00
1.00
1.02
1.04
1.01
2.05
0.99
3.05
f1 (ppm)

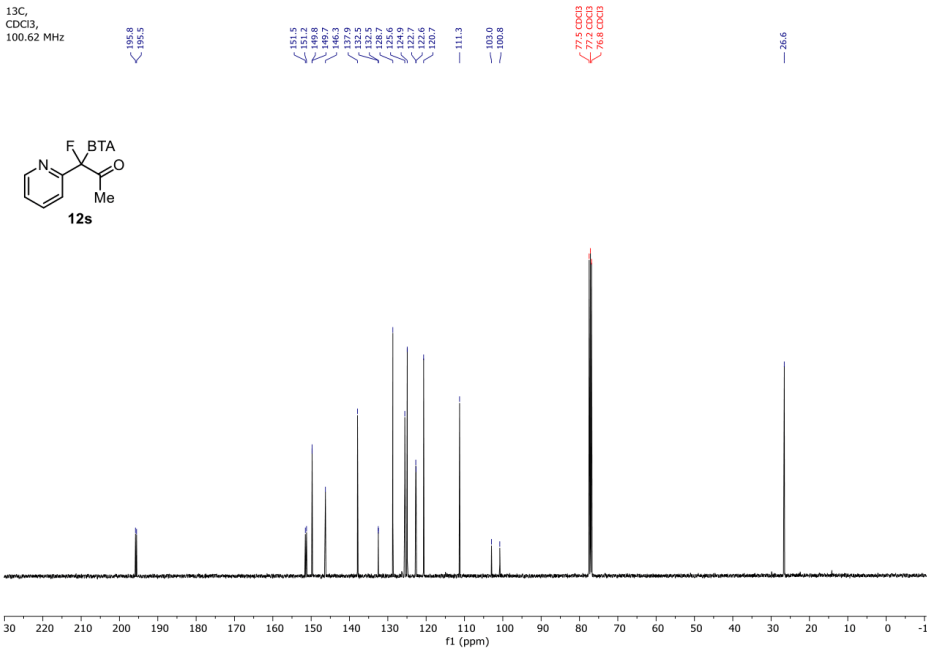
13C,
CDCl3,
100.62 MHz
F
BTA
N
O
Me
12s
f1 (ppm)

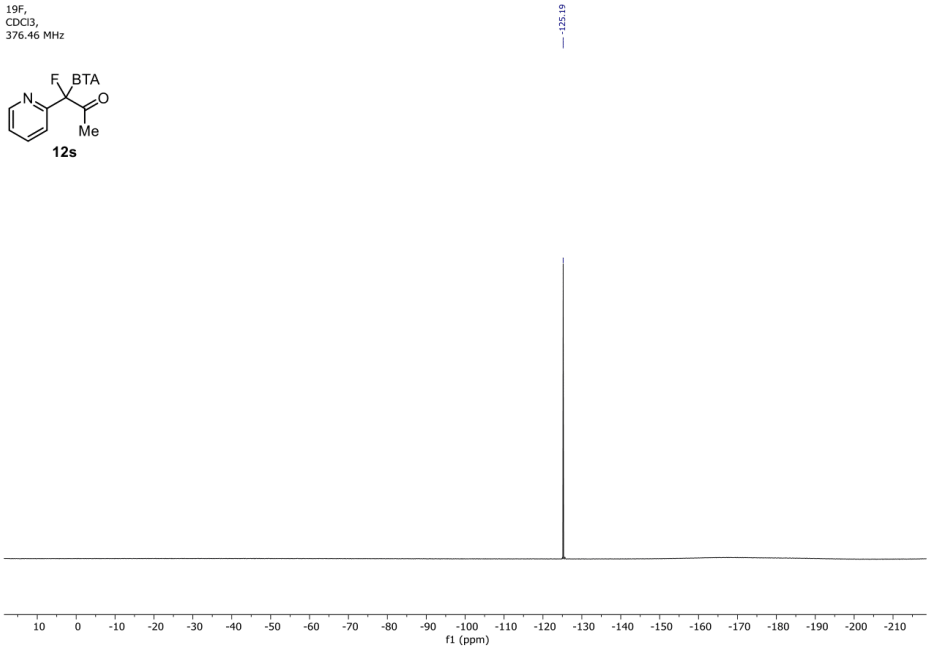
19F,
CDCl3,
376.46 MHz
F
BTA
N
O
Me
12s
-125.19
10 0 -10 -20 -30 -40 -50 -60 -70 -80 -90 -100 -110 -120 -130 -140 -150 -160 -170 -180 -190 -200 -210
f1 (ppm)

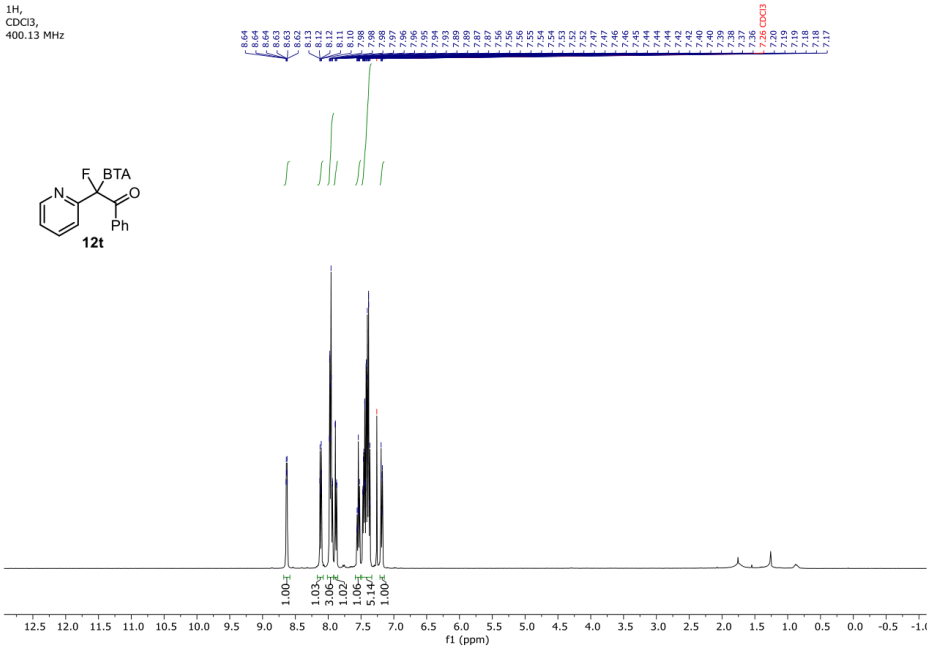
1H,
CDCl3,
400.13 MHz
F
BTA
N
O
Ph
12t
f1 (ppm)

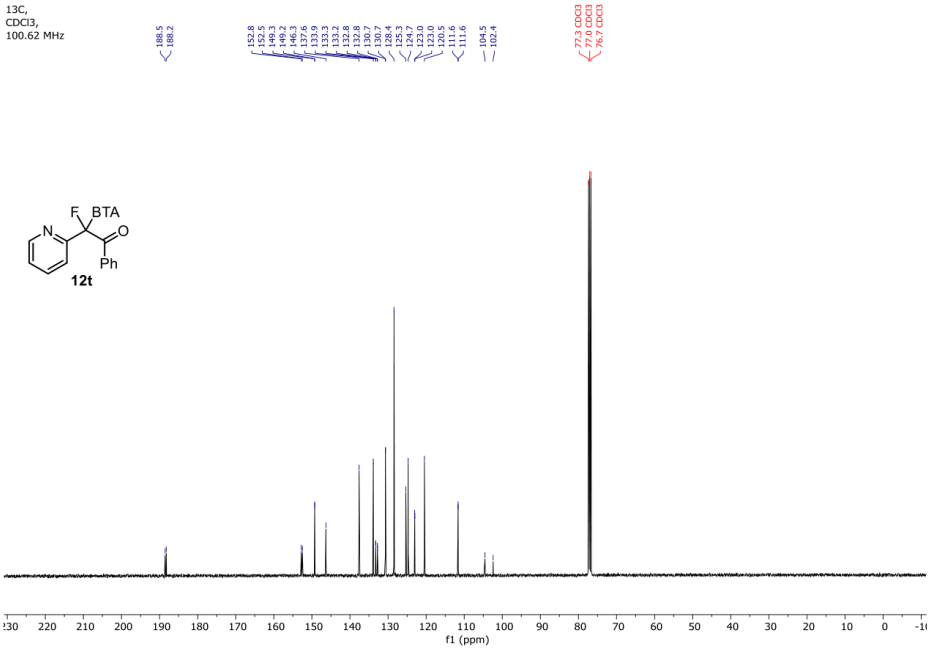
13C,
CDCl3,
100.62 MHz
F
BTA
N
O
Ph
12t
f1 (ppm)

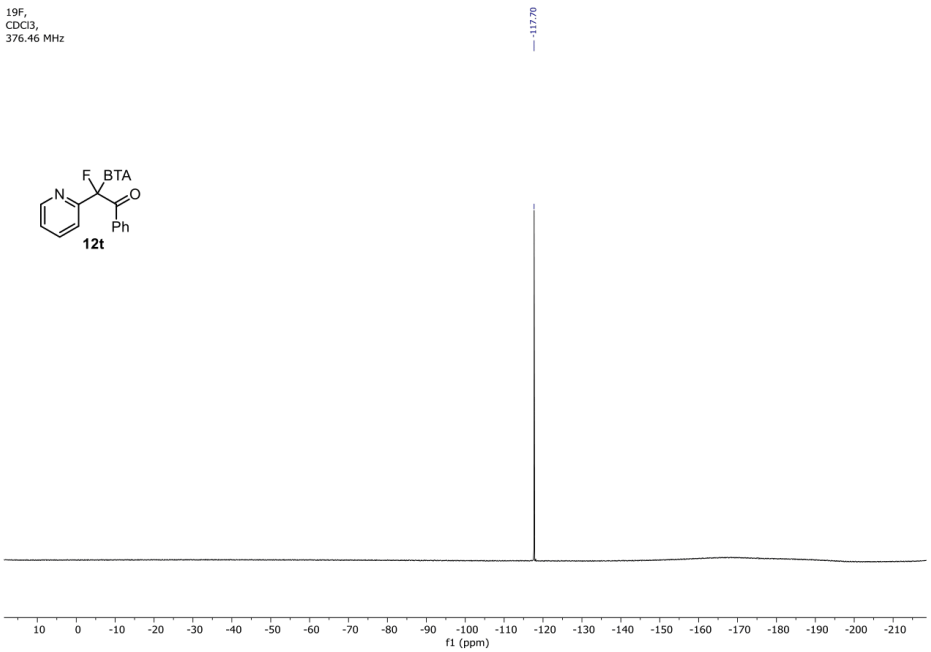
19F,
CDCl3,
376.46 MHz
-117.70
F
BTA
N
O
Ph
12t
10 0 -10 -20 -30 -40 -50 -60 -70 -80 -90 -100 -110 -120 -130 -140 -150 -160 -170 -180 -190 -200 -210
f1 (ppm)

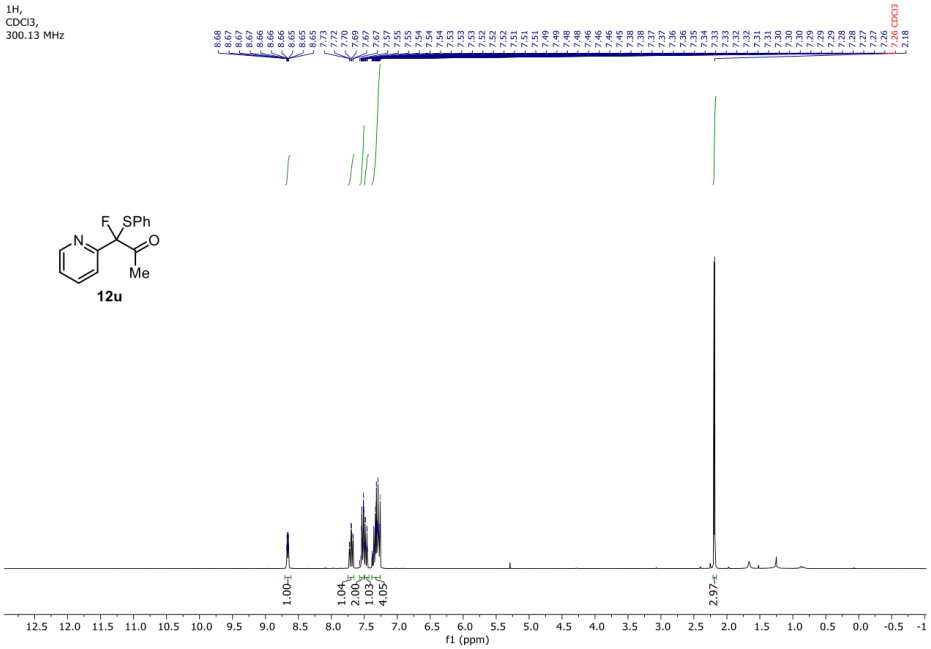
1H,
CDCl3,
300.13 MHz
F
SPh
N
O
Me
12u
1.00
1.04
2.00
1.03
4.05
2.97
f1 (ppm)

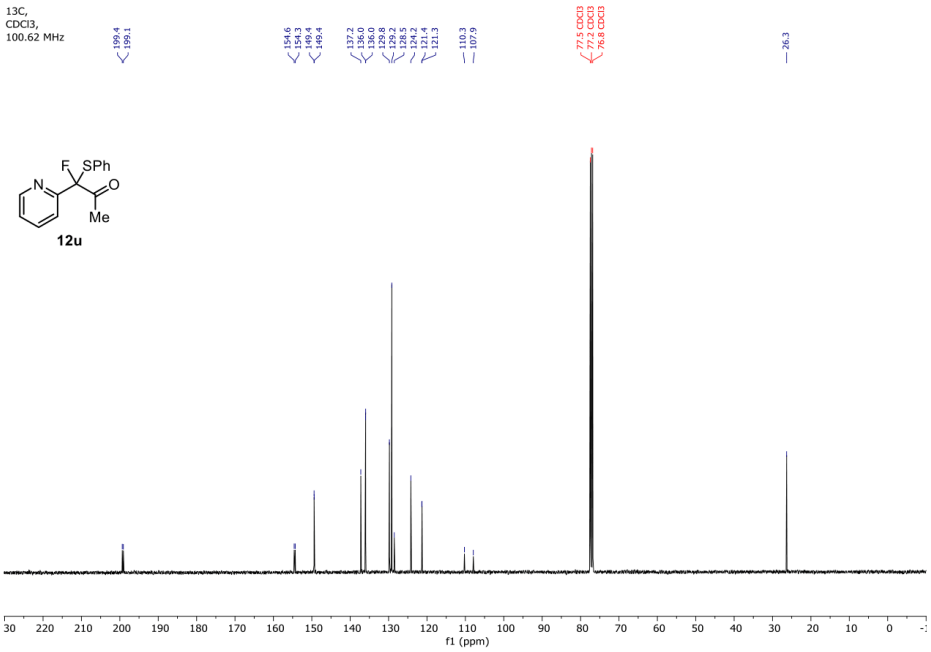
13C,
CDCl3,
100.62 MHz
199.4
199.1
154.6
154.3
149.4
149.4
137.2
136.0
130.0
129.8
129.2
128.5
124.2
121.4
121.3
110.3
107.9
77.5 CDCl3
77.2 CDCl3
76.8 CDCl3
26.3
F
SPh
N
O
Me
12u
f1 (ppm)

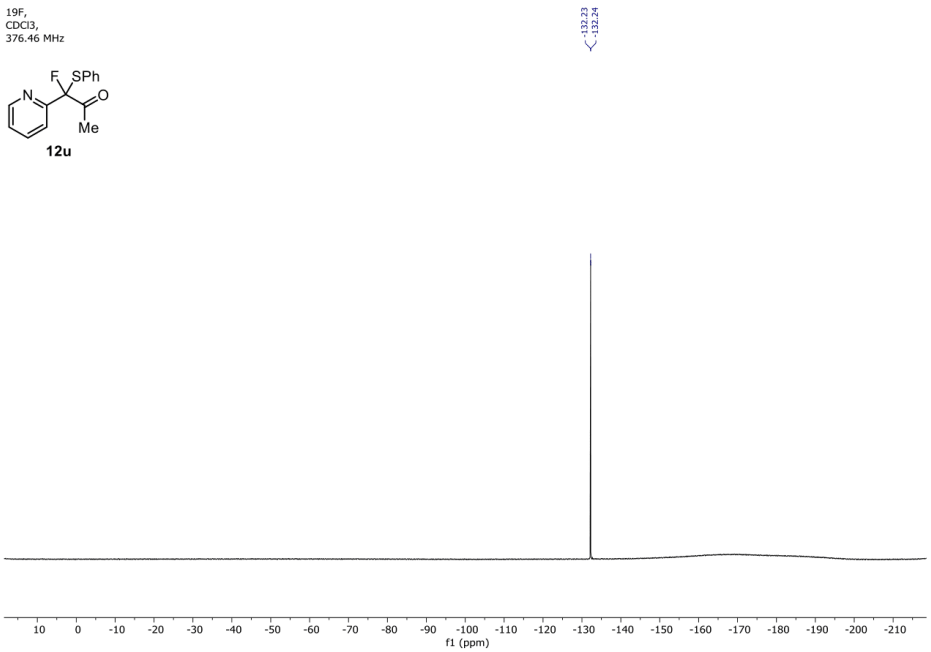
19F,
CDCl3,
376.46 MHz
F
SPh
N
O
Me
12u
-132.23
-132.24
10 0 -10 -20 -30 -40 -50 -60 -70 -80 -90 -100 -110 -120 -130 -140 -150 -160 -170 -180 -190 -200 -210
f1 (ppm)

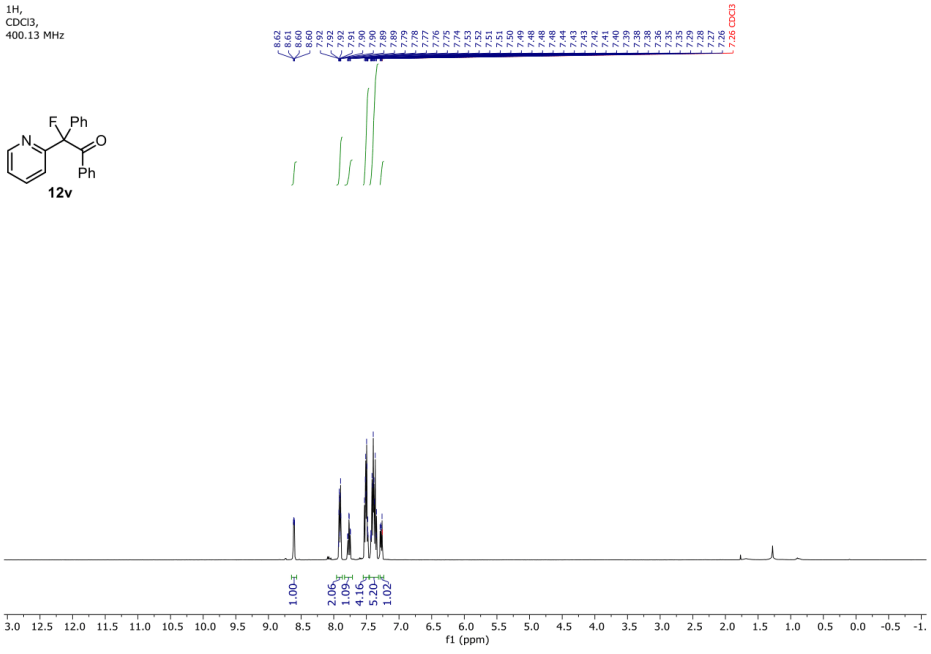
1H,
CDCl3,
400.13 MHz
F
Ph
N
O
Ph
12v
8.62
8.61
8.60
7.92
7.92
7.91
7.90
7.90
7.89
7.89
7.79
7.78
7.77
7.76
7.75
7.74
7.53
7.52
7.51
7.51
7.50
7.49
7.48
7.48
7.46
7.44
7.43
7.43
7.42
7.41
7.40
7.39
7.38
7.38
7.36
7.35
7.35
7.29
7.28
7.27
7.26
7.26 CDCl3
1.00
2.06
1.09
4.16
5.20
1.02
f1 (ppm)

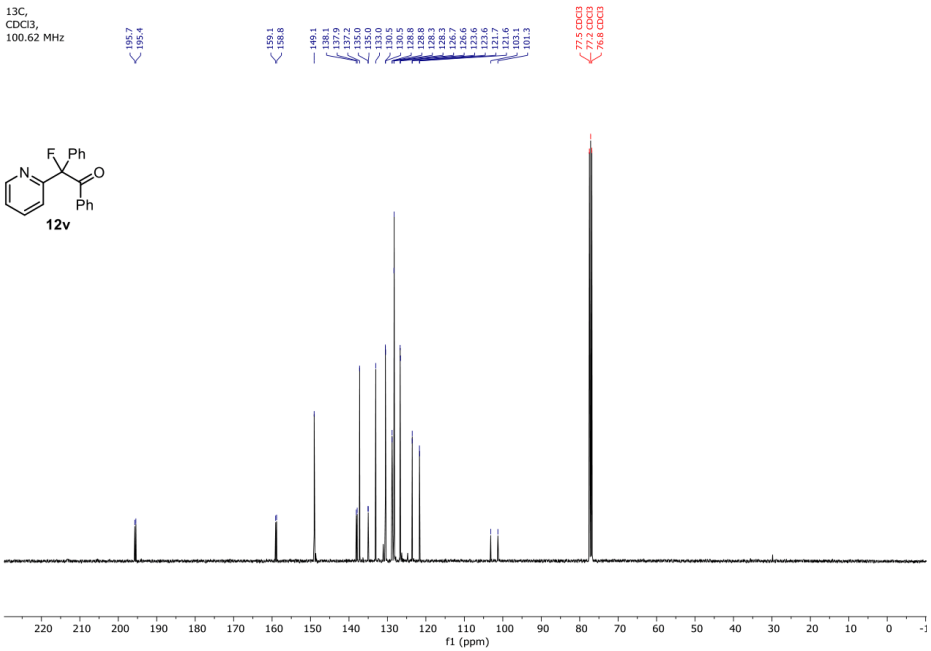
13C,
CDCl3,
100.62 MHz
195.7
195.4
159.1
158.8
149.1
138.1
137.9
137.2
135.0
135.0
133.0
130.5
130.5
128.8
128.8
128.3
128.3
126.7
126.6
123.6
123.6
121.7
121.6
103.1
101.3
77.5 CDCl3
77.2 CDCl3
76.8 CDCl3
F
Ph
N
O
Ph
12v
f1 (ppm)

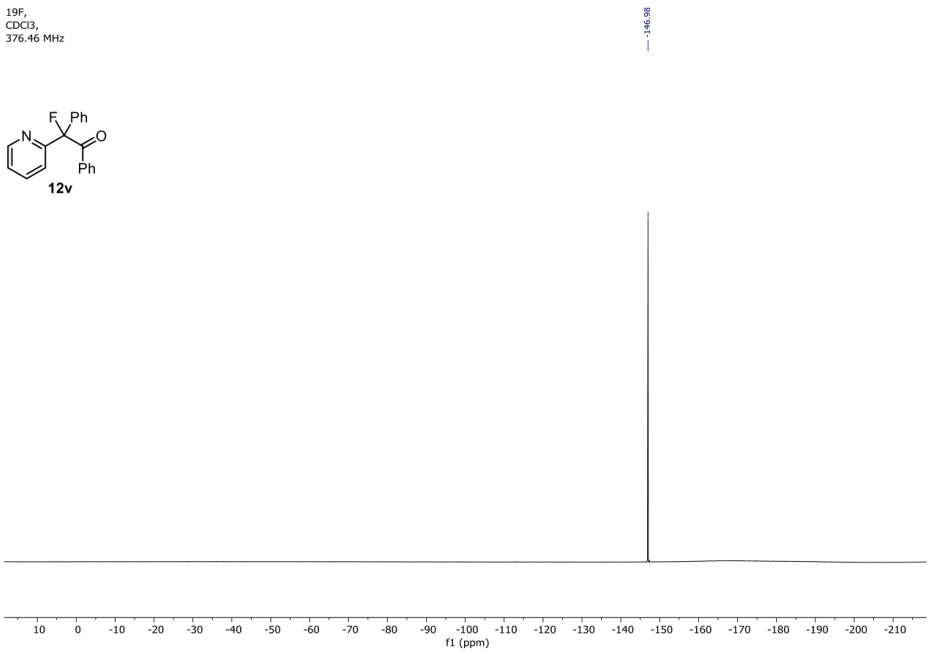
19F,
CDCl3,
376.46 MHz
146.98
F
Ph
N
O
Ph
12v
10 0 -10 -20 -30 -40 -50 -60 -70 -80 -90 -100 -110 -120 -130 -140 -150 -160 -170 -180 -190 -200 -210
f1 (ppm)

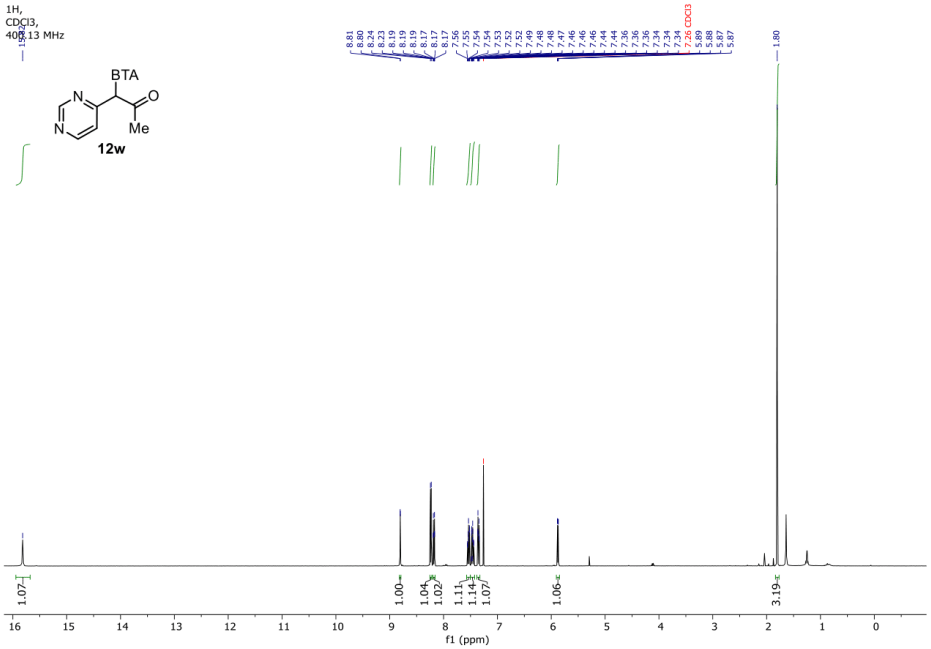
1H,
CDCl3,
400.13 MHz
BTA
Me
12w
f1 (ppm)

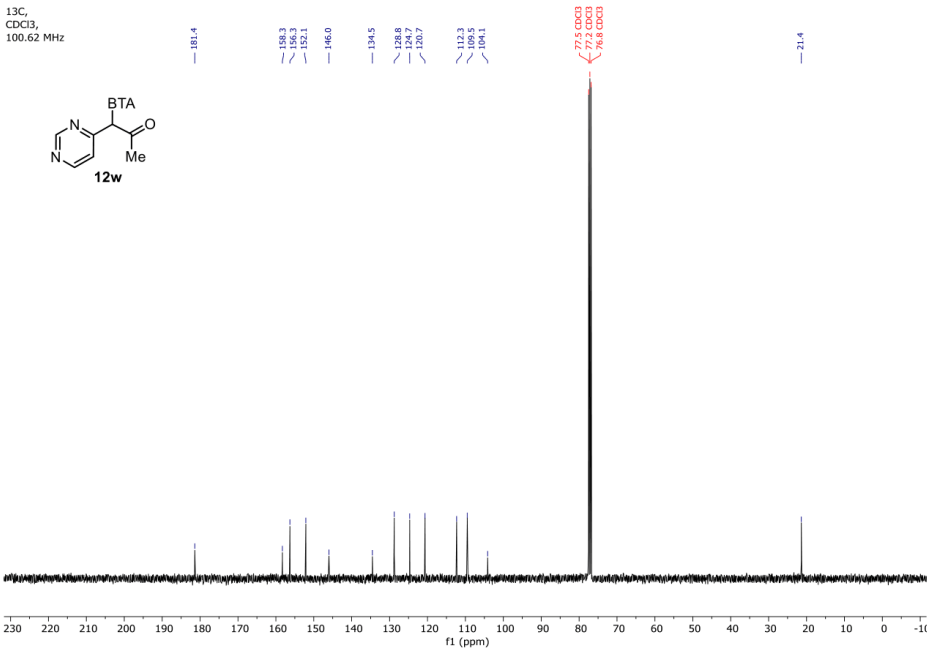
13C,
CDCl3,
100.62 MHz
BTA
Me
12w
f1 (ppm)

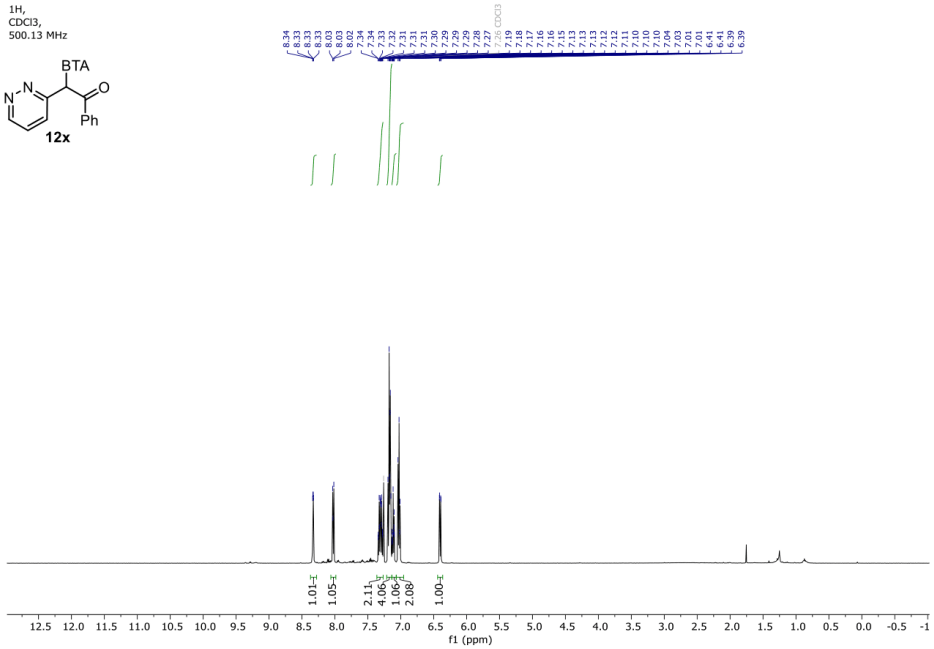
1H,
CDCl3,
500.13 MHz
BTA
Ph
12x
f1 (ppm)

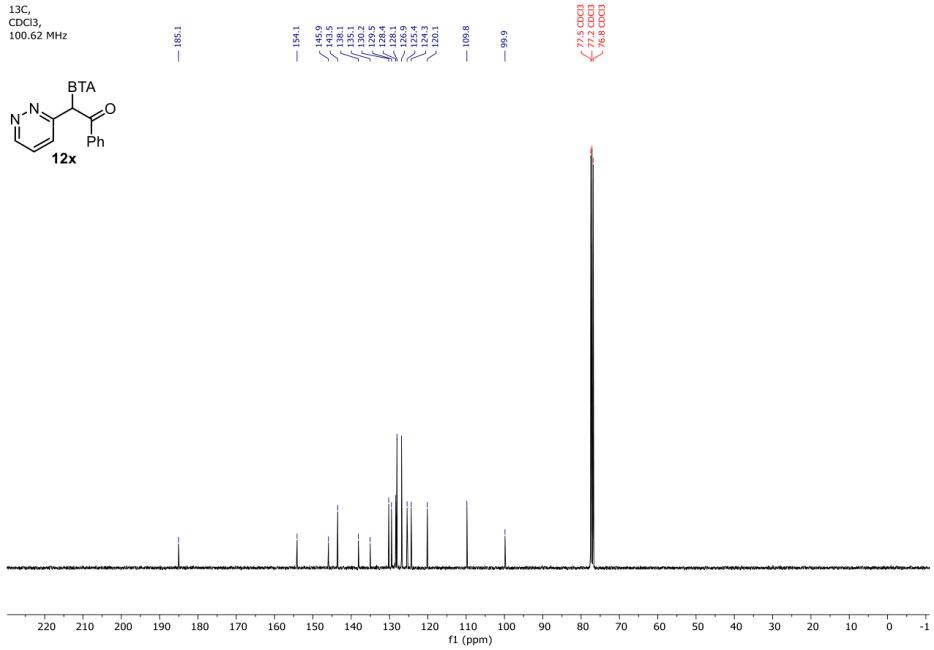
13C,
CDCl3,
100.62 MHz
BTA
Ph
12x
f1 (ppm)

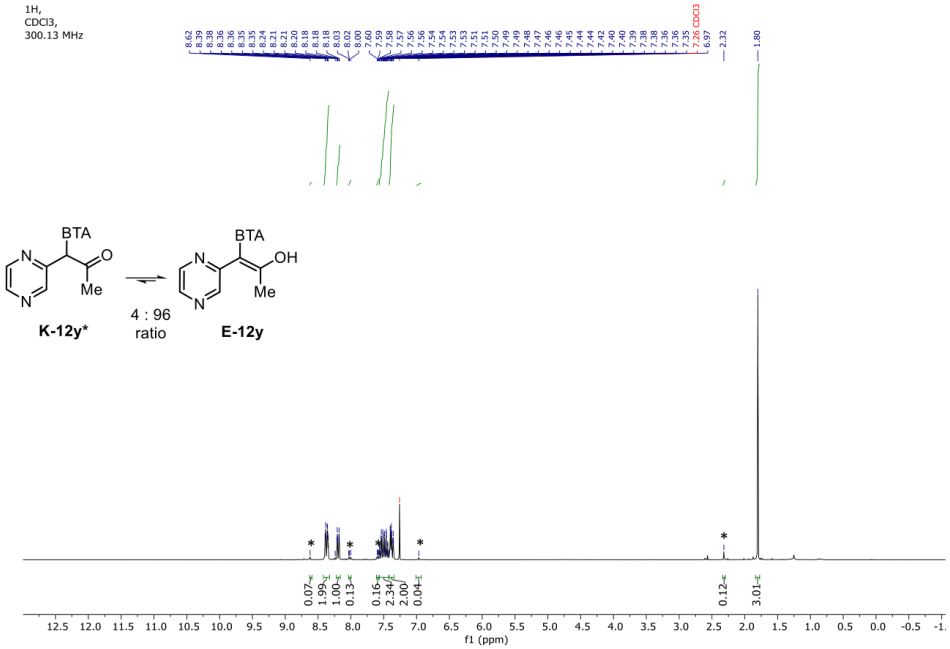
1H,
CDCl3,
300.13 MHz
BTA
Me
K-12y*
4 : 96
ratio
BTA
OH
Me
E-12y
f1 (ppm)

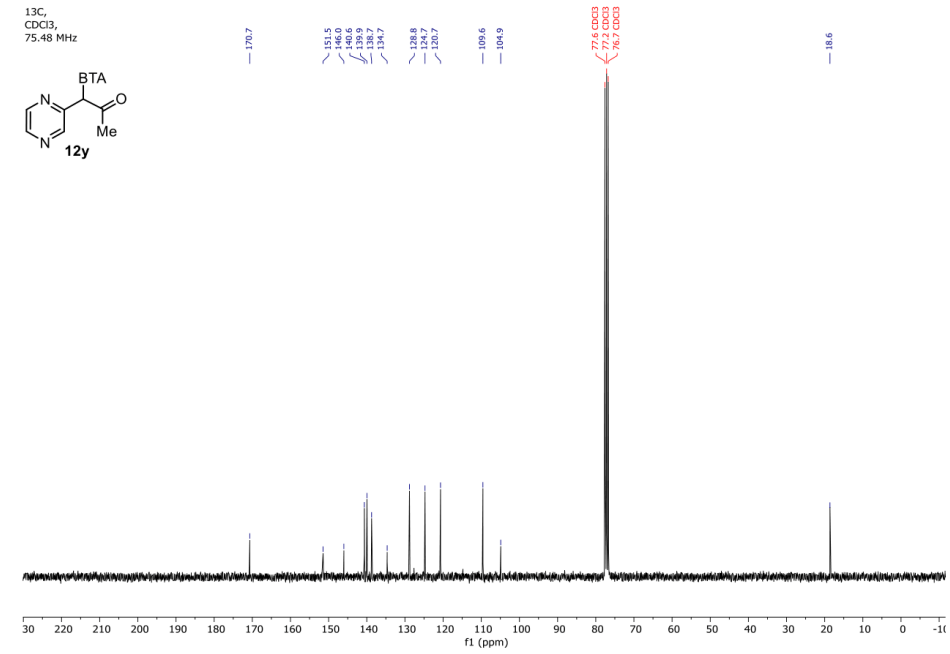
13C,
CDCl3,
75.48 MHz
BTA
Me
12y
f1 (ppm)

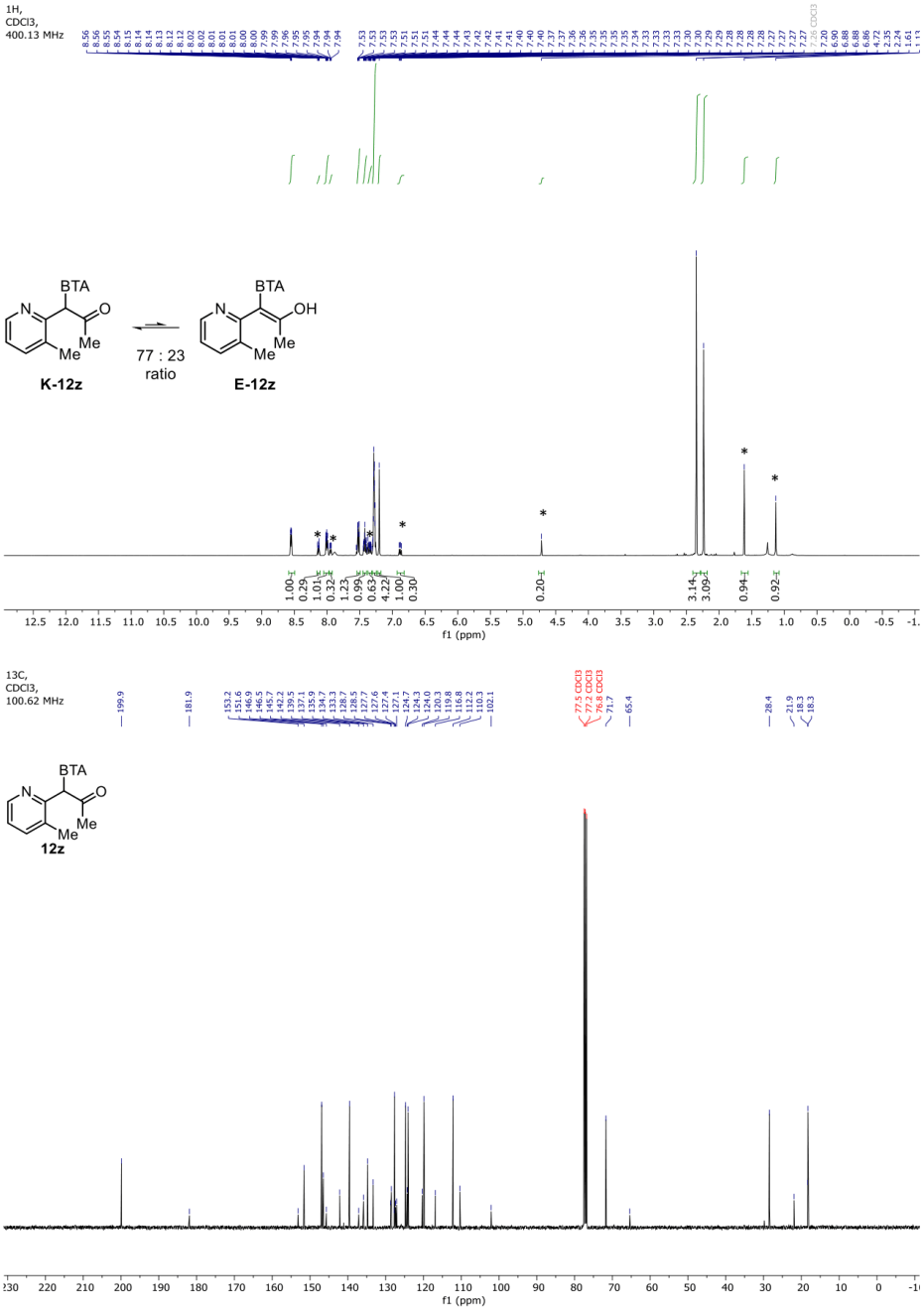
1H,
CDCl3,
400.13 MHz
BTA
Me
K-12z
77 : 23
ratio
E-12z
f1 (ppm)
13C,
CDCl3,
100.62 MHz
12z
f1 (ppm)

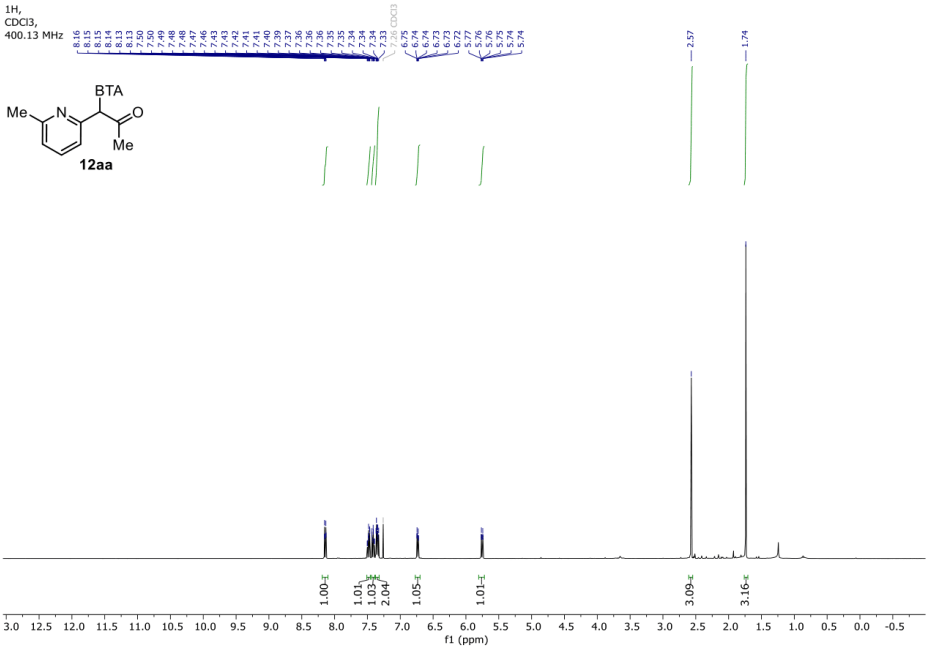
1H,
CDCl3,
400.13 MHz
BTA
Me
N
O
Me
12aa
2.57
1.74
1.00
1.01
1.03
2.04
1.05
1.01
3.09
3.16
f1 (ppm)

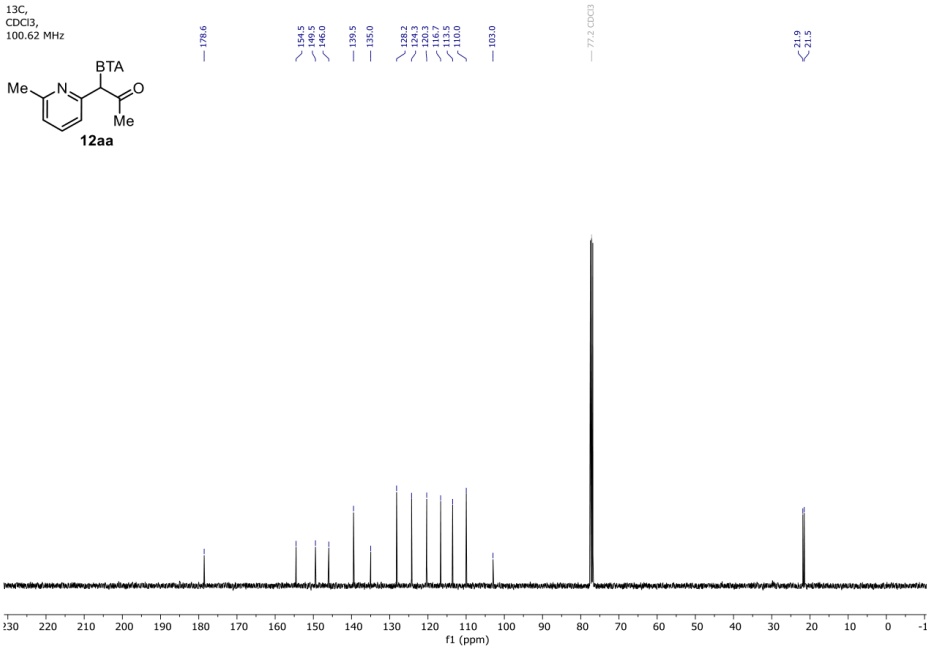
13C,
CDCl3,
100.62 MHz
BTA
Me
N
O
Me
12aa
178.6
154.5
149.5
146.0
139.5
135.0
128.2
124.3
120.3
116.7
113.5
110.0
103.0
77.2 CDCl3
21.9
21.5
f1 (ppm)

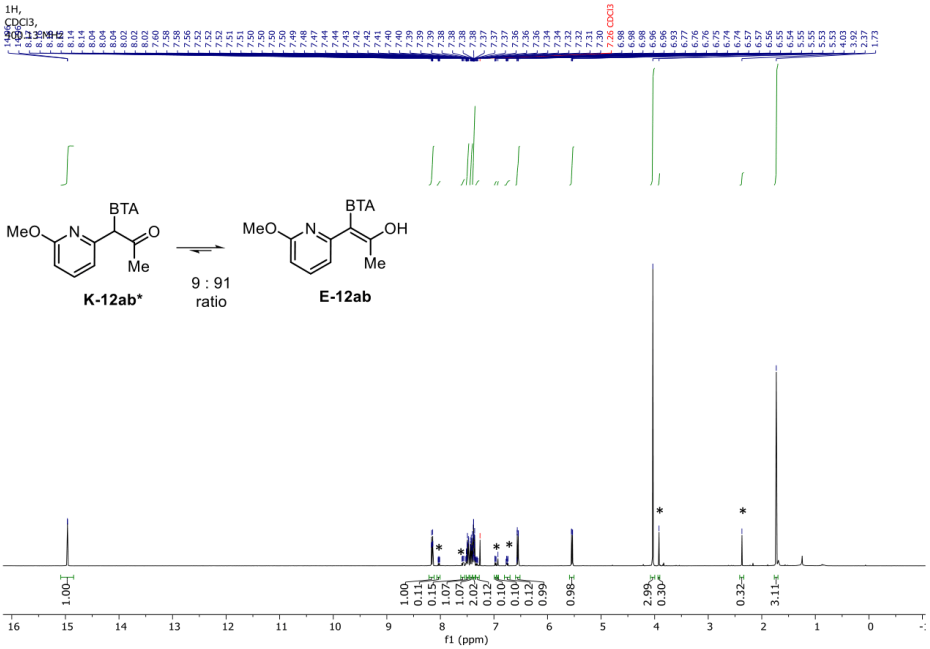
1H,
CDCl3,
400.13 MHz
BTA
MeO
N
O
Me
K-12ab*
9 : 91
ratio
BTA
MeO
N
OH
Me
E-12ab
f1 (ppm)

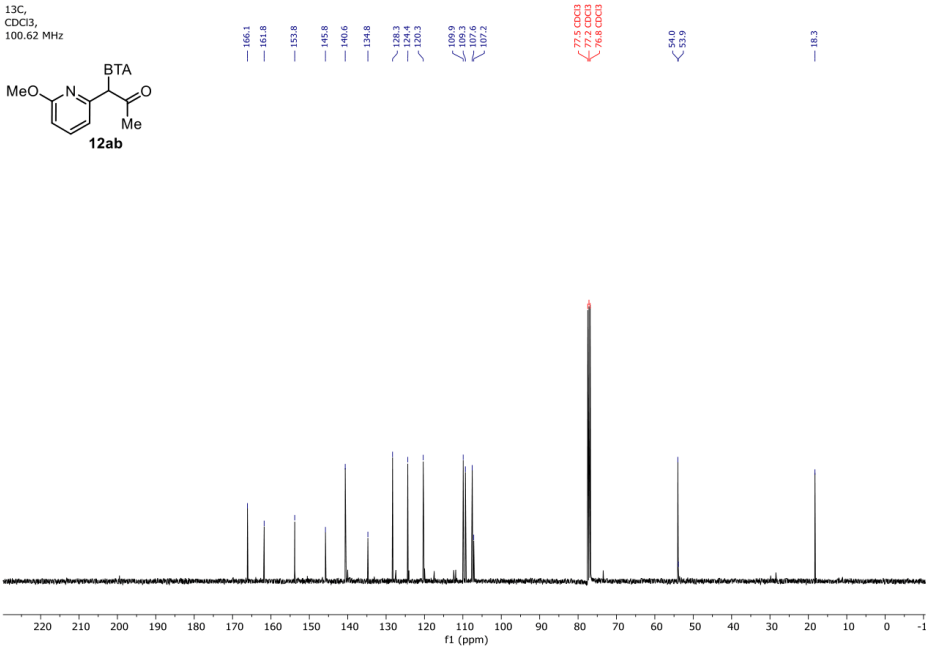
13C,
CDCl3,
100.62 MHz
BTA
MeO
N
O
Me
12ab
f1 (ppm)

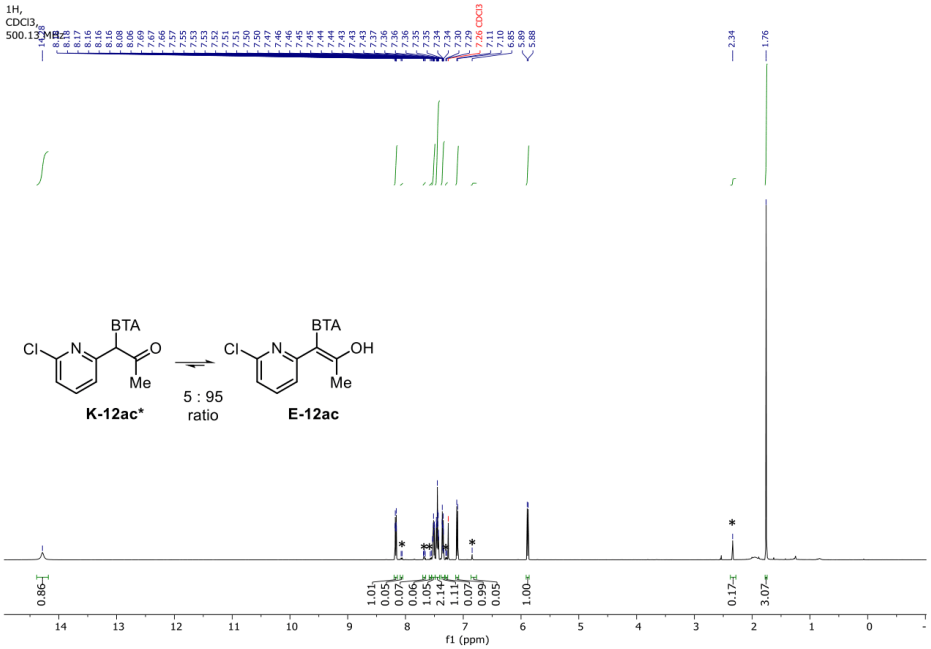
1H,
CDCl3,
500.13 MHz
BTA
Cl
N
O
Me
K-12ac*
5 : 95
ratio
OH
E-12ac
f1 (ppm)

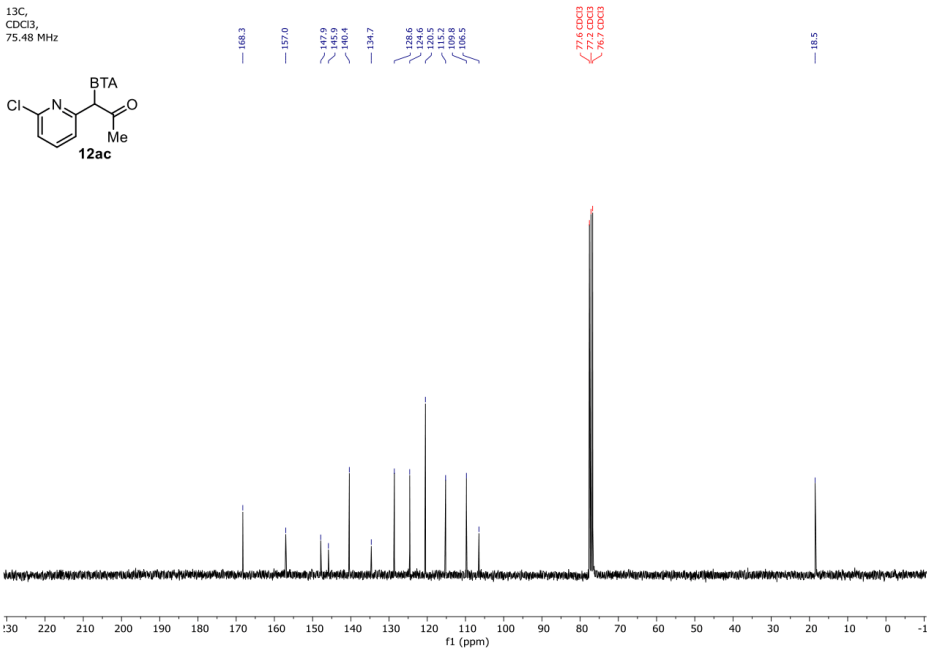
13C,
CDCl3,
75.48 MHz
BTA
12ac
f1 (ppm)

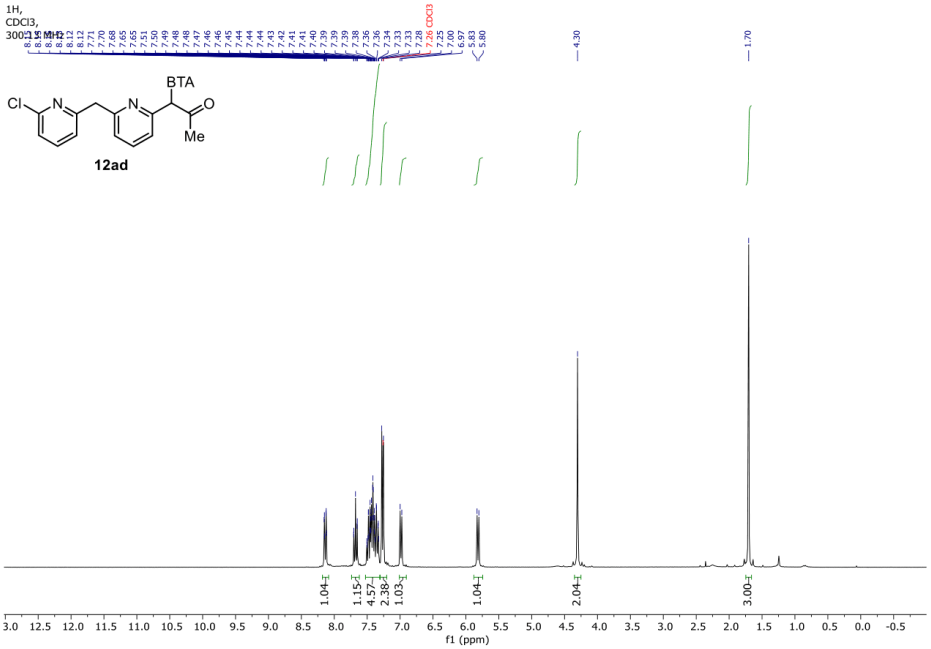
1H,
CDCl3,
BTA
Cl
N
N
O
Me
12ad
4.30
1.70
1.04
1.15
4.57
2.38
1.03
1.04
2.04
3.00
f1 (ppm)

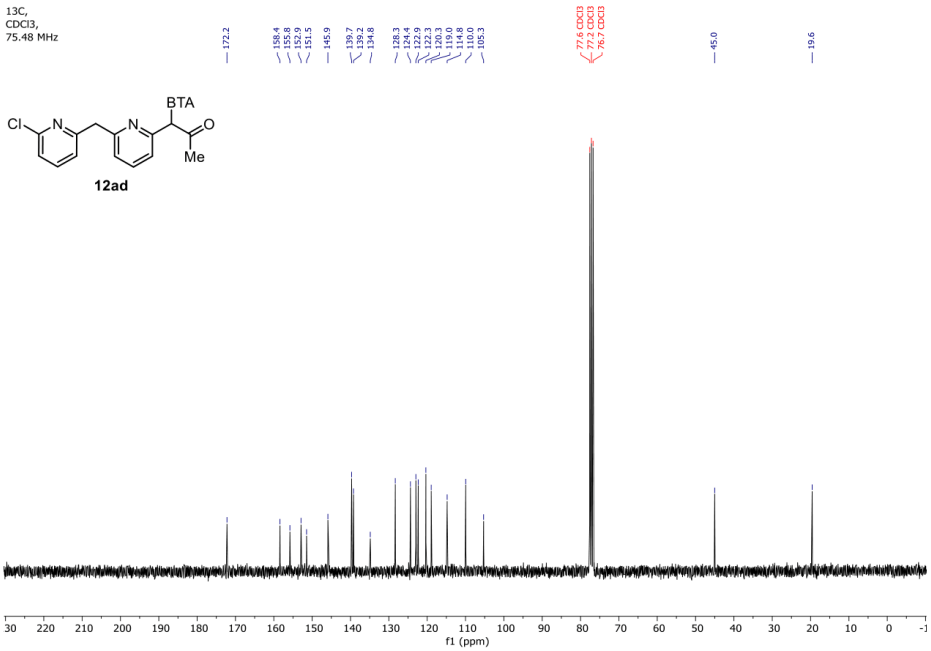
13C,
CDCl3,
75.48 MHz
172.2
158.4
155.8
152.9
151.5
145.9
139.7
139.2
134.8
128.3
124.4
122.9
121.3
120.3
119.0
114.8
110.0
105.3
77.6 CDCl3
77.2 CDCl3
76.7 CDCl3
45.0
19.6
BTA
Cl
N
N
O
Me
12ad
f1 (ppm)

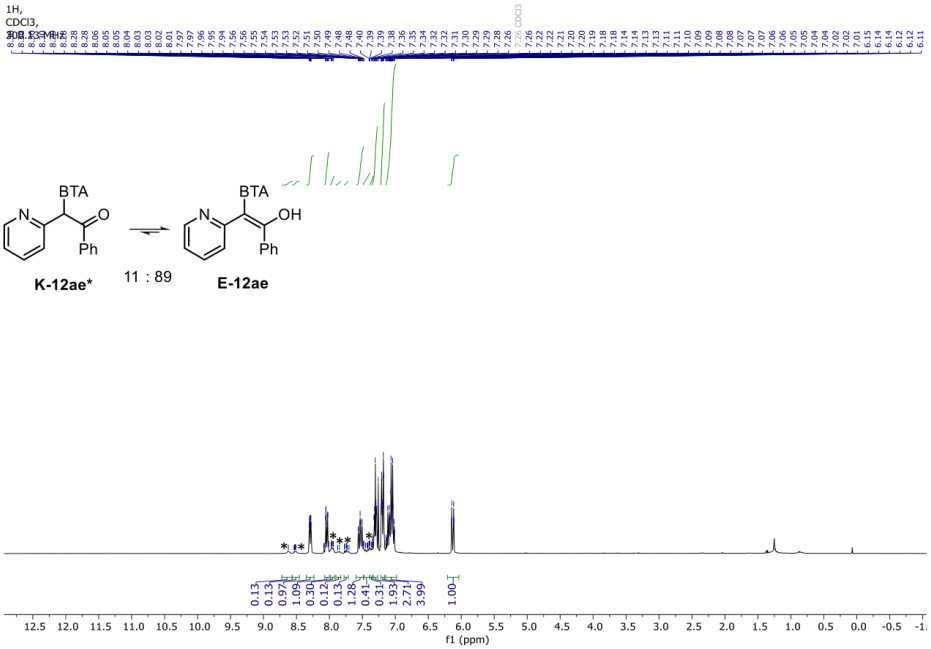
1H,
CDCl3,
BTA
Ph
K-12ae*
11 : 89
BTA
OH
Ph
E-12ae
f1 (ppm)

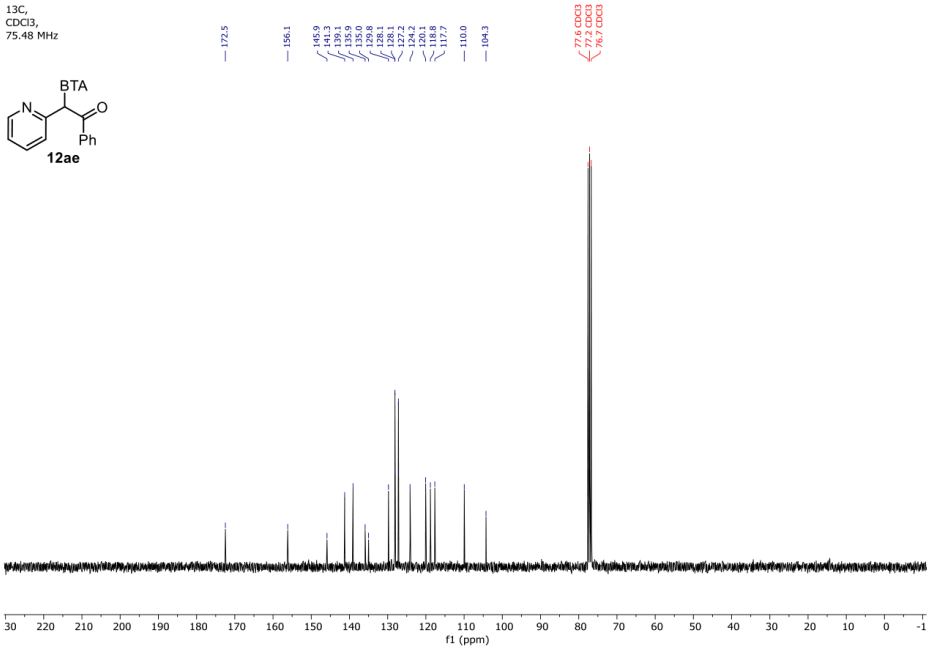
13C,
CDCl3,
75.48 MHz
BTA
Ph
12ae
f1 (ppm)

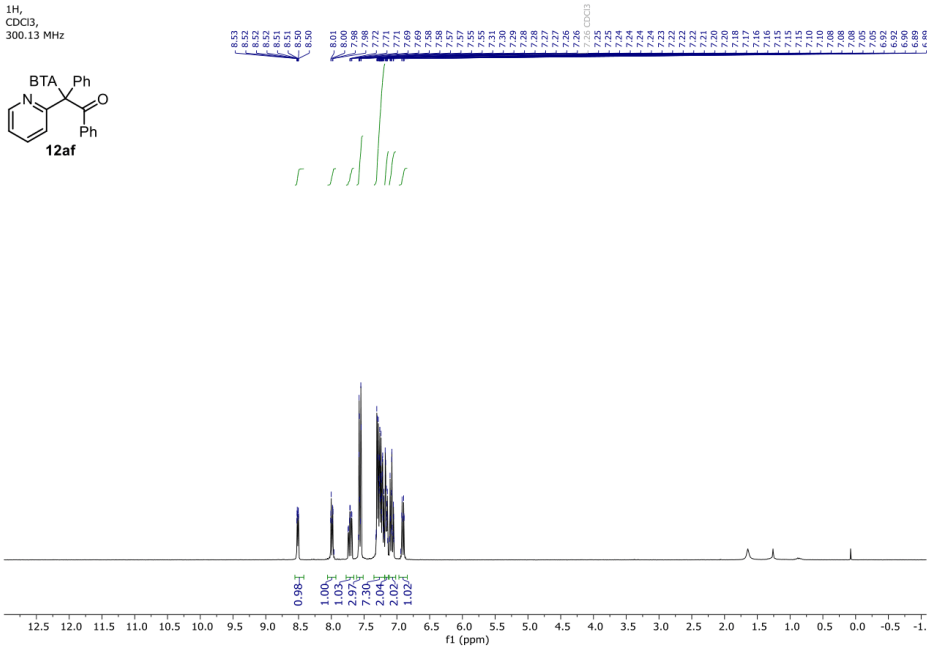
1H,
CDCl3,
300.13 MHz
BTA
Ph
N
O
Ph
12af
0.98
1.00
1.03
2.97
7.30
2.04
2.02
1.02
f1 (ppm)

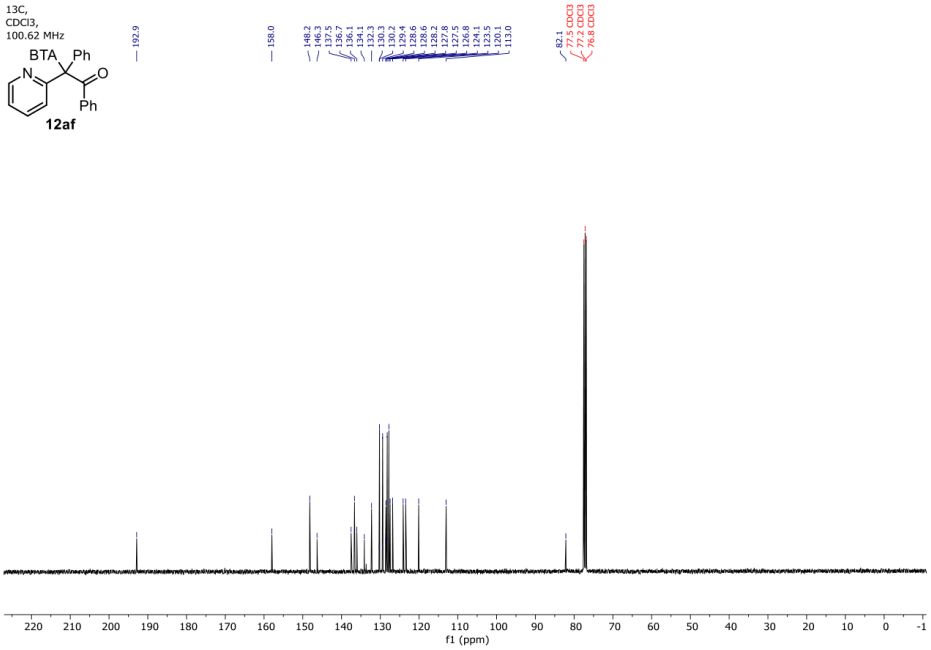
13C,
CDCl3,
100.62 MHz
BTA
Ph
N
O
Ph
12af
192.9
158.0
148.2
146.3
137.5
136.7
136.1
134.1
133.3
130.3
130.2
129.4
128.6
128.6
128.2
127.8
127.5
126.8
124.1
123.5
120.1
113.0
82.1
77.5 CDCl3
77.2 CDCl3
76.8 CDCl3
f1 (ppm)

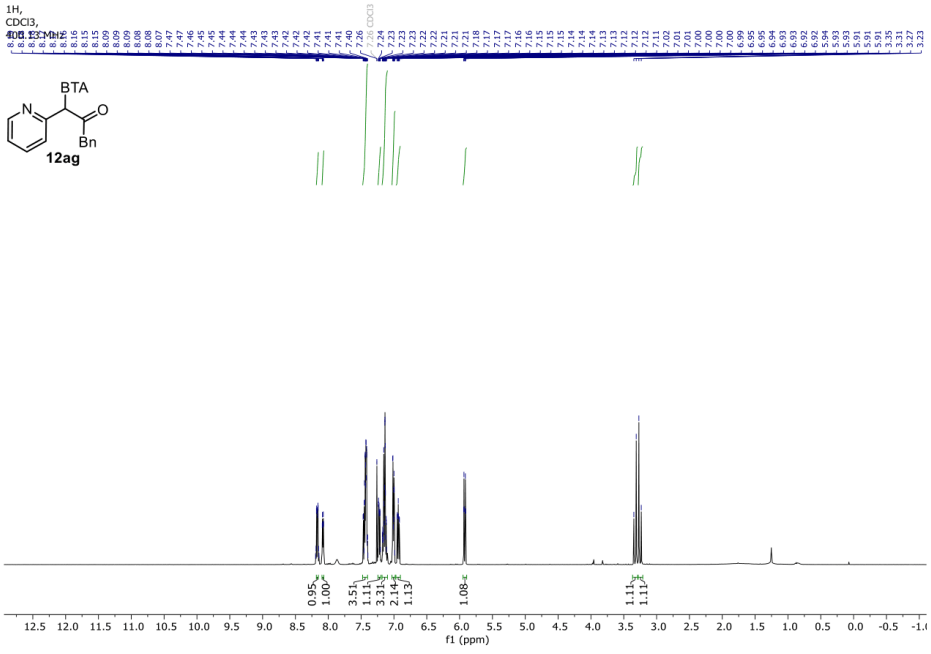
1H,
CDCl3,
BTA
Bn
12ag
f1 (ppm)

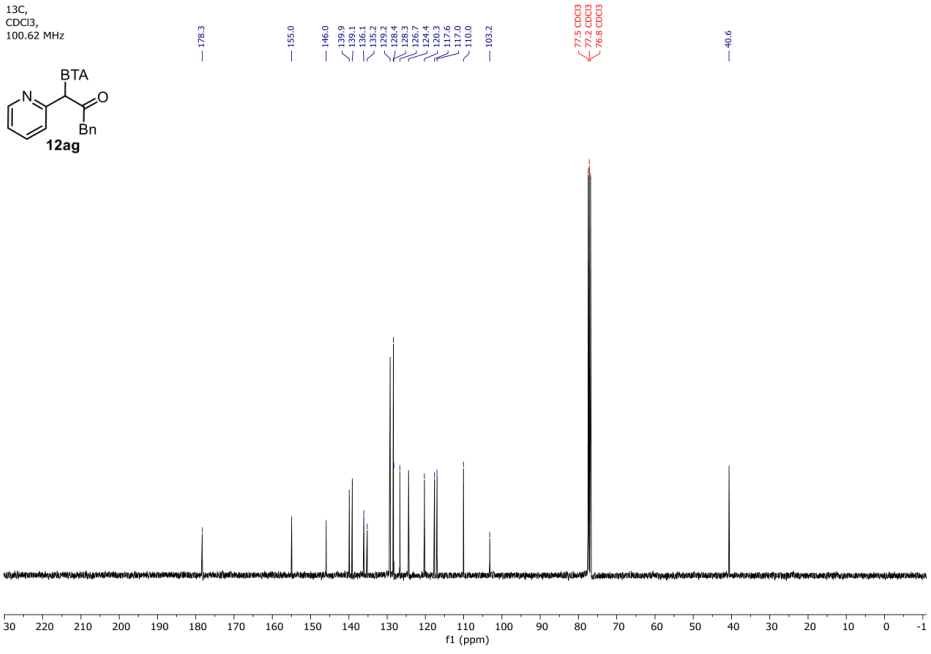
13C,
CDCl3,
100.62 MHz
BTA
Bn
12ag
178.3
155.0
146.0
139.9
139.1
136.1
135.2
132.2
128.4
128.3
126.7
124.4
120.3
117.6
117.0
110.0
103.2
77.5 CDCl3
77.2 CDCl3
76.8 CDCl3
40.6
f1 (ppm)

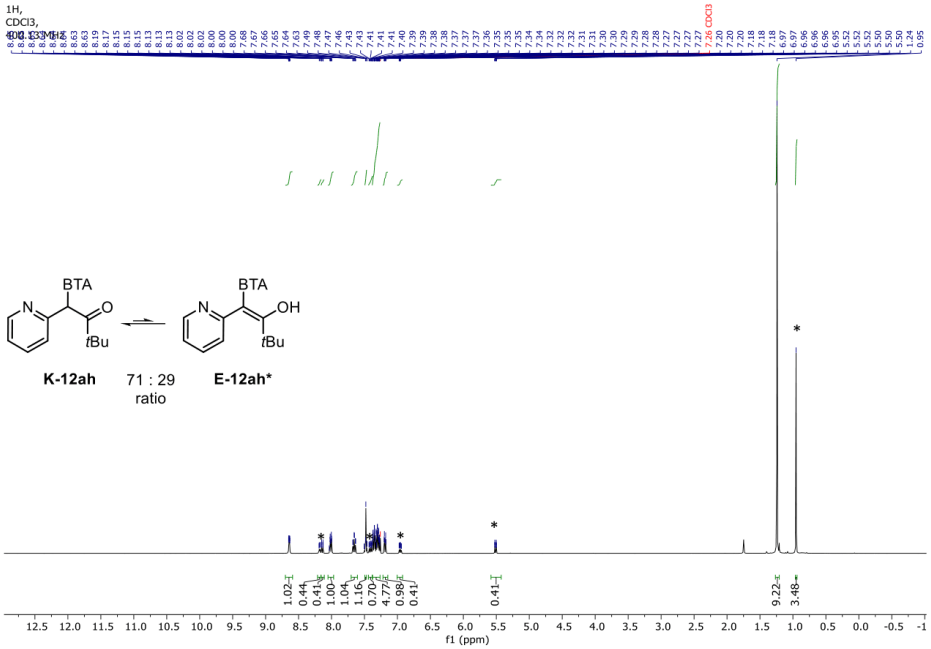
1H,
CDCl3,
BTA
tBu
K-12ah
71 : 29
ratio
E-12ah*
f1 (ppm)

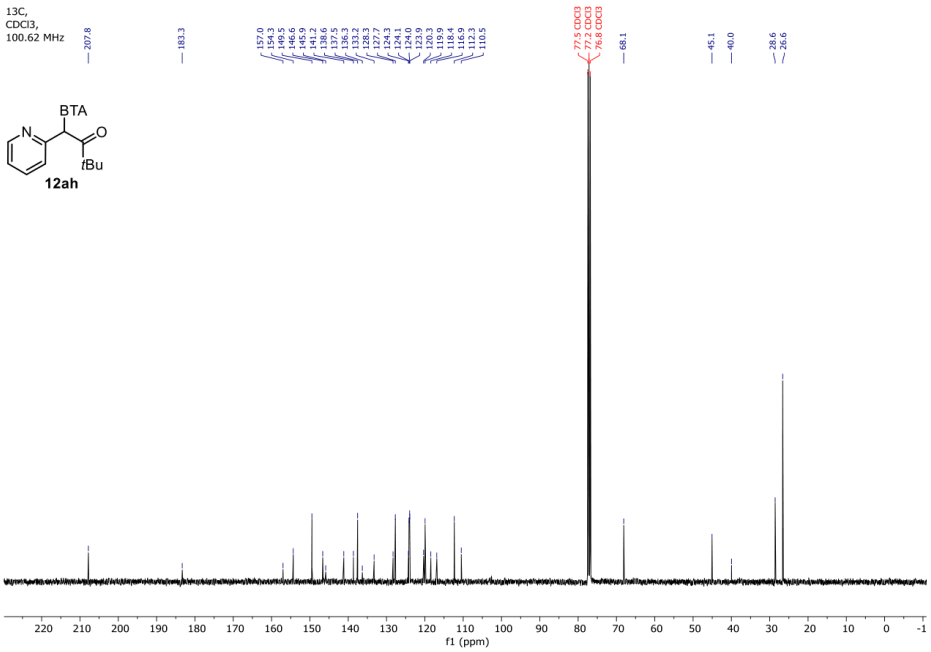
13C,
CDCl3,
100.62 MHz
BTA
tBu
12ah
f1 (ppm)

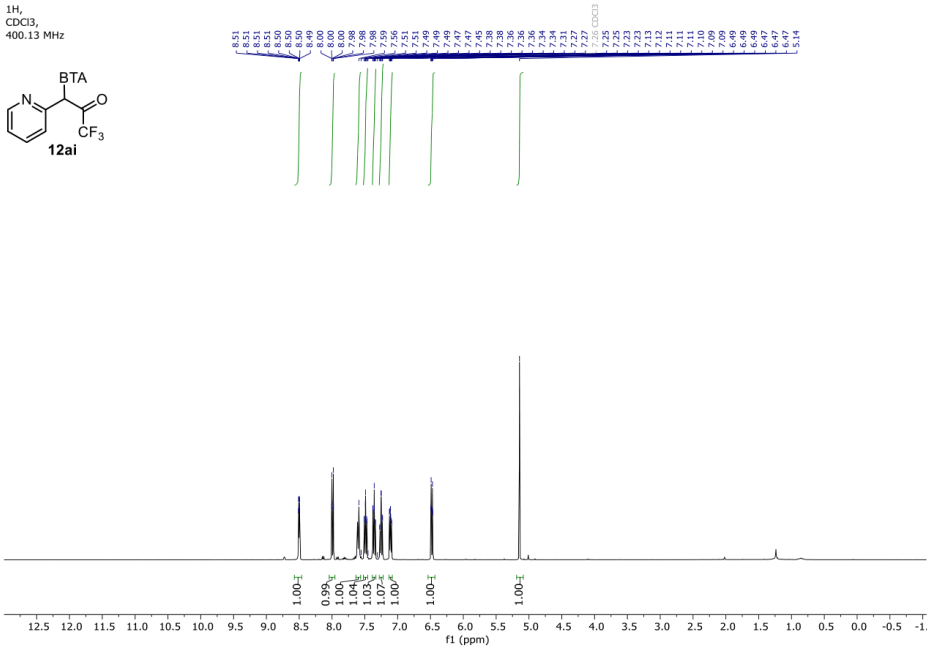
1H,
CDCl3,
400.13 MHz
BTA
CF3
12ai
f1 (ppm)

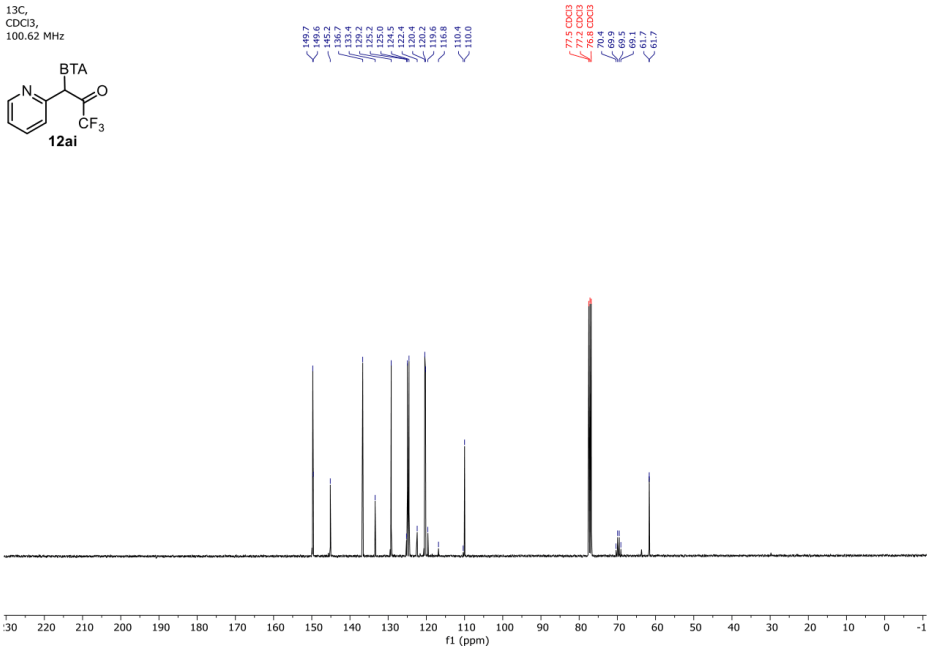
13C,
CDCl3,
100.62 MHz
BTA
CF3
12ai
f1 (ppm)

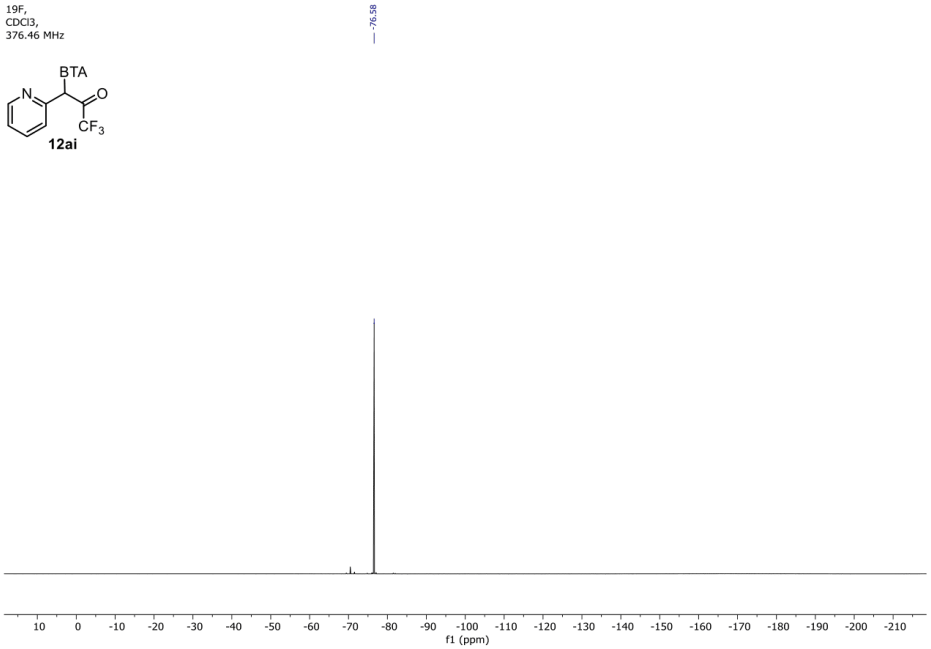
19F,
CDCl3,
376.46 MHz
-76.58
BTA
N
O
CF3
12ai
10 0 -10 -20 -30 -40 -50 -60 -70 -80 -90 -100 -110 -120 -130 -140 -150 -160 -170 -180 -190 -200 -210
f1 (ppm)

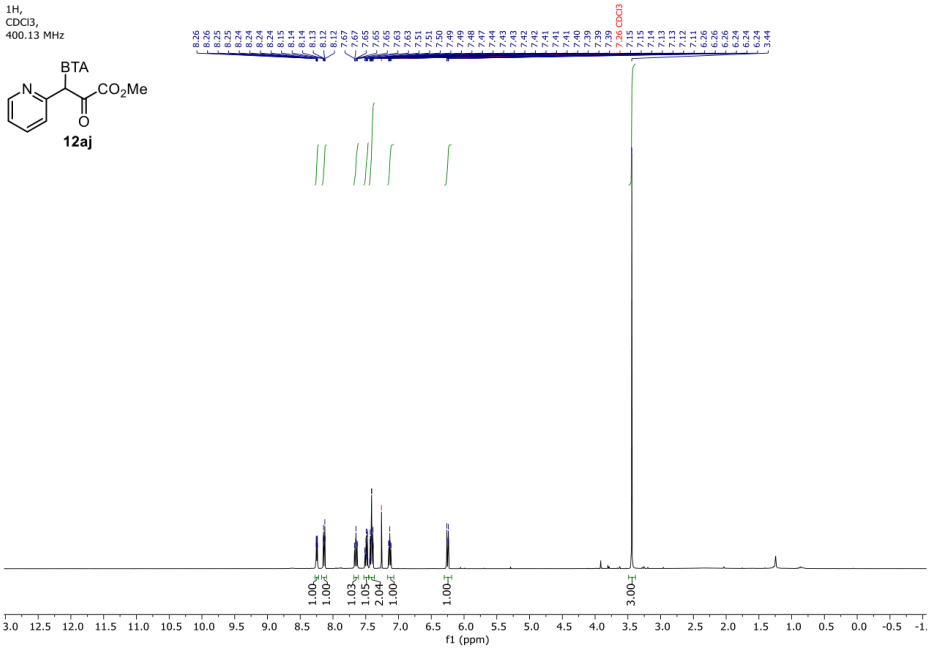
1H,
CDCl3,
400.13 MHz
BTA
CO2Me
O
12aj
f1 (ppm)

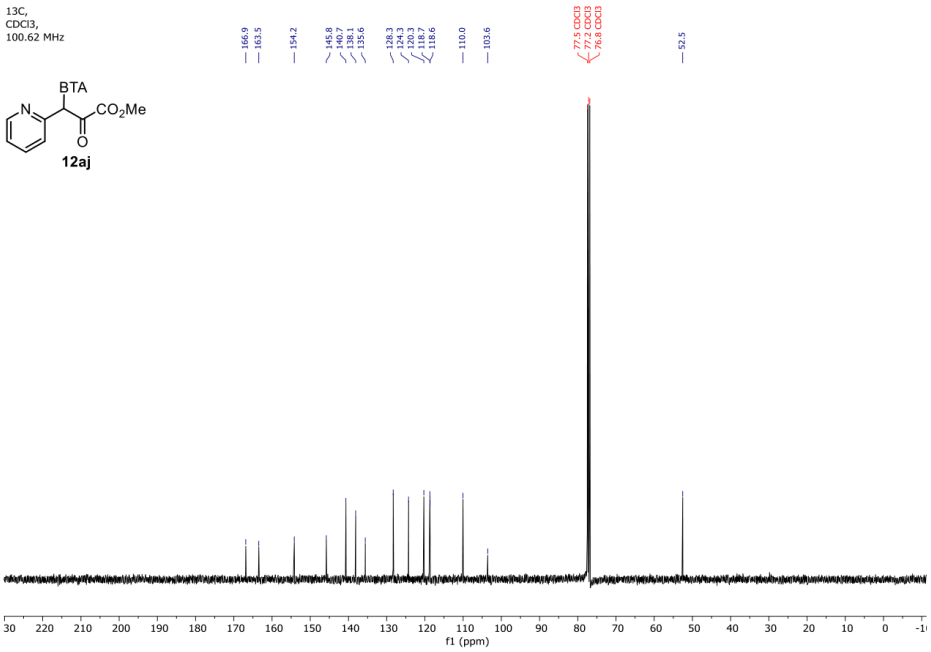
13C,
CDCl3,
100.62 MHz
BTA
CO2Me
O
12aj
f1 (ppm)

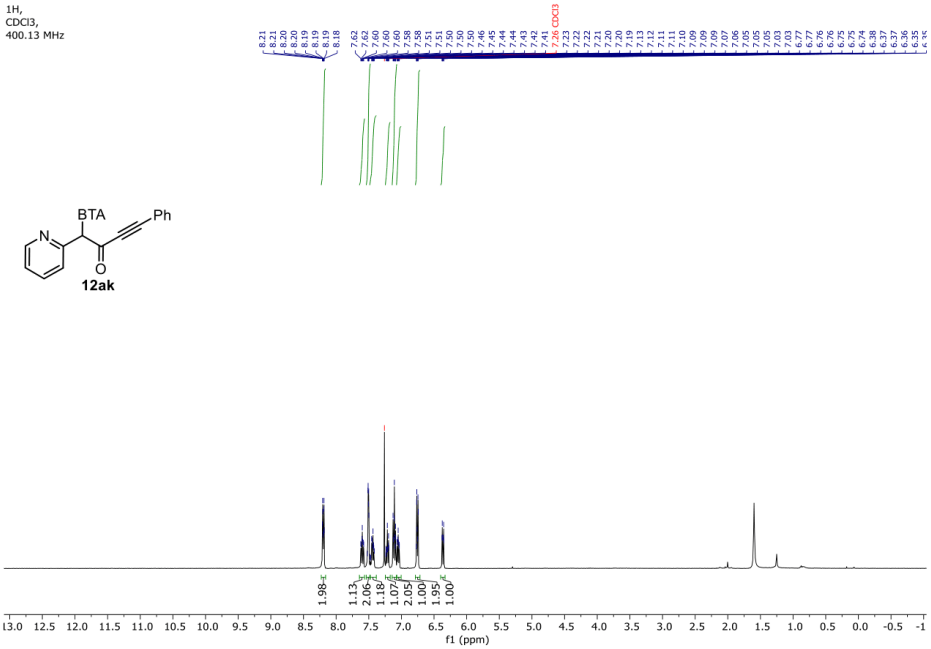
1H,
CDCl3,
400.13 MHz
BTA
Ph
O
12ak
1.98
1.13
2.06
1.18
1.07
2.05
1.00
1.95
1.00
f1 (ppm)

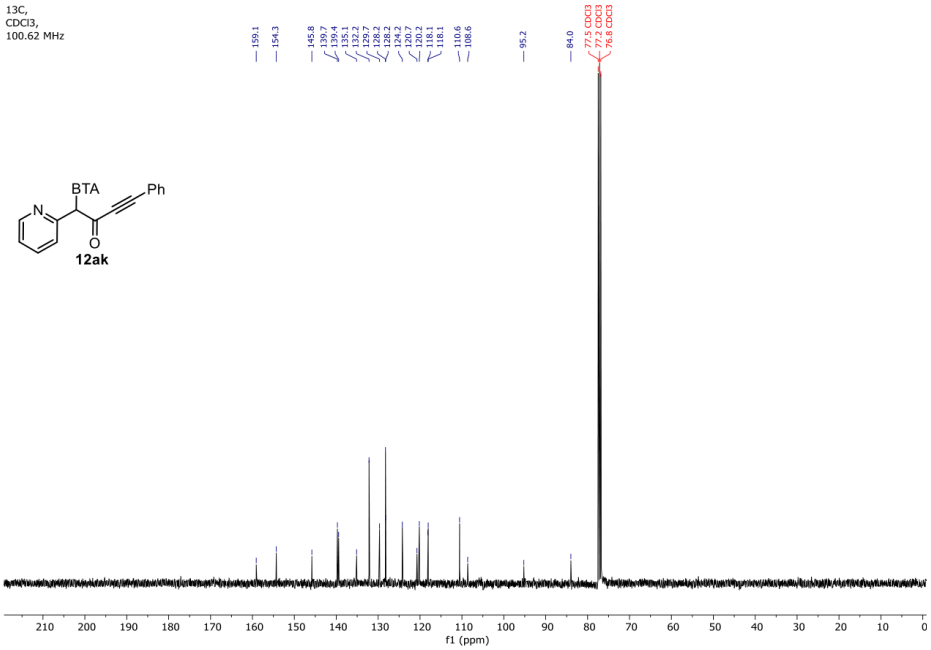
13C,
CDCl3,
100.62 MHz
159.1
154.3
145.8
139.7
139.4
135.1
132.2
129.7
128.2
124.2
120.7
120.2
118.1
110.1
110.6
100.6
95.2
84.0
77.5 CDCl3
77.2 CDCl3
76.8 CDCl3
BTA
Ph
O
12ak
f1 (ppm)

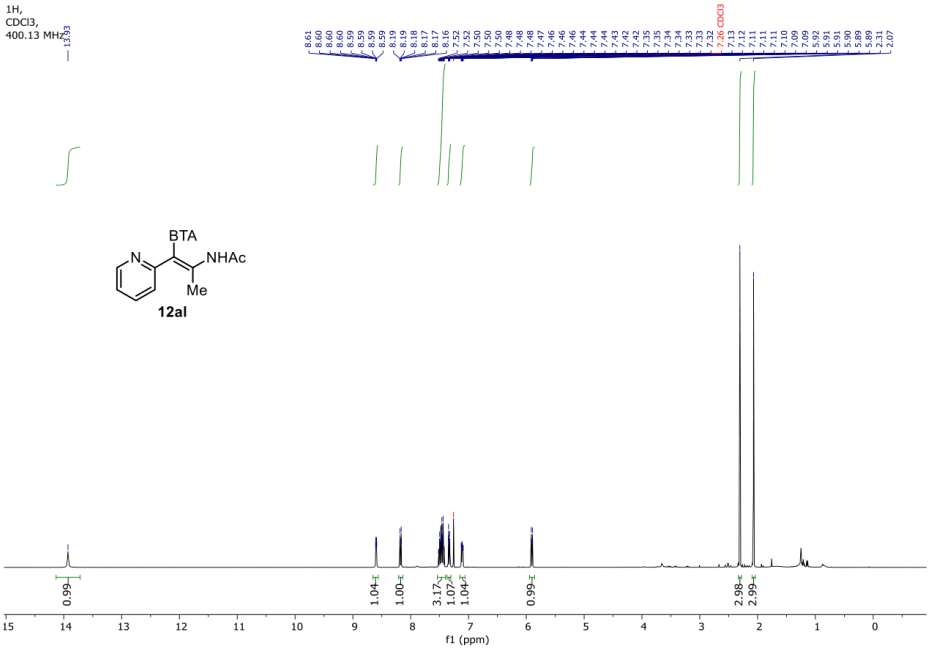
1H,
CDCl3,
400.13 MHz
BTA
NHAc
Me
12al
f1 (ppm)

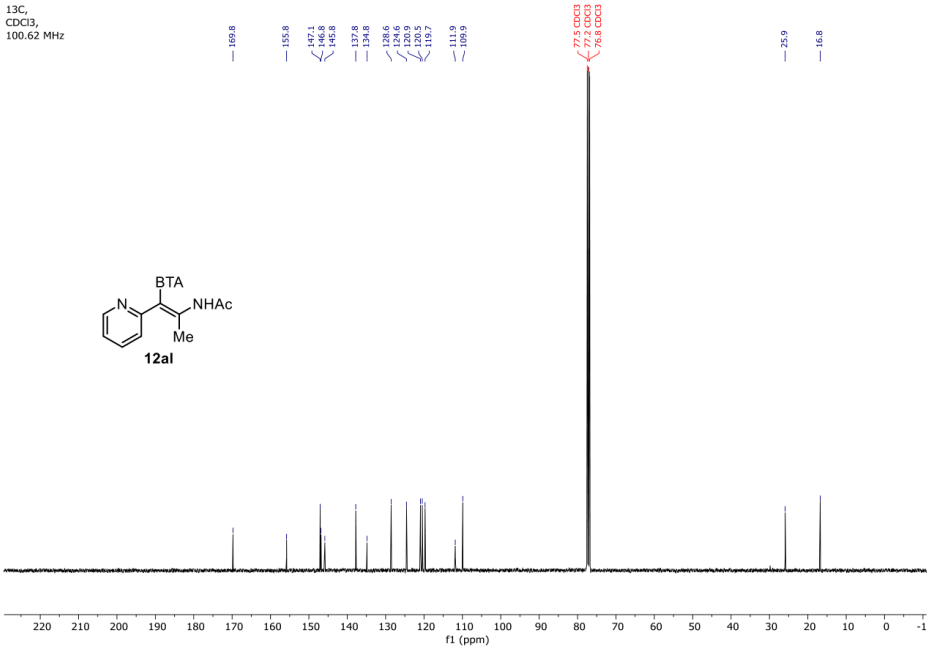
13C,
CDCl3,
100.62 MHz
BTA
NHAc
Me
12al
f1 (ppm)

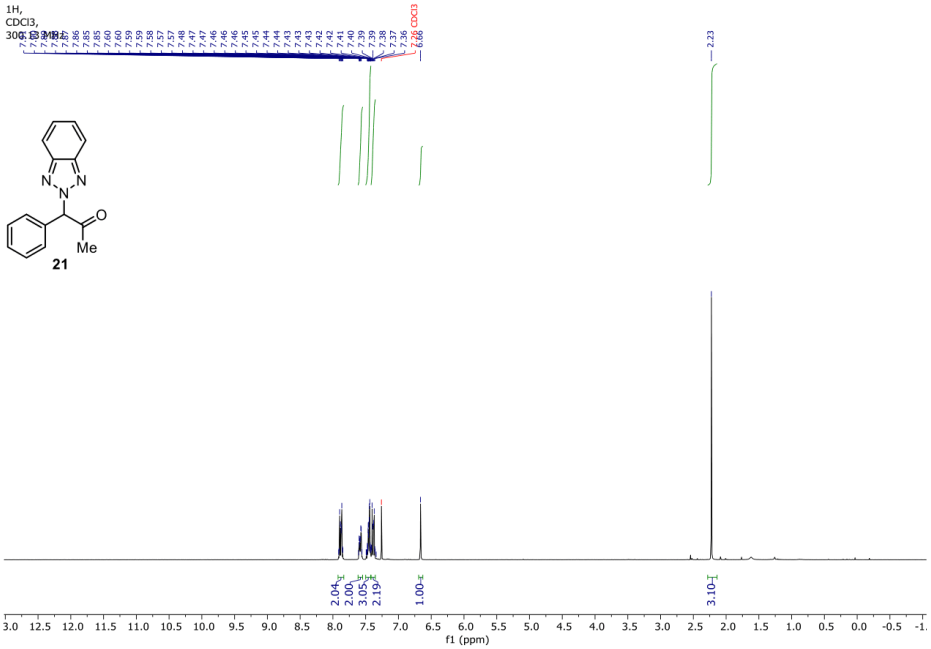
1H,
CDCl3,
300.13 MHz
Me
21
f1 (ppm)

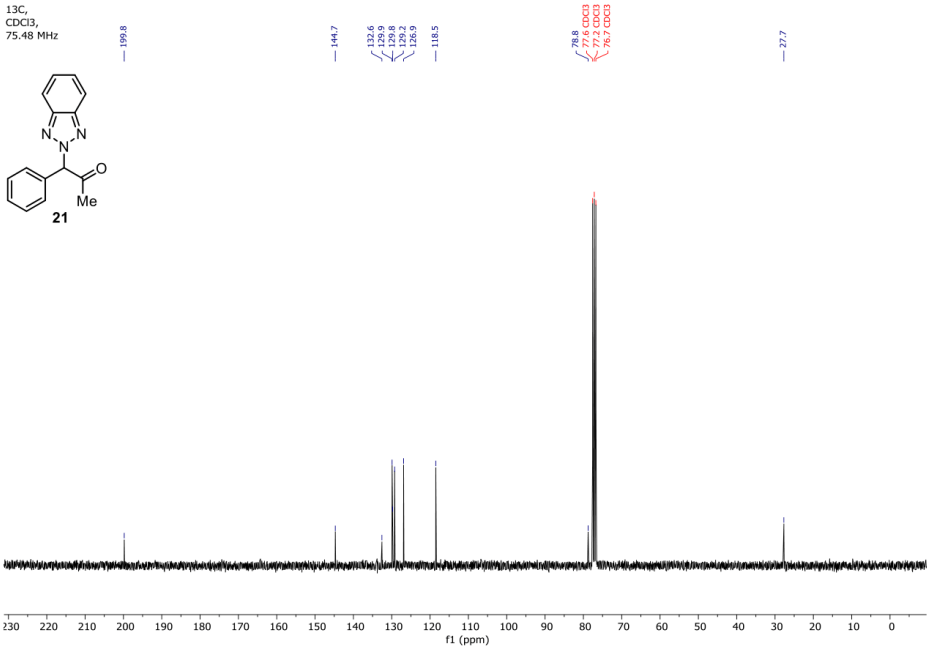
13C,
CDCl3,
75.48 MHz
Me
21
f1 (ppm)

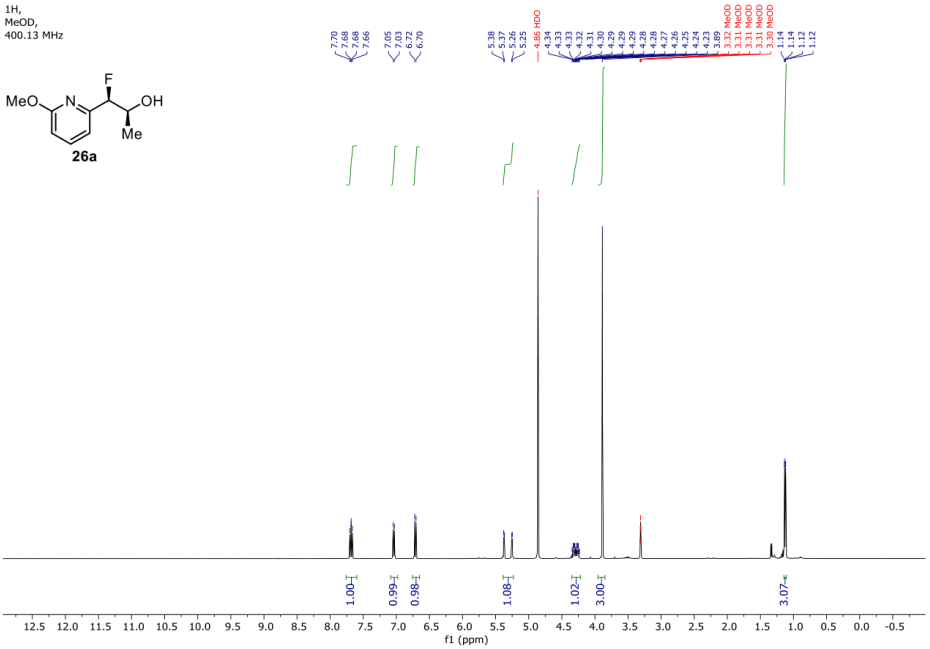
1H,
MeOD,
400.13 MHz
MeO
N
F
OH
Me
26a
f1 (ppm)

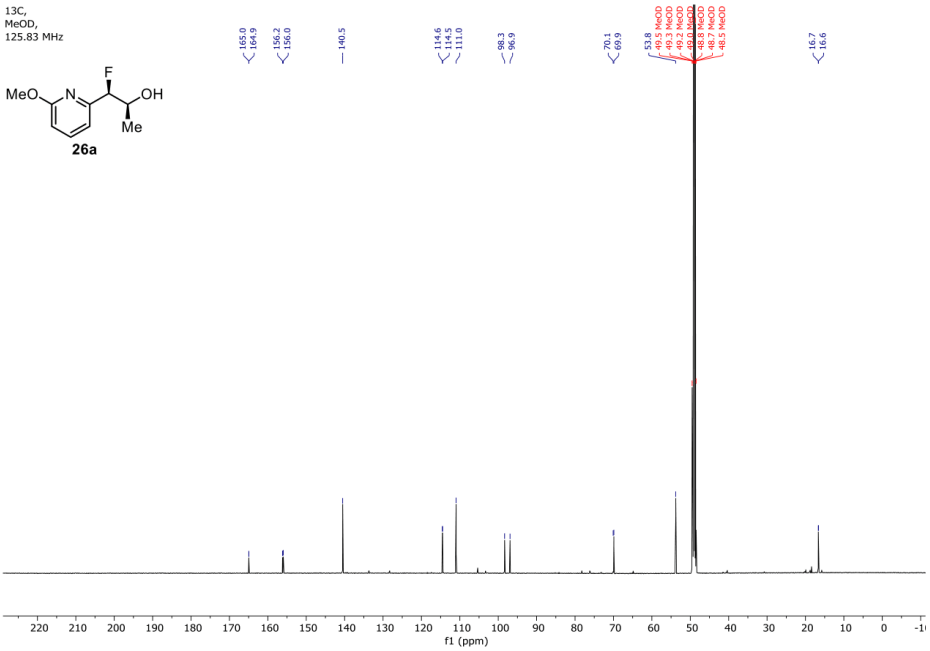
13C,
MeOD,
125.83 MHz
MeO
N
F
OH
Me
26a
f1 (ppm)

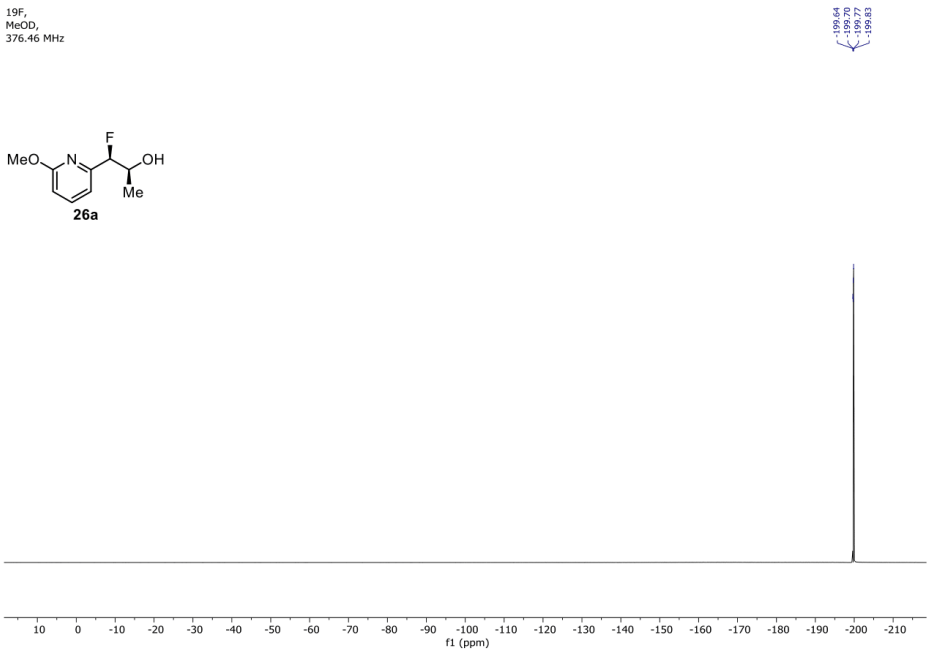
19F,
MeOD,
376.46 MHz
-199.64
-199.70
-199.77
-199.83
F
MeO
N
OH
Me
26a
10 0 -10 -20 -30 -40 -50 -60 -70 -80 -90 -100 -110 -120 -130 -140 -150 -160 -170 -180 -190 -200 -210
f1 (ppm)

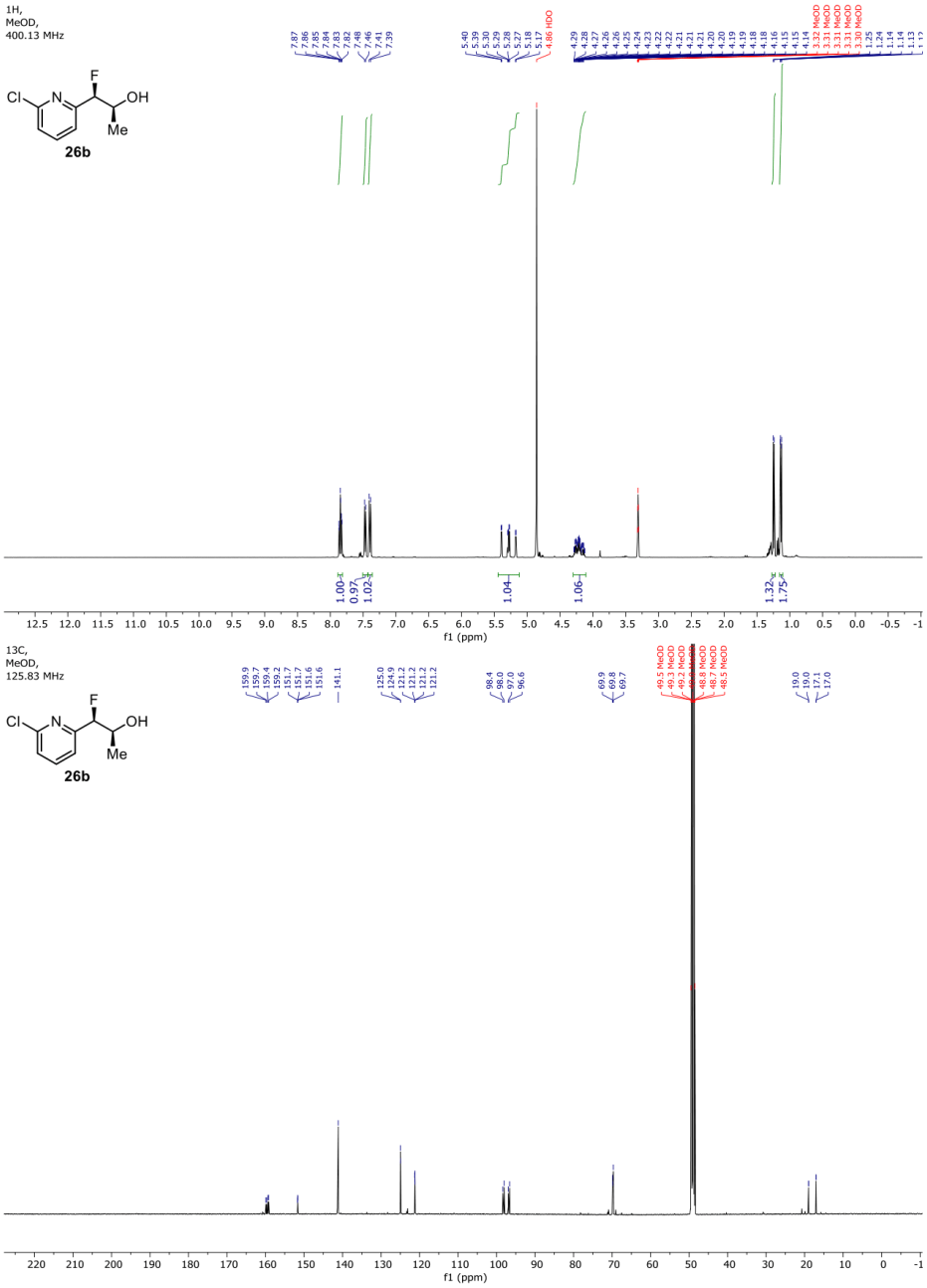
1H,
MeOD,
400.13 MHz
26b
13C,
MeOD,
125.83 MHz
26b
f1 (ppm)

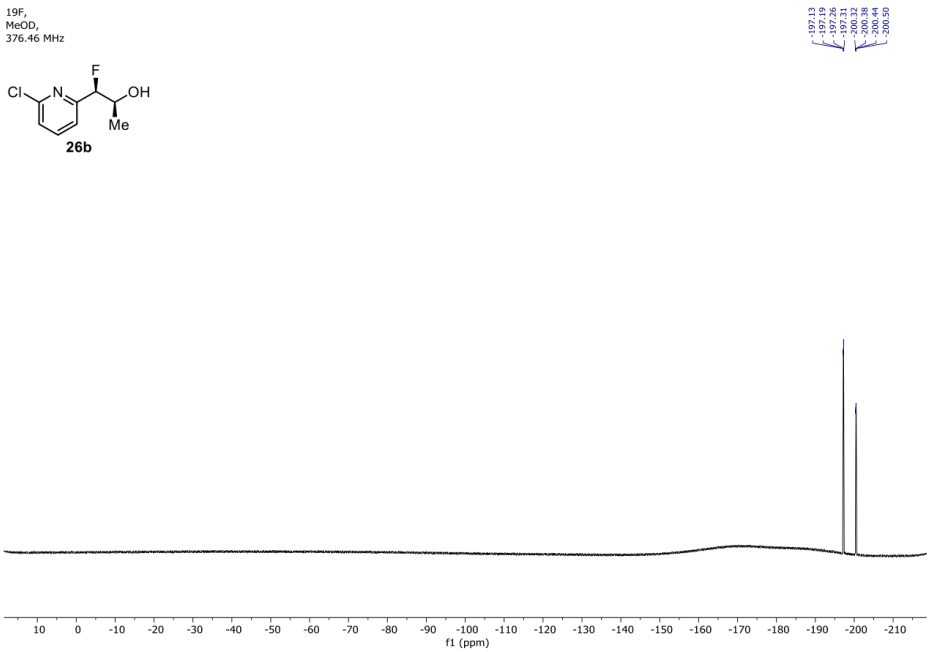
19F,
MeOD,
376.46 MHz
197.13
197.19
197.26
197.31
200.32
200.38
200.44
200.50
F
Cl
N
OH
Me
26b
10 0 -10 -20 -30 -40 -50 -60 -70 -80 -90 -100 -110 -120 -130 -140 -150 -160 -170 -180 -190 -200 -210
f1 (ppm)

IV. Abbreviations

°C	degree Celsius
Å	Ångström
abs.	absolut
Ac	acetyl
Alk/alk	alkyl
aq	aqueous
Ar/ar	aryl
ATR	attenuated total reflection
BHT	butylated hydroxytoluene
Bn	benzyl
Boc	*tert*-butyloxycarbonyl
br	broad
BTA-H	1*H*-benzotriazole
Bu	butyl
Bz	benzoyl
calcd.	calculated
cat.	catalyzed
conc.	concentrated
CSA	camphorsulfonic acid
d.r.	diastereomeric ratio
DCE	1,2-dichloroethane
DCM	dichloromethane
DFT	density functional theory
DMF	*N*,*N*-dimethylformamide
ee	enantiomeric excess
EI	electron ionization
equiv.	equivalent
eq (in schemes)	equivalent
ESI	electrospray ionization
Et	ethyl
EtOH	ethanol
et al.	et alii
Et_2O	diethylether
etc.	*et cetera*
EtOAc	ethylacetate

g	gram
h	hour(s)
HFIP	1,1,1,3,3,3-hexafluoro-2-propanol
Hz	Hertz
*i*Pr	*iso*-propyl
J	coupling constant
K	Kelvin
L	Liter
m	*meta*
*m*CPBA	*meta*-chloroperoxybenzoic acid
M	molar
Me	methyl
MeCN	acetonitrile
MeOH	methanol
MHz	Megahertz
min	minute
MO	molecular orbital
MS	mass spectrometry
Ms	mesyl
m.p.	melting point
m.s.	molecular sieve
NBS	*N*-bromosuccinimide
n.d.	not detected
NMR	Nuclear magnetic resonance
o	*ortho*
OMe	methoxy
p	*para*
Ph	phenyl
Piv	pivaloyl
ppm	*parts per million*
Pr	propyl
Py	pyridine
quant.	quantitative
R	rest
rac.	racemate
R_f	retardation factor
rt	room temperature

s	seconds
sat.	saturated
T	temperature
TBAF	tetra-*N*-butylammonium fluoride
*t*Bu	*tert*-butyl
THF	tetrahydrofuran
Thio	thiophene
TIPS	Triisopropyl silane
TFA	trifluoroacetic acid
TfO	triflate
TLC	thin layer chromatography
Tol	toluene
Ts	tosyl
UV	ultraviolet

V. References

[1] S. Shimizu, N. Watanabe, T. Kataoka, T. Shoji, N. Abe, S. Morishita, H. Ichimura, in *Ullmann's Encyclopedia of Industrial Chemistry*, (Eds.: C. Ley, B. Elvers), Wiley-VCH Verlag GmbH & Co. KGaA, **2000**, 557-589.

[2] H. U. Aeschbacher, U. Wolleb, J. Löliger, J. C. Spadone, R. Liardon, *Fd. Chem. Toxic.* **1989**, *27*, 227-232.

[3] P. Kiuru, J. Yli-Kauhaluoma, in *Heterocycles in Natural Product Synthesis*, (Eds.), **2011**, 267-297.

[4] W. Posselt, L. Reimann, *Geigers Mag. Pharm.* **1828**, *24*, 138-161.

[5] W. H. Organization, **2020, May 27**.

[6] B. D. Holbrook, *Birth Defects Research Part C: Embryo Today: Reviews* **2016**, *108*, 181-192.

[7] D. R. Tattershall, V. L. King, *Vol. US2409345A* (Ed.: A. C. Company), **1946**.

[8] B. Doroftei, O.-D. Ilie, R.-O. Cojocariu, A. Ciobica, R. Maftei, D. Grab, E. Anton, J. McKenna, N. Dhunna, G. Simionescu, *Molecules* **2020**, *25*, 3323.

[9] N. Pollak, C. Dölle, M. Ziegler, *Biochem. J.* **2007**, *402*, 205-218.

[10] R. Percudani, A. Peracchi, *EMBO reports* **2003**, *4*, 850-854.

[11] X. F. Cheng, Z. M. Meng, Z. L. Chen, *Phytochemistry* **1998**, *49*, 2193-2194.

[12] K. V. Rao, W. P. Cullen, *Antibiot. Annu.* **1959**, *7*, 950-953.

[13] E. Vitaku, D. T. Smith, J. T. Njardarson, *J. Med. Chem.* **2014**, *57*, 10257-10274.

[14] a) A. A. Altaf, A. Shahzad, Z. Gul, N. Rasool, A. Badshah, B. Lal, E. Khan, *J. med. chem. drug discov.* **2015**, *1*, 1-11; b) Y. Hamada, in *Pyridine*, (Eds.: P. P. Pandey), BoD – Books on Demand, **2018**, 9-26.

[15] N. C. Desai, M. R. Pandya, K. M. Rajpara, V. V. Joshi, H. V. Vaghani, H. M. Satodiya, *Med. Chem. Res.* **2012**, *21*, 4437-4446.

[16] H. Y. Jung *et al.*, *Bull. Korean Chem. Soc.* **2009**, *30*, 1297-1304.

[17] D. Murdoch, K. L. Goa, S. J. Keam, *Drugs* **2003**, *63*, 2051-2077.

[18] R. Clarke, S. Derry, R. A. Moore, *Cochrane Database of Systematic Reviews* **2014**, 1-34.

[19] J. K. Ayres, C. V. Maani, in *StatPearls*, (Eds.), StatPearls Publishing Copyright © 2020, StatPearls Publishing LLC., Treasure Island (FL), **2020**,

[20] I. Ben-Zvi, S. Kivity, P. Langevitz, Y. Shoenfeld, *Clinic. Rev. Allerg. Immunol.* **2012**, *42*, 145-153.

[21] T. Fiolet, A. Guihur, M. E. Rebeaud, M. Mulot, N. Peiffer-Smadja, Y. Mahamat-Saleh, *Clin. Microbiol. Infect.* **2020**.

[22] Z.-j. Guo, H. Miyoshi, T. Komyoji, T. Haga, T. Fujita, *Biochim. Biophys. Acta Bioenergetics* **1991**, *1056*, 89-92.

[23] P. J. Crowley, in *Comprehensive Heterocyclic Chemistry*, (Eds.: A. R. Katritzky, C. W. Rees), Pergamon, Oxford, **1984**, 185-199.

[24] A. S. Moffat, *Science* **1993**, *261*, 550-551.

[25] A.-Y. Guan, C.-L. Liu, X.-F. Sun, Y. Xie, M.-A. Wang, *Bioorg. Med. Chem.* **2016**, *24*, 342-353.

[26] C. M. Tanner, F. Kamel, G. W. Ross, J. A. Hoppin, S. M. Goldman, M. Korell, C. Marras, G. S. Bhudhikanok, M. Kasten, A. R. Chade, K. Comyns, M. B. Richards, C. Meng, B. Priestley, H. H. Fernandez, F. Cambi, D. M. Umbach, A. Blair, D. P. Sandler, J. W. Langston, *Environ. Health Perspect.* **2011**, *119*, 866-872.

[27] Court of First Instance of the European Communities, *The Court of First Instance annuls the Directive authorising Paraquat as an active plant protection substance*, **2007**.

[28] S. Pal, in *Pyridine*, (Eds.: P. P. Pandey), BoD – Books on Demand, **2018**, 57-74.

[29] J. Arditti, J. B. Tarr, *Amer. J. Bot.* **1979**, *66*, 1105-1113.

[30] K. L. Colabroy, T. P. Begley, *J. Am. Chem. Soc.* **2005**, *127*, 840-841.

[31] Y. Yan, J. Yang, Z. Yu, M. Yu, Y.-T. Ma, L. Wang, C. Su, J. Luo, G. P. Horsman, S.-X. Huang, *Nat. Commun.* **2016**, *7*, 13083.

[32] a) A. E. Chichibabin, *J. Russ. Phys. Chem. Soc.* **1904**, *37*, 1229; b) A. E. Chichibabin, *J. Prakt. Chem.* **1924**, *107*, 122-128.

[33] F. Teplý, *Collect. Czech. Chem. Commun.* **2011**, *76*, 859-917.

[34] J. Klosin, P. P. Fontaine, R. Figueroa, *Acc. Chem. Res.* **2015**, *48*, 2004-2016.

[35] J. M. Brown, *Angew. Chem. Int. Ed.* **1987**, *26*, 190-203.

[36] R. Crabtree, *Acc. Chem. Res.* **1979**, *12*, 331-337.

[37] I. I. Althagafi, M. R. Shaaban, A. Y. Al-dawood, A. M. Farag, *Chem. Cent. J.* **2017**, *11*, 88.

[38] N. R. Haddaway, S. J. Cooke, P. Lesser, B. Macura, A. E. Nilsson, J. J. Taylor, K. Raito, *Environ. Evid.* **2019**, *8*, 9.

[39] E. Negishi, A. O. King, N. Okukado, *J. Org. Chem.* **1977**, *42*, 1821-1823.

[40] M. Ochiai, Y. Takeuchi, T. Katayama, T. Sueda, K. Miyamoto, *J. Am. Chem. Soc.* **2005**, *127*, 12244-12245.

[41] a) A. Ulmer, C. Brunner, A. M. Arnold, A. Pöthig, T. Gulder, *Chem. Eur. J.* **2016**, *22*, 3660-3664; b) A. Andries-Ulmer, C. Brunner, J. Rehbein, T. Gulder, *J. Am. Chem. Soc.* **2018**, *140*, 13034-13041.

[42] J. I. Musher, *Angew. Chem. Int. Ed.* **1969**, *8*, 54-68.

[43] V. V. Zhdankin, *Hypervalent Iodine Chemistry: Preparation, Structure and Synthetic Applications of Polyvalent Iodine Compounds*, John Wiley & Sons, Ltd, **2013**.

[44] C. Willgerodt, *Journal für Praktische Chemie* **1886**, *33*, 154-160.

[45] a) A. Yoshimura, V. V. Zhdankin, *Chem. Rev.* **2016**, *116*, 3328-3435; b) S. V. Kohlhepp, T. Gulder, *Chem. Soc. Rev.* **2016**, *45*, 6270-6288.

[46] V. Meyer, W. Wachter, *Ber. Dtsch. Chem. Ges.* **1892**, *25*, 2632-2635.

[47] C. Willgerodt, *J. Prakt. Chem.* **1894**, *49*, 466.

[48] a) V. Z. Viktor, *Curr. Org. Synth.* **2005**, *2*, 121-145; b) D. P. Hari, P. Caramenti, J. Waser, *Acc. Chem. Res.* **2018**, *51*, 3212-3225.

[49] P. Eisenberger, S. Gischig, A. Togni, *Chem. Eur. J.* **2006**, *12*, 2579-2586.

[50] J. Charpentier, N. Früh, A. Togni, *Chem. Rev.* **2015**, *115*, 650-682.

[51] C. Y. Legault, J. Prévost, *Acta Cryst.* **2012**, *E68*, o1238.

[52] V. Matoušek, E. Pietrasiak, R. Schwenk, A. Togni, *J. Org. Chem.* **2013**, *78*, 6763-6768.

[53] G. C. Geary, E. G. Hope, K. Singh, A. M. Stuart, *Chem. Commun.* **2013**, *49*, 9263-9265.

[54] P. Jeschke, *Pest. Manag. Sci.* **2010**, *66*, 10-27.

[55] J. Wang, M. Sánchez-Roselló, J. L. Aceña, C. del Pozo, A. E. Sorochinsky, S. Fustero, V. A. Soloshonok, H. Liu, *Chem. Rev.* **2014**, *114*, 2432-2506.

[56] R. Berger, G. Resnati, P. Metrangolo, E. Weber, J. Hulliger, *Chem. Soc. Rev.* **2011**, *40*, 3496-3508.

[57] S. Purser, P. R. Moore, S. Swallow, V. Gouverneur, *Chem. Soc. Rev.* **2008**, *37*, 320-330.

[58] W. Yuan, L. Eriksson, K. J. Szabó, *Angew. Chem. Int. Ed.* **2016**, *55*, 8410-8415.

[59] B. K. Mai, K. J. Szabó, F. Himo, *ACS Catal.* **2018**, *8*, 4483-4492.

[60] B. Xing, C. Ni, J. Hu, *Angew. Chem. Int. Ed.* **2018**, *57*, 9896-9900.

[61] N. O. Ilchenko, M. A. Cortés, K. J. Szabó, *ACS Catal.* **2016**, *6*, 447-450.

[62] N. O. Ilchenko, B. O. A. Tasch, K. J. Szabó, *Angew. Chem. Int. Ed.* **2014**, *53*, 12897-12901.

[63] B. Zhou, T. Yan, X.-S. Xue, J.-P. Cheng, *Org. Lett.* **2016**, *18*, 6128-6131.

[64] N. O. Ilchenko, K. J. Szabó, *J. Fluor. Chem.* **2017**, *203*, 104-109.

[65] N. O. Ilchenko, M. Hedberg, K. J. Szabó, *Chemical Science* **2017**, *8*, 1056-1061.

[66] G. C. Geary, E. G. Hope, A. M. Stuart, *Angew. Chem. Int. Ed.* **2015**, *54*, 14911-14914.

[67] B. Yang, K. Chansaenpak, H. Wu, L. Zhu, M. Wang, Z. Li, H. Lu, *Chem. Commun.* **2017**, *53*, 3497-3500.

[68] W. Yuan, K. J. Szabó, *Angew. Chem. Int. Ed.* **2015**, *54*, 8533-8537.

[69] T. Yan, B. Zhou, X.-S. Xue, J.-P. Cheng, *J. Org. Chem.* **2016**, *81*, 9006-9011.

[70] M. A. Cortés González, X. Jiang, P. Nordeman, G. Antoni, K. J. Szabó, *Chem. Commun.* **2019**, *55*, 13358-13361.

[71] M. A. Cortés González, P. Nordeman, A. Bermejo Gómez, D. N. Meyer, G. Antoni, M. Schou, K. J. Szabó, *Chem. Commun.* **2018**, *54*, 4286-4289.

[72] K. Xu, R. Yang, S. Yang, C. Jiang, Z. Ding, *Org. Biomol. Chem.* **2019**, *17*, 8977-8981.

[73] A. Sanz-Marco, S. Martinez-Erro, M. Pauze, E. Gómez-Bengoa, B. Martín-Matute, *Nat. Commun.* **2019**, *10*, 5244.

[74] B.-T. Gröbel, D. Seebach, *Synthesis* **1977**, *1977*, 357-402.

[75] D. Seebach, *Angew. Chem. Int. Ed.* **1979**, *18*, 239-258.

[76] D. Seebach, E. J. Corey, *J. Org. Chem.* **1975**, *40*, 231-237.

[77] O. Miyata, T. Miyoshi, M. Ueda, *ARKIVOC* **2013**, 60-81.

[78] A. W. Erian, S. M. Sherif, H. M. Gaber, *Molecules* **2003**, *8*, 793-865.

[79] F. Mizukami, M. Ando, T. Tanaka, J. Imamura, *Bull. Chem. Soc. Jpn.* **1978**, *51*, 335-336.

[80] E. Merritt, B. Olofsson, *Synthesis* **2011**, *4*, 517-538.

[81] G. F. Koser, A. G. Relenyi, A. N. Kalos, L. Rebrovic, R. H. Wettach, *J. Org. Chem.* **1982**, *47*, 2487-2489.

[82] O. Neiland, B. Karele, *J. Org. Chem. USSR (Engl. Transí.)* **1970**, *6*, 889.

[83] Gerald F. Koser, R. H. Wettach, *J. Org. Chem.* **1977**, *42*, 1476-1478.

[84] J. S. Lodaya, G. F. Koser, *J. Org. Chem.* **1988**, *53*, 210-212.

[85] G. F. Koser, J. S. Lodaya, D. G. Ray, P. B. Kokil, *J. Am. Chem. Soc.* **1988**, *110*, 2987-2988.

[86] J. C. Lee, S. Kim, W. C. Shin, *Synth. Commun.* **2000**, *30*, 4271-4275.

[87] R. M. Moriarty, H. Hu, S. C. Gupta, *Tetrahedron Lett.* **1981**, *22*, 1283-1286.

[88] A. S. Ivanov, I. A. Popov, A. I. Boldyrev, V. V. Zhdankin, *Angew. Chem. Int. Ed.* **2014**, *53*, 9617-9621.

[89] T. Kitamura, K. Muta, K. Muta, *J. Org. Chem.* **2014**, *79*, 5842-5846.

[90] G. C. Geary, E. G. Hope, K. Singh, A. M. Stuart, *RSC Adv.* **2015**, *5*, 16501-16506.

[91] I. Kieltsch, P. Eisenberger, A. Togni, *Angew. Chem. Int. Ed.* **2007**, *46*, 754-757.

[92] M. V. Vita, J. Waser, *Org. Lett.* **2013**, *15*, 3246−3249.

[93] D. Fernández González, J. P. Brand, R. Mondière, J. Waser, *Adv. Synth. Catal.* **2013**, *355*, 1631-1639.

[94] R. D. Richardson, T. K. Page, S. Altermann, S. M. Paradine, A. N. French, T. Wirth, *Synlett* **2007**, 0538-0542.

[95] Urs H. Hirt, Martin F. H. Schuster, Andrew N. French, Olaf G. Wiest, T. Wirth, *Eur. J. Org. Chem.* **2001**, *2001*, 1569-1579.

[96] G. Levitre, A. Dumoulin, P. Retailleau, A. Panossian, F. R. Leroux, G. Masson, *J. Org. Chem.* **2017**, *82*, 11877-11883.

[97] A. H. Abazid, B. J. Nachtsheim, *Angew. Chem. Int. Ed.* **2020**, *59*, 1479-1484.

[98] J. R. Keeffe, A. J. Kresge, in *Enols*, (Eds.: Z. Rappoport), Wiley, Chichester, **1990**, 399-480.

[99] M. Bols, T. Skrydstrup, *Chem. Rev.* **1995**, *95*, 1253-1277.

[100] P. Mizar, T. Wirth, *Angew. Chem., Int. Ed.* **2014**, *53*, 5993-5997.

[101] S. Arava, J. N. Kumar, S. Maksymenko, M. A. Iron, K. N. Parida, P. Fristrup, A. M. Szpilman, *Angew. Chem. Int. Ed.* **2017**, *56*, 2599-2603.

[102] a) P.-O. Norrby, T. B. Petersen, M. Bielawski, B. Olofsson, *Chem. Eur. J.* **2010**, *16*, 8251-8254; b) S. Beaulieu, C. Y. Legault, *Chem. Eur. J.* **2015**, *21*, 11206-11211.

[103] A. A. More, G. K. Pathe, K. N. Parida, S. Maksymenko, Y. B. Lipisa, A. M. Szpilman, *J. Org. Chem.* **2018**, *83*, 2442-2447.

[104] S. Maksymenko, K. N. Parida, G. K. Pathe, A. A. More, Y. B. Lipisa, A. M. Szpilman, *Org. Lett.* **2017**, *19*, 6312-6315.

[105] J. Li, A. Bauer, G. D. Mauro, N. Maulide, *Angew. Chem. Int. Ed.* **2019**.

[106] A. Bauer, G. Di Mauro, J. Li, N. Maulide, *Angew. Chem. Int. Ed. Engl.* **2020**.

[107] H. Shen, J. Li, Q. Liu, J. Pan, R. Huang, Y. Xiong, *J. Org. Chem.* **2015**, *80*, 7212-7218.

[108] R. M. Moriarty, W. Ruwan Epa, R. Penmasta, A. K. Awasthi, *Tetrahedron Lett.* **1989**, *30*, 667-670.

[109] L. Li, Q.-Y. Chen, Y. Guo, *J. Org. Chem.* **2014**, *79*, 5145-5152.

[110] S. Sato, M. Yoshida, S. Hara, *Synthesis* **2005**, *2005*, 2602-2605.

[111] T. Brinck, J. S. Murray, P. Politzer, *International Journal of Quantum Chemistry* **1992**, *44*, 57-64.

[112] a) J. S. Murray, P. Lane, P. Politzer, *J. Mol. Model.* **2009**, *15*, 723-729; b) P. Politzer, J. S. Murray, T. Clark, G. Resnati, *Phys. Chem. Chem. Phys.* **2017**, *19*, 32166-32178.

[113] a) P. Politzer, J. S. Murray, T. Clark, *Phys. Chem. Chem. Phys.* **2013**, *15*, 11178-11189; b) T. Clark, M. Hennemann, J. S. Murray, P. Politzer, *J. Mol. Model.* **2007**, *13*, 291-296.

[114] T. M. Beale, M. G. Chudzinski, M. G. Sarwar, M. S. Taylor, *Chem. Soc. Rev.* **2013**, *42*, 1667-1680.

[115] S. H. Jungbauer, S. M. Walter, S. Schindler, L. Rout, F. Kniep, S. M. Huber, *Chem. Commun.* **2014**, *50*, 6281-6284.

[116] J.-P. Gliese, S. H. Jungbauer, S. M. Huber, *Chem. Commun.* **2017**, *53*, 12052-12055.

[117] F. Heinen, E. Engelage, A. Dreger, R. Weiss, S. M. Huber, *Angew. Chem. Int. Ed.* **2018**, *57*, 3830-3833.

[118] H. Pinto de Magalhães, A. Togni, H. P. Lüthi, *J. Org. Chem.* **2017**, *82*, 11799-11805.

[119] H. Pinto de Magalhães, H. P. Lüthi, P. Bultinck, *Phys. Chem. Chem. Phys.* **2016**, *18*, 846-856.

[120] O. Sala, H. P. Lüthi, A. Togni, *J. Comput. Chem.* **2014**, *35*, 2122-2131.

[121] V. Matoušek, J. Václavík, P. Hájek, J. Charpentier, Z. E. Blastik, E. Pietrasiak, A. Budinská, A. Togni, P. Beier, *Chem. Eur. J.* **2016**, *22*, 417-424.

[122] R. Weiss, J. Seubert, *Angew. Chem. Int. Ed. Engl.* **1994**, *33*, 891-893.

[123] D. C. Georgiou, P. Butler, E. C. Browne, D. J. D. Wilson, J. L. Dutton, *Aust. J. Chem.* **2013**, *66*, 1179-1188.

[124] S. Yannacone, V. Oliveira, N. Verma, E. Kraka, *Inorganics* **2019**, *7*, 47.

[125] R. Weiss, J. Seubert, H. Frank, *Angew. Chem.* **1994**, *106*, 2038-2039.

[126] V. V. Zhdankin, O. Maydanovych, J. Herschbach, J. Bruno, E. D. Matveeva, N. S. Zefirov, *J. Org. Chem.* **2003**, *68*, 1018-1023.

[127] F. Kniep, S. M. Walter, E. Herdtweck, S. M. Huber, *Chem. Eur. J.* **2012**, *18*, 1306-1310.

[128] T. P. Pell, S. A. Couchman, S. Ibrahim, D. J. D. Wilson, B. J. Smith, P. J. Barnard, J. L. Dutton, *Inorg. Chem.* **2012**, *51*, 13034-13040.

[129] J. C. Walters, A. F. Tierno, A. H. Dubin, S. E. Wengryniuk, *Eur. J. Org. Chem.* **2018**, *2018*, 1460-1464.

[130] a) M. Mikhael, S. A. Adler, S. E. Wengryniuk, *Org. Lett.* **2019**, *21*, 5889-5893; b) B. T. Kelley, J. C. Walters, S. E. Wengryniuk, *Org. Lett.* **2016**, *18*, 1896-1899.

[131] R. Corbo, J. L. Dutton, *Coord. Chem. Rev.* **2018**, *375*, 69-79.

[132] V. V. Zhdankin, A. Y. Koposov, N. V. Yashin, *Tetrahedron Lett.* **2002**, *43*, 5735-5737.

[133] I. P. Andrews, N. J. Lewis, A. McKillop, A. S. Wells, *Heterocycles* **1994**, *43*, 713-717.

[134] C. Brunner, A. Andries-Ulmer, G. M. Kiefl, T. Gulder, *Eur. J. Org. Chem.* **2018**, 2615-2621.

[135] X. Jusseau, H. Yin, A. T. Lindhardt, T. Skrydstrup, *Chem. Eur. J.* **2014**, *20*, 15785-15789.

[136] G. M. Kiefl, T. Gulder, *J. Am. Chem. Soc.* **2020**, *142*, 20577-20582.

[137] P. Caramenti, R. K. Nandi, J. Waser, *Chem. Eur. J.* **2018**, *24*, 10049-10053.

[138] a) H. Wang, W. Xu, Z. Wang, L. Yu, K. Xu, *J. Org. Chem.* **2015**, *80*, 2431-2435; b) H. Wang, W. Xu, L. Xin, W. Liu, Z. Wang, K. Xu, *J. Org. Chem.* **2016**, *81*, 3681-3687; c) A. Joshi, D. Chandra Mohan, S. Adimurthy, *Org. Lett.* **2016**, *18*, 464-467; d) M. Li, Y. Xie, Y. Ye, Y. Zou, H. Jiang, W. Zeng, *Org. Lett.* **2014**, *16*, 6232-6235.

[139] A. M. H. Abudken, E. G. Hope, K. Singh, A. M. Stuart, *Org. Biomol. Chem.* **2020**, *18*, 6140-6146.

[140] a) B. Zhou, X.-s. Xue, J.-p. Cheng, *Tetrahedron Lett.* **2017**, *58*, 1287-1291; b) H. K. Minhas, W. Riley, A. M. Stuart, M. Urbonaite, *Org. Biomol. Chem.* **2018**, *16*, 7170-7173; c) K. Matsumoto, M. Nakajima, T. Nemoto, *J. Phys. Org. Chem.* **2019**, *32*, e3961; d) J.-D. Yang, M. Li, X.-S. Xue, *Chin. J. Chem.* **2019**, *37*, 359-363.

[141] J. Chai, W. Ding, J. Wu, N. Yoshikai, *Chem. Asian J.* **2020**, *15*, 2166-2169.

[142] W. A. Herrmann, A. Salzer, *Volume 1: Literature, Laboratory Techniques, and Common Starting Materials*, 1. Auflage, Georg Thieme Verlag, Stuttgart, New York, **1996**.

VI. Attachments

1. Permission for Reprint by ACS Publications / Journal of the American Chemical Society

2. Statutory Declaration

All experimental work in the presented dissertation were done by me, Gabriel Maria Kiefl, during the time span between January 2017 and December 2020 at the department of chemistry in the working group Biomimetic Catalysis at the Technical University of Munich.

This dissertation, titled „Development of novel λ^3-*F*-Iodane based Umpolung strategies for the chemoselective synthesis of α-functionalized ketones" was written by myself without the help of others, except for the indicated references.

_____

Gabriel Maria Kiefl